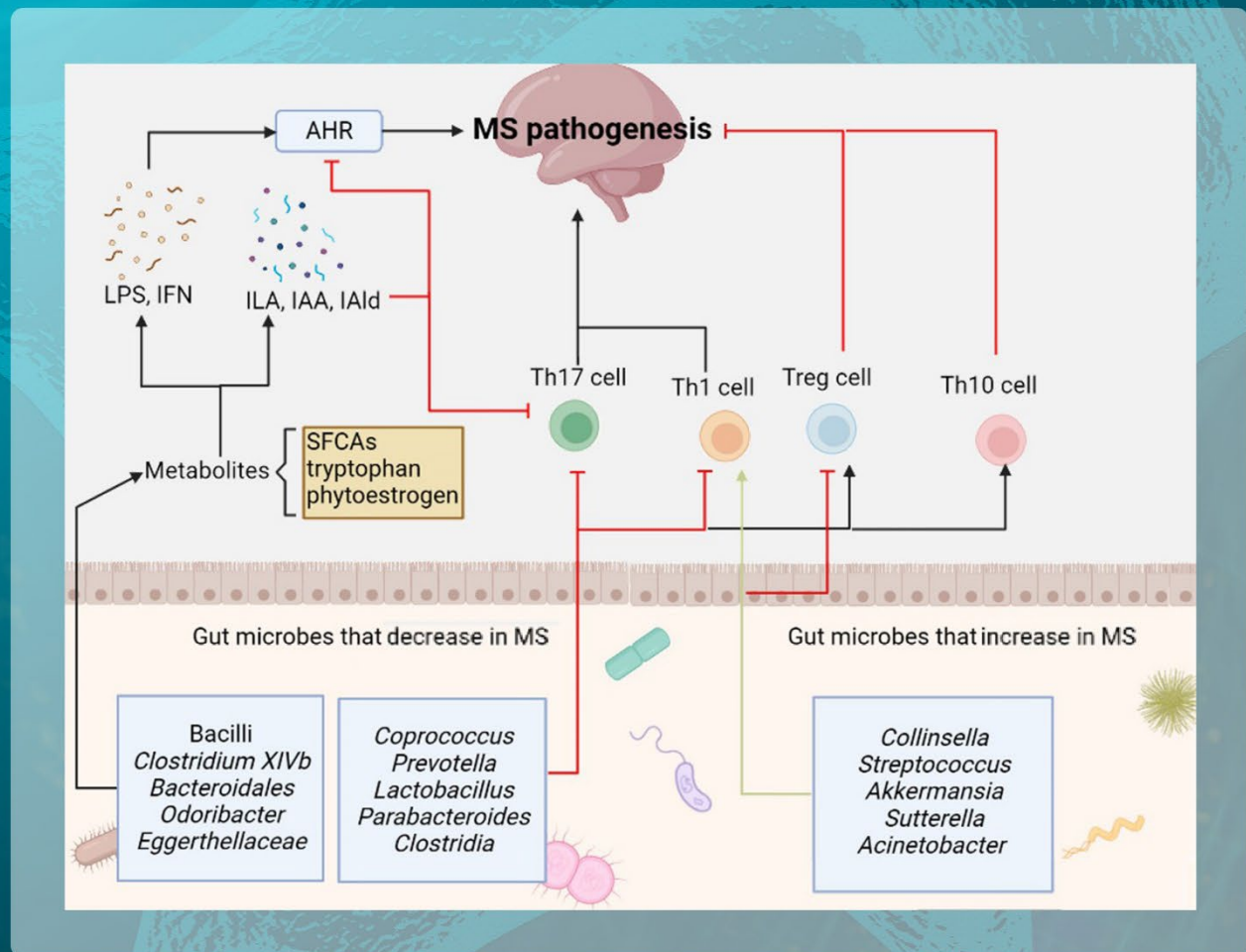


Advanced Neurology



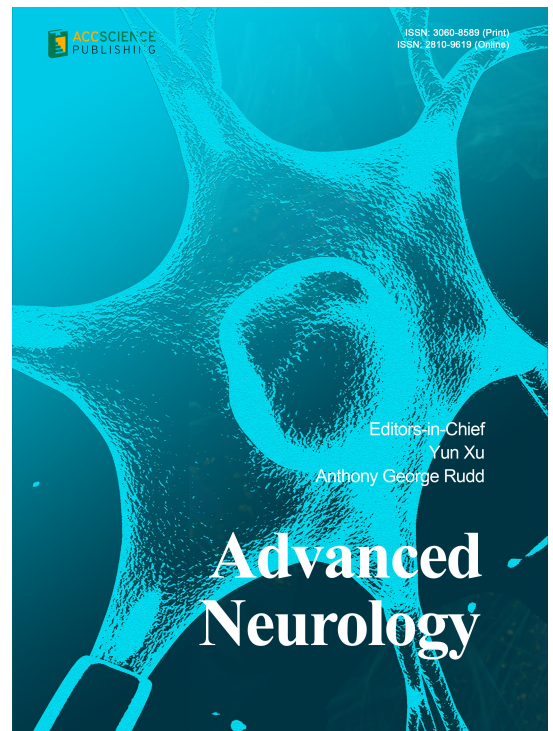
The gut microbiota and associated metabolites in multiple sclerosis

Advanced Neurology

Print ISSN: 3060-8589

Online ISSN: 2810-9619

Advanced Neurology is a peer-reviewed and open-access journal that aims to publish and disseminate novel research on basic, clinical, and translational medicine related to neurological diseases. The journal's mission is to advance our understanding of the diseases related to the nervous system and to provide a platform to showcase the latest findings in fundamental research and clinical research as well as present new ideas that might contribute to the improvement of neurological clinical practice. The target audience of *Advanced Neurology* includes physicians, epidemiologists, and neuroscientists working in the disciplines of neurology, neurosurgery, neuroimaging, neurointervention, neuropsychology, and so on.



About the Publisher

AccScience Publishing is a publishing company based in Singapore. We publish a range of high-quality, open-access, peer-reviewed journals and books from a broad spectrum of disciplines.

Contact Us

Managing Editor
an.office@accscience.sg

AccScience Publishing
8 Burn Road, #15-03 Trivex, Singapore 369977.

Volume 2 • Issue 3 • September 2023
ISSN 3060-8589 (print) ISSN 2810-9619 (online)

ADVANCED NEUROLOGY

Editors-in-Chief

Yun Xu

*The Affiliated Hospital of Nanjing University
Medical School, China*

Anthony George Rudd

King's College London, United Kingdom



Access Science Without Barriers

Full issue copyright © 2023 AccScience Publishing

All rights reserved. Without permission in writing from the publisher, this full issue publication in its entirety may not be reproduced or transmitted for commercial purposes in any form or by any means, electronic or mechanical, including photocopying, recording, or any information storage and retrieval system. Permissions may be sought from an.office@accscience.sg.

Article copyright © Respective Author(s)

See articles for copyright year. All articles in this full issue publication are open-access. There are no restrictions in the distribution and reproduction of individual articles, provided the original work is properly cited. However, permission to reuse copyrighted materials of an article for commercial purposes is applicable if the article is licensed under Creative Commons Attribution-NonCommercial License. Check the specific license before reusing.

ADVANCED NEUROLOGY

ISSN: 3060-8589 (print)

ISSN: 2810-9619 (online)

Editorial and Production Credits

Publisher: AccScience Publishing

Managing Editor: Zoe Zhang

Production Editor: Sharmila Velapasamy

Special Issue Commissioning Editor: Zoe Zhang

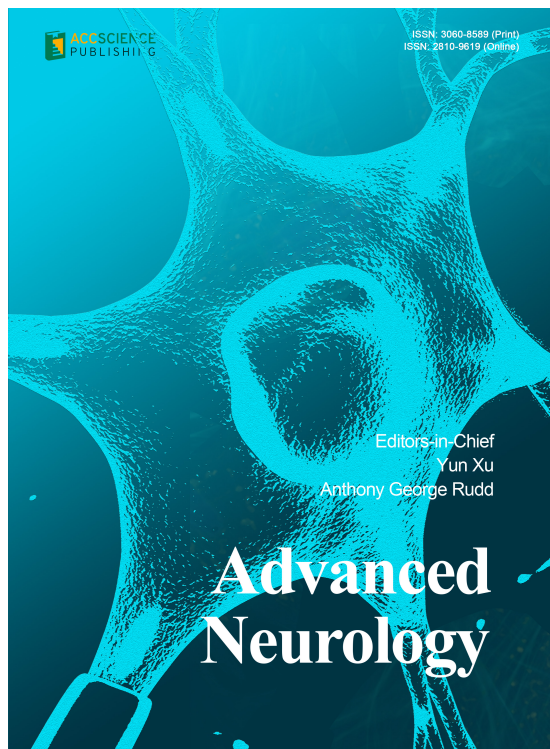
Article Layout and Typeset: Sinjore Technologies (India)

Cover Design: ProPub (China)

For all advertising queries, contact
an.office@accscience.sg.

Supplementary file

Supplementary files of articles can be obtained at
<https://accscience.com/journal/AN/2/3>.



Disclaimer

AccScience Publishing is not liable to the statements, perspectives, and opinions contained in the publications. The appearance of advertisements in the journal shall not be construed as a warranty, endorsement, or approval of the products or services advertised and/or the safety thereof. AccScience Publishing disclaims responsibility for any injury to persons or property resulting from any ideas or products referred to in the publications or advertisements. AccScience Publishing remains neutral with regard to jurisdictional claims in published maps and institutional affiliations.

Advanced Neurology

Editorial Board

Editors-in-Chief

Yun Xu

The Affiliated Hospital of Nanjing University Medical School, China

Anthony George Rudd

King's College London, UK

Associate Editors

Zhong-Ping Feng

University of Toronto, Canada

Chun-Feng Liu

The Second Affiliated Hospital of Soochow University, China

Sheng-Xi Wu

Fourth Military Medical University, China

Liqun Zhang

St George's University Hospital, UK

Ling-Qiang Zhu

Huazhong University of Science and Technology, China

Assistant Editor

Lu Zhang

Jiangsu Province Stroke Association, China

*Editorial Board Members**

Ahmet Hoke, *USA*

Jing Ai, *China*

Nabil J. Alkayed, *USA*

Lars Bertram, *Germany*

Luiz R. Britto, *Brazil*

Deqin Geng, *China*

Xiaoping Gu, *China*

Ying Han, *China*

Jeffrey Henderson, *Canada*

Frank Hoffmann, *Germany*

Bo Hu, *China*

Tao Hong, *China*

Michael F. Jackson, *Canada*

Wolfgang H. Jost, *Germany*

Wolfgang Köhler, *Germany*

Nagaendran Kandiah, *Singapore*

Anna Maria Lavezzi, *Italy*

Giuseppe Lanza, *Italy*

Renyu Liu, *USA*

Francesca Morgante, *UK*

Hengye Man, *USA*

Kenichi Meguro, *Japan*

Marco Mula, *UK*

Hugh Markus, *UK*

Jun Ni, *China*

Michele Roccella, *Italy*

Deidre De Silva, *Singapore*

Hong-Shuo Sun, *Canada*

Jean-Marc Sabatier, *France*

Yun Shi, *China*

Mohammad Wasay, *Pakistan*

Yanzhong Wang, *UK*

Bing Zhang, *China*

Yan Zhang, *China*

Alessio Di Fonzo, *Italy*

Alessandro Pezzini, *Italy*

Giuseppe Biagini, *Italy*

Luis Puellas, *Spain*

Jacek Losy, *Poland*

Jagaralapudi M.K. Murthy, *India*

Péter Halász, *Hungary*

Kheng Seang Lim, *Malaysia*

Franco Valzania, *Italy*

Beata Sarecka-Hujar, *Poland*

*Youth Editorial Board**

Tommaso Lo Barco, *Italy*

*Editorial Board Members as of March 31, 2023

CONTENTS

REVIEW ARTICLES

- 1 **Woven Endobridge embolization: Indications and innovation**
Ashley M. Carter, Bethsabe Romero, Harrison Dai, Simran Phuyal, Danxun Li, Brandon Lucke-Wold
- 2 **The gut microbiota and associated metabolites in multiple sclerosis**
Yunshu Wang, Zihao Li, Yun Xu, Cun-Jin Zhang
- 3 **Multiple sclerosis: Unveiling current immunogenetic factors and their role in etiopathogenesis and clinical aspects**
Benediktas Trumpulis, Rasa Liutkeviciene, Renata Balnyte

ORIGINAL RESEARCH ARTICLES

- 4 **Transient receptor potential melastatin 7 signaling in U251 cell migration and invasion involves calcineurin**
Haifan Gong, Raymond Wong, Julia Bandura, James T. Rutka, Zhong-Ping Feng, Hong-Shuo Sun
- 5 **Distinct behavioral effects of short-term voluntary running in phosphatase and tensin homolog deleted on chromosome 10 neuronal haploinsufficient mice**
Diana Zukas Andreotti, Natália Prudente de Mello, Amanda Galvão Paixão, Cristoforo Scavone, Ana Maria Orellana, Elisa Mitiko Kawamoto
- 6 **Relationship between sleep outcomes and lifestyle factors in young adults who sustained traumatic brain injury in childhood**
Edith Botchway-Commey, Celia Godfrey, Christian L. Nicholas, Vicki Anderson, Cathy Catroppa
- 7 **Cognition damage due to disruption of cyclic adenosine monophosphate-related signaling pathway in melatonin receptor 2 knockout mice**
He-Zhou Huang, Xiang Wang, Dan Liu
- 8 **Estimated glomerular filtration rate and serum neurofilament light chain: Insight from National Health and Nutrition Examination Survey**
Jiangwen Liu

REVIEW ARTICLE

Woven Endobridge embolization: Indications and innovation

Ashley M. Carter¹, Bethsabe Romero¹, Harrison Dai¹, Simran Phuyal¹, Danxun Li¹, and Brandon Lucke-Wold^{2*}¹Eastern Virginia Medical School, Norfolk, Virginia, USA²Department of Neurosurgery, University of Florida, Gainesville, Florida, USA**Abstract**

The treatment of intracranial aneurysms has seen incredible advancements over the last few decades. Long-term occlusion of wide-neck bifurcation aneurysms remains technically challenging. The Woven Endobridge (WEB) embolization device is innovative in its construction and uses. The design of the device has evolved over the last decade. Pre-clinical and clinical trials are ongoing and continue to inform the development of intrasaccular flow-diverting devices. The WEB device is currently approved by the U.S. Food and Drug Administration (FDA) for treating wide-neck aneurysms. The safety and efficacy of the WEB device have yielded promising clinical results that may have additional indications. This review aims to discuss the development of the WEB device and the current state of the WEB device in the treatment of wide-neck aneurysms. We also summarize ongoing clinical studies and potential innovative uses.

Keywords: Woven Endobridge embolization device; Aneurysms; Wide-neck aneurysms; Posterior communicating artery aneurysms; Sidewall aneurysms; Flow-diverting device; Intrasaccular embolization

***Corresponding author:**Brandon Lucke-Wold
(brandon.lucke-wold@
neurosurgery.ufl.edu)

Citation: Carter AM, Romero B, Dai H, *et al.*, 2023, Woven Endobridge embolization: Indications and innovation. *Adv Neuro*, 2(3): 293. <https://doi.org/10.36922/an.293>

Received: December 14, 2022**Accepted:** June 1, 2023**Published Online:** June 13, 2023

Copyright: © 2023 Author(s). This is an Open-Access article distributed under the terms of the Creative Commons Attribution License, permitting distribution, and reproduction in any medium, provided the original work is properly cited.

Publisher's Note: AccScience Publishing remains neutral with regard to jurisdictional claims in published maps and institutional affiliations.

1. Overview of the WEB embolization devices and current treatment approaches

The American Association of Neurological Surgeons (AANS) recommends three broad treatment approaches for brain aneurysms: Endovascular therapy or coiling with or without adjunctive devices, medical intervention, and surgical therapy or clipping^[1]. Endovascular strategies for treating aneurysms have demonstrated great success with embolization coils. Despite this, long-term occlusion of wide-neck and wide-neck bifurcation aneurysms remains technically challenging^[2]. Balloon-assisted and stent-assisted coiling have demonstrated safe and effective treatment of these aneurysms without increased thromboembolic or iatrogenic rupture events^[3-5]. However, the balloon-assisted technique risks temporary occlusion of the parent artery^[6]. Stent-assisted coils eliminate the need for temporary luminal occlusion. Although they are effective for wide-neck aneurysms, they do not adequately treat bifurcation aneurysms as the second branch vessel is often left unprotected and thus risks coil herniation. Various shapes have been developed to address this issue, such as the Y-stent and waffle-cone techniques, which generally provide better coverage^[7,8]; though, the introduction of a stent requires prolonged use of dual antiplatelet therapy^[9].

Flow diversion emerged as a paradigm shift in treating wide-neck and bifurcation aneurysms. Rather than direct intrasaccular embolization, flow diversion aimed to divert flow away from the aneurysm resulting in delayed thrombosis and endothelialization of the parent vessel wall. Devices such as the Pipeline Flex embolization device (PED) achieve flow diversion with lower porosity and approximately 30% higher metal coverage^[10]. The Honeycomb Microporous Covered Stent features a stent covered by a polyurethane film that allows for greater flow-diverting properties than a traditional stent^[11]. While these devices are promising, dual antiplatelet therapy is still required.

The Woven Endobridge (WEB) embolization device is an intrasaccular flow diverter designed to divert flow at the interface between the aneurysm neck and the parent artery^[12]. The device deploys a double-layer (DL) braided oblate nitinol mesh within the aneurysm sac, which self-expands to conform to the aneurysm wall and span the aneurysm neck. As the therapy focuses on stabilization and coverage of the aneurysm neck, the device is designed for both wide-neck and bifurcation aneurysms. The device may also be a single layer (SL) or a single-layer sphere (SLS)^[13]. The inner and outer layers of the mesh are held together by radiopaque markers, which allow direct visualization of the device within the aneurysm with X-ray-based techniques. The thrombogenicity of the WEB device is comparable to that of intrasaccular coils, but the radiopaque marker at the luminal surface of the mesh is not thrombogenic, except where an endoluminal construct is indicated for better support. Long-term antiplatelet therapy is usually unnecessary in most patients^[14].

The WEB embolization device mesh is advanced up to the aneurysm using a VIA[®] catheter, usually with a transfemoral approach. The microcatheter containing the mesh is positioned within the fundus of the aneurysm and deployed within the aneurysm. An angiogram is performed immediately after deployment (Figure 1). If positioning is favorable, the device can be detached and remains within the aneurysm. If not, the device can be



Figure 1. Angiogram of anterior communicating artery aneurysm. (A) Placement of WEB device in aneurysm with early stasis. (B) Final positioning of WEB device in aneurysm dome.

Abbreviation: WEB: Woven Endobridge.

resheathed and repositioned. Serial control angiograms are performed following the deployment, demonstrating progressively rapid cessation of blood flow within the aneurysm, starting distally and progressing toward the aneurysm neck. Complete cessation of intra-aneurysmal blood flow is noted within minutes of placement, and complete occlusion of an aneurysm can be confirmed at 8 weeks^[15]. Endothelialization of the parent vessel by the growth of neo-endothelium within the recessed concavity of the embolization device has been noted^[16]. Thus, the WEB embolization device combines stent-assisted coiling and flow diversion features while minimizing the need for long-term antiplatelet therapy.

2. Clinical trials and ongoing investigations

The WEB embolization device has demonstrated success in pre-clinical trials. Several ongoing clinical trials are investigating the device's effectiveness and safety, while exploring its suitability to various types of intracranial aneurysms. A total of 11 trials using the device have been registered (National Library of Medicine), of which six have been completed (Table 1). Of these six trials, five have results available, while one does not have results available currently. Of the remaining five registered studies, one was withdrawn, one was terminated, one is under recruiting phase, one is not currently recruiting, and one is under unknown status. A summary of clinical trials and their current statuses are found in Table 1.

A prospective, multicenter, and observational study conducted with ten French neurointerventional centers, collectively called French Observatory (NCT01975233), primarily looked at the post-procedure occlusion durability of the aneurysms treated with WEB devices (Table 2)^[17]. The WEBCAST study (NCT01778322) evaluated the safety and efficacy of WEB devices in wide-neck bifurcation aneurysms, mostly unruptured (Table 2)^[18]. A cumulative population study was performed with the patients from the French Observatory trial (NCT01975233) and the WEBCAST trial (NCT01778322)^[19]. In the cumulative study, treatment with WEB was successfully performed in 96.5%. At 1 year, complete aneurysm occlusion was observed in 56.0%, neck remnant in 26.0%, and an aneurysm remnant in 18.0%, of which 2.0% worsened since the procedure. At 1 year, mortality was 3.9%, with three deaths unrelated to an aneurysm or treatment and one related to a partially thrombosed aneurysm^[19].

The WEBCAST-2 was later designed to corroborate further the high degree of safety and efficacy demonstrated by WEBCAST and French Observatory studies^[20]. The study had a comparable protocol to WEBCAST, with a few changes. At 1 year, complete occlusion was achieved

Table 1. Registered trials and their current statuses

Study	Title	Status	Population	References
NCT04621552 (France)	Virtual Simulation for Woven EndoBridge Device Sizing	Completed, results available	Sample size: 186 Inclusion criteria: Patients >18 years treated with WEB for intracranial aneurysms	[64]
NCT01975233 (France)	WEB French Observatory of the WEB Aneurysm Embolization System	Completed, results available	Sample size: 62 Inclusion criteria: Patients >18 years; independent use of WEB device prior to inclusion in French Observatory; Aneurysm characteristic: morphology, saccular, located in BA, MCA bifur, ICA terminus, ACom, or ACA, appropriate diameter and width of aneurysm to be treated with WEB device, and Dome-to-Neck ratio ≥ 1.0	[65]
NCT01778322 (Denmark, France, Germany, Hungary)	WEB Clinical Assessment of Intracranial Aneurysm Therapy (WEBCAST)	Completed, results available	Sample size: 51 Inclusion criteria: Patient ≥ 18 years of age; must sign informed consent form prior to study	[66]
NCT02687607 (France)	Clinical Assessment of WEB Device in Ruptured Aneurysms (CLARYS)	Completed, results available	Sample size: 60 Inclusion criteria: independent use of WEB device prior to inclusion in CLARYS; patient ≥ 18 years and ≤ 80 years; Hunt & Hess score of I, II, or III; Aneurysm characteristic: morphology, saccular, located in BA, MCA bifurcation, ICA terminus, ACom, PCom, or ACA; appropriate diameter, height, and maximum width of 10 mm of aneurysm to be treated with WEB device; patient must be followed up by the physician; patient must comply with all aspects of the study; patient or their legal team must be informed about data collection and its protection, and must sign for consent when mandatory	[67]
NCT03844334 (France, Germany, Hungary)	Clinical Evaluation of WEB 0.017 Device in Intracranial Aneurysms (CLEVER)	Completed, results not yet available	Sample size: 163 Inclusion criteria: Patient ≥ 18 years and <80 years of age; patient must have an intracranial aneurysm; must sign informed consent form prior to any data collection; Hunt & Hess score <III	[68]
NCT02191618 (Canada, Denmark, Germany, Hungary, Turkey, United States)	The WEB-IT Clinical Study	Completed, results available	Sample size: 150 Inclusion criteria: Patient ≥ 18 years and <75 years of age; patient must have a single IA requiring treatment; patient must sign an informed consent form	[69]
NCT03936647 (Canada)	The RISE Trial: A Randomized Trial on Intra-Saccular Endobridge Devices	Currently recruiting	Estimated enrollment: 250 Inclusion criteria: Patient with intracranial aneurysm where WEB device is considered appropriate for treatment; aneurysm diameter of 4–11 mm; can include saccular bifurcation aneurysms of MCA, BA, carotid terminus, or ACom; ruptured aneurysms with WFNS ≤ 3	[70]
NCT03312725 (Belgium)	Mid-term Data Collection of the Treatment of Intracranial Aneurysms with the WEB aneurysm Embolization System	Terminated	-	[71]

(Cont'd...)

Table 1. (Continued)

Study	Title	Status	Population	References
NCT03379714 (Belgium)	Mid-term Data Collection of the Treatment of Intracranial Aneurysms with the WEB aneurysm Embolization System	Withdrawn	-	-
NCT04839705 (United States)	Post Approval Study – Evaluate the Long-term Safety and Effectiveness of the WEB Device (WEB PAS)	Not yet recruiting	-	[72]
NCT03207087 (China)	The WEB-IT China Clinical study	Unknown status	-	[73]

Abbreviations: ACA: Anterior cerebral artery; Acom: Anterior communicating artery; BA: Basilar artery; IA: Intracranial aneurysm; ICA: Internal carotid artery; MCA: Middle cerebral artery; Pcom: Posterior communicating artery.

Table 2. Summary of completed clinical trials result

Study	Title	Study type	Conditions	Interventional treatment	Results	References
NCT04621552 (France)	Virtual Simulation for Woven EndoBridge Device Sizing	Observational	Aneurysm; intracranial aneurysm	Device: WEB embolization	Virtual simulation reduced time of intervention; decreased radiation dose, number of undeployed devices, and need for corrective interventions.	[64]
NCT01975233 (France)	WEB French Observatory of the WEB Aneurysm Embolization System	Observational	Brain aneurysm	Device: WEB aneurysms embolization systems	High rate of complete occlusion (51.7%) and adequate occlusion (79.3%) at 1 year.	[65]
NCT01778322 (Denmark France, Germany, Hungary)	WEB Clinical Assessment of Intrasaccular Aneurysm Therapy (WEBCAST)	Observational	Intracranial aneurysm	Procedure: Intracranial aneurysm embolization	56.1% complete occlusion, 29.3% neck remnant, and 14.6% aneurysm remnant at 6 months.	[66]
NCT02687607 (France)	Clinical Assessment of WEB Device in Ruptured Aneurysms (CLARYS)	Observational	Brain aneurysm	WEB aneurysm embolization system	41.3% complete occlusion and 87% adequate occlusion at 1 year, effective protection against rebleeding.	[67]
NCT02191618 (Canada, Denmark, Germany, Hungary, Turkey, United States)	The WEB-IT Clinical Study	Single group interventional	Wide-neck bifurcation intracranial aneurysms; intracranial aneurysms	Device: WEB	53.8% complete aneurysm occlusion and 84.6% adequate occlusion.	[69]

Abbreviations: CLARYS: Clinical Assessment of WEB Device in Ruptured Aneurysms; WEBCAST: WEB Clinical Assessment of Intrasaccular Aneurysm Therapy; WEB: Woven Endobridge device; WEB-IT: Woven Endobridge Intrasaccular Therapy.

in 54.0% of the aneurysms, neck remnant in 26.0%, and an aneurysm remnant in 20.0%. Adequate occlusion was reported in 80.0%. More recently, data have been published with a cumulative trial population of WEBCAST and WEBCAST-2 at 3 years^[21] and 5-year analysis^[22] that shows long-term aneurysm stability and occlusion rate in aneurysms treated with the WEB devices.

The WEB Intrasaccular Therapy (WEB-IT) study (NCT02191618) also aimed to validate further the WEB

system's safety and effectiveness for treatment of wide-neck bifurcation aneurysms (Table 2)^[23]. Mortality remained 0.0% throughout the entire 12-month study period^[24]. In the case-controlled and multicenter study (NCT04621552), investigators compared a virtual simulation with conventional sizing to determine the appropriate WEB device size for an aneurysm. The results demonstrated fulfillment of the primary outcome measure by shortening the intervention time, lowering the radiation dose, and lowering the number of WEB devices not

deployed (Table 2)^[25]. Finally, the most recently published independent trial is the CLARYS (NCT02687607), which assessed the utility of the WEB embolization specifically in patients with recently ruptured intracranial aneurysms (Table 2)^[26].

3. Outcomes and proposed grading scale for aneurysm recurrence

The most feared complication of intracranial aneurysms is a rupture causing a subarachnoid hemorrhage (SAH), posing a significant risk of morbidity and mortality^[1,27]. Medical intervention, without surgery, is the preferred treatment approach to un-ruptured intracranial aneurysms. Nevertheless, unruptured aneurysms may need surgical intervention, requiring a personalized approach^[1]. The mainstay approach to managing unruptured cerebral aneurysms involves blood pressure control and smoking cessation to prevent further aneurysm development^[27]. Conversely, surgical and endovascular approaches aim to repair aneurysms.

Numerous studies in the literature have demonstrated safety and efficacy in the treatment options for intracranial aneurysms^[28-30]. There are currently several criteria that evaluate the stage, structural morphology, and severity of intracerebral aneurysms, such as the Hunt and Hess classification or Yasargil Grading Scales. However, there remain significant gaps in data examining the long-term recurrence of aneurysms that have been surgically or medically treated^[28-30]. Each modality used to treat intracerebral aneurysms individually estimates re-occurrence rates and outcomes^[28-30]. Evaluating aneurysm re-occurrence remains a highly controversial and active area of research in neurological surgery and neuroradiology.

Several criteria have been proposed to evaluate the future reoccurrence of intracranial aneurysms. Of the criteria that exist, the Raymond-Roy occlusion classification system (RROC) has shown promise. The RROC grades the occlusion of endovascularly-treated aneurysms in an angiographic classification system (Figure 2). Although initially created to assess an aneurysm's occlusion class, the RROC has been modified to predict aneurysmal occurrence after surgical intervention, whereby Mascitelli *et al.* (2015) proposed their modified RROC scale (Figure 2)^[31,32]. The modified scale includes further divided class III to signify progression to occlusion^[31]. A follow-up study in 2015 validated the modified RROC, which demonstrated that specific categories of aneurysms are more likely to reoccur than others^[32,33]. A subsequent 2016 meta-analysis examining the predictiveness of the RROC on aneurysm coiling consisting of 4587 patients found that the RROC

provided a considerable predictive value in reoccurrence for more severe aneurysms treated with coiling^[34].

3.1. Association of WEB device with recurrence and rupture of aneurysm

The recurrence and rupture of wide-neck intracranial aneurysms following treatment with the WEB device are not abundantly reported in the literature^[35,36]. Peterson and Cord (2021) are among the first to focus on the recurrent and residual aneurysms post-WEB that require treatment^[35]. Their meta-analysis included 16 studies and 901 WEB cases and found that $18.7 \pm 11.5\%$ cases of either recurrent or residual aneurysms post-initial WEB device; while $10.7 \pm 11\%$ of cases had to undergo some form of retreatment^[35]. A meta-analysis by Zhang *et al.* that focused on the efficacy of the WEB device in treating wide-neck intracranial aneurysms (36 studies, 1759 patients with 1749 aneurysms) found that the recanalization rate was 9% and intraoperative rupture rate was 3%^[36]. Factors leading to a higher recanalization rate were older-generation WEB devices, posterior circulation, and rupture status^[36]. Thus far, the most likely treatment for the recurrence of an aneurysm following an operation with the WEB device is stent-assisted coiling (SAC). Some other techniques used include flow diversions, additional coiling, clipping, and additional WEB devices, and all have shown success^[35,37]. Further investigation into long-term association of recurrence and rupture rates of wide-neck intracranial aneurysms post-treatment with the WEB devices would provide value to the literature. The ability to keep up with the rapid pace of WEB device innovations within the literature as it relates to the recurrence and rupture rate of each new generation can also provide value for clinicians.

4. Discuss how pre-clinical studies are seeking to improve the devices

The WEB device has been in clinical use for over 10 years^[38]. The first pre-clinical study evaluated the short-term performance of the WEB II device^[12]. The WEB II device was improved by adding more than a single layer of nitinol mesh. The device was implanted in two patients to assess occlusion's short-term performance and durability. One patient had an unruptured middle cerebral artery (MCA) trifurcation aneurysm, while the other had a basilar tip aneurysm. The device was successfully implanted in both patients without complications of hemorrhage or peri or post-procedural thromboembolism. Complete aneurysm occlusion was achieved within minutes of device placement. Eight weeks later, angiography confirmed stable occlusion in both patients^[12].

A stable construct across the neck of the aneurysm is critical for achieving durable occlusion^[39]. Failure of

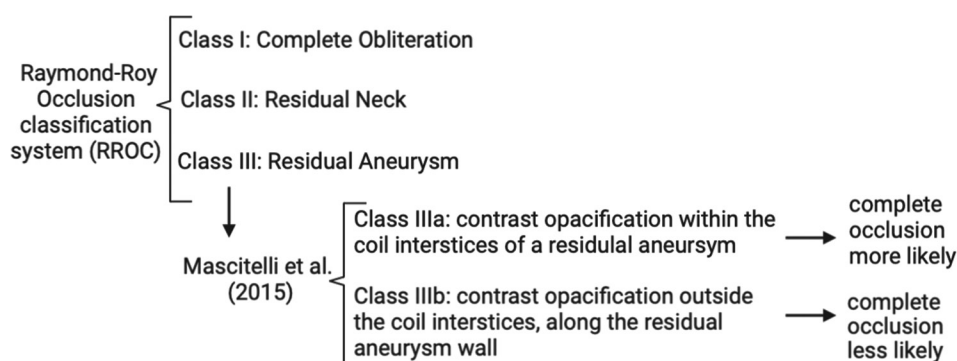


Figure 2. Current classification for intracranial or cerebral aneurysm recurrence. Class III is divided to indicate progression to occlusion. Class IIIb complete occlusion is less likely versus Class IIIa (85.11% vs. 16.67%, $p < 0.001$)^[31,43]. This image was generated using Biorender.

the WEB II device was documented in a case study of a patient who presented with regrowth of an unruptured MCA aneurysm 9 months after implantation^[40]. During the patient's 6-month follow-up, the magnetic resonance imaging (MRI) showed continued progression of aneurysm neck filling, pushing the device distally. Balloon-assisted coiling was used to treat the regrown aneurysm according to standard neurointerventional approaches^[41,42]. Although not desired, device failure can reveal deficiencies that lead to improvement of subsequent device models.

Pre-clinical studies continue to inform the modification and development of these devices. Several changes have been made to the device since its introduction in 2011^[12]. The current devices, the WEB SLS and WEB SL model, are spheroid and cylindrical shaped devices composed of single layers of braided nitinol^[24]. Another change was incorporation of platinum into nitinol strands to enhance visualization in the WEB SLS EV and WEB SL models^[43]. In the U.S., 27 cylindrical and eight spheroid devices are available, differing in diameters and heights^[43]. These improvements have expanded European treatment indications to treat distal and sidewall aneurysms and wide-neck bifurcation aneurysms^[44,45].

5. Discuss novel innovations for wide-neck aneurysms

Decades of research and development have been invested to make endovascular treatments the standard of care for intrasaccular aneurysms. However, treating wide-neck aneurysms can be technically challenging as they have a higher risk of recanalization^[46,47]. It has been demonstrated that coil embolization can successfully treat aneurysm but is limited by several factors, including neck size and the dome-to-neck ratio^[48-51]. In addition, the instability of coils can lead to herniation of the parent artery, and herniated coils may migrate or lead to thromboembolism and incomplete occlusion^[12].

Over the past decade, a paradigm shift has occurred in the treatment of wide-neck aneurysms. A new treatment model emerged in 2011 when the FDA approved the first flow-diverting device^[12,14]. Conventionally, endovascular treatment involves direct intrasaccular embolization, followed by immediate protection^[39]. On the contrary, flow-diverting devices delay aneurysm occlusion, an approach different from the traditional treatment model. The device diverts blood flow away from the aneurysm, allowing for thrombosis to occur. Over time, endothelialization of the device takes place in the aneurysm's parent vessel wall^[39,52].

Several flow-diverting devices are under clinical trials, and the FDA has approved various devices for treating wide-neck aneurysms (Table 3)^[11,53-57]. The WEB aneurysm embolization system (MicroVention Terumo, Aliso Viejo, CA, USA) is a flow-diverting device that differs from traditional flow diverters^[2,38,58]. Rather than occupying the parent vessel's lumen, the WEB device is intrasaccular and composed of nitinol-based braided wire^[38]. The device is not limited by the use of dual antiplatelet therapy and can be used to treat both ruptured and unruptured aneurysms^[38,59].

6. Discussion

The WEB device is unique in its innovation and indications, yet further research and development is warranted in several areas. At present, the proposed grading scale, the RROC, with its modifications by Mascitelli *et al.*, should be additionally classified based on the treatment used^[31]. It would be advantageous to assess the rate of complications with WEB devices versus stents or clipping. Pre-clinical studies are crucial to advancing the WEB device to its fullest potential. Accurate WEB device size selection is imperative to a safe and effective procedure; automated volumetric software and digital subtraction angiography (DSA) are actively being studied to improve this aspect of the device^[60]. The need for guidelines for successful implantation could

Table 3. Wide-neck aneurysm treatment devices with FDA approval

Year of approval	Wide-neck aneurysm treatment devices	Manufacturer	References
2014	Barrel Vascular Reconstruction Device	Reverse Medical Corporation (Irvine, CA, USA)	[56,74]
2019	Comaneci Device	Rapid Medical, (Yokneam, Israel)	[55,56]
2015	eCLIPS Device	EVASC Neurovascular Enterprises (Vancouver, BC, Canada)	[54,56]
2017	PulseRider Aneurysm Neck Reconstruction Device	Pulsar Vascular Inc., (Los Gatos, CA, USA)	[53,56]
2011	Woven EndoBridge	MicroVention Terumo (Aliso Viejo, CA, USA)	[12,24,43,56]

All treatment devices names are as listed. Abbreviation: FDA: Food and drug administration.

also prove beneficial as it may decrease waste and provide efficiency in practice. As novel innovations for wide-neck aneurysms continue to be investigated, it is essential to continue to evaluate the effectiveness and indications of the WEB embolization device.

In recent years, novel advancements in neurological surgery, such as the WEB device, have broadened surgical and endovascular aneurysm management^[30]. The WEB device can treat anatomically complex bifurcation aneurysms, and the treatment is safer and more effective than the traditional approach. Conventionally, the placement of stent-assisted coiling would require antiplatelet therapy, which has the risk of hemorrhagic complications^[24]. Some of the advantages of the WEB device treatment are that it does not require dual antiplatelet therapy, and the procedure can be performed within a shorter timeframe, resulting in improved cost-effectiveness and decreased anesthesia exposure^[61]. The WEB device is currently only FDA approved to treat wide-neck bifurcation aneurysms^[24]; however, several ongoing clinical trials are investigating the device's suitability in various intracranial aneurysms. As the results from these clinical studies emerge, the device and its applications will likely evolve.

Recently, a multicenter study evaluated the use of the WEB device in both sidewall and bifurcation intracranial aneurysms^[62]. When 91 pairs of aneurysms were compared, outcomes were not significantly different between the two groups. In particular occlusion status, device deployment success and complication rates were not significantly different — indicating that the WEB device may be used off-label for sidewall aneurysms. A small cohort study of 15 patients was also performed to evaluate the use of the WEB device in posterior communicating artery (PCoMA) aneurysms^[63]. The authors reported complete and adequate occlusion. Retreatment was required for two patients and no intraoperative ruptures occurred. Considering the common occurrence of aneurysms in the PCoMA and their rates of rupture, the off-label use of the WEB device is a promising alternative for PCoMA aneurysms.

Acknowledgments

None.

Funding

None.

Conflict of interest

The authors declare that they have no competing interests.

Author contributions

Conceptualization: Brandon Lucke-Wold, Ashley M. Carter, Bethsabe Romero

Writing – original draft: All authors

Writing – review & editing: Brandon Lucke-Wold, Ashley M. Carter, Bethsabe Romero, Simran Phuyal

Ethics approval and consent to participate

Not applicable.

Consent for publication

Not applicable.

Availability of data

Not applicable.

References

1. Cerebral Aneurysm Secondary Cerebral Aneurysm. Available from: <https://www.aans.org/en/patients/neurosurgical-conditions-and-treatments/cerebral-aneurysm> [Last accessed on 2023 Feb 27].
2. Pierot L, Moret J, Barreau X, *et al.*, 2018, Safety and efficacy of aneurysm treatment with WEB in the cumulative population of three prospective, multicenter series. *J Neurointerv Surg*, 10: 553–559.
<https://doi.org/10.1136/neurintsurg-2017-013448>
3. Moret J, Cognard C, Weill A, *et al.*, 1997, The “Remodelling Technique” in the treatment of wide neck intracranial aneurysms. Angiographic results and clinical follow-up in

- 56 cases. *Interv Neuroradiol*, 3: 21–35.
<https://doi.org/10.1177/159101999700300103>
4. Shapiro M, Babb J, Becske T, *et al.*, 2008, Safety and efficacy of adjunctive balloon remodeling during endovascular treatment of intracranial aneurysms: A literature review. *AJNR Am J Neuroradiol*, 29: 1777–1781.
<https://doi.org/10.3174/ajnr.A1216>
 5. Sluzewski M, van Rooij WJ, Beute GN, *et al.*, 2006, Balloon-assisted coil embolization of intracranial aneurysms: Incidence, complications, and angiography results. *J Neurosurg*, 105: 396–399.
<https://doi.org/10.3171/jns.2006.105.3.396>
 6. Fargen KM, Hoh BL, Welch BG, *et al.*, 2012, Long-term results of enterprise stent-assisted coiling of cerebral aneurysms. *Neurosurgery*, 71: 239–244; discussion 244.
<https://doi.org/10.1227/neu.0b013e3182571953>
 7. Chow MM, Woo HH, Masaryk TJ, *et al.*, 2004, A novel endovascular treatment of a wide-necked basilar apex aneurysm by using a Y-configuration, double-stent technique. *AJNR Am J Neuroradiol*, 25: 509–512.
 8. Horowitz M, Levy E, Sauvageau E, *et al.*, 2006, Intra/extraneurysmal stent placement for management of complex and wide-necked-bifurcation aneurysms: Eight cases using the waffle cone technique. *Neurosurgery*, 58: ONS–258–262; discussion ONS–262.
<https://doi.org/10.1227/01.neu.0000204713.24945.d2>
 9. Gresele P, 2013, Antiplatelet agents in clinical practice and their haemorrhagic risk. *Blood Transfus*, 11: 349–356.
<https://doi.org/10.2450/2013.0248-12>
 10. Cho SH, Jo WI, Jo YE, *et al.*, 2017, Bench-top comparison of physical properties of 4 commercially-available self-expanding intracranial stents. *Neurointervention*, 12: 31–39.
<https://doi.org/10.5469/neuroint.2017.12.1.31>
 11. Nakayama Y, Satow T, Funayama M, *et al.*, 2016, Construction of 3 animal experimental models in the development of honeycomb microporous covered stents for the treatment of large wide-necked cerebral aneurysms. *J Artif Organs*, 19: 179–187.
<https://doi.org/10.1007/s10047-015-0879-0>
 12. Klisch J, Sychra V, Strasilla C, *et al.*, 2011, The Woven EndoBridge cerebral aneurysm embolization device (WEB II): Initial clinical experience. *Neuroradiology*, 53: 599–607.
<https://doi.org/10.1007/s00234-011-0891-x>
 13. Goyal N, Hoit D, DiNitto J, *et al.*, 2020, How to WEB: A practical review of methodology for the use of the Woven EndoBridge. *J Neurointerv Surg*, 12: 512–520
<https://doi.org/10.1136/neurintsurg-2019-015506>
 14. Ding YH, Lewis DA, Kadirvel R, *et al.*, 2011, The Woven EndoBridge: A new aneurysm occlusion device. *AJNR Am J Neuroradiol*, 32: 607–611.
<https://doi.org/10.3174/ajnr.A2399>
 15. Goertz L, Liebig T, Siebert E, *et al.*, 2019, Extending the indication of Woven EndoBridge (WEB) embolization to internal carotid artery aneurysms: A multicenter safety and feasibility study. *World Neurosurg*, 126: e965–e974.
<https://doi.org/10.1016/j.wneu.2019.02.198>
 16. Rouchaud A, Brinjikji W, Ding YH, *et al.*, 2016, Evaluation of the angiographic grading scale in aneurysms treated with the WEB device in 80 rabbits: Correlation with histologic evaluation. *AJNR Am J Neuroradiol*, 37: 324–329.
<https://doi.org/10.3174/ajnr.A4527>
 17. Pierot L, Moret J, Turjman F, *et al.*, 2016, WEB treatment of intracranial aneurysms: Clinical and anatomic results in the french observatory. *AJNR Am J Neuroradiol*, 37: 655–659.
<https://doi.org/10.3174/ajnr.a4578>
 18. Pierot L, Costalat V, Moret J, *et al.*, 2016, Safety and efficacy of aneurysm treatment with WEB: Results of the WEBCAST study. *J Neurosurg*, 124: 1250–1256.
<https://doi.org/10.3171/2015.2.jns.142634>
 19. Pierot L, Spelle L, Molyneux A, *et al.*, 2016, Clinical and anatomical follow-up in patients with aneurysms treated with the WEB device: 1-year follow-up report in the cumulated population of 2 prospective, multicenter series (WEBCAST and French observatory). *Neurosurgery*, 78: 133–141
<https://doi.org/10.1227/neu.0000000000001106>
 20. Pierot L, Gubucz I, Buhk JH, *et al.*, 2017, Safety and efficacy of aneurysm treatment with the WEB: Results of the WEBCAST 2 study. *AJNR Am J Neuroradiol*, 38: 1151–1155.
<https://doi.org/10.3174/ajnr.a5178>
 21. Pierot L, Szikora I, Barreau X, *et al.*, 2021, Aneurysm treatment with WEB in the cumulative population of two prospective, multicenter series: 3-year follow-up. *J Neurointerv Surg*, 13: 363–368.
<https://doi.org/10.1136/neurintsurg-2020-016151>
 22. Pierot L, Szikora I, Barreau X, *et al.*, 2022, Aneurysm treatment with the Woven EndoBridge (WEB) device in the combined population of two prospective, multicenter series: 5-year follow-up. *J Neurointerv Surg*, 15: 552–557.
<https://doi.org/10.1136/neurintsurg-2021-018414>
 23. Fiorella D, Molyneux A, Coon A, *et al.*, 2017, Demographic, procedural and 30-day safety results from the WEB Intra-saccular Therapy Study (WEB-IT). *J Neurointerv Surg*, 9: 1191–1196.
<https://doi.org/10.1136/neurintsurg-2016-012841>

24. Arthur AS, Molyneux A, Coon AL, *et al.*, 2019, The safety and effectiveness of the Woven EndoBridge (WEB) system for the treatment of wide-necked bifurcation aneurysms: Final 12-month results of the pivotal WEB Intrasaccular Therapy (WEB-IT) Study. *J Neurointerv Surg*, 11: 924–930.
<https://doi.org/10.1136/neurintsurg-2019-014815>
25. Cagnazzo F, Marnat G, Ferreira I, *et al.*, 2021, Comparison of Woven EndoBridge device sizing with conventional measurements and virtual simulation using the Sim&Size software: A multicenter experience. *J Neurointerv Surg*, 13: 924–929.
<https://doi.org/10.1136/neurintsurg-2020-017060>
26. Spelle L, Herbreteau D, Caroff J, *et al.*, 2022, CLinical Assessment of WEB device in Ruptured aneurYSms (CLARYS): 12-month angiographic results of a multicenter study. *J Neurointerv Surg*, Published Online First: 1–6.
<https://doi.org/10.1136/neurintsurg-2022-018749>
27. Chalouhi N, Hoh BL, Hasan D, 2013, Review of cerebral aneurysm formation, growth, and rupture. *Stroke*, 44: 3613–3622.
<https://doi.org/10.1161/strokeaha.113.002390>
28. Linzey JR, Griauzde J, Guan Z, *et al.*, 2017, Stent-assisted coiling of cerebrovascular aneurysms: Experience at a large tertiary care center with a focus on predictors of recurrence. *J Neurointerv Surg*, 9: 1081–1085.
<https://doi.org/10.1136/neurintsurg-2016-012704>
29. Ries T, Siemonsen S, Thomalla G, *et al.*, 2007, Long-term follow-up of cerebral aneurysms after endovascular therapy prediction and outcome of retreatment. *AJNR Am J Neuroradiol*, 28: 1755–1761.
<https://doi.org/10.3174/ajnr.A0649>
30. Kabbasch C, Goertz L, Siebert E, *et al.*, 2019, WEB embolization versus stent-assisted coiling: Comparison of complication rates and angiographic outcomes. *J Neurointerv Surg*, 11: 812–816.
<https://doi.org/10.1136/neurintsurg-2018-014555>
31. Mascitelli JR, Moyle H, Oermann EK, *et al.*, 2015, An update to the Raymond-Roy Occlusion Classification of intracranial aneurysms treated with coil embolization. *J Neurointerv Surg*, 7: 496–502.
<https://doi.org/10.1136/neurintsurg-2014-011258>
32. Greve T, Sukopp M, Wostrack M, *et al.*, 2021, Initial Raymond-Roy Occlusion classification but not packing density defines risk for recurrence after aneurysm coiling. *Clin Neuroradiol*, 31: 391–399.
<https://doi.org/10.1007/s00062-020-00926-x>
33. Stapleton CJ, Torok CM, Rabinov JD, *et al.*, 2016, Validation of the Modified Raymond-Roy classification for intracranial aneurysms treated with coil embolization. *J Neurointerv Surg*, 8: 927–933.
<https://doi.org/10.1136/neurintsurg-2015-012035>
34. Darflinger R, Thompson LA, Zhang Z, *et al.*, 2016, Recurrence, retreatment, and rebleed rates of coiled aneurysms with respect to the Raymond-Roy scale: A meta-analysis. *J Neurointerv Surg*, 8: 507–511.
<https://doi.org/10.1136/neurintsurg-2015-011668>
35. Peterson C, Cord BJ, 2021, Recurrent and residual aneurysms after Woven EndoBridge (WEB) therapy: What's next? *Cureus*, 13: e14404.
<https://doi.org/10.7759/cureus.14404>
36. Zhang SM, Liu LX, Ren PW, *et al.*, 2020, Effectiveness, safety and risk factors of Woven EndoBridge device in the treatment of wide-neck intracranial aneurysms: Systematic review and meta-analysis. *World Neurosurg*, 136: e1–e23.
<https://doi.org/10.1016/j.wneu.2019.08.023>
37. Srinivasan VM, Dmytriw AA, Regenhardt RW, *et al.*, 2022, Retreatment of residual and recurrent aneurysms after embolization with the woven EndoBridge device: Multicenter case series. *Neurosurgery*, 90: 569–580.
<https://doi.org/10.1227/neu.0000000000001883>
38. Pierot L, 2021, Ten years of clinical evaluation of the woven EndoBridge: A safe and effective treatment for wide-neck bifurcation aneurysms. *Neurointervention*, 16: 211–221.
<https://doi.org/10.5469/neuroint.2021.00395>
39. McPheeters MJ, Vakharia K, Munich SA, *et al.*, 2019, Wide-necked cerebral artery aneurysms: Where do we stand? *Endovascular Today*, 18: 70–79.
40. Wallner AK, Broussalis E, Hauser T, *et al.*, 2012, Coiling after treatment with the woven EndoBridge cerebral aneurysm embolization device. A case report. *Interv Neuroradiol*, 18: 208–212.
<https://doi.org/10.1177/159101991201800214>
41. Turjman F, Massoud TF, Ji C, *et al.*, 1994, Combined stent implantation and endosaccular coil placement for treatment of experimental wide-necked aneurysms: A feasibility study in swine. *AJNR Am J Neuroradiol*, 15: 1087–1090.
42. Modi J, Eesa M, Menon BK, *et al.*, 2011, Balloon-assisted rapid intermittent sequential coiling (BRISC) technique for the treatment of complex wide-necked intracranial aneurysms. *Interv Neuroradiol*, 17: 64–69.
<https://doi.org/10.1177/159101991101700110>
43. Secondary. Available from: <https://radiopaedia.org/articles/raymondroy-occlusion-classification-of-intracranial-aneurysms-1?lang=us> [Last accessed on 2023 Feb 27].
44. Pierot L, Biondi A, Narata AP, *et al.*, 2017, Should indications for WEB aneurysm treatment be enlarged? Report of a series of 20 patients with aneurysms in “atypical” locations for WEB treatment. *J Neuroradiol*, 44: 203–209.

- <https://doi.org/10.1016/j.neurad.2016.12.011>
45. Zimmer S, Maus V, Maurer C, *et al.*, 2021, Widening the indications for intrasaccular flow disruption: WEB 17 in the treatment of aneurysm locations different from those in the good clinical practice trials. *AJNR Am J Neuroradiol*, 42: 524–529.
<https://doi.org/10.3174/ajnr.A6946>
46. Pierot L, Cognard C, Anxionnat R, *et al.*, 2012, Endovascular treatment of ruptured intracranial aneurysms: Factors affecting midterm quality anatomic results: Analysis in a prospective, multicenter series of patients (CLARITY). *AJNR Am J Neuroradiol*, 33: 1475–1480.
<https://doi.org/10.3174/ajnr.A3003>
47. Fargen KM, Velat GJ, Lawson MF, *et al.*, 2013, The stent anchor technique for distal access through a large or giant aneurysm. *J Neurointerv Surg*, 5: e24.
<https://doi.org/10.1136/neurintsurg-2012-010276>
48. Hope JK, Byrne JV, Molyneux AJ, 1999, Factors influencing successful angiographic occlusion of aneurysms treated by coil embolization. *AJNR Am J Neuroradiol*, 20: 391–399.
49. Turjman F, Massoud TF, Sayre J, *et al.*, 1998, Predictors of aneurysmal occlusion in the period immediately after endovascular treatment with detachable coils: A multivariate analysis. *AJNR Am J Neuroradiol*, 19: 1645–1651.
50. Mine B, Bonnet T, Vazquez-Suarez JC, *et al.*, 2018, Comparison of stents used for endovascular treatment of intracranial aneurysms. *Expert Rev Med Devices* 15: 793–805.
<https://doi.org/10.1080/17434440.2018.1538779>
51. Morsy A, Mahmoud M, Abokresha AE, *et al.*, 2022, Intracranial wide neck aneurysms: Clinical and angiographic outcomes of endovascular management. *Egypt J Neurol Psychiatr Neurosurg*, 58: 108.
<https://doi.org/10.1186/s41983-022-00546-x>
52. Kadirvel R, Ding YH, Dai D, *et al.*, 2014, Cellular mechanisms of aneurysm occlusion after treatment with a flow diverter. *Radiology*, 270: 394–399.
<https://doi.org/10.1148/radiol.13130796>
53. Spiotta AM, Derdeyn CP, Tateshima S, *et al.*, 2017, Results of the ANSWER trial using the PulseRider for the treatment of broad-necked, bifurcation aneurysms. *Neurosurgery*, 81: 56–65.
<https://doi.org/10.1093/neuros/nyx085>
54. Ricci DR, de Vries J, Blanc R, 2017, Role of preliminary registry data in development of a clinical trial for an innovative device: A small but integral piece of a health policy initiative. *J Mark Access Health Policy*, 5: 1283106.
<https://doi.org/10.1080/20016689.2017.1283106>
55. Fischer S, Weber A, Carolus A, *et al.*, 2017, Coiling of wide-necked carotid artery aneurysms assisted by a temporary bridging device (Comaneci): Preliminary experience. *J Neurointerv Surg*, 9: 1039–1097.
<https://doi.org/10.1136/neurintsurg-2016-012664>
56. Jia ZY, Shi HB, Miyachi S, *et al.*, 2018, Development of new endovascular devices for aneurysm treatment. *J Stroke*, 20: 46–56.
<https://doi.org/10.5853/jos.2017.02229>
57. Sirakov S, Panayotova A, Sirakov A, *et al.*, 2019, Treatment of recurrent wide neck bifurcation aneurysm with the barrel vascular reconstruction device. *Front Neurol*, 10, 1159.
<https://doi.org/10.3389/fneur.2019.01159>
58. Armoiry X, Turjman F, Hartmann DJ, *et al.*, 2016, Endovascular treatment of intracranial aneurysms with the WEB device: A systematic review of clinical outcomes. *AJNR Am J Neuroradiol*, 37: 868–872.
<https://doi.org/10.3174/ajnr.A4611>
59. Fiorella D, Arthur AS, Chiacchierini R, *et al.*, 2017, How safe and effective are existing treatments for wide-necked bifurcation aneurysms? Literature-based objective performance criteria for safety and effectiveness. *J Neurointerv Surg*, 9: 1197–1201.
<https://doi.org/10.1136/neurintsurg-2017-013223>
60. Ansari S, Zevallos CB, Farooqui M, *et al.*, 2021, Optimal Woven EndoBridge (WEB) device size selection using automated volumetric software. *Brain Sci*, 11: 901.
<https://doi.org/10.3390/brainsci11070901>
61. Rai AT, Turner RC, Brotman RG, *et al.*, 2021, Comparison of operating room variables, radiation exposure and implant costs for WEB versus stent assisted coiling for treatment of wide neck bifurcation aneurysms. *Interv Neuroradiol*, 27: 465–472.
<https://doi.org/10.1177/1591019920965392>
62. Adeeb N, Dibas M, Diestro JD, *et al.*, 2022, Multicenter study for the treatment of sidewall versus bifurcation intracranial aneurysms with use of woven EndoBridge (WEB). *Radiology*, 304: 372–382.
<https://doi.org/10.1148/radiol.212006>
63. Aguiar G, Caroff J, Mihalea C, *et al.*, 2022, WEB device for treatment of posterior communicating artery aneurysms. *J Neurointerv Surg*, 14: 362–365.
<https://doi.org/10.1136/neurintsurg-2021-017405>
64. Virtual Simulation for Woven EndoBridge Device Sizing. Available from: <https://clinicaltrials.gov/show/nct04621552> [Last accessed on 2023 Feb 27].
65. WEB French Observatory of the WEB Aneurysm Embolization System. Available from: <https://clinicaltrials.gov/show/nct01975233> [Last accessed on 2023 Feb 27].

66. WEB Clinical Assessment of IntraSaccular Aneurysm Therapy. Available from: <https://clinicaltrials.gov/show/nct01778322> [Last accessed on 2023 Feb 27].
67. CLARYS: CLinical Assessment of WEB® Device in Ruptured aneuRysms. Available from: <https://clinicaltrials.gov/show/nct02687607> [Last accessed on 2023 Feb 27].
68. CLinical EValuation of WEB 0.017 Device in Intracranial AneuRysms. Available from: <https://clinicaltrials.gov/show/nct03844334> [Last accessed on 2023 Feb 27].
69. The WEB-IT Clinical Study. Available from: <https://clinicaltrials.gov/show/nct02191618> [Last accessed on 2023 Feb 27].
70. The RISE Trial: A Randomized Trial on Intra-saccular Endobridge Devices. Available from: <https://clinicaltrials.gov/show/nct03936647> [Last accessed on 2023 Feb 27].
71. Mid-term Data Collection of the Treatment of Intracranial Aneurysms with the WEB™ Aneurysm Embolization System. Available from: <https://clinicaltrials.gov/show/nct03379714> [Last accessed on 2023 Feb 27].
72. Post Approval Study-evaluate the Long-term Safety and Effectiveness of the WEB Device. Available from: <https://clinicaltrials.gov/show/nct04839705> [Last accessed on 2023 Feb 27].
73. The WEB®-IT China Clinical Study. Available from: <https://clinicaltrials.gov/show/nct03207087> [Last accessed on 2023 Feb 27].
74. Givens JL, Tjia J, 2002, Depressed medical students' use of mental health services and barriers to use. *Acad Med*, 77: 918–921.
<https://doi.org/10.1097/00001888-200209000-00024>

REVIEW ARTICLE

The gut microbiota and associated metabolites in multiple sclerosis

Yunshu Wang¹, Zihao Li², Yun Xu², and Cun-Jin Zhang^{1,2*}¹Department of Basic Research, Medical School of Nanjing University, Nanjing, Jiangsu, China²Department of Neurology, Nanjing Drum Tower Hospital, Nanjing University, Nanjing, Jiangsu, China**Abstract**

Multiple sclerosis (MS) is a severe central nervous system autoimmune inflammatory disease featured by the presence of infiltrated immune cells, demyelination, and degeneration. Recent research has shown that gut microbiota, including some commensal bacteria, is capable of interacting with the host immune system and remarkably influencing the development and outcome of experimental autoimmune encephalomyelitis, a classic animal model of MS. In addition, gut dysbiosis, presented with a significantly altered composition of commensal bacteria, is linked to the immune response and inflammation, such as Th17 activation and B cell function. Moreover, it has been observed that microbiota impacts the immune system by regulating the metabolites in the gut. In this review, we summarize the new research on the relationship and mechanism between the gut microbiota and MS, as well as the implications for developing new strategies in MS by modulating the gut microbiota and metabolites.

***Corresponding author:**
Cun-Jin Zhang
(zhangcunjn516@163.com)

Citation: Wang Y, Li Z, Xu Y, *et al.*, 2023, The gut microbiota and associated metabolites in multiple sclerosis. *Adv Neuro*, 2(3): 413. <https://doi.org/10.36922/an.413>

Received: March 30, 2023

Accepted: July 10, 2023

Published Online: July 26, 2023

Copyright: © 2023 Author(s). This is an Open Access article distributed under the terms of the Creative Commons Attribution License, permitting distribution, and reproduction in any medium, provided the original work is properly cited.

Publisher's Note: AccScience Publishing remains neutral with regard to jurisdictional claims in published maps and institutional affiliations.

Keywords: Gut; Microbiota; Metabolites; Multiple sclerosis; Inflammation

1. Introduction

Multiple sclerosis (MS) is an inflammatory and degenerative disorder of the central nervous system (CNS) with features of demyelination, neuronal loss, permanent axonal damage, and progressive neurological dysfunction. About 2.5 million people are diagnosed with MS, and it is more common in young women than in men^[1-3]. Currently, the mechanism of MS is only partially known and still requires further investigation. The pathophysiology of MS is thought to be driven by an autoimmune reaction^[4]. A key factor in the development of MS is abnormal immune cell activation. The blood-brain barrier (BBB) can be breached by immune cells, cytokines, and inflammatory mediators, allowing for neurological injury. Activation of myelin-specific CD4⁺ T cells, in particular, is crucial in the pathogenesis and is shown in many animal models, including the experimental autoimmune encephalomyelitis (EAE) model. Targeting CNS self-antigens, Th1 and Th17 cells are thought to have a role in the etiology of MS. Interferon (IFN)- γ , which can act on microglia and trigger M1-type polarization, is mostly secreted by Th1 cells, whereas interleukin-17A (IL-17A) and IL-21 are primarily produced by Th17 cells. This may cause the astroglia to release IL-1 and IL-6, which amplify the inflammatory response associated with EAE^[5,6].

Intestinal microflora has recently emerged as an important environmental component that may provide important clues to the progression of inflammation and the development of MS. An abnormal intestinal flora was found to be differentially abundant among MS patients compared with healthy controls (HCs), though with little consistency in the bacterial taxa^[7-10]. In MS patients, the composition of the intestinal flora is aberrant, including a rise in potentially pathogenic microbes and a reduction in the number of helpful bacteria, according to metagenomic research^[11-13]. Another study on how the intestinal microbiota affects people with MS was done by Kadowaki *et al.* They discovered that the connections between the T cell C-C chemokine receptor type 9 (CCR9) and its ligand C-C chemokine ligand 25 (CCL25) were affected by the gut microbiota. The small intestine epithelium is involved in this interaction, which affects T cell growth and immunity. CCR9 function was shown to be diminished in MS patients. CD4⁺ T cells increased the expression of CCR9⁺ on T cells. The number of CCR9⁺ memory T (Tm) cells in peripheral blood was reduced as a result of blocking the CCR9-CCL25 interaction. To ascertain if the gut microbiota has an impact on CCR9⁺ Tm cells, CD4⁺ Tm cells from peripheral blood of germ-free (GF) mice conditions have been examined. In GF mice, the number of CCR9⁺ Tm cells decreased. The researchers also gave wild-type mice short-term antibiotic therapy after inducing EAE in them. Treatment with antibiotics increased the number of CCR9⁺ Tm cells and significantly reduced the severity of EAE^[14]. This finding supports the possibility that gut dysbiosis, through affecting the gut-systemic immunological axis, contributes to the genesis of MS. Furthermore, immunoglobulin A (IgA) protects the mucosal epithelium from invading pathogens, toxins, and food-derived antigens but also regulates gut microbial composition^[15]. The effectiveness of anti-B treatments and novel genetic research has highlighted the significance that B cells regulate neuroinflammation in MS^[16,17]. Plasma cells of secretory IgA (IgA⁺ PC)'s gut origins have been shown in the EAE mouse model, and they decreased inflammation of the nervous system under an IL-10-dependent way, underscoring the growing significance of mucosal immune deficiency in MS. IgA⁺ PC gut-derived intraepithelial lymphocytes suppressed neuroinflammation, prevented EAE, and decreased the number of CD4⁺ T cells that cause granulocyte-macrophage colony-stimulating factor as they moved from the gut to the periphery and subsequently to the inflamed CNS, which patients with MS have seen a comparable decrease in IgA-bound fecal bacteria following relapse^[18]. In all, emerging evidence established a critical link between the gut and MS.

2. The gut microbes in the pathogenesis and progression of MS

2.1. Preclinical evidence from the EAE model

Segmented filamentous bacteria (SFB) are important communicators for the differentiation of Th17 cells^[19]. It was demonstrated that actively generated EAE is reduced in GF mice yet is recovered through SFB gut colonization^[20]. In addition, Berer *et al.* showed that EAE-resistant GF animals spontaneously acquire EAE without any treatment with adjuvant or pertussis toxin following recolonization with native microbes or a variety of SFB utilizing a T-cell receptor (TCR) transgenic mouse model of EAE^[21]. Notably, the majority of SFB-induced Th17 cells respond to SFB antigens, emphasizing the importance of microbial antigens during the activation of effector T cells within the gut^[22]. In fact, after SFB colonization, SFB-specific CD4⁺ T cells of mesenteric lymph nodes (MLNs) are prepared to develop into Th17 cells^[23]. Through processes of bystander activation or cross-reactivity between SFB and as of yet uncharacterized CNS antigens, SFB may stimulate T lymphocytes with CNS reactivity. SFB-specific Th17 cells may either recirculate to the CNS after migrating to intestinal mucosa following priming in MLNs or might straight enter the CNS through the systemic circulation. Intriguingly, it has recently been discovered that gut nociceptor neurons, which are often linked to protective reflexes, regulate SFB levels. This suggests that their activity might obliquely govern the development of CNS-reactive Th17 cells^[24].

It is worth noting that the impacts of MS on the composition and variety of gut microbes differed in animal models. Omura *et al.* created an MS model using Theiler's murine encephalomyelitis virus (TMEV)-infected SJL/J mice and collected feces from TMEV mice on day 4 (pre-onset phase), day 7 (acute phase), and day 35 (chronic phase). According to RNA sequencing, the abundance of individual bacteria genera *Marvinbryantia* increased on days 7 and 35, while *Coprococcus* increased on day 35. However, neither the microbial biodiversity nor the overall microbiota pattern was altered^[25]. Moreover, after the EAE induction, the gut microbiota composition of EAE-resistant Albino Oxford rats was more stable, whereas the gut bacterial diversity of EAE-susceptible Dark Agouti rats was higher^[26]. Constipation-induced intestinal dysbiosis worsens EAE symptoms in C57BL/6 mice while also reducing the abundance and diversity of the intestinal microbiota^[27]. These contradictory results hint indirectly at the potential influence of mice species on gut microbes.

2.2. Clinical evidence from MS patients

2.2.1. *Akkermansia*

A mucus-degrader called *Akkermansia* converts mucin to short-chain fatty acids (SCFAs) which could influence the effects on the immune system^[15]. It has been found to have both regulatory and inflammatory activities^[28]. Alternately, pro-inflammatory pathways, such as the actuation of complement and coagulation cascades as well as the over-expression of genes related to antigen-presentation, B cell, and TCR signaling, and pro-inflammatory pathways, have been linked to *Akkermansia*^[29]. Its capacity to break down mucus, which results in the collapse of the intestinal epithelium barrier as well as a greater barring of local immune cells to microbial antigens, may be the cause of these inflammation-promoting characteristics^[30].

Gene sequencing of the gut microbes in stool samples from patients with MS showed *Acinetobacter calcoaceticus* and *Akkermansia muciniphila* had much higher levels whereas *Parabacteroides distasonis* had significantly lower levels. *A. muciniphila* promoted Th1 cell differentiation, causing pro-inflammatory responses in mononuclear cells of MS patients. When MS patient microbiota was given to GF mice, the animals had more severe EAE symptoms and fewer regulatory T cells (Tregs)^[7]. In untreated MS twins, *Akkermansia* species were also found to be increased^[31]. *Faecalibacterium* levels were found to be lower in MS patients. They also looked into variations in bacterial makeup between patients who received glatiramer acetate treatment and those who did not (*Bacteroidaceae*, *Faecalibacterium*, *Ruminococcus*, *Lactobacillaceae*, *Clostridium*, and other Clostridiales). Patients with MS, who were not given any treatment, showed a rise among the species *Akkermansia*, *Faecalibacterium*, and *Coprococcus* following vitamin D administration in comparison to the other groups^[8]. Although the detailed mechanism of vitamin D is still uncertain, some studies have reported that it binds to the vitamin D receptor and downregulates NLRP3/Caspase-1/GSDMD pyroptosis pathway, which is also activated in gut epithelial cells and associated with gut inflammation^[32-34]. A change in intestinal microbes from MS patients was observed by Jangi *et al.* Rise in *Methanobrevibacter* and *Akkermansia* with lessening in *Butyricimonas* are among the microbiome changes associated with MS, which are also connected to changes in the activation of genes related to dendritic cell (DC) maturation, IFN signaling, as well as Nuclear factor kappa B signaling pathways among circulating T cells and monocytes. When compared to those who are not receiving treatment, patients receiving disease-modified treatment had higher abundances of *Prevotella* and *Sutterella* and lower abundances of *Sarcina*^[35]. EAE was

alleviated by *Akkermansia* cultured from MS patients, and this improvement was associated with a decrease in $\gamma\delta^+$ and IL-17-producing T cells^[36].

2.2.2. *Clostridia*

There were important differences in the species abundance of 21 species noted in the gut of roughly 20 Japanese MS patients. Of the 21 species, a reduction in 19 species was noticeable in MS samples, and 14 of them belonged to Clostridia clusters XIVa and IV. It has been identified that several organisms, including *Parabacteroides* and *Prevotella* (Bacteroidetes), *Adlercreutzia* and *Collinsella* (Actinobacteria), and *Erysipelotrichaceae* (Firmicutes), were decreased in relapsing-remitting MS (RRMS) as compared to HCs^[37]. *Prevotella*, *Parabacteroides*, and *Adlercreutzia* are linked to the metabolism of phytoestrogens as well as the plant-derived xenoestrogen, whereas *Parabacteroides* and *Erysipelotrichaceae* are involved in bile acid metabolism, which also plays a critical role in Th17 inflammation and MS^[38-40]. In addition, there was a study that analyzed the gut microbes of MS patients who had yet to receive therapy in the early stages of the disease and compared them among Caucasians, Hispanics, and African Americans. Early-stage MS patients from all three ethnic groups had an elevated relative abundance of Clostridia, indicating a connection between the etiology of MS and Clostridia. Two studies identified variations in specific *Clostridium* operational taxonomic units between treated and untreated MS people, while no appreciable alterations between all MS patients and controls, raising the possibility that these drugs' antibacterial capabilities might change the microbiome^[8,35]. A strain that proportionally increased in MS, *Collinsella*, has currently been found to be related to the changes in intestinal permeability in MS patients as well as the rise of the pro-inflammatory cytokine IL-17A^[41,42].

2.2.3. *Prevotella*

Cosorich *et al.* investigated the potential relationship with changes in the intestinal microbiota of MS patients. They examined the microbes that were separated from small intestinal tissues and noticed that in comparison to HCs and MS patients without clinical symptoms, those with increased disease activity and a rise in the number of intestinal Th17 cells had an elevated Firmicutes/Bacteroidetes ratio, a larger relative abundance of *Streptococcus*, and fewer *Prevotella* strains. It showed that the relative frequency of *Prevotella* strains in the human small intestine is negatively correlated with the frequency of gut Th17 cells. It demonstrates that abnormal Th17 cell growth in the human gut and certain microbiome changes are linked to cerebral autoimmunity^[10]. Mangalam *et al.* also report that *Prevotella histicola*

can restrain EAE symptoms in HLA class-II transgenic model. *P. histicola* restrains disease by the alteration of systemic immune responses, leading to a decrease in pro-inflammatory Th1 and Th17 cells as well as a rise in the frequencies of CD4⁺FoxP3⁺ regulatory T cells, tolerogenic DC, and suppressive macrophage^[43]. These findings point to functional relationships between variations in certain gut bacteria and a change toward a pro-inflammatory T-cell profile that may amplify or sustain autoimmune responses, perhaps discovering a previously unidentified environmental factor to MS pathogenesis.

2.2.4. Other evidence

Although immunological markers (such as Th2, Th17, and Treg) did not change between cases and controls in research of 24 kids (15 in relapsing remission and 9 in controls), gut microbiota associations did. Species richness and Th17 showed a positive correlation for relapsing remission patients. Bacteroidetes had a negative correlation with Th17 in relapsing remission patients, whereas *Fusobacteria* had a positive correlation with Tregs in control patients^[13]. Another study that included 18 pediatric RRMS cases and 17 controls discovered that, in comparison to controls, MS cases had a significant depletion in *Lachnospiraceae* and *Ruminococcaceae* as well as enrichment in members of the *Desulfovibrionaceae* (*Bilophila*, *Desulfovibrio*, and *Christensenellaceae*). Microbial genes with expression higher in MS than in control are involved in glutathione metabolism, and this result remains the same regardless of the administration of immunomodulatory drugs^[9]. Additional studies have shown that a lower abundance of butyrate-producing microbes, such as *Butyricoccus desmolans* and *Odoribacter*, is linked to a higher risk of MS disease recurrence among children^[44].

3. Microbial metabolites in the pathogenesis of MS

3.1. SCFAs

With chain lengths ranging from one to six carbon atoms, SCFAs are the primary component of dietary fiber fermentation in the colon. Butyrate, acetate, and propionate are the most common. SCFA helps to keep the intestinal barrier intact, and butyrate, in particular, improves intestinal barrier function by regulating the expression of tight junction proteins^[45]. Intracellular butyrate, propionate, and acetate inhibit histone deacetylases (HDACs) activity and promote histone hyperacetylation; SCFAs appear to inhibit monocyte, macrophage, and DC maturation by suppressing HDACs, reduce pro-inflammatory cytokine production, and promote T cell differentiation into Th1 cells, Th17 cells, IL-10⁺ T cells, as well as Treg cells^[46].

Among them, butyrate increases cellular metabolism and improves the memory capacity of activated CD8⁺ T cells^[47]. It is worth noting that SCFAs can move across the BBB and there are functional SCFA receptors in the CNS^[48,49]. It is also notable that some SCFA-producing bacteria, including *A. muciniphila*, *Roseburia inulinivorans*^[50], *Butyricimonas*^[35], and *Faecalibacterium prausnitzii*^[51], have been characterized.

Acetate, propionate, and butyrate concentrations in feces and blood samples are lower in MS patients than in HCs, possibly pointing to a protective role for SCFAs in MS^[41,52-54]. Notably, compared to healthy people, secondary progressive MS patients had lower blood levels of acetate, propionate, and butyrate. The feces sample of RRMS patients likewise revealed identical findings, indicating that these changes happen independently of the disease types^[52,54]. Decreased relative abundance of recognized SCFA-producers among the MS microbes, such as *Roseburia*, *Coprococcus*, *Blautia*, *Faecalibacterium*, *Dorea*, *Butyricoccus*, and *Clostridium XIVb*, is correlated with decreases in fecal SCFAs^[41,55].

SCFAs have implications for MS disease. Serum caproic acid (CA) concentrations increased in MS patients as butyrate and acetate concentrations decreased. CA was also found to be positively associated with CD4⁺IFN- γ ⁺ T cells^[41]. Similarly, another study discovered that acetate concentration decreased in MS patients, which was associated with a negative relationship with the pro-inflammatory biomarker IFN. In addition, it decreased the count of effector T cells in the intestine and increased the release of IL-10 by regulatory B cells, which improved EAE^[56].

Current studies on propionic acid confirm that it can improve the severity of MS. With propionate supplementation, the number of peripheral Tregs and their ability to inhibit MS symptoms *ex vivo* and *in vitro* were found to increase with propionic acid in a way that was IL-10-dependent^[53]. Furthermore, Tregs treated with propionate were transferred to EAE mice to lessen the severity of the illness. Last but not least, propionate also raises the quantity of Treg in the spleen and spinal cord^[57]. According to these findings, propionate reduces CNS autoimmunity by raising the number of Treg cells throughout the body, including the CNS, where they are likely to suppress continuing inflammation.

Notably, Th17 cells treated with acetate exacerbated the EAE progression. As a result, this might tip the immune response in favor of a Th17 response^[52]. Surprisingly, elevated levels of acetate were found in the plasma of MS patients and were connected to higher numbers of CD8⁺ IL-17⁺ T cells and greater neurological impairment^[58]. It was

also discovered that MS patients have a higher proportion of butyrate and propionate levels that are compared to HCs and that both butyrate and valerate are positively correlated with pro-inflammatory cytokines^[59]. These findings may suggest a labyrinthine function of SCFAs in the regulation of CNS autoimmune inflammation.

3.2. Tryptophan

Tryptophan is a naturally occurring monoamine alkaloid with a function as an agonist of the aromatic hydrocarbon receptor and is also produced by gut microbiota metabolism. The metabolic products of tryptophan include indole-3-lactic acid (ILA), indole-3-acetic acid (IAA), and indole-3-carboxaldehyde (IAld). Furthermore, other metabolic products (kynurenine, kynurenic acid, and xanthurenic acid) act as ligands for the aryl hydrocarbon receptor (AhR) and can have immune- and neuro-modulatory impacts.

When compared to HCs, serum tryptophan concentrations were lower and kynurenine levels were higher in MS patients, indicating that tryptophan metabolism may be disturbed in this condition^[60]. Dietary tryptophan shortage exacerbated the clinical course of EAE in mice. When tryptophan was added back into the diet, it alleviated the condition in wild-type mice but not in AhR^{-/-} mice^[61]. The analysis of tryptophan derivatives now includes AhR ligands as a result of recent investigations. Elevated blood indole-3-propionic acid (IPA) and IAA concentrations in children with MS are linked to higher rates of cognitive processing and less severe illness^[62]. In addition, a lower risk of recurrence was linked to the fecal microbiota's enrichment of tryptophan catabolism-related genes. This is supported by the finding that AhR ligand levels in the blood are lower in RRMS patients compared to HCs, exception for patients with benign disease (long-standing diagnosis, but mild clinical symptoms) and those who are actively relapsing, where they might be upregulated in an anti-inflammatory feedback loop^[63].

Laquinimod, a synthetic indole-containing substance, reduced EAE by activating AhR-dependent signaling in astrocytes. Laquinimod clinical trials, however, have had conflicting outcomes^[64,65]. Laquinimod did not significantly slow the course of RRMS despite a considerable reduction in brain shrinkage (Clinical Trial NCT01707992)^[66]. When *Lactobacillus murinus* and *Lactobacillus reuteri* are administered as probiotics, fecal levels of tryptophan metabolites such as ILA, IAA, and IAld are raised and ameliorate EAE. Although this impact was not investigated with the other metabolites, it was hypothesized that ILA would have a protective role by lowering Th17 polarization and IL-17A production from myelin oligodendrocyte glycoprotein peptide (MOG)-reactive T cells^[67].

The start of EAE in mice is paradoxically prevented by a complete lack of dietary tryptophan before vaccination due to the microbiota-dependent harm to brain T cells^[64,65]. However, mice fed with a control diet started to show a reduction in EAE symptoms, whereas clinical disease worsens if dietary tryptophan is withdrawn after the onset of EAE^[65]. Another study showed that IFN- β causes the AhR expression of astrocytes, which might lead to a therapeutic IFN- β 's role in MS through increasing glial cell responsiveness to anti-inflammatory AhR ligands. In addition, the AhR ligands indoxyl 3-sulfate, IPA, and IAld all alleviated EAE via AhR signaling and restricted astrocyte production of IL-6, tumor necrosis factor (TNF)- α , CCL2, and inducible nitric oxide synthase^[68].

3.3. Phytoestrogens

Phytoestrogens are dietary substances generated from plants that share structural similarities with 17-estradiol. Given this, phytoestrogens may also affect immune function in MS^[69,70]. *Prevotella*, *Parabacteroides*, *Adlercreutzia*, *Slackia*, and *Lactobacillus*, which metabolize phytoestrogens as well as improve bioavailability, diminished among MS patients, hence demonstrating that phytoestrogen is linked to the etiology of MS^[71-73]. Recently, an eating plan that contains phytoestrogen decreased EAE disease from a manner that depended on phytoestrogen-metabolizing bacteria. In addition, it is demonstrated that mice given this diet and devoid of phytoestrogens had intestinal flora compositions that were strikingly comparable to those of MS patients. These findings imply that commensal bacterially generated food phytoestrogen metabolites may have an impact on CNS autoimmunity.

Isoflavones are phytoestrogens that are only metabolized by the human body via gut microbes. It was discovered that the number of bacteria capable of metabolizing isoflavones was low in MS patients, and further research revealed that isoflavone diet mice had an altered gut microbial composition as well as an anti-inflammatory phenotype that inhibited EAE^[37,38,74].

4. Therapeutic implications for microbiota in MS

4.1. Probiotics

Much research in recent years has focused on probiotics to restore the balance of the gut microbiota. It is thought that these live microorganisms work by altering the gut microbes to encourage intestinal barrier integrity as well as the differentiation and activation of immunoregulatory cell subsets over inflammatory cell subsets^[75,76]. Oral probiotics improved gut microbiota diversity by increasing the abundance of many species,

including *Bacteroides*, *Odoribacter*, *Lactobacillus*, *Sutterella*, and *Bifidobacterium*^[77-79]. Probiotic use also reduced the abundance of strains previously linked to MS intestinal dysbiosis such as *Akkermansia* and *Blautia*^[80]. Two commercial multi-species probiotics, Lactibianeiki and Vivomixx, induce peripheral immune tolerance in EAE mice by regulating DC number and phenotype. The Lactibianeiki group had a higher frequency of Tregs with a lower frequency of plasma cells^[78]. Furthermore, oral Vivomixx inhibited the proliferation of microglia, astrocytes, and leukocyte infiltration, while activating the proliferation of regulatory B cells (Bregs) in the CNS of TMEV mice^[77]. It is worth noting that Lactibianeiki and Vivomixx are commercial products that can be quickly translated into clinical use. In mice, a kind of probiotic, *Lactobacillus acidipiscis*, induced the generation of $\gamma\delta 1^+$ Treg cells and $CD4^+Foxp3^+$ Treg cells while inhibiting the differentiation of cerebrospinal Th1 as well as Th17 cells^[81]. Oral probiotics also can modulate immune cells, inhibit pro-inflammatory cytokine expression such as IL-1/6/17, and IFN- γ , and promote the anti-inflammatory cytokine IL-10 expression in EAE mice^[77,82,83].

Probiotic treatment has only been tested in three research addressing MS, and there are few human studies on the subject. In two small double-blinded randomized controlled trials (RCTs), the MS group receiving a combination of *Lactobacillus* and *Bifidobacterium* every day for 12 weeks displayed meaningful ameliorations among disability score, depression, anxiety, and inflammatory markers, with decreased IL-8 and TNF- α expression of peripheral blood mononuclear cells^[84,85]. Similarly, Tankou *et al.* discovered a reduction of CD80 protein production in peripheral monocytes after giving MS patients as well as HCs a probiotic combination including *Lactobacillus*, *Bifidobacterium*, and *Streptococcus* twice daily for 2 months. After taking probiotics, the documented modifications to the immune system and gut microbiota composition were not sustained^[80].

An analysis of GF mice mono-colonized with a new strain of the *Erysipelotrichaceae* family, however, revealed that *Lactobacillus reuteri* treatment increased MOG-specific responses. It was suggested that the molecular similarity between MOG and the *uvrA* gene product of *Lactobacillus reuteri* could be the mechanism causing EAE exacerbation^[86]. Following the study, it is important to take into account the synergistic impact that these microorganisms have when determining the pathogenicity of MS. Similarly, another study discovered that *Lactobacillus reuteri* aggravated EAE in mice with certain genetic predispositions^[87].

4.2. Antibiotics

In mice models, antibiotic intervention in the gut microbiota is currently yielding positive results. Researchers report that oral prophylactic antibiotics during the presymptomatic transition phase, in particular, prevented motor dysfunction in TMEV mice and reduced susceptibility to EAE; however, antibiotic treatment after an EAE episode did not reduce the severity of the illness^[88,89]. *Clostridium butyricum* and norfloxacin, as gut microbiota interventions, may alleviate EAE by inhibiting the Th17/Treg-related pathway. Treatment with *Clostridium butyricum* reduced the number of Th1 cells in the spleen^[90]. According to a recent study, oral ampicillin therapy reduced the severity of EAE. Researchers also discovered two molecules produced by *Lactobacillus reuteri* and a newly discovered strain of the *Erysipelotrichaceae* family that work together to cause the accumulation of MOG-specific Th17 cells in the small bowel^[86]. The data also support a link of the gut-microbiota-CNS axis.

There is not much research on the impact of antibiotic therapy on MS. In comparison to IFN- β -only therapy, two small studies looking at the effects of doxycycline and IFN- β in MS found lower rates of relapse, better indices of disability, and fewer gadolinium-enhancing lesions^[91,92]. Minocycline delayed the conversion of patients with clinically isolated syndrome (CIS) to MS during a 6-month but not a 24-month timeframe, according to another double-blind, randomized trial^[93]. A bigger investigation into those with CIS is continuing (Clinical Trial NCT04291456). Indeed, one study found that using ampicillin during clinical EAE worsened the disease, whereas using vancomycin had no clinical effect^[61]. There are dangers associated with continuous antibiotic treatment for MS, including the growth of fungus, opportunistic pathogens such as *Clostridium difficile*, and antibiotic-resistant infections^[94].

4.3. Diet

Diet has a significant impact on the gastrointestinal tract, and dietary treatments can help to correct intestinal microflora imbalances^[95-97]. A study in marmosets showed that a targeted dietary intervention lowers pro-inflammatory T cells that respond to recombinant human MOG and improves brain remyelination^[98]. Another study, by taking mice on intermittent fasting (IF), found that IF improved the clinical course and pathology of EAE in mice by improving intestinal dysregulation, which increased microbial abundance and enrichment, increasing ketone formation and glutathione metabolism, and enhancing antioxidant pathways, leading to less inflammation, demyelination, and axonal damage^[99].

Different diet preferences may have an impact on MS. MS relapse rates and the expanded disability status scale scores showed a decrease in the high-vegetable/low-protein diet group, and both Th17 cells and programmed cell death protein 1-expressing CD4⁺ T cells were reduced^[100]. In addition, the Mediterranean diet was found to have a favorable impact on MS in a multi-center, cross-sectional investigation^[101]. An RCT found that 15 days of a periodic calorie limitation diet was highly tolerable and showed a lower level of the proinflammatory adipokine leptin without changes in adiponectin among 16 MS patients recovering from relapsing MS as compared to an *ad libitum* diet. This study found that dietary restriction enriched *Faecalibacterium*, *Lachnospiraceae incertaesedis*, and *Blautia* populations in the gut and that adiponectin levels were positively linked with *Faecalibacterium*^[99]. The metabolic and gut microbiota alterations between mice and MS patients receiving IF showed a consistent pattern and highlighted the possibility for translation of IF. Nonetheless, there are drawbacks to the human study, including limited sample

size, brief research duration, and the impossibility of a blind clinical trial regarding the participating patients' diet allocation.

4.4. Fecal microbiota transplantation (FMT)

Many intestinal illnesses, such as *Clostridium difficile* infection^[102], ulcerative colitis^[103], and irritable bowel syndrome^[104], respond well to FMT. FMT has mostly been used in animal models in MS investigations. Transplanting the intestinal bacteria of EAE-resistant mice into EAE-susceptible or EAE-provoked mice can alleviate EAE^[105,106]. However, there is evidence of the opposite effect, where the transfer of the gut microbes from PWD mice, which is resistant to EAE, to EAE-susceptible B6 mice exasperates EAE, whereas the transfer of the gut microbes from B6 mice to PWD mice increases susceptibility to EAE; this could be due to the presence of genetic susceptibility, making the role of gut microbes less important in EAE, implying that animal models with different genetic background may interfere to some extent with the study of gut microbial facets of MS^[87].

Table 1. The change and functions of gut microbiota in multiple sclerosis

	Phylum	Class	Family	Genus/species	Functions in MS	References		
Decrease in MS	Firmicutes	Clostridia	Lachnospiraceae	<i>Blautia</i> , <i>Dorea</i> , <i>Roseburia inulinivorans</i>	Produce SCFAs	[41,50]		
			Ruminococcaceae	<i>Faecalibacterium</i>	[8,41]			
			Oscillospiraceae	<i>Faecalibacterium prausnitzii</i>	[51]			
				<i>Butyricoccus desmolans</i>	[53]			
			Clostridium XIVb	-	[41]			
			Bacilli	Lactobacillaceae	<i>Lactobacillus</i>	Metabolize phytoestrogens	[69,70,104]	
				Erysipelotrichaceae	-	Metabolize SCFAs	[38]	
			Bacteroidetes	Bacteroidia	Bacteroidales	-	Affect cellular immunity	[13]
						<i>Parabacteroides (Parabacteroides distasonis)</i>	Metabolize phytoestrogens and SCFAs	[37,40,69]
						<i>Prevotella</i>	Affect cellular immunity	[12,37]
<i>Slackia</i>	Metabolize phytoestrogens	[69,70,104]						
Actinobacteria	Coriobacteriia	Eggerthellaceae	<i>Adlercreutzia</i>	Metabolize phytoestrogens	[69,70,104]			
			<i>Odoribacter</i>	Produce SCFAs	[44]			
Increase in MS	Firmicutes	Clostridia	Streptococcaceae	-	Affect cellular immunity	[12]		
			Actinobacteria	Coriobacteriia	Coriobacteriaceae	<i>Collinsella</i>	-	[29]
	Proteobacteria	Betaproteobacteria	Sutterellaceae	<i>Sutterella</i>	-	[37]		
			Gammaproteobacteria	Moraxellaceae	<i>Acinetobacter calcoaceticus</i>	-	[7]	
			Deltaproteobacteria	Desulfovibrionaceae	-	-	[9]	
	Verrucomicrobia	Verrucomicrobiae	Akkermansiaceae	<i>Akkermansia (Akkermansia muciniphila)</i>	Affect cellular immunity	[7,36,37]		
				Produce SCFAs				

Abbreviations: MS: Multiple sclerosis, SCFAs: Short-chain fatty acids.

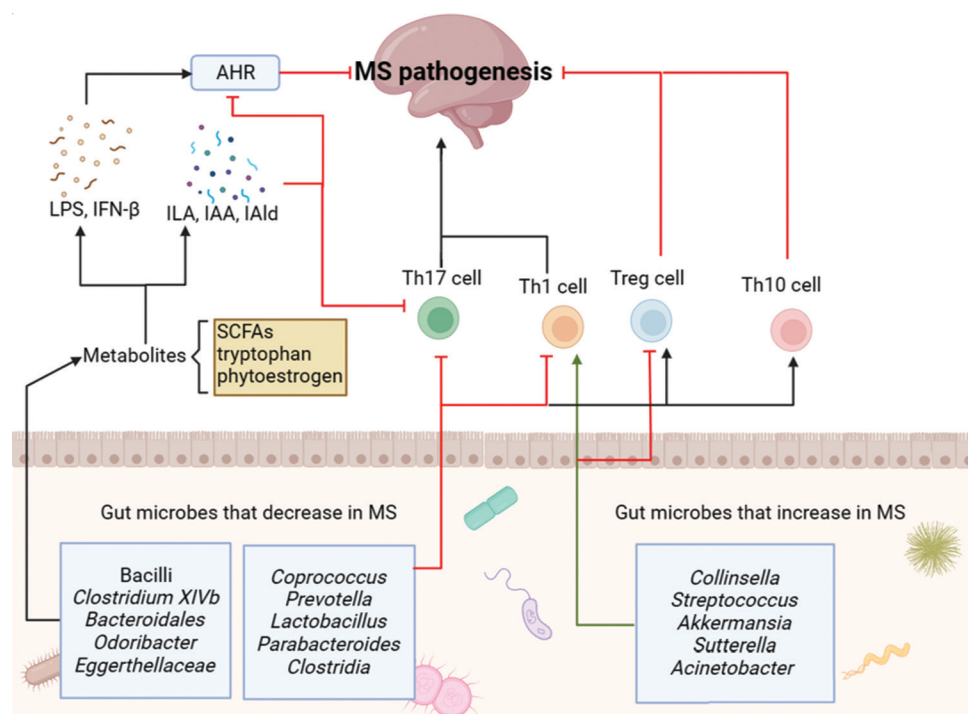


Figure 1. The role of gut microflora and associated metabolites in multiple sclerosis (MS). During the pathogenesis of MS, one of the signature changes is the intestinal flora disturbance. While the abundance of some microbes (such as *Bacilli*, *Clostridium XIVb*, *Bacteroidales*, *Odoribacter*, *Eggerthellaceae*, *Coprococcus*, *Prevotella*, *Lactobacillus*, *Parabacteroides*, and *Clostridia*) decreased in MS, some other microbes (such as *Collinsella*, *Streptococcus*, *Akkermansia*, *Sutterella*, and *Acinetobacter*) increased in MS. These changes microbes could either modulate the distinct T cell subsets directly or regulate the production of different metabolites to boost the immune system and impact the MS pathogenesis.

5. Conclusion

In summary, gut microbes play a crucial role in the progression of MS together with the exacerbation of neuroinflammation by acting as environmental factors through the gut-brain axis. Multiple microbiome species, particularly *Akkermansia* as well as *Collinsella*, are more prevalent in MS patients. The number of SCFA-producing genera, many of which are *Firmicutes* or *Bacteroidetes*, is decreasing (Table 1). To further understand the molecular connections between gut and brain functions as well as how they affect CNS autoimmunity, more study is required. An experimental idea of FMT is to transplant gut microbiota from the group in the experiment that received the active intervention. EAE improved in FMT mice when compared to those given 60 min of strength training^[107]; similar results were seen in FMT mice compared to mice given delta-9tetrahydrocannabinol (THC) and Cannabidiol (CBD) treatment (THC and CBD are drugs used to treat muscle spasms in MS patients), and the improvement in EAE may be attributed to microbiota changes in the mice through bacterial transplantation^[108]. This could reveal novel MS treatment pathways. Pomegranate peel extract is a natural compound that acts as a prebiotic and has anti-EAE properties. Intestinal flora from PPE-treated mice

was transplanted into EAE mice, which prevented illness development^[109]. These studies demonstrated that fine-tuning the gut bacteria may be an interesting approach to MS treatment.

Studies showed that MS is influenced by the changes in microbiota-derived metabolites, including SCFAs, phytoestrogens, and tryptophan derivatives. In preclinical models and clinical trials, interventions that affect the microbe, such as probiotics, antibiotics, diet, and FMT, are currently being studied. In a case study, an RRMS patient that was given FMTs from five donors daily showed raised levels of propionate, butyrate, and brain-derived neurotrophic factor as well as decreased levels of pro-inflammatory cytokines and relative abundance of *F. prausnitzii* in the weeks after the transplant. Clinical tests revealed that the patient's ability to walk and maintain balance had improved^[110]. The above studies suggest that FMT might be an emerging treatment for MS. It may complement currently available therapeutic choices for MS patients (Figure 1).

Acknowledgments

None.

Funding

This study was supported by the National Natural Science Fund for Excellent Young Scholars (82022019 to C.-J. Zhang); Nanjing special fund for Medical Science and Technology Development Projects for Distinguished Young Scholars (JQX19005 to C.-J. Zhang), National Natural Science Foundation of China (81701235 to C.-J. Zhang, 81991514 to C.-J. Zhang); The Fundamental Research Funds for the Central Universities the Key Research (021414380446 to C.-J. Zhang).

Conflict of interest

The authors declare that they have no competing interests.

Author contributions

Conceptualization: Yunshu Wang, Yun Xu, Cun-Jin Zhang
Writing – original draft: Yunshu Wang, Zihao Li, Cun-Jin Zhang
Writing – review & editing: Cun-Jin Zhang.

Ethics approval and consent to participate

Not applicable.

Consent for publication

Not applicable.

Availability of data

Not applicable.

References

- Dendrou CA, Fugger L, Friese MA, 2015, Immunopathology of multiple sclerosis. *Nat Rev Immunol*, 15: 545–558.
<https://doi.org/10.1038/nri3871>
- Fox EJ, 2004, Immunopathology of multiple sclerosis. *Neurology* 63: S3–S7.
https://doi.org/10.1212/wnl.63.12_suppl_6.s3
- Harbo HF, Gold R, Tintore M, 2013, Sex and gender issues in multiple sclerosis. *Ther Adv Neurol Disord*, 6: 237–248.
<https://doi.org/10.1177/1756285613488434>
- Sospedra M, Martin R, 2005, Immunology of multiple sclerosis. *Annu Rev Immunol*, 23: 683–747.
<https://doi.org/10.1146/annurev.immunol.23.021704.115707>
- Bar-Or A, Li R, 2021, Cellular immunology of relapsing multiple sclerosis: Interactions, checks, and balances. *Lancet Neurol*, 20: 470–483.
[https://doi.org/10.1016/S1474-4422\(21\)00063-6](https://doi.org/10.1016/S1474-4422(21)00063-6)
- Fletcher JM, Lalor SJ, Sweeney CM, *et al.*, 2010, T cells in multiple sclerosis and experimental autoimmune encephalomyelitis. *Clin Exp Immunol*, 162: 1–11.
<https://doi.org/10.1111/j.1365-2249.2010.04143.x>
- Cekanaviciute E, Yoo BB, Runia TF, *et al.*, 2017, Gut bacteria from multiple sclerosis patients modulate human T cells and exacerbate symptoms in mouse models. *Proc Natl Acad Sci U S A*, 114: 10713–10718.
<https://doi.org/10.1073/pnas.1711235114>
- Cantarel BL, Waubant E, Chehoud C, *et al.*, 2015, Gut microbiota in multiple sclerosis: Possible influence of immunomodulators. *J Investig Med*, 63: 729–734.
<https://doi.org/10.1097/JIM.0000000000000192>
- Tremlett H, Zhu F, Arnold D, *et al.*, 2021, The gut microbiota in pediatric multiple sclerosis and demyelinating syndromes. *Ann Clin Transl Neurol*, 8: 2252–2269.
<https://doi.org/10.1002/acn3.51476>
- Cosorich I, Dalla-Costa G, Sorini C, *et al.*, 2017, High frequency of intestinal T_H17 cells correlates with microbiota alterations and disease activity in multiple sclerosis. *Sci Adv*, 3: e1700492.
<https://doi.org/10.1126/sciadv.1700492>
- Miyake S, Kim S, Suda W, *et al.*, 2015, Dysbiosis in the gut microbiota of patients with multiple sclerosis, with a striking depletion of species belonging to clostridia XIVa and IV clusters. *PLoS One*, 10: e0137429.
<https://doi.org/10.1371/journal.pone.0137429>
- Zeng Q, Gong J, Liu X, *et al.*, 2019, Gut dysbiosis and lack of short chain fatty acids in a Chinese cohort of patients with multiple sclerosis. *Neurochem Int*, 129: 104468.
<https://doi.org/10.1016/j.neuint.2019.104468>
- Tremlett H, Fadrosch DW, Faruqi AA, *et al.*, 2016, Associations between the gut microbiota and host immune markers in pediatric multiple sclerosis and controls. *BMC Neurol*, 16: 182.
<https://doi.org/10.1186/s12883-016-0703-3>
- Kadowaki A, Saga R, Lin Y, *et al.*, 2019, Gut microbiota-dependent CCR9+CD4+ T cells are altered in secondary progressive multiple sclerosis. *Brain*, 142: 916–931.
<https://doi.org/10.1093/brain/awz012>
- Scher JU, Ubeda C, Artacho A, *et al.*, 2015, Decreased bacterial diversity characterizes the altered gut microbiota in patients with psoriatic arthritis, resembling dysbiosis in inflammatory bowel disease. *Arthritis Rheumatol*, 67: 128–139.
<https://doi.org/10.1002/art.38892>
- Steri M, Orrù V, Idda ML, *et al.*, 2017, Overexpression of the cytokine BAFF and autoimmunity risk. *N Engl J Med*, 376: 1615–1626.
<https://doi.org/10.1056/NEJMoa1610528>

17. Hauser SL, Waubant E, Arnold DL, *et al.*, 2008, B-cell depletion with rituximab in relapsing-remitting multiple sclerosis. *N Engl J Med*, 358: 676–688.
<https://doi.org/10.1056/NEJMoa0706383>
18. Rojas OL, Pröbstel AK, Porfilio EA, *et al.*, 2019, Recirculating intestinal iga-producing cells regulate neuroinflammation via IL-10. *Cell*, 177: 492–493.
<https://doi.org/10.1016/j.cell.2019.03.037>
19. Ivanov II, Atarashi K, Manel N, *et al.*, 2009, Induction of intestinal Th17 cells by segmented filamentous bacteria. *Cell*, 139: 485–498.
<https://doi.org/10.1016/j.cell.2009.09.033>
20. Lee YK, Menezes JS, Umesaki Y, *et al.*, 2011, Proinflammatory T-cell responses to gut microbiota promote experimental autoimmune encephalomyelitis. *Proc Natl Acad Sci U S A*, 108 Suppl 1: 4615–4622.
<https://doi.org/10.1073/pnas.1000082107>
21. Berer K, Mues M, Koutrolos M, *et al.*, 2011, Commensal microbiota and myelin autoantigen cooperate to trigger autoimmune demyelination. *Nature*, 479: 538–541.
<https://doi.org/10.1038/nature10554>
22. Yang Y, Torchinsky MB, Gobert M, *et al.*, 2014, Focused specificity of intestinal TH17 cells towards commensal bacterial antigens. *Nature*, 510: 152–156.
<https://doi.org/10.1038/nature13279>
23. Sano T, Huang W, Hall JA, *et al.*, 2015, An IL-23R/IL-22 Circuit regulates epithelial serum amyloid A to promote local effector Th17 responses. *Cell*, 163: 381–393.
<https://doi.org/10.1016/j.cell.2015.08.061>
24. Lai NY, Musser MA, Pinho-Ribeiro FA, *et al.*, 2020, Gut-innervating nociceptor neurons regulate peyer's patch microfold cells and SFB levels to mediate *Salmonella* host defense. *Cell*, 180: 33–49, e22.
<https://doi.org/10.1016/j.cell.2019.11.014>
25. Omura S, Sato F, Park AM, *et al.*, 2020, Bioinformatics analysis of gut microbiota and CNS transcriptome in virus-Induced acute myelitis and chronic Inflammatory demyelination; potential association of distinct bacteria with CNS IgA upregulation. *Front Immunol*, 11: 1138.
<https://doi.org/10.3389/fimmu.2020.01138>
26. Stanisavljević S, Lukić J, Soković S, *et al.*, 2016, Correlation of gut microbiota composition with resistance to experimental autoimmune encephalomyelitis in rats. *Front Microbiol*, 7: 2005.
<https://doi.org/10.3389/fmicb.2016.02005>
27. Lin X, Liu Y, Ma L, *et al.*, 2021, Constipation induced gut microbiota dysbiosis exacerbates experimental autoimmune encephalomyelitis in C57BL/6 mice. *J Transl Med*, 19: 317.
<https://doi.org/10.1186/s12967-021-02995-z>
28. Derrien M, Vaughan EE, Plugge CM, *et al.*, 2004, *Akkermansia muciniphila* gen. nov., sp. nov., a human intestinal mucin-degrading bacterium. *Int J Syst Evol Microbiol*, 54: 1469–1476.
<https://doi.org/10.1099/ijs.0.02873-0>
29. Derrien M, Van Baarlen P, Hooiveld G, *et al.*, 2011, Modulation of mucosal immune response, tolerance, and proliferation in mice colonized by the mucin-degrader *Akkermansia muciniphila*. *Front Microbiol*, 2: 166.
<https://doi.org/10.3389/fmicb.2011.00166>
30. Ganesh BP, Klopffleisch R, Loh G, *et al.*, 2013, Commensal *Akkermansia muciniphila* exacerbates gut inflammation in *Salmonella* Typhimurium-infected gnotobiotic mice. *PLoS One*, 8: e74963.
<https://doi.org/10.1371/journal.pone.0074963>
31. Berer K, Gerdes LA, Cekanaviciute E, *et al.*, 2017, Gut microbiota from multiple sclerosis patients enables spontaneous autoimmune encephalomyelitis in mice. *Proc Natl Acad Sci U S A*, 14: 10719–10724.
<https://doi.org/10.1073/pnas.1711233114>
32. Nunes PR, Romao-Veiga M, Matias ML, *et al.*, 2022, Vitamin D decreases expression of NLRP1 and NLRP3 inflammasomes in placental explants from women with preeclampsia cultured with hydrogen peroxide. *Hum Immunol*, 83: 74–80.
<https://doi.org/10.1016/j.humimm.2021.10.002>
33. Jiang S, Zhang H, Li X, *et al.*, 2021, Vitamin D/VDR attenuate cisplatin-induced AKI by down-regulating NLRP3/Caspase-1/GSDMD pyroptosis pathway. *J Steroid Biochem Mol Biol*, 206: 105789.
<https://doi.org/10.1016/j.jsbmb.2020.105789>
34. Donovan C, Liu G, Shen S, *et al.*, 2020, The role of the microbiome and the NLRP3 inflammasome in the gut and lung. *J Leukoc Biol*, 108: 925–935.
<https://doi.org/10.1002/JLB.3MR0720-472RR>
35. Jangi S, Gandhi R, Cox LM, *et al.*, 2016, Alterations of the human gut microbiome in multiple sclerosis. *Nat Commun*, 7: 12015.
<https://doi.org/10.1038/ncomms12015>
36. Cox LM, Maghzi AH, Liu S, *et al.*, 2021, Gut microbiome in progressive multiple sclerosis. *Ann Neurol*, 89: 1195–1211.
<https://doi.org/10.1002/ana.26084>
37. Chen J, Chia N, Kalari KR, *et al.*, 2016, Multiple sclerosis patients have a distinct gut microbiota compared to healthy controls. *Sci Rep*, 6: 28484.
<https://doi.org/10.1038/srep28484>

38. Korkina L, Kostyuk V, De Luca C, *et al.*, 2011, Plant phenylpropanoids as emerging anti-inflammatory agents. *Mini Rev Med Chem*, 11: 823–835.
<https://doi.org/10.2174/138955711796575489>
39. Schogor AL, Huws SA, Santos GT, *et al.*, 2014, Ruminant *Prevotella* spp. may play an important role in the conversion of plant lignans into human health beneficial antioxidants. *PLoS One*, 9: e87949.
<https://doi.org/10.1371/journal.pone.0087949>
40. Toh H, Oshima K, Suzuki T, *et al.*, 2013, Complete genome sequence of the equol-producing bacterium *Adlercreutzia equolifaciens* DSM 19450T. *Genome Announc*, 1.
<https://doi.org/10.1128/genomeA.00742-13>
41. Saresella M, Marventano I, Barone M, *et al.*, 2020, Alterations in circulating fatty acid are associated with gut microbiota dysbiosis and inflammation in multiple sclerosis. *Front Immunol*, 11: 1390.
<https://doi.org/10.3389/fimmu.2020.01390>
42. Barone M, Mendozzi L, D'Amico F, *et al.*, 2021, Influence of a high-impact multidimensional rehabilitation program on the gut microbiota of patients with multiple sclerosis. *Int J Mol Sci*, 22: 7173.
<https://doi.org/10.3390/ijms22137173>
43. Mangalam A, Shahi SK, Luckey D, *et al.*, 2017, Human gut-derived commensal bacteria suppress CNS inflammatory and demyelinating disease. *Cell Rep*, 20: 1269–1277.
<https://doi.org/10.1016/j.celrep.2017.07.031>
44. Horton MK, McCauley K, Fadrosch D, *et al.*, 2021, Gut microbiome is associated with multiple sclerosis activity in children. *Ann Clin Transl Neurol*, 8: 1867–1883.
<https://doi.org/10.1002/acn3.51441>
45. Peng L, Li ZR, Green RS, *et al.*, 2009, Butyrate enhances the intestinal barrier by facilitating tight junction assembly via activation of AMP-activated protein kinase in Caco-2 cell monolayers. *J Nutr*, 139: 1619–1625.
<https://doi.org/10.3945/jn.109.104638>
46. Dalile B, Van Oudenhove L, Vervliet B, *et al.*, 2019, The role of short-chain fatty acids in microbiota-gut-brain communication. *Nat Rev Gastroenterol Hepatol*, 16: 461–478.
<https://doi.org/10.1038/s41575-019-0157-3>
47. Bachem A, Makhoulouf C, Binger KJ, *et al.*, 2019, Microbiota-derived short-chain fatty acids promote the memory potential of antigen-activated CD8⁺ T Cells. *Immunity*, 51: 285–297.e5.
<https://doi.org/10.1016/j.immuni.2019.06.002>
48. Mitchell RW, On NH, Del Bigio MR, *et al.*, 2011, Fatty acid transport protein expression in human brain and potential role in fatty acid transport across human brain microvessel endothelial cells. *J Neurochem*, 117: 735–746.
<https://doi.org/10.1111/j.1471-4159.2011.07245.x>
49. Bonini JA, Anderson SM, Steiner DF, 1997, Molecular cloning and tissue expression of a novel orphan G protein-coupled receptor from rat lung. *Biochem Biophys Res Commun*, 234: 190–193.
<https://doi.org/10.1006/bbrc.1997.6591>
50. Kim CH, 2018, Immune regulation by microbiome metabolites. *Immunology*, 154: 220–229.
<https://doi.org/10.1111/imm.12930>
51. Deleu S, Machiels K, Raes J, *et al.*, 2021, Short chain fatty acids and its producing organisms: An overlooked therapy for IBD? *EBioMedicine*, 66: 103293.
<https://doi.org/10.1016/j.ebiom.2021.103293>
52. Park J, Wang Q, Wu Q, *et al.*, 2019, Bidirectional regulatory potentials of short-chain fatty acids and their G-protein-coupled receptors in autoimmune neuroinflammation. *Sci Rep*, 9: 8837.
<https://doi.org/10.1038/s41598-019-45311-y>
53. Duscha A, Gisevius B, Hirschberg S, *et al.*, 2020, Propionic acid shapes the multiple sclerosis disease course by an immunomodulatory mechanism. *Cell*, 180: 1067–1080.e16.
<https://doi.org/10.1016/j.cell.2020.02.035>
54. Takewaki D, Suda W, Sato W, *et al.*, 2020, Alterations of the gut ecological and functional microenvironment in different stages of multiple sclerosis. *Proc Natl Acad Sci U S A*, 117: 22402–22412.
<https://doi.org/10.1073/pnas.2011703117>
55. Ling Z, Cheng Y, Yan X, *et al.*, 2020, Alterations of the fecal microbiota in Chinese patients with multiple sclerosis. *Front Immunol*, 11: 590783.
<https://doi.org/10.3389/fimmu.2020.590783>
56. Luu M, Pautz S, Kohl V, *et al.*, 2019, The short-chain fatty acid pentanoate suppresses autoimmunity by modulating the metabolic-epigenetic crosstalk in lymphocytes. *Nat Commun*, 10: 760.
<https://doi.org/10.1038/s41467-019-08711-2>
57. Haase S, Mäurer J, Duscha A, *et al.*, 2021, Propionic acid rescues high-fat diet enhanced immunopathology in autoimmunity via effects on Th17 responses. *Front Immunol*, 12: 701626.
<https://doi.org/10.3389/fimmu.2021.701626>
58. Perez-Perez S, Domínguez-Mozo MI, Alonso-Gómez A, *et al.*, 2020, Acetate correlates with disability and immune response in multiple sclerosis. *PeerJ*, 8: e10220.
<https://doi.org/10.7717/peerj.10220>

59. Olsson A, Gustavsen S, Nguyen TD, *et al.*, 2021, Serum short-chain fatty acids and associations with inflammation in newly diagnosed patients with multiple sclerosis and healthy controls. *Front Immunol*, 12: 661493.
<https://doi.org/10.3389/fimmu.2021.661493>
60. Lim CK, Bilgin A, Lovejoy DB, *et al.*, 2017, Kynurenine pathway metabolomics predicts and provides mechanistic insight into multiple sclerosis progression. *Sci Rep*, 7: 41473.
<https://doi.org/10.1038/srep41473>
61. Rothhammer V, Mascanfroni ID, Bunse L, *et al.*, 2016, Type I interferons and microbial metabolites of tryptophan modulate astrocyte activity and central nervous system inflammation via the aryl hydrocarbon receptor. *Nat Med*, 22: 586–597.
<https://doi.org/10.1038/nm.4106>
62. Nourbakhsh B, Bhargava P, Tremlett H, *et al.*, 2018, Altered tryptophan metabolism is associated with pediatric multiple sclerosis risk and course. *Ann Clin Transl Neurol*, 5: 1211–1221.
<https://doi.org/10.1002/acn3.637>
63. Rothhammer V, Borucki DM, Sanchez MI, *et al.*, 2017, Dynamic regulation of serum aryl hydrocarbon receptor agonists in MS. *Neurol Neuroimmunol Neuroinflamm*, 4: e359.
<https://doi.org/10.1212/NXI.0000000000000359>
64. Kaye J, Piryatinsky V, Birnberg T, *et al.*, 2016, Laquinimod arrests experimental autoimmune encephalomyelitis by activating the aryl hydrocarbon receptor. *Proc Natl Acad Sci U S A*, 113: E6145–E6152.
<https://doi.org/10.1073/pnas.1607843113>
65. Rothhammer V, Kenison JE, Li Z, *et al.*, 2021, Aryl hydrocarbon receptor activation in astrocytes by laquinimod ameliorates autoimmune inflammation in the CNS. *Neurol Neuroimmunol Neuroinflamm*, 8: e946.
<https://doi.org/10.1212/NXI.0000000000000946>
66. Vollmer TL, Sorensen PS, Selmaj K, *et al.*, 2014, A randomized placebo-controlled phase III trial of oral laquinimod for multiple sclerosis. *J Neurol*, 261: 773–783.
<https://doi.org/10.1007/s00415-014-7264-4>
67. Wilck N, Matus MG, Kearney SM, *et al.*, 2017, Salt-responsive gut commensal modulates TH17 axis and disease. *Nature*, 551: 585–589.
<https://doi.org/10.1038/nature24628>
68. Rothhammer V, Borucki DM, Tjon EC, *et al.*, 2018, Microglial control of astrocytes in response to microbial metabolites. *Nature*, 557: 724–728.
<https://doi.org/10.1038/s41586-018-0119-x>
69. Rietjens IMC, Louisse J, Beekmann K, 2017, The potential health effects of dietary phytoestrogens. *Br J Pharmacol*, 174: 1263–1280.
<https://doi.org/10.1111/bph.13622>
70. Masilamani M, Wei J, Sampson HA, 2012, Regulation of the immune response by soybean isoflavones. *Immunol Res*, 54: 95–110.
<https://doi.org/10.1007/s12026-012-8331-5>
71. Rafii F, 2015, The role of colonic bacteria in the metabolism of the natural isoflavone daidzin to equol. *Metabolites*, 5: 56–73.
<https://doi.org/10.3390/metabo5010056>
72. Clavel T, Borrmann D, Braune A, *et al.*, 2006, Occurrence and activity of human intestinal bacteria involved in the conversion of dietary lignans. *Anaerobe*, 12: 140–147.
<https://doi.org/10.1016/j.anaerobe.2005.11.002>
73. Freedman SN, Shahi SK, Mangalam AK, 2018, The “gut feeling”: Breaking down the role of gut microbiome in multiple sclerosis. *Neurotherapeutics*, 15: 109–125.
<https://doi.org/10.1007/s13311-017-0588-x>
74. Jensen SN, Cady NM, Shahi SK, *et al.*, 2021, Isoflavone diet ameliorates experimental autoimmune encephalomyelitis through modulation of gut bacteria depleted in patients with multiple sclerosis. *Sci Adv*, 7: eabd4595.
<https://doi.org/10.1126/sciadv.abd4595>
75. Suez J, Zmora N, Segal E, *et al.*, 2019, The pros, cons, and many unknowns of probiotics. *Nat Med*, 25: 716–729.
<https://doi.org/10.1038/s41591-019-0439-x>
76. Morshedi M, Hashemi R, Moazzen S, *et al.*, 2019, Immunomodulatory and anti-inflammatory effects of probiotics in multiple sclerosis: A systematic review. *J Neuroinflammation*, 16: 231.
<https://doi.org/10.1186/s12974-019-1611-4>
77. Mestre L, Carrillo-Salinas FJ, Feliú A, *et al.*, 2020, How oral probiotics affect the severity of an experimental model of progressive multiple sclerosis? Bringing commensal bacteria into the neurodegenerative process. *Gut Microbes*, 12: 1813532.
<https://doi.org/10.1080/19490976.2020.1813532>
78. Calvo-Barreiro L, Eixarch H, Ponce-Alonso M, *et al.*, 2020, A commercial probiotic induces tolerogenic and reduces pathogenic responses in experimental autoimmune encephalomyelitis. *Cells*, 9: 906.
<https://doi.org/10.3390/cells9040906>
79. Colpitts SL, Kasper EJ, Keever A, *et al.*, 2017, A bidirectional association between the gut microbiota and CNS disease in a biphasic murine model of multiple sclerosis. *Gut Microbes*, 8: 561–573.
<https://doi.org/10.1080/19490976.2017.1353843>

80. Tankou SK, Regev K, Healy BC, *et al.*, 2018. A probiotic modulates the microbiome and immunity in multiple sclerosis. *Ann Neurol*, 83: 1147–1161.
<https://doi.org/10.1002/ana.25244>
81. Abdurasulova IN, Matsulevich AV, Tarasova EA, *et al.*, 2016, *Enterococcus faecium* strain L-3 and glatiramer acetate ameliorate experimental allergic encephalomyelitis in rats by affecting different populations of immune cells. *Benef Microbes*, 7: 719–729.
<https://doi.org/10.3920/BM2016.0018>
82. Secher T, Kassem S, Benamar M, *et al.*, 2017, Oral administration of the probiotic strain *Escherichia coli* Nissle 1917 reduces susceptibility to neuroinflammation and repairs experimental autoimmune encephalomyelitis-induced intestinal barrier dysfunction. *Front Immunol*, 8: 1096.
<https://doi.org/10.3389/fimmu.2017.01096>
83. He B, Hoang TK, Tian X, *et al.*, 2019, *Lactobacillus reuteri* reduces the severity of experimental autoimmune encephalomyelitis in mice by modulating gut microbiota. *Front Immunol*, 10: 385.
<https://doi.org/10.3389/fimmu.2019.00385>
84. Kouchaki E, Tamtaji OR, Salami M, *et al.*, 2017, Clinical and metabolic response to probiotic supplementation in patients with multiple sclerosis: A randomized, double-blind, placebo-controlled trial. *Clin Nutr*, 36: 1245–1249.
<https://doi.org/10.1016/j.clnu.2016.08.015>
85. Tamtaji OR, Kouchaki E, Salami M, *et al.*, 2017, The effects of probiotic supplementation on gene expression related to inflammation, insulin, and lipids in patients with multiple sclerosis: A randomized, double-blind, placebo-controlled trial. *J Am Coll Nutr*, 36: 660–665.
<https://doi.org/10.1080/07315724.2017.1347074>
86. Miyauchi E, Kim SW, Suda W, *et al.*, 2020, Gut microorganisms act together to exacerbate inflammation in spinal cords. *Nature*, 585: 102–106.
<https://doi.org/10.1038/s41586-020-2634-9>
87. Montgomery TL, Künstner A, Kennedy JJ, *et al.*, 2020, Interactions between host genetics and gut microbiota determine susceptibility to CNS autoimmunity. *Proc Natl Acad Sci U S A*, 117: 27516–27527.
<https://doi.org/10.1073/pnas.2002817117>
88. Mestre L, Carrillo-Salinas FJ, Mecha M, *et al.*, 2019, Manipulation of gut microbiota influences immune responses, axon preservation, and motor disability in a model of progressive multiple sclerosis. *Front Immunol*, 10: 1374.
<https://doi.org/10.3389/fimmu.2019.01374>
89. Gödel C, Kunkel B, Kashani A, *et al.*, 2020, Perturbation of gut microbiota decreases susceptibility but does not modulate ongoing autoimmune neurological disease. *J Neuroinflammation*, 17: 79.
<https://doi.org/10.1186/s12974-020-01766-9>
90. Chen H, Ma X, Liu Y, *et al.*, 2019, Gut microbiota interventions with *Clostridium butyricum* and norfloxacin modulate immune response in experimental autoimmune encephalomyelitis mice. *Front Immunol*, 10: 1662.
<https://doi.org/10.3389/fimmu.2019.01662>
91. Minagar A, Alexander JS, Schwendimann RN, *et al.*, 2008, Combination therapy with interferon beta-1a and doxycycline in multiple sclerosis: An open-label trial. *Arch Neurol*, 65: 199–204.
<https://doi.org/10.1001/archneurol.2007.41>
92. Mazdeh M, Mobaien AR, 2012, Efficacy of doxycycline as add-on to interferon beta-1a in treatment of multiple sclerosis. *Iran J Neurol*, 11: 70–73.
93. Metz LM, Eliasziw M, 2017, Trial of minocycline in clinically isolated syndrome of multiple sclerosis. *N Engl J Med*, 377: 789.
<https://doi.org/10.1056/NEJMc1708486>
94. Ross CL, Spinler JK, Savidge TC, 2016, Structural and functional changes within the gut microbiota and susceptibility to *Clostridium difficile* infection. *Anaerobe*, 41: 37–43.
<https://doi.org/10.1016/j.anaerobe.2016.05.006>
95. Zmora N, Suez J, Elinav E, 2019, You are what you eat: Diet, health and the gut microbiota. *Nat Rev Gastroenterol Hepatol*, 16: 35–56.
<https://doi.org/10.1038/s41575-018-0061-2>
96. Sonnenburg ED, Smits SA, Tikhonov M, *et al.*, 2016, Diet-induced extinctions in the gut microbiota compound over generations. *Nature*, 529: 212–215.
<https://doi.org/10.1038/nature16504>
97. Sonnenburg JL, Backhed F, 2016, Diet-microbiota interactions as moderators of human metabolism. *Nature*, 535: 56–64.
<https://doi.org/10.1038/nature18846>
98. Kap YS, Bus-Spoor C, van Driel N, *et al.*, 2018, Targeted diet modification reduces multiple sclerosis-like disease in adult marmoset monkeys from an outbred colony. *J Immunol*, 201: 3229–3243.
<https://doi.org/10.4049/jimmunol.1800822>
99. Cignarella F, Cantoni C, Ghezzi L, *et al.*, 2018, Intermittent fasting confers protection in CNS autoimmunity by altering the gut microbiota. *Cell Metab*, 27: 1222–1235.e6.
<https://doi.org/10.1016/j.cmet.2018.05.006>
100. Saresella M, Mendozzi L, Rossi V, *et al.*, 2017, Immunological and clinical effect of diet modulation of the gut microbiome in

- multiple sclerosis patients: A pilot study. *Front Immunol*, 8: 1391.
<https://doi.org/10.3389/fimmu.2017.01391>
101. Esposito S, Sparaco M, Maniscalco GT, *et al.*, 2021, Lifestyle and Mediterranean diet adherence in a cohort of Southern Italian patients with Multiple Sclerosis. *Mult Scler Relat Disord*, 47: 102636,
<https://doi.org/10.1016/j.msard.2020.102636>
102. Kao D, Roach B, Silva M, *et al.*, 2017, Effect of oral capsule-vs colonoscopy-delivered fecal microbiota transplantation on recurrent *Clostridium difficile* infection: A randomized clinical trial. *JAMA*, 318: 1985–1993.
<https://doi.org/10.1001/jama.2017.17077>
103. Cammarota G, Ianiro G, 2019, FMT for ulcerative colitis: Closer to the turning point. *Nat Rev Gastroenterol Hepatol*, 16: 266–268.
<https://doi.org/10.1038/s41575-019-0131-0>
104. El-Salhy M, Hatlebakk JG, Gilja OH, *et al.*, 2020, Efficacy of faecal microbiota transplantation for patients with irritable bowel syndrome in a randomised, double-blind, placebo-controlled study. *Gut*, 69: 859–867.
<https://doi.org/10.1136/gutjnl-2019-319630>
105. Stanisavljević S, Dinić M, Jevtić B, *et al.*, 2018, Gut microbiota confers resistance of albino Oxford rats to the induction of experimental autoimmune encephalomyelitis. *Front Immunol*, 9: 942.
<https://doi.org/10.3389/fimmu.2018.00942>
106. Chitralla KN, Guan H, Singh NP, *et al.*, 2017, CD44 deletion leading to attenuation of experimental autoimmune encephalomyelitis results from alterations in gut microbiome in mice. *Eur J Immunol*, 47: 1188–1199.
<https://doi.org/10.1002/eji.201646792>
107. Chen H, Shen L, Liu Y, *et al.*, 2021, Strength exercise confers protection in central nervous system autoimmunity by altering the gut microbiota. *Front Immunol*, 12: 628629.
<https://doi.org/10.3389/fimmu.2021.628629>
108. Al-Ghezi ZZ, Busbee PB, Alghetaa H, *et al.*, 2019, Combination of cannabinoids, delta-9-tetrahydrocannabinol (THC) and cannabidiol (CBD), mitigates experimental autoimmune encephalomyelitis (EAE) by altering the gut microbiome. *Brain Behav Immun*, 82: 25–35.
<https://doi.org/10.1016/j.bbi.2019.07.028>
109. Lu XY, Han B, Deng X, *et al.*, 2020, Pomegranate peel extract ameliorates the severity of experimental autoimmune encephalomyelitis via modulation of gut microbiota. *Gut Microbes*, 12: 1857515.
<https://doi.org/10.1080/19490976.2020.1857515>
110. Engen PA, Zaferiou A, Rasmussen H, *et al.*, 2020, Single-arm, non-randomized, time series, single-subject study of fecal microbiota transplantation in multiple sclerosis. *Front Neurol*, 11: 978.
<https://doi.org/10.3389/fneur.2020.00978>

REVIEW ARTICLE

Multiple sclerosis: Unveiling current immunogenetic factors and their role in etiopathogenesis and clinical aspects

Benediktas Trumpulis^{1*}, Rasa Liutkeviciene², and Renata Balnyte³¹Lithuanian University of Health Sciences, Medical Academy, Eiveniu 2 Street, Kaunas, Lithuania²Neuroscience Institute, Lithuanian University of Health Sciences, Medical Academy, Eiveniu Street 2, Kaunas, Lithuania³Department of Neurology, Lithuanian University of Health Sciences, Medical Academy, Eiveniu 2 Street, Kaunas, Lithuania

Abstract

Multiple sclerosis (MS) is the most common cause of neurological deficits among the young population. While the prevalence of MS is increasing worldwide, the incidence rate of MS is also undergoing a similar trend in Lithuania. Globally, women are twice as likely to be affected by MS as men. Unilateral optic neuritis is the most common initial symptom of MS. The signs and symptoms of MS vary greatly from patient to patient and depend on the location and severity of the nerve fiber damage in the central nervous system. Most people with MS have a relapsing-remitting disease course or clinically isolated syndrome. They experience periods of new symptoms or relapses that develop over days or weeks and usually resolve partially or completely. These relapses are followed by quiet periods of disease remission that may last months or even years. Data accumulated over the years suggest a complex interplay between environment and immunogenetics (strong associations with a large number of immune and genetic markers), and an increasingly convincing role of an underlying degenerative process leading to demyelination (in both white and gray matter), axonal and neurosynaptic damage, and a persistent innate inflammatory response, with T-cell-mediated autoimmunity appearing to play a diminishing role as the MS develops and progresses. In the absence of clinically proven, accurate, and reliable biomarkers, the disease can take a progressive course in case of late treatment, signifying the critical need for early diagnosis. This article therefore discusses the etiopathogenesis and clinical aspects of MS.

Keywords: Multiple sclerosis; Etiopathogenesis; Clinical aspects

***Corresponding author:**Benediktas Trumpulis
(benediktas.trumpulis@stud.lsmu.lt)**Citation:** Trumpulis B, Liutkeviciene R, Balnyte R, 2023, Multiple sclerosis: Unveiling current immunogenetic factors and their role in etiopathogenesis and clinical aspects. *Adv Neuro*, 2(3): 1319. <https://doi.org/10.36922/an.1319>**Received:** July 18, 2023**Accepted:** September 14, 2023**Published Online:** September 29, 2023**Copyright:** © 2023 Author(s). This is an Open-Access article distributed under the terms of the Creative Commons Attribution License, permitting distribution, and reproduction in any medium, provided the original work is properly cited.**Publisher's Note:** AccScience Publishing remains neutral with regard to jurisdictional claims in published maps and institutional affiliations.

1. Introduction

Multiple sclerosis (MS) is the most common cause of neurological deficits among the young population, with the prevalence increasing worldwide, particularly in Western countries^[1]. The number of people affected by MS has increased to 2.8 million in 2020. The global prevalence of MS is estimated to be 35.9/100,000 people in 2022. The number of documented cases has increased by 14.69% globally since 2013^[2]. MS has different

prevalence rates in different regions, for example, up to 140/100,000 population in North America, 108/100,000 in Europe, and around 2.2/100,000 in East Asia and sub-Saharan Africa^[3]. Worldwide, women are twice as likely as men to develop MS^[2]. An increase in the incidence rate of MS was also observed in Lithuania. According to the 2001 – 2015 data derived from the Statutory Health Insurance Information System, there had been an annual increase of MS diagnoses in the period 2001 – 2015. In 2001, 162 new MS cases were recorded, while in 2015, there were 343 new cases. The incidence rate of MS during the period 2001 – 2015 was 6.5 cases/100,000 persons. The gender-specific prevalence of MS is also consistent with some other European countries. Women were 1.5 – 2 times more likely than men to have MS in the period 2001 – 2015. In 2015, the incidence rate of MS was 8.1 and 4.9/100,000 people for women and men, respectively^[4].

Relapsing-remitting MS (RRMS) is the most common phenotype of MS and accounts for approximately 85% of all cases of MS, regardless of disease types. The remaining patients usually have a primary progressive MS (PPMS) course since disease onset. The majority (50 – 80%) of patients with RRMS tend to develop a progressive disease course (secondary progressive MS [SSMS]) 15 – 20 years after the initial onset of the disease, with about 5% of patients progressing from RRMS to SPMS per year^[5-7]. It is quite clear that both degenerative and immunogenetic processes are involved in the pathophysiology of MS. Unfortunately, the close interconnection between these two processes, which run through all phases of the disease, makes it extremely difficult for researchers to definitively resolve the “outside-in” versus “inside-out” controversy. Similarly, to other neurodegenerative diseases, the initial trigger is unknown. The mechanism of chronic MS progression remains the most significant mystery, when solved it could shed light on the prevention of irreversible disability^[8]. Delays in early diagnosis of progressive MS are quite common^[6,9,10]. It has been observed that SPMS remained undiagnosed for 2 – 3 years before a definitive diagnosis^[11]. With the help of the revised McDonald criteria of 2017, the diagnosis of PPMS has become much more systemic and easier for neurologists. These new guidelines emphasize the importance of cerebrospinal fluid (CSF)-specific oligoclonal bands and spatial spread of lesions on magnetic resonance imaging (MRI)^[12]. It is crucial to rule out other causes of disease that present as chronic myelopathy with temporal progression. This article therefore discusses the etiopathogenesis and clinical aspects of MS.

2. Methods

For this review, we searched through PubMed, ScienceDirect, and SpringerLink databases. We included

relevant animal-based meta-analyses, systematic reviews, observational studies, and randomized control trials published from 2014 to 2023. The majority of these papers described researches conducted in the populations of Europe, North America, and Asian countries. After thoroughly examining the published articles focusing on etiopathogenesis, epidemiology, genetics, current diagnostic and screening methods, and identifying applicable studies from the articles' reference lists, we collected a total of 100 articles for our review.

3. Etiology

The pathogenesis of MS relies on both genetic predisposition and environmental exposure. Nevertheless, genetic predisposition to MS is considered a rare phenomenon in the population (<7.3%), and specific combinations of non-additive genetic risk factors are required for MS pathogenesis^[13]. Moreover, genetic changes contributed to a higher percentage of T cell variation (30%) than B cell variation. This is thought to be caused by human leukocyte antigen (HLA) variations and T cell receptors^[14]. A consensus holds that MS is polygenic: Multiple independent or interactive genes and risk alleles in the population are at play in MS pathogenesis, exerting a differential effect, from low to moderate, on the development of MS^[13]. A variety of environmental risk factors are also suspected^[3]. However, Epstein-Barr virus (EBV) seroconversion precedes almost 99% of the new cases of MS and likely predates the first clinical symptoms^[15]. A recent study by Bjornevik *et al.* examined a cohort of 10 million participants and strongly implicated EBV and its association with MS. The study has shown a 32-fold risk increase (95% confidence interval [CI]: 4.3 – 245.3, $P < 0.001$) of MS development after EBV infection, but no increase after other virus infections^[16]. A prevailing theory postulates that EBV increases the risk for MS and plays a part of MS pathogenesis because of molecular mimicry. It is thought that EBV being a cross-reactive antigen (molecular mimic) and being a B-cell trophic virus providing various cytokines, as well as costimulation, are the requisite for the stimulation of T cell differentiation, which leads to the activation of pathogenic autoreactive T cell leading up to the development of MS^[17]. Other studies suggested that low levels of 25-hydroxyvitamin D (25[OH]D) may be associated with increased disease activity in people with MS. Large-scale genome-wide association studies suggested that 25(OH)D levels are partly genetically determined^[18].

HLAs are part of the major histocompatibility complex (MHC) and their association with MS was first mentioned several decades ago. The focus remains that MS is primarily an antigen-associated autoimmune disease.

Ongoing research on MHC maps identified the *HLA-DRB1* gene, specifically the *DRB1*15:01* allele, with six statistically independent effects. The function of the non-classical HLA and non-HLA genes in the MHC is also highlighted. This allele remains the most potent genetic risk factor with an average odds ratio (OR) of 3.08^[13,19,20]. The majority of risk alleles associated with MS outside the *HLA* region have been detected in intronic and intragenic regions^[20]. *HLA-DRB1*15:01* correlates with higher rates of IgG abnormalities in CSF. Optic nerve involvement, *that is*, optic neuritis (ON), was observed at increased rates in individuals with *DRB1*15:01* and also *DRB1*04:05* compared to individuals without these alleles. Individuals with *DRB1*15:01*-positive MS had statistically significant ($P = 0.036$) IgG abnormalities in the CSF and were more likely ($P = 0.044$) to have optic nerve damage than those with *DRB1*15:01*-negative MS. In addition, they tended to have higher foveal sensitivity visual function scores compared to allele-negative patients ($P = 0.060$)^[19]. Genome-wide association studies (GWAS) have identified at least 200 single nucleotide polymorphisms outside the *MHC* region, which are associated with the risk for MS development^[21,22]. An extensive genetic association study on MS found 233 significant independent MS susceptibility genomic factors, 200 of which were in the autosomal non-*MHC* genome. In the same study, microglia and various immune system cells (B, T, natural killer, and myeloid cells) were also associated with an excess of MS-linked genes. The mentioned genome-wide significant SNPs had odd ratios from 1.06 to 2.06 and the allele frequencies of the respective risk allele also varied from 2.1% to 98.4%^[20]. It has been found that these types of mutations were quite common (>2.1% risk allele frequency) and were also observed in healthy individuals^[22].

No variants were found on the male sex chromosome Y whose P -value was lower than 0.05. In contrast, analyses on the X chromosome identified rs2807267 as genome-wide significant with OR = 1.0 ($P = 6.86 \times 10^{-9}$)^[20]. These results justify the higher rates of MS in females, although the X chromosome cannot be the sole explanation for why MS occurs predominantly in females. Remarkable enrichment of MS susceptibility loci was found in various immune cell types and tissues, whereas CNS profiles showed no enrichment at the tissue level. In addition to the intensively studied T and B cells, cell types belonging to the innate immune system, namely, natural killer cells and dendritic cells, were highly enriched in MS. It is worth noting that microglia, rather than neurons and astrocytes, showed enrichment of MS-linked genes. This draws attention to the fact that local immune cells of the CNS may play a role in MS susceptibility. The study concluded that heritability of MS accounts for up to 48% of all cases, which can be

estimated by large-scale genome-wide association studies data^[20]. Therefore, there is no single predominant factor causing MS; instead, a multitude of various genetic and environmental components, as well as their complex interaction, that lead to increased risk and development of this disease should be taken into consideration.

4. Pathogenesis

In progressive MS, neuron degeneration is a predominant hallmark, whereas in RRMS, inflammation, which tends to lessen over the course of MS, is the main factor causing RRMS. Neuroaxonal damage is more prevalent in individuals with progressive MS (PMS) than in those with other phenotypes of MS^[5]. Despite the fact that the coexistence of inflammatory responses and neurodegeneration is common in the patients and they are usually manifested in all lesions at all stages of the disease, innate cells and B cells are often cited as the culprits of neurodegeneration, while a complex interplay between oxidative stress, activation of microglia, remyelination deficiency and its failure, iron toxicity, mitochondrial dysfunction, and many other processes is also suspected to support the process of neuronal injury and progression of MS^[5,10,23-25].

By releasing perforin or granzymes, T cells induce a cytotoxic effect on structures, interact with microglia, and increase inflammation and neurotoxicity^[26]. B cells are usually located in the meninges and perivascular spaces of postcapillary venules and secrete antibodies that damage the cortex. In addition, B cells also secrete cytotoxic factors that can lead to direct destruction of oligodendrocytes and neurons^[27]. Lymphoid follicles, consisting of T and B lymphocytes, plasma cells, and macrophages, are formed in the CNS of patients with PMS^[28]. Microglia and macrophages are thought to be strongly involved in the process of neurodegeneration. Increased numbers of these cells are associated with the occurrence of demyelination and axonal damage. A positron emission tomography (PET)-based study found that the activation of microglia/macrophages could predict disability of MS^[29]. Through the release of myeloperoxidase, proteases, and matrix metalloproteinases, microglia/macrophages can exert a direct cytotoxic effect^[30]. It is worth noting that microglia and macrophages play an important role in remyelination: These cells phagocytose myelin remnants and synthesize growth factors needed for successful repair of damaged neuronal sheaths, although long-term activation of these cells stimulates pro-inflammatory responses, resembling the activation of microglia in slowly expanding lesions (SELS)^[31,32]. Astrocytes also play a role in the progression of MS, exemplified by reactive astrogliosis that is common in MS plaques and causes continuous secretion of tumor

necrosis factor-alpha (TNF α), reactive oxygen species (ROS), and reactive nitrogen species (RNS). This type of astrocyte reaction is thought to be an innate immune response of the brain to various injuries^[5].

Mitochondrial dysfunction is also associated with neuronal damage in MS. Mitochondria are highly susceptible to ROS-induced oxidative damage. The inflammatory process disrupts the movement of mitochondria from the soma to the axon due to kinesin dysfunction, and it has been revealed that stimulating mitochondrial supply from the soma into axons reduced neuroaxonal damage^[33,34]. Another study called attention to changes in motor proteins responsible for the movement of mitochondria to axons and that neurons in deep cortical layers have mitochondria with mtDNA deletions^[35]. Analyses of biomarkers in CSF have shown that CSF lactate concentration is correlated with the rate of progression of MS, reinforcing mitochondrial involvement in PPMS^[36]. Iron is an important component in the process of myelin formation by oligodendrocytes; it is first stored in ferritin and then in the myelin sheath^[37]. Iron metabolism is susceptible to disruption by inflammation, resulting in the release of iron from myelin and accumulation in the immediate environment, which in turn leads to iron-induced oxidative stress. Iron accumulation is a major feature of MS and is associated with neuronal degeneration^[38]. Therefore, remyelination does not confer wide-scale protection when axon degeneration is already underway, but it supports and protects axons from further deterioration by providing supportive factors such as energy sources for the production of ATP^[39,40]. Demyelination is particularly pronounced in SEL, indicating that chronic inflammation prevents remyelination, which in turn affects axonal survival^[41]. Studies conducted with PET have shown that patients with a higher potential for dynamic remyelination tend to have lower levels of clinical disability^[42]. The rate of myelin repair varies in patients depending on the presence of oligodendrocyte progenitor cells and their ability to mature into oligodendrocytes^[43]. Remyelination-stimulating treatment may prove to be very effective, but the consensus remains that therapies need to be initiated before neurodegeneration begins^[40]. In another study, inflammation of neuronal tissue in mice and humans was found to lead to induction and toxic accumulation of the synaptic protein Bassoon (Bsn). Genetic disruption of *Bsn* and pharmacological proteasome activation has resulted in improved clearance of Bsn deposits and increased neuronal survival^[44].

Misfolding of cellular prion proteins has been cited as one of the factors contributing to neurodegeneration. In addition, citrullination and disruption of myelin

proteins in brain tissue have been observed in autopsies from MS-affected individuals^[45]. MS becomes a clinically progressive disease when the extent of lesions exceeds the neuroplasticity of the CNS and symptoms of disability begin to appear^[46]. These changes may explain why disease-modifying treatments are effective in RRMS but not in PMS, as treatment starts late, when neurodegeneration is already pervasive and CNS functional reserve has diminished. This is also confirmed by recent studies on the administration of the highly effective disease-modifying therapy, which was started in the early stages of PMS when the patients had reduced disability progression^[5,47]. At the time of writing, there are no specific guidelines or statistically significant measurements that could be used to determine progression of MS, although the search for reliable and objective measures of the progression of MS is ongoing^[48]. Early detection of SPMS has been sought through the use of algorithms and biomarkers^[11]. The expanded disability status scale (EDSS) score remains the primary measure of clinical MS. Various imaging biomarkers are being investigated to better detect and monitor the progression of MS in the clinic^[49]. At present, new T2 and/or gadolinium contrast of the lesions in conventional MRI is considered the most important marker of clinical MS relapse. Additional imaging biomarkers, such as leptomeningeal contrast enhancement, newly highlighted SELs within the white matter, and T2 lesion volume, show strong correlation with clinical and/or MRI measures of MS progression^[11]. SELs have been found to correlate with signs of acute axonal injury in the environment^[50]. SELs occur more frequently in PMS than in RRMS^[5]. It is important to note that another MRI study found that the corners of SELs contain active microglia/macrophages, which often have iron deposition. However, a more recent study using the TMEM119 marker, which is selective for microglia, showed that microglial cells predominate in SELs^[32]. Global brain atrophy, SELs, and inflammation mainly triggered by microglia/macrophages are the main pathological features of PMS^[5]. At the edges of SELs, activated microglia are involved in the failure of remyelination, which in turn leads to additional destruction of adjacent neural tissue^[51].

Offering simple and widespread accessibility as well as management and accurate diagnostic prospects, fluid-based biomarkers are at the forefront of current research, boasting a huge potential in MS diagnosis. In a review, Kaisey *et al.* described a plethora of laboratory diagnostic biomarkers^[52]. Oligoclonal bands in CSF are an important biomarker based on the McDonald diagnostic criteria but have limited utility as a marker of progression in RRMS and SPMS^[12]. Some cytoskeletal proteins, discovery of neurofilament light chains (NfL), glial fibrillary acid protein, and kappa-free light chains (κ FLC) were considered potential sensitive

diagnostic markers used in the screening for MS^[52]. NfL are important components of the axon cytoskeleton. During neuroaxonal injury, these molecules are released into the interstitial fluid, then into the CSF, and then into the serum. While other clinical parameters remain stable, NfL measurements in serum may indicate future or ongoing disease activity. NfL is regularly associated with new or enlarging T2 lesions, current inflammation, and future brain atrophy in progressive MS, and is also a promising marker of response to treatment with immunosuppressive disease-modifying therapies. It can be said that the increase in NfL concentration reflects neurodegeneration and disease activity in the years that follow^[5,53-55]. Interestingly, serum samples from asymptomatic individuals have shown that an increase in NfL concentration was observed as early as 6 years before the diagnosis of MS^[56]. EBV-infected individuals who later developed MS tended to have elevated levels of NfL after the initial infection, but before MS development^[16]. Therefore, to avoid neurodegeneration, early initiation with effective neuroprotective drugs proves beneficial in retarding the progression of PMS^[5]. Serum NfL is believed to be a plausible biomarker of neurodegeneration, and its measurement is high accurate, sensitive, and reproducible. However, standardization of sample processing and analysis is needed before it can be used as one of the PMS markers^[55,57]. κFLC offers logistical advantages, such as diagnostic speed, lower cost, and no requirement of paired serum samples, and performs similarly to CSF oligoclonal bands. Although further research concerning the influence of blood- and saliva-derived κFLC and steroid therapy on κFLC levels are needed, Kaisey *et al.* brought up in their review osteopontin (OPN), a glycoprotein which functions as an extracellular matrix protein and a cytokine^[52]. OPN is associated with immune cell migration, and recent research has found a notable increase of serum OPN in persons with MS in comparison to healthy control group^[58]. The authors deemed chitinase-3-like protein 1 as a non-specific biomarker of neurovegetative disease. Utilizing extracellular vesicles in diagnostics is a challenge because of their origins, subtypes, and content, and thus, further research is warranted to devise strategies for differentiating patients with MS from those without MS and to predict the conversion of clinically isolated syndrome (CIS) to MS^[52]. Another serum and CSF biomarker – glial fibrillary acidic protein (GFAP) – is associated with astrocyte activation. In addition, the glycoprotein chitinase 3-like 1 (CHI3L1) synthesized by astrocytes and microglia, sCD163, which is a marker for microglia and macrophages, and chemoattractant CXCL13, was detected in MS patients. NfL levels were associated with brain volume loss, while CHI3L1 levels correlated with spinal atrophy. However, the clinical utility of these biomarkers remains unconfirmed^[54,59]. It has long

been known that aging is the most important risk factor for the occurrence of neurodegenerative diseases and a likely cause of progression of MS^[60]. A recent study showed that a shorter leukocyte telomere length, which is a biological aging biomarker, was associated with more severe clinical disability and loss of brain volume in MS patients, who maintained higher EDSS and lower brain volume at baseline for more than 10 years^[61]. MRI studies have shown that the brain volume of MS patients decreases by approximately 0.5% to 1.3% per year, which is outside the physiological range^[62].

Growth-associated protein 43 (GAP-43) is highly expressed during axon growth and there is no such expression during MS progression. In this study, it was found that CSF GAP-43 levels significantly decreased during the progression of MS compared with the healthy control group ($P = 0.004$) and with RRMS individuals ($P \leq 0.001$). The concentration of GAP-43 was higher in RRMS subjects who had signs of active inflammatory disease than in subjects in remission ($P = 0.042$)^[63]. Despite the benefits in serological testing, the application of GAP-43 in routine MS clinical assessment may result in unnecessary diagnostic hold-up, excessive testing and increased costs. During the study, 150 patients had undergone 823 serologic tests, and only 40 individuals were MS-positive and thus required further testing^[64].

There is growing interest in the role of the gut microbiome and its impact on the immune system, particularly in autoimmune diseases. Recent studies have compared the gut microbiota of MS patients and healthy controls. In MS patients, a large amount of *Akkermansia muciniphila* and *Methanobrevibacter* bacteria was found. These two types of bacteria were consistent with the expression of genes affecting the adaptive immune system^[65,66]. *In vitro*, *A. muciniphila* increased Th1 lymphocyte differentiation^[67]. In addition, the prevalence of *Butyricoccus* was found to be lower in PMS patients compared to RRMS patients^[68]. Despite the abundant ongoing research on biomarkers and their importance in mechanisms of MS pathogenesis, disease progression, and severity, biomarker use in clinical practice is still limited. These novel biological markers remain a subject of research and, in our opinion, clinicians should continue testing with the most important biomarkers, such as oligoclonal bands, neurofilaments, and immunoglobulin G in CSF, in the effort to detect MS. We remain hopeful that carrying out more clinical studies with other biomarkers in the future may lead to discoveries of more biomarkers applicable in routine clinical practice for MS screening, diagnosis, prognosis, and treatment.

Figure 1 illustrates the mechanism of MS development, taking into account environment factors, infectious factors, and genetic factors.

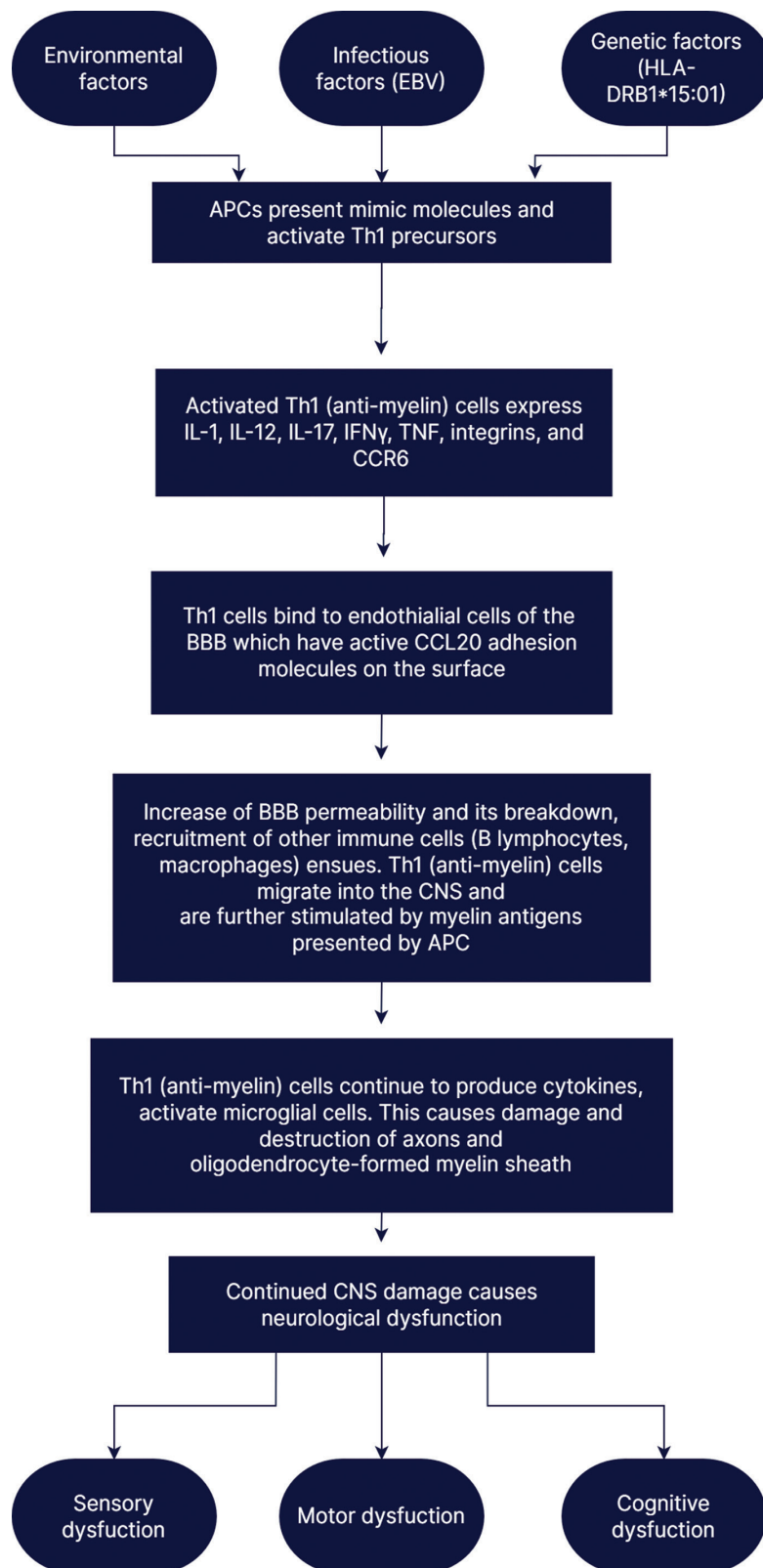


Figure 1. Proposed mechanism of multiple sclerosis development.

Abbreviations: APC: Antigen-presenting cell; BBB: Blood-brain barrier; CCL20: Chemokine (C-C motif) ligand 20; CCR6: C-C chemokine receptor type 6; CNS: Central nervous system; EBV: Epstein-Barr virus; IFN γ : Interferon-gamma; IL: Interleukin; TNF: Tumor necrosis factor.

5. Smouldering MS

Progression independent of relapse activity or smouldering MS is characterized by impairment progression while the patient is in remission with no obvious MRI lesion findings^[69]. It is suggested that the “real MS” originates from a primary smouldering process that coexists with inflammation^[70]. Whether MS is an autoimmune disease or a CNS-intrinsic disease remains contentious in the scientific literature. The autoimmune hypothesis of MS, also called outside-in, is supported by the fact that immunosuppressive therapies, such as alemtuzumab, hematopoietic stem cell transplantation, or natalizumab, are effective in the treatment process. However, in RRMS, effective suppression of the immune system does not always prevent disability in the long-term^[69].

It is suggested that MS is an inside-out disease in which focal inflammatory activity is a concomitant feature of primary CNS neurodegeneration. Some possible pathogenetic components of smouldering MS include acute axonal and synaptic loss, demyelination, CNS microglia/macrophage activation, chronic oxidative stress, iron accumulation, mitochondrial damage and dysfunction, and infection^[70].

There is a strong contrast between clinical, MRI, and pathologic studies. Clinical and MRI data have classified MS as a biphasic disease, dominated by inflammation at baseline and preceded by non-inflammatory neurodegeneration. In contrast, pathologic findings show continuous inflammation and demyelination even in the later or terminal stages of MS^[25,71]. Since therapies for

acute inflammation do not further halt the development of progressive volume loss of the brain and spinal cord, it has been proposed that smouldering MS plays a role in the process of CNS volume loss^[70-73].

Table 1 shows the clinical characteristics of different subtypes of multiple sclerosis.

The typical manifestation of RRMS is ON, which is present in 25% of patients. The analysis of clinical, imaging, and genetic data suggested that PPMS and SPMS share a high level of similarities^[6]. The risk of conversion from ON to MS is explained by laboratory, clinical, and radiological findings. Lesions suggestive of demyelination on MRI examinations are the most compelling factors indicating the conversion to MS^[74,75]. A study on the Turkish patients who had undergone the first seizure ON found that unilateral ON was present in 67.3% of patients (104 total), positive CSF in 62.5%, and Vitamin D deficiency in 65.2%. The ON in 83 patients (79.9%) converted to MS, and it took an average of 2.74 years for the second relapse to occur^[74]. In the Iranian population, the ON in only 42.2% of patients converted to MS. The study also found that women were more likely to become converters (OR = 3.4, CI = 1.83 – 6.32, $P \leq 0.001$). Brain lesions were also found in 63.2% of patients with original ON, and white matter lesions were the most significant factor determining the higher risk of conversion to MS (OR = 5.15 CI = 2.64 – 10.07, $P < 0.001$)^[75]. In the MSBase cohort study of demographics, conversion to MS was observed in 741 (66.2%) of 1119 patients with CIS. Time taken for conversion to MS was longer in treated compared with non-treated subjects:

Table 1. Clinical characteristics of multiple sclerosis subtypes

	Relapsing-remitting	Secondary progressive	Primary progressive
Mean age	20–40 years	10–15 years after initial disease onset	≥40 years
Female to male ratio	3:1	3:1	1:1
Manifestations	Optic neuritis, acute partial transverse myelitis, brainstem syndromes	Progressive myelopathy, brainstem or cerebellar syndrome	Progressive myelopathy, brainstem or cerebellar syndrome
Frequency of manifestations at the beginning	85%	Not applicable	10 – 15%
Course	Episodes of acute worsening of neurologic functioning with total or partial recovery	Gradual neurologic deterioration following a relapsing course with or without relapses	Steady functional decline from disease onset without relapses or remission
Conventional brain MRI	Lesion load burden is higher compared with primary progressive MS: Active lesions are common, cortical lesions are less common	Rare active lesions: subpial demyelination and cortical atrophy are more common	Lesion load burden is lower compared with relapsing MS: Rare active lesions, subpial demyelination and cortical atrophy are more common
Conventional spinal cord MRI	Lower lesion load	Higher lesion load	Higher lesion load

Adapted from Amezcua^[6].

Abbreviation: MRI: Magnetic resonance imaging

Median survival 1.0 year (interquartile range [IQR] = 0.7 – 2.3, range = 0.3 – 6.2) and 0.6 years (IQR = 0.4 – 1.1, range = 0.3 – 7.5) ($P < 0.001$). The findings of the study are congruent with the age and the presence of brain MRI lesions at baseline being the high-risk predictors of conversion to MS^[76].

After examining electronic medical records of military patients, researchers found that the prevalence of ON was 8.1/100,000 between 2006 and 2018, and the incidence rates were about 3 times higher in women than in men, which also increased with age^[77]. It has been shown that sex hormones, such as estrogen, progesterone, prolactin, and androgen, and their function in immune system have a bearing on the unbalanced development of MS among male and female individuals. It is thought that the use of oral contraceptives, smoking and dietary habits, and tendency for Western women to have fewer children and also at older maternal age may influence this inequality^[78]. There were 136 cases registered after ON eventually converted to MS. In women, the MS probability of conversion was 12% at 6 months, 18% at 5 years, and 19% at 10 years; in men, it was 8%, 12%, and 14% at 6 months, 5 years, and 10 years, respectively^[77]. In Korea, a retrospective study utilizing data from 2010 to 2016 was conducted^[79]. There were 531 diagnosed pediatric ON cases and 7183 adult ON cases^[79]. A total of 111 patients presenting with ON as the first symptom converted to MS. The cumulative conversion rate to MS was estimated to be 10.6% in the overall population. MS conversion rate in the pediatric cohort was 13.8% and 11.4% in the adult population^[79].

Optical coherence tomography was used to quantitatively assess the different retinal layers. The results of the study showed that the thickness of the ganglion cell layer and the inner plexiform layer (GCIPL) as well as the peripapillary retinal nerve fiber layer and the inferonasal sector of the GCIPL of the contralateral eye predicted the development of MS with statistical significance (hazard ratio [HR] = 0.922, 95% CI = 0.861 – 0.988, $P = 0.021$; HR = 0.939, 95% CI = 0.891 – 0.989, $P = 0.0179$; HR = 0.924, 95% CI = 0.867 – 0.986, $P = 0.0172$)^[80]. Changes in diagnostic criteria may provide an answer to why milder courses of MS are becoming more common. Recently, a new radiological biomarker for inflammatory demyelination in radiologically isolated syndrome has been proposed – an MRI-detectable central vein within white matter lesions^[81,82]. According to the most recent MS diagnostic guidelines, the McDonalds criteria (2017), CIS can be designated as MS if it meets the MRI criteria for spatial (DIS) and temporal spread (DIT) or DIS is presented with oligoclonal bands in the CSF^[12]. This indicates that more individuals with a lower disease

activity profile could be diagnosed with MS, increasing the sensitivity and prevalence of MS^[83]. The application of the 2017 McDonalds criteria increased the frequency of MS diagnoses by an additional 41.7% of patients and categorized 87.7% of patients previously diagnosed with CIS as fulfilling the new criteria for RRMS, increasing the total RRMS cases to 94.1%, with the rest (5.8%) being CIS patients^[84]. The increase in survival rates of MS (excess mortality decreased from 11.29% to 2.56%) has led to a shift in prevalence toward the elderly population^[85].

Because of the inclusion of CIS in RRMS, a decrease in relapse rates and fewer persistent symptoms have been noted. Notably, an increase in milder disease progression could be attributed to declining tobacco use in Western Europe and North America^[12,86]. Despite the fact that current MS diagnostic criteria revisions and available diagnostic tools should allow for earlier MS identification, delays seem inevitable. Solomon *et al.* conducted a worldwide study to identify the causes of “major barriers” to early MS diagnosis^[87]. A total of 107 countries participated in this study and completed the Atlas questionnaire based on MS diagnosis. The 2017 McDonald criteria were the most commonly used criteria for MS diagnosis (84 [79%] countries). Higher-income countries tended to use the 2017 McDonald criteria more often than lower-income countries (66 [90%] vs. 18 [58%], $P < 0.001$). The majority of countries (83%) showed at least 1 major barrier to early MS diagnosis. The most prevalent causes for the delays of MS diagnosis were “lack of awareness of MS symptoms among general public” (68%), “lack of awareness of MS symptoms among health-care professionals” (59%), and “lack of availability of health-care professionals with knowledge to diagnose MS” (44%)^[87].

6. Association of MS with optic neuritis

At MS, ON presents as the initial manifestation of the disease in 20% of those affected, and about half of those patients with MS develop ON later in life^[88]. Studies have recorded very low rates of bilateral optic nerve involvement in MS (in 427 patients with MS, bilateral ON was diagnosed only in 2 patients [0.42%])^[89]. It has been hypothesized that obesity may play a role in the development and progression of MS, as well as the treatment response. Several adipocytokines have been suggested, including resistin, leptin, and adiponectin. These molecules are mediators in the proliferation of T cells and the production of pro-inflammatory cytokines, such as interleukin (IL)-1, IL-6, IL-12, and TNF α , and finally the activation of monocytes and macrophages. The increase in adipocytokines, with the exception of adiponectin, has been noted in patients with MS,

suggesting their involvement in the progression of MS^[90]. Numerous studies have shown that individuals who develop ON as the first clinical symptom of MS have a lower degree of disability, whereas MS first appears in other neurological structures. Serum adiponectin, leptin, and resistin concentration were remarkably lower in patients with ON as the first symptom compared to ON negative as first symptom (adiponectin $P = 0.004$, leptin $P = 0.013$, resistin $P = 0.006$). Curiously, healthy control subjects and patients with ON as their first clinical episode had similar adiponectin, leptin, and resistin levels^[90].

Research was conducted to evaluate the changes in brain structural volume. In MS active individuals, the loss of ganglion cell volume and inner plexiform layer as well as total brain mass was two times greater and five times faster in thalamic regions than in MS-stable patients during the first 2 years after the onset of MS, although these strong contrasts decreased 5 years after the onset of MS^[91]. With the aid of optical coherence tomography, retinal damage was found in association with neuroinflammation, particularly in acute ON, and similar changes have been observed in patients with MS. Under the premise of the association of retinal atrophy with brain atrophy, researchers used MS model to study acute and chronic *in vivo* molecules in the retina during acute and chronic ON by employing the Raman spectroscope. Ten different molecules that correlate with cellular energy and axon biology were selected. It was found that age was the major determinant of the concentration changes of some molecules. The most striking alteration was the change in metabolites related to mitochondria and energy supply (NADH and FAD)^[92].

One study examined the relationship between visual evoked potentials and thiol-disulfide homeostasis, a measure of redox imbalance. The study provided evidence that during an episode of ON in MS, there was a delay in nerve signal transmission from the retina to the visual cortices, known as P100 wave latency, while the thiol-disulfide balance shifted in favor of disulfides^[93].

Since MS is mainly triggered by autoimmune reactions against the CNS, CSF examination should be the priority in the search for biomarkers. A study has shown that the epitopes of A and B likely mimic the high-affinity antigenic epitopes of cytomegalovirus and EBV, corroborating these epitopes as potent candidates for serological biomarkers^[94]. The high-antigenic epitopes of glycoprotein B cytomegalovirus and VCA p18 EBV suggest their role in the pathogenesis of MS, although how the humoral response of the immune system against

these epitopes is related to CNS antigens remains an open question^[94].

Studies are still underway to better understand how inflammatory demyelination processes in the optic nerve leads to loss of retinal ganglion cells in the retinal layer of the eye. Research on the early molecules of the complement pathway, C1q and C3, has led to the hypothesis that deviation in complement expression by astroglia leads to neurotoxicity^[95]. In addition, recent studies have shown that C3 is primarily expressed in neurotoxic astrocytes^[96,97]. Immunohistochemical staining has identified a neurotoxic subtype of optic nerve astrocytes that express greater amounts of complement component 3 (C3)^[98]. Early complement pathway molecules such as C1q and C3 may have the ability to mediate neurodegenerative processes in MS^[21]. Yes-associated protein (YAP) has been implicated in the mechanism of neuroinflammation and may upregulate the expression of transforming growth factor beta (TGF β) to prevent inflammatory responses, demyelination, and retinal ganglion cell death in ON^[99]. Based on research and also clinical practice, not only the pathogenesis of ON, but also the clinical features are linked with MS. Therefore, further investigation may lead to the discovery of markers for detecting early-stage demyelination, which is instrumental for predicting disease development and if necessary, initiating early treatment.

7. Conclusions

In Western countries, MS is the leading cause of neurological disability and typically occurs more frequently in women than in men. The etiopathogenesis of MS is a complex and multistage process encompassing inflammation, demyelination, and neurodegeneration, in which genetic and environmental factors are at play. The smouldering MS hypothesis may help explain disease progression during the remission phase. Early diagnosis of the disease could be realized using biological markers for disease detection, but the search for specific and accurate diagnostic markers is currently in progress. Optic neuritis is an important manifestation of MS, which is part of the criteria for early diagnosis of demyelinating disease. In conclusion, establishing a more comprehensive set of diagnostic criteria for MS is a prerequisite for earlier detection and diagnosis of MS, which is crucial for earlier prescription of treatments to improve the patient's condition and halt disease progression.

Acknowledgments

None.

Funding

None.

Conflict of interest

The authors declare that they have no competing interests.

Author contributions

Conceptualization: All authors

Writing – original draft: Benediktas Trumpulis

Writing – review & editing: Rasa Liutkeviciene, Renata Balnyte

Ethics approval and consent to participate

Not applicable.

Consent for publication

Not applicable.

Availability of data

Not applicable.

References

- Wallin MT, Culpepper WJ, Nichols E, *et al.*, 2019, Global, regional, and national burden of multiple sclerosis 1990–2016: A systematic analysis for the Global Burden of Disease Study 2016. *Lancet Neurol*, 18: 269–285.
[https://doi.org/10.1016/S1474-4422\(18\)30443-5](https://doi.org/10.1016/S1474-4422(18)30443-5)
- Walton C, King R, Rechtman L, *et al.*, 2020, Rising prevalence of multiple sclerosis worldwide: Insights from the Atlas of MS, third edition. *Mult Scler*, 26: 1816–1821.
<https://doi.org/10.1177/1352458520970841>
- Leray E, Moreau T, Fromont A, *et al.*, 2016, Epidemiology of multiple sclerosis. *Rev Neurol (Paris)*, 172: 3–13.
<https://doi.org/10.1016/j.neurol.2015.10.006>
- Valadkeviciene D, Kavaliunas A, Kizlaitiene R, *et al.*, 2019, Incidence rate and sex ratio in multiple sclerosis in Lithuania. *Brain Behav*, 9: e01150.
<https://doi.org/10.1002/brb3.1150>
- Yong HYE, Yong VW, 2022, Mechanism-based criteria to improve therapeutic outcomes in progressive multiple sclerosis. *Nat Rev Neurol*, 18: 40–55.
<https://doi.org/10.1038/s41582-021-00581-x>
- Amezcuca L, 2022, Progressive multiple sclerosis. *Continuum (Minneapolis)*, 28: 1083–1103.
<https://doi.org/10.1212/CON.0000000000001157>
- Reich DS, Lucchinetti CF, Calabresi PA, 2018, Multiple sclerosis. *N Engl J Med*, 378: 169–180.
<https://doi.org/10.1056/NEJMra1401483>
- Stys PK, Tsutsui S, 2019, Recent advances in understanding multiple sclerosis. *F1000Res*, 8: 2100.
<https://doi.org/10.12688/f1000research.20906.1>
- Sellebjerg F, Börnsen L, Ammitzbøll C, *et al.*, 2017, Defining active progressive multiple sclerosis. *Mult Scler*, 23: 1727–1735.
<https://doi.org/10.1177/1352458517726592>
- Pozzilli C, Pugliatti M, Vermersch P, *et al.*, 2023, Diagnosis and treatment of progressive multiple sclerosis: A position paper. *Eur J Neurol*, 30: 9–21.
<https://doi.org/10.1111/ene.15593>
- Ziemssen T, Bhan V, Chataway J, *et al.*, 2023, Secondary progressive multiple sclerosis: A review of clinical characteristics, definition, prognostic tools, and disease-modifying therapies. *Neurol Neuroimmunol Neuroinflamm*, 10: e200064.
<https://doi.org/10.1212/NXI.0000000000200064>
- Thompson AJ, Banwell BL, Barkhof F, *et al.*, 2018, Diagnosis of multiple sclerosis: 2017 revisions of the McDonald criteria. *Lancet Neurol*, 17: 162–173.
[https://doi.org/10.1016/S1474-4422\(17\)30470-2](https://doi.org/10.1016/S1474-4422(17)30470-2)
- Goodin DS, Khankhanian P, Gourraud PA, *et al.*, 2021, The nature of genetic and environmental susceptibility to multiple sclerosis. *PLoS One*, 16: e0246157.
<https://doi.org/10.1371/journal.pone.0246157>
- Gerdes LA, Janoschka C, Eveslage M, *et al.*, 2020, Immune signatures of prodromal multiple sclerosis in monozygotic twins. *Proc Natl Acad Sci U S A*, 117: 21546–21556.
<https://doi.org/10.1073/pnas.200339117>
- Ortega-Hernandez OD, Martínez-Cáceres EM, Presas-Rodríguez S, *et al.*, 2023, Epstein-barr virus and multiple sclerosis: A convoluted interaction and the opportunity to unravel predictive biomarkers. *Int J Mol Sci*, 24: 7407.
<https://doi.org/10.3390/ijms24087407>
- Bjornevik K, Cortese M, Healy BC, *et al.*, 2022, Longitudinal analysis reveals high prevalence of Epstein-Barr virus associated with multiple sclerosis. *Science*, 375: 296–301.
<https://doi.org/10.1126/science.abj8222>
- Kuchroo VK, Weiner HL, 2022, How does Epstein-Barr virus trigger MS? *Immunity*, 55: 390–392.
<https://doi.org/10.1016/j.immuni.2022.02.008>
- Vasileiou ES, Hu C, Bernstein CN, *et al.*, 2022, Association of Vitamin D polygenic risk scores and disease outcome in people with multiple sclerosis. *Neurol Neuroimmunol Neuroinflamm*, 10: e20006.
<https://doi.org/10.1212/NXI.0000000000200062>

19. Watanabe M, Nakamura Y, Sato S, *et al.*, 2021, HLA genotype-clinical phenotype correlations in multiple sclerosis and neuromyelitis optica spectrum disorders based on Japan MS/NMOSD Biobank data. *Sci Rep*, 11: 607.
<https://doi.org/10.1038/s41598-020-79833-7>
20. International Multiple Sclerosis Genetics Consortium, 2019, Multiple sclerosis genomic map implicates peripheral immune cells and microglia in susceptibility. *Science*, 365: eaav7188.
<https://doi.org/10.1126/science.aav7188>
21. Fitzgerald KC, Kim K, Smith MD, *et al.*, 2019, Early complement genes are associated with visual system degeneration in multiple sclerosis. *Brain*, 142: 2722–2736.
<https://doi.org/10.1093/brain/awz188>
22. Gresle MM, Jordan MA, Stankovich J, *et al.*, 2020, Multiple sclerosis risk variants regulate gene expression in innate and adaptive immune cells. *Life Sci Alliance*, 3: e202000650.
<https://doi.org/10.26508/lsa.202000650>
23. Baecher-Allan C, Kaskow BJ, Weiner HL, 2018, Multiple sclerosis: Mechanisms and immunotherapy. *Neuron*, 97: 742–768.
<https://doi.org/10.1016/j.neuron.2018.01.021>
24. Heidker RM, Emerson MR, LeVine SM, 2017, Metabolic pathways as possible therapeutic targets for progressive multiple sclerosis. *Neural Regen Res*, 12: 1262–1267.
<https://doi.org/10.4103/1673-5374.213542>
25. Lassmann H, 2018, Pathogenic mechanisms associated with different clinical courses of multiple sclerosis. *Front Immunol*, 9: 3116.
<https://doi.org/10.3389/fimmu.2018.03116>
26. Dong Y, Yong VW, 2019, When encephalitogenic T cells collaborate with microglia in multiple sclerosis. *Nat Rev Neurol*, 15: 704–717.
<https://doi.org/10.1038/s41582-019-0253-6>
27. Lisak RP, Nedelkoska L, Benjamins JA, *et al.*, 2017, B cells from patients with multiple sclerosis induce cell death via apoptosis in neurons *in vitro*. *J Neuroimmunol*, 309: 88–99.
<https://doi.org/10.1016/j.jneuroim.2017.05.004>
28. Mahad DH, Trapp BD, Lassmann H, 2015, Pathological mechanisms in progressive multiple sclerosis. *Lancet Neurol*, 14: 183–193.
[https://doi.org/10.1016/S1474-4422\(14\)70256-X](https://doi.org/10.1016/S1474-4422(14)70256-X)
29. Sucksdorff M, Matilainen M, Tuisku J, *et al.*, 2020, Brain TSPO-PET predicts later disease progression independent of relapses in multiple sclerosis. *Brain*, 143: 3318–3330.
<https://doi.org/10.1093/brain/awaa275>
30. Calabrese M, Magliozzi R, Ciccarelli O, *et al.*, 2015, Exploring the origins of grey matter damage in multiple sclerosis. *Nat Rev Neurosci*, 16: 147–158.
<https://doi.org/10.1038/nrn3900>
31. Berghoff SA, Spieth L, Sun T, *et al.*, 2021, Microglia facilitate repair of demyelinated lesions via post-squalene sterol synthesis. *Nat Neurosci*, 24: 47–60.
<https://doi.org/10.1038/s41593-020-00757-6>
32. Jäckle K, Zeis T, Schaeren-Wiemers N, *et al.*, 2020, Molecular signature of slowly expanding lesions in progressive multiple sclerosis. *Brain*, 143: 2073–2088.
<https://doi.org/10.1093/brain/awaa158>
33. Campbell G, Mahad DJ, 2018, Mitochondrial dysfunction and axon degeneration in progressive multiple sclerosis. *FEBS Lett*, 592: 1113–1121.
<https://doi.org/10.1002/1873-3468.13013>
34. Licht-Mayer S, Campbell GR, Canizares M, *et al.*, 2020, Enhanced axonal response of mitochondria to demyelination offers neuroprotection: Implications for multiple sclerosis. *Acta Neuropathol*, 140: 143–167.
<https://doi.org/10.1007/s00401-020-02179-x>
35. Campbell GR, Worrall JT, Mahad DJ, 2014, The central role of mitochondria in axonal degeneration in multiple sclerosis. *Mult Scler*, 20: 1806–1813.
<https://doi.org/10.1177/1352458514544537>
36. Abdelhak A, Hottenrott T, Mayer C, *et al.*, 2017, CSF profile in primary progressive multiple sclerosis: Re-exploring the basics. *PLoS One*, 12: e0182647.
<https://doi.org/10.1371/journal.pone.0182647>
37. Lee NJ, Ha SK, Sati P, *et al.*, 2019, Potential role of iron in repair of inflammatory demyelinating lesions. *J Clin Invest*, 129: 4365–4376.
<https://doi.org/10.1172/JCI126809>
38. Raz E, Branson B, Jensen JH, *et al.*, 2015, Relationship between iron accumulation and white matter injury in multiple sclerosis: A case-control study. *J Neurol*, 262: 402–409.
<https://doi.org/10.1007/s00415-014-7569-3>
39. Lubetzki C, Zalc B, Williams A, *et al.*, 2020, Remyelination in multiple sclerosis: From basic science to clinical translation. *Lancet Neurol*, 19: 678–688.
[https://doi.org/10.1016/S1474-4422\(20\)30140-X](https://doi.org/10.1016/S1474-4422(20)30140-X)
40. Micu I, Plemel JR, Caprariello AV, *et al.*, 2018, Axo-myelinic neurotransmission: A novel mode of cell signalling in the central nervous system. *Nat Rev Neurosci*, 19: 49–58.
<https://doi.org/10.1038/nrn.2017.128>
41. Correale J, Gaitán MI, Ysrraelit MC, *et al.*, 2017, Progressive multiple sclerosis: From pathogenic mechanisms to

- treatment. *Brain*, 140: 527–546.
<https://doi.org/10.1093/brain/aww258>
42. Bodini B, Veronese M, Garcia-Lorenzo D, *et al.*, 2016, Dynamic imaging of individual remyelination profiles in multiple sclerosis. *Ann Neurol*, 79: 726–738.
<https://doi.org/10.1002/ana.24620>
43. Franklin RJM, Frisén J, Lyons DA, 2021, Revisiting remyelination: Towards a consensus on the regeneration of CNS myelin. *Semin Cell Dev Biol*, 116: 3–9.
<https://doi.org/10.1016/j.semcdb.2020.09.009>
44. Schattling B, Engler JB, Volkmann C, *et al.*, 2019, Bassoon proteinopathy drives neurodegeneration in multiple sclerosis. *Nat Neurosci*, 22: 887–896.
<https://doi.org/10.1038/s41593-019-0385-4>
45. Luchicchi A, Hart B, Frigerio I, *et al.*, 2021, Axon-myelin unit blistering as early event in MS normal appearing white matter. *Ann Neurol*, 89: 711–725.
<https://doi.org/10.1002/ana.26014>
46. Schumacher AM, Mahler C, Kerschensteiner M, 2017, Pathology and pathogenesis of progressive multiple sclerosis: Concepts and controversies. *Neurol Int Open*, 1: E171–E181.
<https://doi.org/10.1055/s-0043-106704>
47. He A, Merkel B, Brown JW, *et al.*, 2020, Timing of high-efficacy therapy for multiple sclerosis: A retrospective observational cohort study. *Lancet Neurol*, 19: 307–316.
[https://doi.org/10.1016/S1474-4422\(20\)30067-3](https://doi.org/10.1016/S1474-4422(20)30067-3)
48. Tavazzi E, Zivadinov R, Dwyer MG, *et al.*, 2020, MRI biomarkers of disease progression and conversion to secondary-progressive multiple sclerosis. *Expert Rev Neurother*, 20: 821–834.
<https://doi.org/10.1080/14737175.2020.1757435>
49. Filippi M, Preziosa P, Langdon D, *et al.*, 2020, Identifying progression in multiple sclerosis: New perspectives. *Ann Neurol*, 88: 438–452.
<https://doi.org/10.1002/ana.25808>
50. Frischer JM, Weigand SD, Guo Y, *et al.*, 2015, Clinical and pathological insights into the dynamic nature of the white matter multiple sclerosis plaque. *Ann Neurol*, 78: 710–721.
<https://doi.org/10.1002/ana.24497>
51. Absinta M, Sati P, Masuzzo F, *et al.*, 2019, Association of chronic active multiple sclerosis lesions with disability *in vivo*. *JAMA Neurol*, 76: 1474–1483.
<https://doi.org/10.1001/jamaneurol.2019.2399>
52. Kaisey M, Lashgari G, Fert-Bober J, *et al.*, 2022, An update on diagnostic laboratory biomarkers for multiple sclerosis. *Curr Neurol Neurosci Rep*, 22: 675–688.
<https://doi.org/10.1007/s11910-022-01227-1>
53. Williams T, Zetterberg H, Chataway J, 2021, Neurofilaments in progressive multiple sclerosis: A systematic review. *J Neurol*, 268: 3212–3222.
<https://doi.org/10.1007/s00415-020-09917-x>
54. Pitt D, Lo CH, Gauthier SA, *et al.*, 2022, Toward precision phenotyping of multiple sclerosis. *Neurol Neuroimmunol Neuroinflamm*, 9: e200025.
<https://doi.org/10.1212/NXI.000000000200025>
55. Siller N, Kuhle J, Muthuraman M, *et al.*, 2019, Serum neurofilament light chain is a biomarker of acute and chronic neuronal damage in early multiple sclerosis. *Mult Scler*, 25: 678–686.
<https://doi.org/10.1177/1352458518765666>
56. Bjornevik K, Munger KL, Cortese M, *et al.*, 2020, Serum neurofilament light chain levels in patients with presymptomatic multiple sclerosis. *JAMA Neurol*, 77: 58–64.
<https://doi.org/10.1001/jamaneurol.2019.3238>
57. Kapoor R, Smith KE, Allegretta M, *et al.*, 2020, Serum neurofilament light as a biomarker in progressive multiple sclerosis. *Neurology*, 95: 436–444.
<https://doi.org/10.1212/WNL.000000000010346>
58. Golabi M, Fathi F, Samadi M, *et al.*, 2022, Identification of potential biomarkers in the peripheral blood mononuclear cells of relapsing-remitting multiple sclerosis patients. *Inflammation*, 45: 1815–1828.
<https://doi.org/10.1007/s10753-022-01662-9>
59. Abdelhak A, Huss A, Kassubek J, *et al.*, 2018, Serum GFAP as a biomarker for disease severity in multiple sclerosis. *Sci Rep*, 8: 14798.
<https://doi.org/10.1038/s41598-018-33158-8>
60. Hou Y, Dan X, Babbar M, *et al.*, 2019, Ageing as a risk factor for neurodegenerative disease. *Nat Rev Neurol*, 15: 565–581.
<https://doi.org/10.1038/s41582-019-0244-7>
61. Krysko KM, Henry RG, Cree BA, *et al.*, 2019, Telomere length is associated with disability progression in multiple sclerosis. *Ann Neurol*, 86: 671–682.
<https://doi.org/10.1002/ana.25592>
62. Meca-Lallana V, Berenguer-Ruiz L, Carreres-Polo J, *et al.*, 2021, Deciphering multiple sclerosis progression. *Front Neurol*, 12: 608491.
<https://doi.org/10.3389/fneur.2021.608491>
63. Sandelius Å, Sandgren S, Axelsson M, *et al.*, 2019, Cerebrospinal fluid growth-associated protein 43 in multiple sclerosis. *Sci Rep*, 9: 17309.
<https://doi.org/10.1111/j.1365-2990.2006.00730.x>
64. Shah AA, Piche J, Stewart B, *et al.*, 2023, Limited diagnostic utility of serologic testing for neurologic manifestations of

- systemic disease in the evaluation of suspected multiple sclerosis: A single-center observational study. *Mult Scler Relat Disord*, 69: 104443.
<https://doi.org/10.1016/j.msard.2022.104443>
65. Berer K, Gerdes LA, Cekanaviciute E, *et al.*, 2017, Gut microbiota from multiple sclerosis patients enables spontaneous autoimmune encephalomyelitis in mice. *Proc Natl Acad Sci U S A*, 114: 10719–10724.
<https://doi.org/10.1073/pnas.1711233114>
66. Jangi S, Gandhi R, Cox LM, *et al.*, 2016, Alterations of the human gut microbiome in multiple sclerosis. *Nat Commun*, 7: 12015.
<https://doi.org/10.1038/ncomms12015>
67. Cekanaviciute E, Yoo BB, Runia TF, *et al.*, 2017, Gut bacteria from multiple sclerosis patients modulate human T cells and exacerbate symptoms in mouse models. *Proc Natl Acad Sci U S A*, 114: 10713–10718.
<https://doi.org/10.1073/pnas.1711235114>
68. Reynders T, Devolder L, Valles-Colomer M, *et al.*, 2020, Gut microbiome variation is associated to multiple sclerosis phenotypic subtypes. *Ann Clin Transl Neurol*, 7: 406–419.
<https://doi.org/10.1002/acn3.51004>
69. Kappos L, Wolinsky JS, Giovannoni G, *et al.*, 2020, Contribution of relapse-independent progression vs relapse-associated worsening to overall confirmed disability accumulation in typical relapsing multiple sclerosis in a pooled analysis of 2 randomized clinical trials. *JAMA Neurol*, 77: 1132–1140.
<https://doi.org/10.1001/jamaneurol.2020.1568>
70. Giovannoni G, Popescu V, Wuerfel J, *et al.*, 2022, Smouldering multiple sclerosis: The “real MS”. *Ther Adv Neurol Disord*, 15: 17562864211066751.
<https://doi.org/10.1177/17562864211066751>
71. Luchetti S, Franssen NL, Van Eden CG, *et al.*, 2018, Progressive multiple sclerosis patients show substantial lesion activity that correlates with clinical disease severity and sex: A retrospective autopsy cohort analysis. *Acta Neuropathol*, 135: 511–528.
<https://doi.org/10.1007/s00401-018-1818-y>
72. Sastre-Garriga J, Pareto D, Rovira À, 2017, Brain atrophy in multiple sclerosis: Clinical relevance and technical aspects. *Neuroimaging Clin N Am*, 27: 289–300.
<https://doi.org/10.1016/j.nic.2017.01.002>
73. Tintore M, Vidal-Jordana A, Sastre-Garriga J, 2019, Treatment of multiple sclerosis—success from bench to bedside. *Nat Rev Neurol*, 15: 53–58.
<https://doi.org/10.1038/s41582-018-0082-z>
74. Koseoglu M, Tutuncu M, 2020, Conversion of optic neuritis to relapsing remitting multiple sclerosis: A retrospective comorbidity cohort study. *Eur Neurol*, 83: 287–292.
<https://doi.org/10.1159/000507547>
75. Abri Aghdam K, Aghajani A, Kanani F, *et al.*, 2021, A novel decision tree approach to predict the probability of conversion to multiple sclerosis in Iranian patients with optic neuritis. *Mult Scler Relat Disord*, 47: 102658.
<https://doi.org/10.1016/j.msard.2020.102658>
76. Kenney R, Liu M, Patil S, *et al.*, 2021, Long-term outcomes in patients presenting with optic neuritis: Analyses of the MSBase registry. *J Neurol Sci*, 430: 118067.
<https://doi.org/10.1016/j.jns.2021.118067>
77. Gu W, Tagg NT, Panchal NL, *et al.*, 2021, Incidence of optic neuritis and the associated risk of multiple sclerosis for service members of U.S. Armed forces. *Mil Med*, 188: usab352.
<https://doi.org/10.1093/milmed/usab352>
78. Ysraaelit MC, Correale J, 2019, Impact of sex hormones on immune function and multiple sclerosis development. *Immunology*, 156: 9–22.
<https://doi.org/10.1111/imm.13004>
79. Lee JY, Han J, Yang M, *et al.*, 2020, Population-based incidence of pediatric and adult optic neuritis and the risk of multiple sclerosis. *Ophthalmology*, 127: 417–425.
<https://doi.org/10.1016/j.ophtha.2019.09.032>
80. Pihl-Jensen G, Wanscher B, Frederiksen JL, 2021, Predictive value of optical coherence tomography, multifocal visual evoked potentials, and full-field visual evoked potentials of the fellow, non-symptomatic eye for subsequent multiple sclerosis development in patients with acute optic neuritis. *Mult Scler*, 27: 391–400.
<https://doi.org/10.1177/1352458520917924>
81. Sorensen PS, Sellebjerg F, Hartung HP, *et al.*, 2020, The apparently milder course of multiple sclerosis: Changes in the diagnostic criteria, therapy and natural history. *Brain*, 143: 2637–2652.
<https://doi.org/10.1093/brain/awaa145>
82. Sati P, Oh J, Constable RT, *et al.*, 2016, The central vein sign and its clinical evaluation for the diagnosis of multiple sclerosis: A consensus statement from the North American imaging in multiple sclerosis cooperative. *Nat Rev Neurol*, 12: 714–722.
<https://doi.org/10.1038/nrneurol.2016.166>
83. Van der Vuurst de Vries RM, Mescheriakova JY, Samijn JP, *et al.*, 2018, Application of the 2017 revised McDonald criteria for Multiple Sclerosis to patients with a typical clinically isolated syndrome. *JAMA Neurol*, 75: 1392–1398.
<https://doi.org/10.1001/jamaneurol.2018.2160>

84. Lee DH, Peschke M, Utz KS, *et al.*, 2019, Diagnostic value of the 2017 McDonald criteria in patients with a first demyelinating event suggestive of relapsing-remitting multiple sclerosis. *Eur J Neurol*, 26: 540–545.
<https://doi.org/10.1111/ene.13853>
85. Koch-Henriksen N, Thygesen LC, Stenager E, *et al.*, 2018, Incidence of MS has increased markedly over six decades in Denmark particularly with late onset and in women. *Neurology*, 90: e1954–e1963.
<https://doi.org/10.1212/WNL.0000000000005612>
86. Petersen ER, Søndergaard HB, Laursen JH, *et al.*, 2019, Smoking is associated with increased disease activity during natalizumab treatment in multiple sclerosis. *Mult Scler*, 25: 1298–1305.
<https://doi.org/10.1177/1352458518791753>
87. Solomon AJ, Marrie RA, Viswanathan S, *et al.*, 2023, Global barriers to the diagnosis of multiple sclerosis: Data from the multiple sclerosis international federation atlas of MS, third edition. *Neurology*, 101: e624–e635.
<https://doi.org/10.1212/WNL.0000000000207481>
88. Chun BY, Kim JH, Jung YK, *et al.*, 2021, Protective role of limitrin in experimental autoimmune optic neuritis. *Invest Ophthalmol Vis Sci*, 62: 8.
<https://doi.org/10.1167/iovs.62.9.8>
89. Winter A, Chwalisz B, 2020, MRI characteristics of NMO, MOG and MS related optic neuritis. *Semin Ophthalmol*, 35: 333–342.
<https://doi.org/10.1080/08820538.2020.1866027>
90. Çoban A, Düzel B, Tüzün E, *et al.*, 2017, Investigation of the prognostic value of adipokines in multiple sclerosis. *Mult Scler Relat Disord*, 15: 11–14.
<https://doi.org/10.1016/j.msard.2017.04.006>
91. Pulido-Valdeolivas I, Andorrà M, Gómez-Andrés D, *et al.*, 2020, Retinal and brain damage during multiple sclerosis course: Inflammatory activity is a key factor in the first 5 years. *Sci Rep*, 10: 13333.
<https://doi.org/10.1038/s41598-020-70255-z>
92. Alba-Arbalat S, Andorra M, Sanchez-Dalmau B, *et al.*, 2021, *In vivo* molecular changes in the retina of patients with multiple sclerosis. *Invest Ophthalmol Vis Sci*, 62: 11.
<https://doi.org/10.1167/iovs.62.6.11>
93. Vural G, Gümüşyayla Ş, Deniz O, *et al.*, 2019, Relationship between thiol-disulphide homeostasis and visual evoked potentials in patients with multiple sclerosis. *Neurol Sci*, 40: 385–391.
<https://doi.org/10.1007/s10072-018-3660-3>
94. Sadam H, Pihlak A, Jaago M, *et al.*, 2021, Identification of two highly antigenic epitope markers predicting multiple sclerosis in optic neuritis patients. *EBioMedicine*, 64: 103211.
<https://doi.org/10.1016/j.ebiom.2021.103211>
95. Gharagozloo M, Smith MD, Jin J, *et al.*, 2021, Complement component 3 from astrocytes mediates retinal ganglion cell loss during neuroinflammation. *Acta Neuropathol*, 142: 899–915.
<https://doi.org/10.1007/s00401-021-02366-4>
96. Liddelow SA, Guttenplan KA, Clarke LE, *et al.*, 2017, Neurotoxic reactive astrocytes are induced by activated microglia. *Nature*, 541: 481–487.
<https://doi.org/10.1038/nature21029>
97. Roostaei T, Sadaghiani S, Mashhadi R, *et al.*, 2019, Convergent effects of a functional C3 variant on brain atrophy, demyelination, and cognitive impairment in multiple sclerosis. *Mult Scler*, 25: 532–540.
<https://doi.org/10.1177/1352458518760715>
98. Jin J, Smith MD, Kersbergen CJ, *et al.*, 2019, Glial pathology and retinal neurotoxicity in the anterior visual pathway in experimental autoimmune encephalomyelitis. *Acta Neuropathol Commun*, 7: 125.
<https://doi.org/10.1186/s40478-019-0767-6>
99. Wu Q, Miao X, Zhang J, *et al.*, 2021, Astrocytic YAP protects the optic nerve and retina in an experimental autoimmune encephalomyelitis model through TGF- β signaling. *Theranostics*, 11: 8480–8499.
<https://doi.org/10.7150/thno.60031>

ORIGINAL RESEARCH ARTICLE

Transient receptor potential melastatin 7 signaling in U251 cell migration and invasion involves calcineurin

Haifan Gong¹, Raymond Wong¹, Julia Bandura¹, James T. Rutka²,
Zhong-Ping Feng^{1*}, and Hong-Shuo Sun^{1,2,3,4*}¹Department of Physiology, Temerty Faculty of Medicine, University of Toronto, Toronto, Ontario, Canada²Department of Surgery, Temerty Faculty of Medicine, University of Toronto, Toronto, Ontario, Canada³Department of Pharmacology and Toxicology, Temerty Faculty of Medicine, University of Toronto, Toronto, Ontario, Canada⁴Leslie Dan Faculty of Pharmacy, University of Toronto, Toronto, Ontario, Canada**Abstract**

Transient receptor potential melastatin 7 (TRPM7) is a divalent cation channel that has crucial functions in glioblastoma (GBM), which remains the most prevalent and lethal primary brain tumor in adults. Altering TRPM7 activity has previously been reported to affect GBM cell function (i.e., migration, invasion, and proliferation), thus elucidating the TRPM7-mediated signaling pathway in GBM could reveal novel therapeutic targets. Calcineurin, a Ca²⁺-dependent phosphatase, also influences GBM cell survival and migration. However, the role or the relationship between TRPM7 and calcineurin in GBM signaling has not previously been investigated. In this study, we provide evidence that there is a possible interaction between TRPM7 and calcineurin in the GBM cell line U251. Moreover, we employed pharmacological approaches to show that TRPM7 regulates calcineurin function, thereby suggesting that calcineurin is a potential downstream target of TRPM7 signaling in U251 cell migration and invasion.

Keywords: Glioblastoma; Transient receptor potential melastatin 7 channels; Calcineurin***Corresponding authors:**Zhong-Ping Feng
(zp.feng@utoronto.ca)
Hong-Shuo Sun
(hss.sun@utoronto.ca)**Citation:** Gong H, Wong R, Bandura J, *et al.*, 2023, Transient receptor potential melastatin 7 signaling in U251 cell migration and invasion involves calcineurin.
Adv Neuro, 2(3): 334.<https://doi.org/10.36922/an.334>**Received:** January 19, 2023**Accepted:** July 10, 2023**Published Online:** July 24, 2023**Copyright:** © 2023 Author(s). This is an Open-Access article distributed under the terms of the Creative Commons Attribution License, permitting distribution, and reproduction in any medium, provided the original work is properly cited.**Publisher's Note:** AccScience Publishing remains neutral with regard to jurisdictional claims in published maps and institutional affiliations.**1. Introduction**

The ubiquitously expressed transient receptor potential melastatin 7 (TRPM7) channel is involved in the cellular homeostasis of divalent ions^[1-3]. Containing both an ion channel and a kinase domain^[4-6], TRPM7 plays a critical role in cancer cell function, and inhibition of overexpressed TRPM7 has been identified as a potential pharmaceutical intervention^[7-11].

Glioblastoma (GBM) is the most lethal malignant primary brain tumor in adults, with an estimated 5-year survival rate of 5.1%^[12,13]. Current treatment approaches, including surgical resection, radiotherapy, and chemotherapy, are untargeted, resulting in suboptimal outcomes^[14]. Thus, novel treatment options are urgently required. Over the past decade, there has been growing evidence demonstrating the critical role of TRPM7 in regulating

GBM cell function. Several publications have shown that whereas TRPM7 inhibition in GBM reduced its cell function (i.e., migration, invasion, and proliferation)^[15-19], TRPM7 potentiation conversely promoted GBM cell function^[20,21]. Furthermore, our previous studies have also revealed that changes in TRPM7 activity affected the phosphorylation of proteins in the PI3K/AKT and MEK/ERK pathways^[16,20]. Nonetheless, there needs to be a higher level of granularity in our understanding of the TRPM7 signaling pathway in GBM before TRPM7 can be pursued as a drug target for future clinical application.

Previous proteomic analysis data from our laboratory showed a change in the expression of the calcium-dependent Ser/Thr phosphatase, calcineurin, following pharmacological inhibition of TRPM7^[22]. Interestingly, inhibiting calcineurin has also been shown to reduce GBM cell function^[23,24]. However, it is unclear (1) if calcineurin and TRPM7 interact in GBM, and (2) whether calcineurin and TRPM7 act within the same pathway to regulate GBM cell function. In this study, we demonstrated the interaction between TRPM7 and calcineurin proteins using co-immunoprecipitation and pull-down assays. Furthermore, inhibiting calcineurin upregulated TRPM7 protein and mRNA expression levels in the human GBM cell line U251. Finally, following pharmacological potentiation of TRPM7 activity in U251, enhancement in cell migration and invasion was prevented by inhibition of calcineurin, thus suggesting that calcineurin is a downstream target of TRPM7 signaling.

2. Materials and methods

2.1. Cell culture

The human GBM cell line U251 was obtained from the American Type Culture Collection (Manassas, VA, USA) and maintained with Dulbecco's Modified Eagle Medium (DMEM, Sigma-Aldrich) containing 10% heat-inactivated fetal bovine serum (FBS, Wisent, CA) and 100 U/mL penicillin-streptomycin (Gibco, CA). Stably transfected Flag-TRPM7 human embryonic kidney (HEK293) cells were maintained with Minimum Essential Medium (MEM, Sigma-Aldrich, USA) containing 10% heat-inactivated FBS and 100 U/mL penicillin-streptomycin. All cell cultures were maintained in an incubator at 37°C (5% CO₂; 95% humidified air).

2.2. Reagents

The stock solution of cyclosporine A (CsA, ab120114, Abcam, UK) was prepared in DMSO at 100 mM. The stock solution of Naltriben mesylate (Naltriben, 0892, Tocris, UK) was prepared in DMSO at 50 mM. Tetracycline (87128) and dimethyl sulfoxide (DMSO, 472301) were obtained from Sigma-Aldrich (USA).

2.3. Co-immunoprecipitation (co-IP)

Overexpression of recombinant mouse Flag-TRPM7 protein in HEK cells was induced by tetracycline (1 µL/mL in MilliQ water). After 18 – 24 h, the cells were lysed using co-IP lysis buffer (20 mM Tris-HCl, pH 7.5, 150 mM NaCl, 1 mM EDTA, 1 mM EGTA, 1% NP-40, 0.25% sodium deoxycholate, protease inhibitors: 1 µg/mL pepstatin A, 5 µg/mL leupeptin, 2 µg/mL aprotinin, 1 mM sodium orthovanadate, 0.1 mM PMSE, 10 mM NaF). After centrifuging at 13,000 rpm, the protein concentration of the supernatant was determined using Pierce BCA Protein Assay Kit (Thermo Fisher Scientific, USA). Anti-Flag antibody (F3165, Sigma-Aldrich, USA) was added to the protein lysate and incubated on a rotator overnight at 4°C. Protein A/G agarose beads (sc2003, Santa Cruz, USA) were then added and incubated for 1 – 3 h. The beads were washed three times with lysis buffer. An antibody-free negative control was run alongside the experimental samples. All samples were subsequently analyzed using Western blot.

2.4. His-tagged protein synthesis and purification

Human calmodulin (*CALM1*) cDNA was amplified using PCR with the following primers: ATGGCTGATCAGCTGACCGAA (forward), TTTTGCAGTCATCATCTGTACG (reverse). The product was inserted into a pET28-BIOH vector using the In-Fusion HD EcoDry Cloning Kit (Takara, Japan) and transformed into *Escherichia coli* DH5α cells by heat shock. DNA was then isolated using the QIAprep Spin Miniprep Kit (Qiagen, Germany) and sequenced. Plasmids were transformed into *E. coli* BL21 by heat shock and 1 mM IPTG (BioShop, CA) was used to induce protein overexpression. The bacterial broth was centrifuged at 6,000 rpm at 4°C and the pellet was sonicated in equilibrium buffer (20 mM Tris, 150 mM NaCl, pH 8.0, 2 mM 2-mercaptoethanol). The supernatant after centrifugation at 12,000 rpm was incubated with Ni-NTA agarose beads (Qiagen, Germany). The beads were loaded onto the column and washed using equilibrium buffer containing 20 mM and then 30 mM imidazole (Bioshop, CA), at ×10 the resin volume. Finally, proteins were eluted using ×1 resin volume of equilibrium buffer containing 250 mM imidazole. The protein of interest was purified using ion exchange chromatography with HiTrap Q HP anion column (GE Healthcare, USA) with solution A (20 mM Tris, pH 8.0, 2 mM 2-mercaptoethanol) and B (20 mM Tris, pH 8.0, 2 mM 2-mercaptoethanol, 1 M NaCl) at a gradient of 0–80% of buffer B running 10×column volume. After confirming using sodium dodecyl-sulfate polyacrylamide gel electrophoresis (SDS-PAGE), the eluted samples containing proteins of the desired molecular weight were carried to gel filtration chromatography, which was performed

with a Superdex 16/60 75 columns (GE Healthcare, USA) with buffer (20 mM Tris, pH 8.0, 200 mM NaCl, 2 mM 2-mercaptoethanol). Samples containing proteins of desired molecular weight validated by SDS-PAGE were concentrated and quantified using NanoDrop (Thermo Fisher Scientific, USA). The quality of the final protein product was evaluated by mass spectrometry.

2.5. Pull-down assay

The pull-down assay was performed using HisPur cobalt beads according to the manufacturer's instructions (Thermo Fisher Scientific, USA). In brief, cells were lysed using pull-down lysis buffer (20 mM Tris-HCl, pH 7.5, 150 mM NaCl, 1% NP-40, 0.25% sodium deoxycholate, and protease inhibitors), and the lysate was incubated with the 6×His-calmodulin on a rotator at 4°C overnight. HisPur cobalt beads were incubated with the pull-down mixture, washed three times with lysis buffer, and eluted with pull-down lysis buffer containing 150 mM imidazole. All samples were subsequently analyzed using Western blot.

2.6. Cell viability assay

U251 cells were seeded at 3×10^3 cells/well in 96-well plates and incubated in a medium containing 10 – 80 μ M CsA. After 24 h, the Cell Counting Kit-8 (CCK-8, Dojindo, Japan) solution was added and incubated for 3 h. The absorbance at 450 nm was determined using a microplate reader (Synergy H1, Biotek, USA).

2.7. Quantitative reverse transcription PCR (qRT-PCR)

Total RNA was extracted using the PureLink RNA Mini Kit (Thermo Fisher Scientific, USA) and quantified using Nanodrop (Thermo Fisher Scientific, USA). High-Capacity cDNA Reverse Transcription Kit (Applied Biosystems, USA) was used to synthesize cDNA. cDNA was then amplified with TRPM7 and GAPDH primers using Platinum SYBR Green qPCR SuperMix-UDG with ROX (Thermo Fisher Scientific, USA) in the 7900HT Fast Real-Time PCR System (Applied Biosystems, USA). TRPM7 RT-qPCR primers: CCAGAAACCAAGCGCTTTCC (forward); GCCATGACCTGCCTCTTCAT (reverse). GAPDH primers: ACTCCACTCACGGCAAATTC (forward); CCAGTAGACTCCACGGACATACT (reverse). The quantity mean of TRPM7 in each sample was calculated by SDS Software v2.4 (Thermo Fisher Scientific, USA) and normalized to the reference gene, *GAPDH*.

2.8. Western blot

Cells were resuspended in RIPA buffer (20 mM Tris-HCl, pH 7.5, 150 mM NaCl, 1% NP-40, 0.5% sodium deoxycholate, 0.1% SDS, protease inhibitors) and the

protein concentration in the centrifuged supernatant was measured with Pierce BCA Protein Assay Kit (Thermo Fisher Scientific, USA). Samples were boiled and 40 μ g protein was loaded into each well of the SDS-PAGE gel. The gel was transferred to a 0.2 μ m PVDF membrane (Bio-Rad, USA) and blocked using 5% skim milk. Membranes were incubated in the appropriate primary antibodies overnight at 4°C: anti-TRPM7 (1:1000, ab85016, Abcam, UK); anti-calcineurin A (1:500, G182-1847; BD Pharmingen, CA); anti-phospho-AKT (1:1000, 9271S, CST, USA); anti-AKT (1:1000, 2920S, CST, USA); anti-phospho-ERK (1:1000, 5726S, CST, USA); anti-ERK (1:1000, 4695S, CST, USA); anti-GAPDH (1:5000, 2118S, CST, USA); anti-6×His (1:1000, Y1010, UBPBio, USA). Following incubation with the respective mouse (1:7500, 7076S, CST, USA) or rabbit (1:10000, 7074S, CST, USA) secondary antibodies, protein signals were detected using X-ray film (Clonex, CA) after incubating blots in enhanced chemiluminescence reagents (Bio-Rad, USA). The intensity of each protein band was analyzed using ImageJ.

2.9. Wound healing migration assay

A vertical wound was created on the U251 cell layer in 12-well plates. Culture medium containing 1% FBS and drug treatments were added to corresponding wells. Four representative images at marked locations along the wound were captured per well using a phase-contrast Olympus microscope ($\times 10$ objective, CKX41) at 0 and 24 h after treatment. The images were analyzed using ImageJ and the following formula: Percentage of closure = $\text{Gap}(T_{24} - T_0) / \text{Gap}T_0 \times 100\%$.

2.10. Oris migration assay

The Oris migration assay was performed according to the manufacturer's instructions (Platypus Technologies, USA). In brief, U251 cells were seeded into the Oris 96-well plate at 2.5×10^4 cells/mL and a circular wound was created in each well after the removal of the stoppers. A culture medium containing 1% FBS and drug treatments were added to each well. An image was taken for each well using a phase-contrast Olympus microscope ($\times 4$ objective) at 0-, 12-, 24-, and 48-h post-treatment. The percentage of closure was analyzed in the same fashion as the wound healing assay.

2.11. Cell invasion assay

The Corning BioCoat Matrigel invasion assay was conducted according to the manufacturer's instructions (Corning, USA). In summary, U251 cells were seeded into the 24-well Matrigel chambers at 5×10^4 cells/mL in serum-free DMEM and placed into the companion plate containing a chemoattractant (DMEM with 10% FBS).

After 24 h, the invaded cells were fixed with methanol and stained using 1% Toluidine blue. Four fields of each chamber were imaged using a phase-contrast Olympus microscope ($\times 10$ objective) and the cells were quantified using ImageJ.

2.12. Statistics and data analysis

Data are presented as means \pm SEM. Student's *t*-test was used to assess the statistical significance of the difference in two experimental groups or one-way ANOVA for more than two groups. Statistical significance was defined as a probability level lower than 0.05 ($P < 0.05$). For each of the figures shown below, the following summarizes the number of times each experiment was repeated to obtain the total indicated sample size, respectively: Figure 1A (4 times), Figure 1B (1 time), Figure 2 (1 time), Figure 3A (3 times), Figure 3B and C (4 times), Figure 3D (3 times), Figure 4A and B (6 times), Figure 4C and D (1 time), Figure 4E (1 time), and Figure 5 (4 times; AKT and ERK experiments were run together).

3. Results

3.1. Flag-TRPM7 immunoprecipitates calcineurin A-subunit from both HEK293 and U251 cell lysates

To investigate the interaction between TRPM7 and calcineurin, the tetracycline-inducible expression system (Figure S1) was used to overexpress Flag-tagged mouse TRPM7 protein in HEK293 cells. Anti-Flag antibody was used to immunoprecipitated Flag-TRPM7 and its associated protein complexes from HEK293 cells, as well as U251 cells. TRPM7 (212 kDa) and calcineurin A-subunit (61 kDa) were detected using Western blot (Figure 1). The regulatory calcineurin B-subunit (19 kDa), known to bind to calcineurin A, was also present in the precipitated mixture (Figure S2). This suggested that calcineurin binds

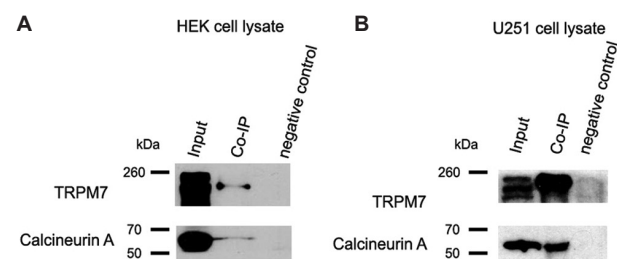


Figure 1. Flag-TRPM7 immunoprecipitates calcineurin A-subunit in HEK293 and U251 cells. The Flag-TRPM7-associated protein complexes from (A) HEK293 cell lysate and (B) U251 cell lysate were analyzed by Western blot. Both TRPM7 (212 kDa) and calcineurin A (61 kDa) were present in the co-IP and input (HEK293 or U251 cell total lysate) lanes, while neither appeared in the negative control lanes (a result of co-IP performed without anti-Flag antibody).

Abbreviation: TRPM7: Transient receptor potential melastatin 7.

TRPM7, either directly or indirectly, thus indicating that both proteins potentially participate in the same signaling pathway to regulate GBM cell function.

3.2. Calmodulin does not function as a mediator in the TRPM7-calcineurin interaction

We hypothesized that there may be a protein mediator that binds both TRPM7 and calcineurin in this protein complex. One such candidate protein is calmodulin, which classically binds calcineurin^[25] and also has the potential to bind to TRPM7 due to the presence of conserved calmodulin-interacting TRPM3 regions on TRPM7 (Figure S3). In U251 cells, 6 \times His-tagged human calmodulin (His-calmodulin) full-length protein was used for a pull-down assay (Figure 2). Both calcineurin A and His-calmodulin were present in the elution product of the pull-down experiment and absent from the negative control sample, which is consistent with previous reports^[25]. However, TRPM7 was not pulled down. Thus, this suggested that calmodulin was unlikely to be involved in the interaction between TRPM7 and calcineurin in U251 cells.

3.3. Inhibition of calcineurin increases the expression of TRPM7 protein

To investigate whether calcineurin is an upstream regulator of TRPM7 function in GBM, we inhibited calcineurin and examined the expression level of TRPM7 in U251 cells. When evaluating the cytotoxicity of the calcineurin inhibitor cyclosporine A (CsA), we found a concentration-

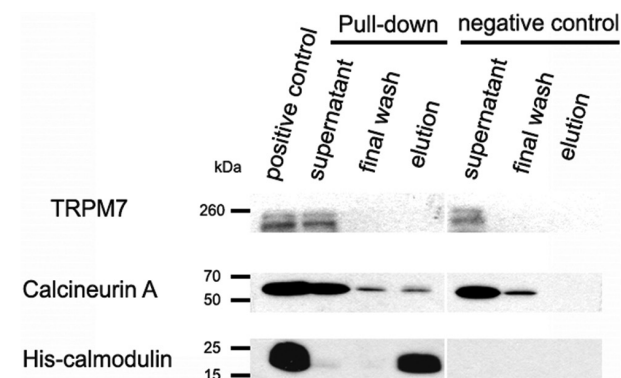


Figure 2. His-calmodulin pulls down calcineurin A but not TRPM7 from the U251 cell lysate. Purified 6 \times His-tagged calmodulin was added to U251 total cell lysate. Protein complexes were then pulled down in the absence of Ca^{2+} and analyzed using Western blot. The positive input control contained both U251 cell lysate and His-calmodulin protein. A pull-down experiment was also performed without His-calmodulin as a negative control. Both can (61 kDa) and His-calmodulin (20 kDa) were present in the pull-down elution sample whereas the TRPM7 channel (212 kDa) protein was only present in the supernatants.

Abbreviation: TRPM7: Transient receptor potential melastatin 7.

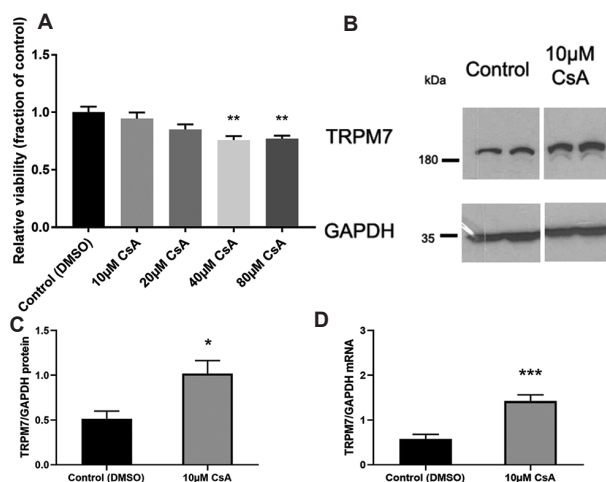


Figure 3. Calcineurin inhibition increases TRPM7 protein and mRNA levels. (A) CCK-8 assay on U251 cells was conducted following treatment with vehicle (DMSO; control) or CsA (10, 20, 40, or 80 μ M) for 24 h ($n = 10$ /group). The analysis was performed with one-way ANOVA ($**p < 0.01$). (B–D) Cells were treated with vehicle (DMSO; control) or 10 μ M CsA 24 h before RNA or protein isolation. (B) Representative images and (C) exposure intensities of Western blot bands, normalized using the loading control GAPDH, were processed with ImageJ and statistically analyzed using Student's *t*-test ($*p < 0.05$; $n = 8$ or 9 /group). (D) TRPM7 mRNA levels were assessed using qRT-PCR and normalized using GAPDH as the reference gene. The difference between the control and treatment groups was analyzed using Student's *t*-test ($***p < 0.001$; $n = 6$ /group). Abbreviations: TRPM7: Transient receptor potential melastatin 7; CsA: Cyclosporine A.

dependent decrease in U251 cell viability, consistent with a previous report^[23] (Figure 3A). Furthermore, we observed that treatment with 10 μ M CsA had no significant effect on the viability of U251 cells, and thus this concentration was used for subsequent experiments.

Our data showed that CsA treatment significantly increased ($p < 0.05$) TRPM7 protein levels (Figure 3B and C). Consistently, CsA treatment resulted in a significant increase ($p < 0.001$) in mRNA levels of *TRPM7* compared to control (Figure 3D). These findings indicated that calcineurin inhibition can increase protein and mRNA levels of TRPM7 in U251 cells.

3.4. Treatment with TRPM7 activator does not reverse the effects of calcineurin inhibition on U251 cell migration and invasion

Next, we wanted to examine whether TRPM7 acted upstream of calcineurin in regulating GBM cell function. After treating U251 cells for 24 h with 10 μ M CsA, 25 μ M naltriben, or co-treatment, the rate of cell migration was assessed using wound healing assays. We found that 10 μ M CsA significantly lowered the rate of U251 cell migration whereas 25 μ M naltriben significantly increased the rate

of migration ($p < 0.05$) (Figure 4A–D), consistent with previous findings^[20]. However, naltriben was unable to reverse the inhibitory effect of CsA. Specifically, the rate of wound closure in the co-treatment group was significantly lower than in the naltriben-only group ($p < 0.0001$) and not significantly different compared to the CsA-only group. Since CsA appeared to occlude naltriben's effect of enhancing U251 cell migration, this suggested that calcineurin acts downstream of TRPM7 to promote GBM cell migration.

In addition to migration, CsA treatment has also been previously shown to inhibit the rate of GBM cell invasion^[24]. Conversely, treatment with naltriben has been reported to increase invasion^[20]. We confirmed these findings by using the Corning BioCoat Matrigel Invasion Chamber. Specifically, we showed that the rate of U251 cell invasion was significantly increased following treatment with naltriben for 24 h ($p < 0.001$), whereas a decreasing trend for the invasion was observed in the CsA-treated group ($p = 0.131$). Consistent with migration assay results, co-treatment with CsA and naltriben resulted in an invasion rate that was not significantly different from that of the CsA-only group, while being significantly lower ($p < 0.0001$) than the naltriben-only group (Figure 4E). Thus, calcineurin may act downstream of the TRPM7 pathway that promotes GBM cell function.

3.5. CsA-induced changes in PI3K/AKT and MAPK/ERK signaling pathways are not affected by naltriben

Previous studies have demonstrated that both pharmacological inhibition and genetic knockdown of TRPM7 resulted in decreased phosphorylation of AKT and ERK^[16,17]. In contrast, calcineurin inhibition by CsA has been reported to increase p-AKT^[26]. In the present study, we showed that 24-h CsA treatment elevated p-AKT levels significantly, whereas naltriben treatment had no significant effect (Figure 5A and B). Levels of p-AKT levels were significantly increased in the naltriben and CsA co-treatment group compared to the naltriben-only group, but they were not significantly different from the CsA-only group.

Interestingly, although statistical significance was not observed, treatment of U251 cells with CsA appeared to trend towards a decrease in ERK phosphorylation. Similarly, the naltriben and CsA co-treatment group also showed a decreasing trend in p-ERK levels compared to the control group (Figure 5D and E). These findings provide further evidence that calcineurin acts as a downstream target in the TRPM7-mediated signaling that is involved in regulating GBM cell function.

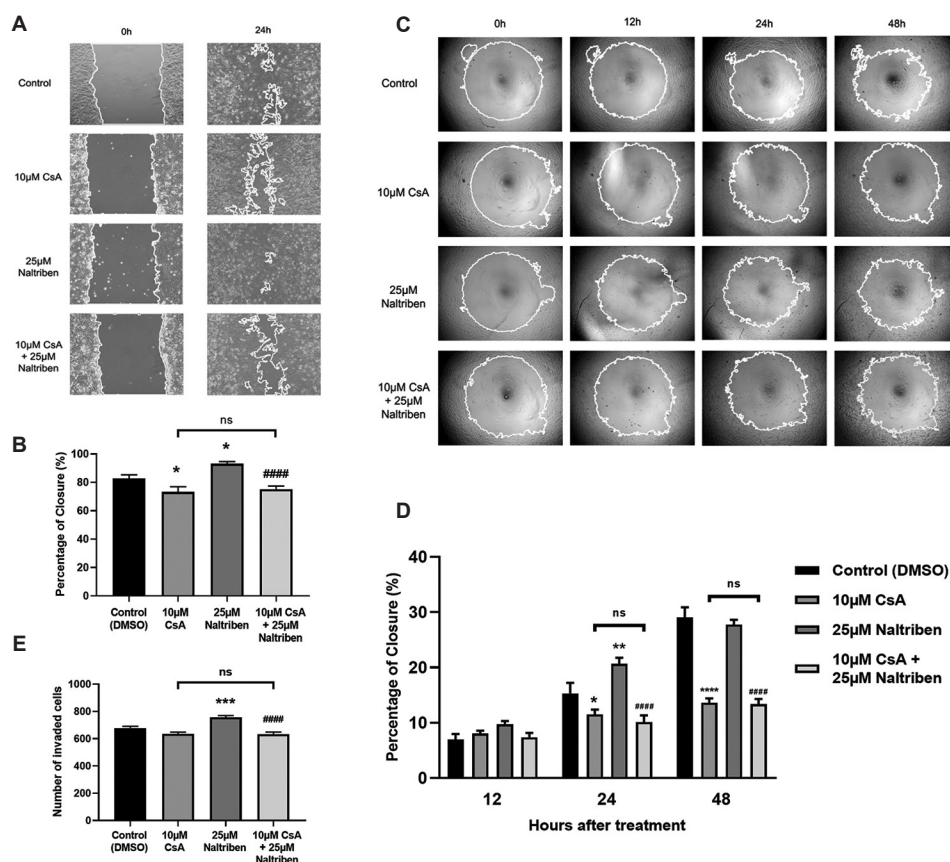


Figure 4. CsA and naltriben co-treatment reduces U251 cell migration and invasion similarly to CsA-only treatment. Cells were treated with DMSO vehicle, CsA, and/or naltriben (10 and 25 µM, respectively). (A) Wound healing assay. Images were taken 0 and 24 h following the scratch wound, and wound size was outlined using ImageJ. (B) One-way ANOVA and Tukey *post hoc* test were used to compare the percentage of wound closure between groups (* $p < 0.05$; compared to the 25 µM naltriben group: **** $p < 0.0001$; and compared to the 10 µM CsA group: ns, no significance; $n = 7$ /group). When comparing the 10 µM CsA group compared to the control, there was a significant moderate reduction ($p < 0.05$). (C) Oris migration assay. Images were taken at 0, 12, 24, and 48 h following wound formation, and the size of the wound was outlined using ImageJ. (D) One-way ANOVA and Tukey *post hoc* test were used to compare the percentage of closure of the wound between groups (* $p < 0.05$; ** $p < 0.01$; compared to the 25 µM naltriben group: **** $p < 0.0001$; and compared to the 10 µM CsA group: ns, no significance; $n = 7$ /group). € Matrigel invasion assay. One-way ANOVA and Tukey *post hoc* test were used to assess statistical significance (ns, no significance; ** $p < 0.01$ compared to control; **** $p < 0.0001$ compared to 25 µM naltriben group; $n = 3$ /group). When comparing the 10 µM CsA group compared to the control, there was a trend toward moderate reduction ($p = 0.131$). Abbreviations: CsA: Cyclosporin A; ANOVA: Analysis of variance.

4. Discussion

The current study investigated the relationship between TRPM7 and calcineurin, and the role of this interaction in GBM cell migration and invasion. We found that: (1) There is a possible interaction between TRPM7 and the calcineurin A-subunit proteins; (2) calcineurin inhibition appears to affect TRPM7 protein and mRNA levels; and (3) calcineurin potentially acts as a downstream target of TRPM7 and is likely involved in one of the pathways by which TRPM7 promotes GBM cell function.

We showed that the calcineurin A-subunit was immunoprecipitated with Flag-tagged mouse TRPM7 protein in both HEK293 and U251 cells (Figure 1A and B),

thus suggesting a potential interaction between TRPM7 and calcineurin A. It has been previously reported that the calcineurin phosphatase region can directly bind to phosphorylation sites on the C-terminus of TRPM7^[27]. This may modulate TRPM7 kinase activity and its subsequent signaling pathways^[28]. In contrast, the function of N-terminal phosphorylation sites on TRPM7 remains largely undefined^[29], and none of the known consensus sequences of calcineurin (i.e., PXIXIT^[30], LXVP^[31], and LQLP^[32]) are found at the TRPM7 N-terminus.

If the interaction between TRPM7 and calcineurin is indirect, a mediator protein would be required to facilitate the binding. Calmodulin (CaM), a calcium-binding protein,

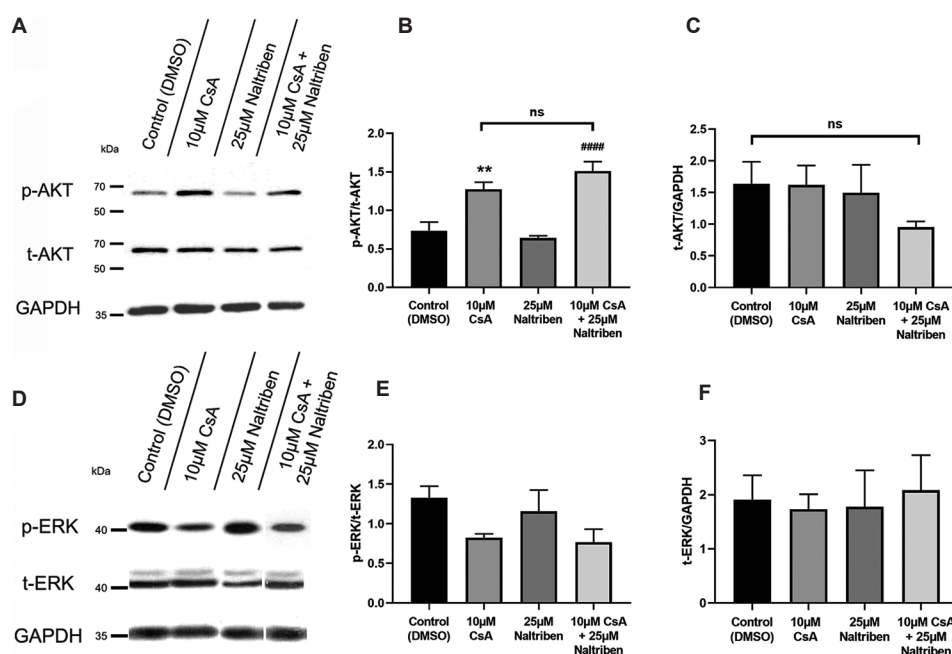


Figure 5. CsA and naltriben co-treatment affects AKT and ERK phosphorylation levels similarly to CsA-only treatment. Cells were treated with vehicle, CsA, and/or naltriben (10 or 25 μM, respectively) 24 h before protein collection for Western blot. Optic density was analyzed with ImageJ. (A) Representative images and (B and C) statistical analysis of p-AKT and t-AKT levels. One-way ANOVA and Tukey post hoc test were used to assess significant differences (** $p < 0.01$ compared to control; #### $p < 0.0001$ compared to 25 μM naltriben group; $n = 7$ /group). (D) Representative images and (E and F) statistical analysis of p-ERK and t-ERK levels. One-way ANOVA and Tukey post hoc test were used to assess statistical significance (no significance between any groups; $n = 4$ /group). Note that although there were trends toward reduction in the 10 μM CsA and co-treatment groups when compared to the control, we did not observe significance ($p > 0.05$).

Abbreviations: CsA: Cyclosporine A; ANOVA: Analysis of variance.

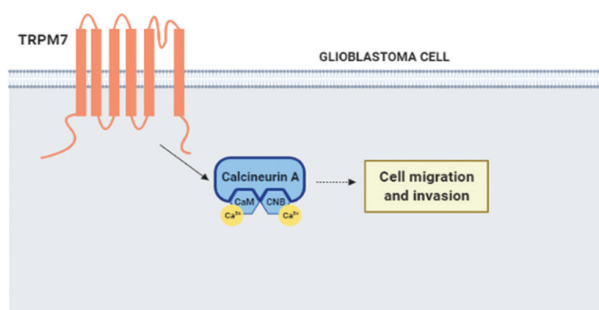


Figure 6. Graphical summary created with Biorender.

may mediate this binding since CaM has been shown to interact with both TRPM7 and calcineurin^[31,33]. Consistent with a previous finding^[25], we showed that calcineurin A was precipitated alongside His-CaM. However, TRPM7 was not found in the pull-down protein mixture in the absence of Ca²⁺ (Figure 2). This suggested that either Ca²⁺ is crucial for this interaction, or calmodulin may not be required for the TRPM7/calcineurin interaction. Nonetheless, there are limitations to our current experimental approach. Future co-IP studies may consider using anti-TRPM7 antibodies to precipitate endogenous

human TRPM7 protein and reverse IP experiments to precipitate endogenous or overexpressed can. Importantly, reciprocal co-immunoprecipitation assay should be employed to validate the interaction between Flag-TRPM7 and the calcineurin A-subunit. Furthermore, investigators can employ approaches such as PLA assay or confocal microscopy to examine the subcellular dispositions of TRPM7 and calcineurin. Finally, potential mediators of this interaction can be investigated using *in silico* protein docking simulations or affinity purification-mass spectrometry approaches, potentially testing different concentrations of Ca²⁺ to investigate the Ca²⁺ dependency of this interaction.

The inhibition of either TRPM7 or calcineurin has previously been shown to decrease the rate of migration and invasion of GBM cells^[17,20,23]. The AKT and ERK pathways, which play important roles in GBM function, have been reported to act downstream of both TRPM7 and calcineurin^[26,34]. Thus, in U251 cells, we applied the TRPM7 agonist naltriben together with the calcineurin inhibitor CsA to determine whether TRPM7 activation can reverse the CsA-induced reduction in GBM cell function and signaling. Consistent with previous findings, results

from our migration assay showed that CsA significantly decreased U251 cell migration, and naltriben alone had the opposite effect (Figure 4A-D). However, CsA and naltriben co-treatment significantly reduced migration compared to the naltriben-only group, and not significantly different compared to the CsA-only group. Similar trends were found in the rate of cell invasion (Figure 4E), and phosphorylation levels of AKT and ERK (Figure 5). Taken together, CsA treatment appears to occlude the potentiating effect of naltriben on GBM cell function, thereby suggesting that calcineurin acts downstream of TRPM7. To strengthen this finding, future studies can simultaneously investigate if pharmacological TRPM7 inhibition, such as with the use of carvacrol or waixenicin A^[15,16], has similar effects on GBM cell function as pharmacological inhibition of calcineurin. In addition, 24-h CsA treatment increased TRPM7 mRNA and protein levels in U251 cells (Figure 3B-D). One possible explanation is that reduction of calcineurin activity due to CsA-mediated inhibition may stimulate the cell to synthesize excess TRPM7 protein as compensation for the loss of downstream calcineurin-related signaling. Overall, our results suggested that TRPM7 may function as an upstream regulator of calcineurin activity in GBM.

Since the activation of the MEK/ERK pathway is involved in GBM invasiveness, migration, and death resistance^[35,36], the decreasing trend in p-ERK level following CsA treatment was expected (Figure 5E). However, in contrast with a previous report^[20], higher p-ERK levels following naltriben treatment were not observed. This may be due to the lower dosage (i.e., 25 μ M instead of 50 μ M) used in the present experiments to preserve cell viability in the naltriben and CsA co-treatment group. Furthermore, we employed a different GBM cell line from this previous study (i.e., U251 instead of U87), suggesting potential cell line-dependent effects^[20]. Nevertheless, the co-treatment group showed a decreasing trend in p-ERK levels, similar to the CsA-only group, and trended towards reduction when compared to control or naltriben groups. These results were consistent with our migration and invasion assay findings. Interestingly, p-AKT levels in U251 cells were significantly elevated with CsA treatment, consistent with previous reports in other cell types, where it has been rationalized that the loss of dephosphorylating activity due to calcineurin inhibition would lead to higher p-AKT levels^[24,26]. However, the literature shows that the activation of the PI3K/AKT pathway promotes GBM proliferation and tumor invasion, and inhibiting TRPM7 decreases the p-AKT level^[16,37]. One possible explanation is that any potential GBM-enhancing effects due to CsA-mediated upregulation of p-AKT are outweighed by the collective inhibitory effects of CsA on other mechanisms involved in GBM cell function. To build on our present findings,

the next steps should involve genetic manipulation of calcineurin levels by employing techniques such as RNA interference. In summary, calcineurin is a downstream player in the TRPM7-mediated signaling pathway that regulates GBM cell function.

5. Conclusion

The present findings provide evidence that the transient receptor potential melastatin 7 (TRPM7) channel interacts with calcineurin A-subunit proteins, either directly or indirectly. Aberrant TRPM7 activity can upregulate GBM cell function through various pathways, and calcineurin is potentially one of its downstream targets (Figure 6). In this study, we employed one GBM cell line (i.e., U251) to elucidate the proposed mechanism. It is important to note that the present findings with the U251 cell line may not necessarily reflect the nature of TRPM7-mediated signaling in glioma stem cells. Moving forward, future studies should consider confirming the interaction between TRPM7 and calcineurin using other GBM cell lines as well as glioma stem cells. By identifying potential drug targets within the TRPM7-mediated signaling pathway, the ultimate goal is to advance the development of novel chemotherapeutic agents for the treatment of GBM.

Acknowledgments

We would like to thank Haorui Zhang, Neruja Loganathan, and Andy Tran for their technical assistance.

Funding

This work was supported by the following grants: Canadian Institutes of Health Research (CIHR PJT-153155) to ZPF; Natural Sciences and Engineering Research Council of Canada (NSERC) Discovery Grants (RGPIN-2016-04574) to HSS.

Conflict of interest

The authors declare that they have no conflicts of interest with the contents of this article.

Author contributions

Conceptualization: Zhong-Ping Feng, Hong-Shuo Sun

Formal analysis: All authors

Investigation: Haifan Gong

Writing – original draft: Haifan Gong, Raymond Wong, Julia Bandura

Writing – review & editing: All authors

Ethics approval and consent to participate

Not applicable.

Consent for publication

Not applicable.

Availability of data

The data that support the findings of this study are available from the corresponding author upon reasonable request.

References

1. Nadezhdin KD, Correia L, Narangoda C, *et al.*, 2023, Structural mechanisms of TRPM7 activation and inhibition. *Nat Commun*, 14: 2639.
<https://doi.org/10.1038/s41467-023-38362-3>
2. Nadler MJ, Hermosura MC, Inabe K, *et al.*, 2001, LTRPC7 is a Mg.ATP-regulated divalent cation channel required for cell viability. *Nature*, 411: 590–595.
<https://doi.org/10.1038/35079092>
3. Monteilh-Zoller MK, Hermosura MC, Nadler MJS, *et al.*, 2003, TRPM7 provides an ion channel mechanism for cellular entry of trace metal ions. *J Gen Physiol*, 121: 49–60.
<https://doi.org/10.1085/jgp.20028740>
4. Krapivinsky G, Krapivinsky L, Manasian Y, *et al.*, 2014, The TRPM7 channel is cleaved to release a chromatin-modifying kinase. *Cell*, 157: 1061–1072.
<https://doi.org/10.1016/j.cell.2014.03.046>
5. Runnels LW, Yue L, Clapham DE, 2001, TRP-PLIK, a bifunctional protein with kinase and ion channel activities. *Science*, 291: 1043–1047.
<https://doi.org/10.1126/science.1058519>
6. Demeuse P, Penner R, Fleig A, 2006, TRPM7 channel is regulated by magnesium nucleotides via its kinase domain. *J Gen Physiol*, 127: 421–434.
<https://doi.org/10.1085/jgp.200509410>
7. Ji D, Fleig A, Horgen FD, *et al.*, 2022, Modulators of TRPM7 and its potential as a drug target for brain tumours. *Cell Calcium*, 101: 102521.
<https://doi.org/10.1016/j.ceca.2021.102521>
8. Cao R, Meng Z, Liu T, *et al.*, 2016, Decreased TRPM7 inhibits activities and induces apoptosis of bladder cancer cells via ERK1/2 pathway. *Oncotarget*, 7: 72941–72960.
<https://doi.org/10.18632/oncotarget.12146>
9. Huang J, Furuya H, Faouzi M, *et al.*, 2017, Inhibition of TRPM7 suppresses cell proliferation of colon adenocarcinoma *in vitro* and induces hypomagnesemia *in vivo* without affecting azoxymethane-induced early colon cancer in mice. *Cell Commun Signal*, 15: 30.
<https://doi.org/10.1186/s12964-017-0187-9>
10. Middelbeek J, Kuipers AJ, Henneman L, *et al.*, 2012, TRPM7 is required for breast tumor cell metastasis. *Cancer Res*, 72: 4250–4261.
<https://doi.org/10.1158/0008-5472.can-11-3863>
11. Chen JP, Luan Y, You CX, *et al.*, 2010, TRPM7 regulates the migration of human nasopharyngeal carcinoma cell by mediating Ca(2+) influx. *Cell Calcium*, 47: 425–432.
<https://doi.org/10.1016/j.ceca.2010.03.003>
12. Ostrom QT, Gittleman H, Fulop J, *et al.*, 2015, CBTRUS statistical Report: Primary brain and central nervous system tumors diagnosed in the United States in 2008–2012. *Neuro Oncol*, 17: iv1–iv62.
<https://doi.org/10.1093/neuonc/nov189>
13. Stupp R, Mason WP, van den Bent MJ, *et al.*, 2005, Radiotherapy plus concomitant and adjuvant temozolomide for glioblastoma. *N Engl J Med*, 352: 987–996.
<https://doi.org/10.1056/nejmoa043330>
14. Wu W, Klockow JL, Zhang M, *et al.*, 2021, Glioblastoma multiforme (GBM): An overview of current therapies and mechanisms of resistance. *Pharmacol Res*, 171: 105780.
<https://doi.org/10.1016/j.phrs.2021.105780>
15. Wong R, Gong H, Alanazi R, *et al.*, 2020, Inhibition of TRPM7 with waixenicin A reduces glioblastoma cellular functions. *Cell Calcium*, 92: 102307.
<https://doi.org/10.1016/j.ceca.2020.102307>
16. Chen WL, Barszczyk A, Turlova E, *et al.*, 2015, Inhibition of TRPM7 by carvacrol suppresses glioblastoma cell proliferation, migration and invasion. *Oncotarget*, 6: 16321–16340.
<https://doi.org/10.18632/oncotarget.3872>
17. Chen WL, Turlova E, Sun CLF, *et al.*, 2015, Xyloketal B suppresses glioblastoma cell proliferation and migration *in vitro* through inhibiting TRPM7-regulated PI3K/Akt and MEK/ERK signaling pathways. *Mar Drugs*, 13: 2505–2525.
<https://doi.org/10.3390/md13042505>
18. Leng TD, Li MH, Shen JF, *et al.*, 2015, Suppression of TRPM7 inhibits proliferation, migration, and invasion of malignant human glioma cells. *CNS Neurosci Ther*, 21: 252–261.
<https://doi.org/10.1111/cns.12354>
19. Liu M, Inoue K, Leng T, *et al.*, 2014, TRPM7 channels regulate glioma stem cell through STAT3 and Notch signaling pathways. *Cell Signal*, 26: 2773–2781.
<https://doi.org/10.1016/j.cellsig.2014.08.020>
20. Wong R, Turlova E, Feng ZP, *et al.*, 2017, Activation of TRPM7 by naltriben enhances migration and invasion of glioblastoma cells. *Oncotarget*, 8: 11239–11248.
<https://doi.org/10.18632/oncotarget.14496>
21. Tian Y, Yang T, Yu S, *et al.*, 2018, Prostaglandin E2 increases

- migration and proliferation of human glioblastoma cells by activating transient receptor potential melastatin 7 channels. *J Cell Mol Med*, 22: 6327–6337.
<https://doi.org/10.1111/jcmm.13931>
22. Turlova E, Wong R, Xu B, *et al.*, 2021, TRPM7 mediates neuronal cell death upstream of calcium/calmodulin-dependent protein kinase II and calcineurin mechanism in neonatal hypoxic-ischemic brain injury. *Transl Stroke Res*, 12: 164–184.
<https://doi.org/10.1007/s12975-020-00810-3>
23. Brun M, Glubrecht DD, Baksh S, *et al.*, 2013, Calcineurin regulates nuclear factor I dephosphorylation and activity in malignant glioma cell lines. *J Biol Chem*, 288: 24104–24115.
<https://doi.org/10.1074/jbc.M113.455832>
24. Sliwa M, Markovic D, Gabrusiewicz K, *et al.*, 2007, The invasion promoting effect of microglia on glioblastoma cells is inhibited by cyclosporin A. *Brain*, 130: 476–489.
<https://doi.org/10.1093/brain/awl263>
25. Kaleka KS, Petersen AN, Florence MA, *et al.*, 2012, Pull-down of calmodulin-binding proteins. *J Vis Exp*, 59: 3502.
<https://doi.org/10.3791/3502>
26. Han W, Ming M, He TC, *et al.*, 2010, Immunosuppressive cyclosporin A activates AKT in keratinocytes through PTEN suppression: Implications in skin carcinogenesis. *J Biol Chem*, 285: 11369–11377.
<https://doi.org/10.1074/jbc.M109.028142>
27. Kim TY, Shin SK, Song MY, *et al.*, 2012, Identification of the phosphorylation sites on intact TRPM7 channels from mammalian cells. *Biochem Biophys Res Commun*, 417: 1030–1034.
<https://doi.org/10.1016/j.bbrc.2011.12.085>
28. Clark K, Middelbeek J, Morrice NA, *et al.*, 2008, Massive autophosphorylation of the Ser/Thr-rich domain controls protein kinase activity of TRPM6 and TRPM7. *PLoS One*, 3: e1876.
<https://doi.org/10.1371/journal.pone.0001876>
29. Hornbeck PV, Zhang B, Murray B, *et al.*, 2015, PhosphoSitePlus, 2014: Mutations, PTMs and recalibrations. *Nucleic Acids Res*, 43: D512–D520.
30. Czirják G, Enyedi P, 2006, Targeting of calcineurin to an NFAT-like docking site is required for the calcium-dependent activation of the background K⁺ channel, TRESK. *J Biol Chem*, 281: 14677–14682.
<https://doi.org/10.1074/jbc.M602495200>
31. Li H, Rao A, Hogan PG, 2011, Interaction of calcineurin with substrates and targeting proteins. *Trends Cell Biol*, 21: 91–103.
<https://doi.org/10.1016/j.tcb.2010.09.011>
32. Czirják G, Enyedi P, 2014, The LQLP calcineurin docking site is a major determinant of the calcium-dependent activation of human TRESK background K⁺ channel. *J Biol Chem*, 289: 29506–29518.
<https://doi.org/10.1074/jbc.M114.577684>
33. Ryazanova LV, Dorovkov MV, Ansari A, *et al.*, 2004, Characterization of the protein kinase activity of TRPM7/ChaK1, a protein kinase fused to the transient receptor potential ion channel. *J Biol Chem*, 279: 3708–3716. <https://doi.org/10.1074/jbc.M308820200>
34. Yang X, Li G, Xue Q, *et al.*, 2017, Calcineurin/P-ERK/Egr-1 pathway is involved in fear memory impairment after isoflurane exposure in mice. *Sci Rep*, 7: 13947.
<https://doi.org/10.1038/s41598-017-13975-z>
35. Schreck KC, Allen AN, Wang J, *et al.*, 2020, Combination MEK and mTOR inhibitor therapy is active in models of glioblastoma. *Neurooncol Adv*, 2: vdaa138.
<https://doi.org/10.1093/oaajnl/vdaa138>
36. Kim JY, Kim YJ, Lee S, *et al.*, 2009, The critical role of ERK in death resistance and invasiveness of hypoxia-selected glioblastoma cells. *BMC Cancer*, 9: 27.
<https://doi.org/10.1186/1471-2407-9-27>
37. Behrooz AB, Talaie Z, Jusheghani F, *et al.*, 2022, Wnt and PI3K/Akt/mTOR survival pathways as therapeutic targets in glioblastoma. *Int J Mol Sci*, 23: 1353.
<https://doi.org/10.3390/ijms23031353>

ORIGINAL RESEARCH ARTICLE

Distinct behavioral effects of short-term voluntary running in phosphatase and tensin homolog deleted on chromosome 10 neuronal haploinsufficient mice

Diana Zukas Andreotti¹, Natália Prudente de Mello¹, Amanda Galvão Paixão¹, Cristoforo Scavone², Ana Maria Orellana^{1,2}, and Elisa Mitiko Kawamoto^{1*}

¹Laboratory of Molecular and Functional Neurobiology, Department of Pharmacology, Institute of Biomedical Sciences, University of São Paulo, São Paulo, Brazil

²Laboratory of Molecular Neuropharmacology, Department of Pharmacology, Institute of Biomedical Sciences, University of São Paulo, São Paulo, Brazil

Abstract

Phosphatase and tensin homolog deleted on chromosome ten (PTEN) is a tumor suppressor with functions related to its phosphatase activity. PTEN plays various roles, such as cell proliferation, survival, and migration and is involved in neurogenesis and synaptic plasticity in the central nervous system. It has been reported that running could have protective effects against the aging process and neurodegenerative diseases. Therefore, we aimed to evaluate the effects of physical exercise on behavioral and biochemical aspects of PTEN-conditioned knockout female mice. We observed that 10 days of voluntary running positively affected fear memory but caused no changes in anxiety-like behavior. However, it was unable to counteract the social recognition memory deficit in PTEN neuronal haploinsufficient mice. In terms of biochemical aspects, we observed that short-term running reduced S6 phosphorylation in PTEN heterozygous mice and PTEN protein expression independent of the genotype. In addition, PTEN heterozygous mice presented reduced N-methyl-D-aspartate subunit NR1 protein expression. Our results regarding decreased S6 phosphorylation in HT mice suggest that short-term voluntary running could have induced a protective effect in reducing dysregulated cell growth, possibly related to the downregulation of tumor suppressor expression/activity such as PTEN. Moreover, running induced distinct behavioral effects in PTEN-conditioned knockout mice.

Keywords: Memory; Brain; Anxiety; Plasticity; Sociability; Running

***Corresponding author:**
Elisa Mitiko Kawamoto
(elisamk@usp.br)

Citation: Andreotti DZ, de Mello NP, Paixão AG, *et al.*, 2023, Distinct behavioral effects of short-term voluntary running in phosphatase and tensin homolog deleted on chromosome 10 neuronal haploinsufficient mice. *Adv Neuro*, 2(3): 0872.
<https://doi.org/10.36922/an.0872>

Received: April 27, 2023

Accepted: July 10, 2023

Published Online: August 2, 2023

Copyright: © 2023 Author(s). This is an Open-Access article distributed under the terms of the Creative Commons Attribution License, permitting distribution, and reproduction in any medium, provided the original work is properly cited.

Publisher's Note: AccScience Publishing remains neutral with regard to jurisdictional claims in published maps and institutional affiliations.

1. Introduction

Originally known as a tumor suppressor protein, phosphatase and tensin homolog deleted on chromosome 10 (PTEN)^[1,2] is a dual phosphatase with both protein and lipid phosphatase activities regulating several cellular functions. Through its lipid phosphatase motif, PTEN dephosphorylates 3,4,5-phosphatidylinositol triphosphate (PIP₃), converting it into 4,5-phosphatidylinositol bisphosphate (PIP₂), which negatively

modulates protein kinase B (AKT) and its downstream targets, such as the ribosomal protein S6 kinase (S6k) and the mechanistic target of rapamycin (mTOR). This regulatory mechanism regulates major cell functions, including cell growth, size, proliferation, survival, and metabolism^[3-5].

In the central nervous system (CNS), PTEN is located in the spines and dendrites of neurons in the cerebral cortex, hippocampus, olfactory bulb, and cerebellum^[6]. Several reports provide evidence that PTEN deletion results in alterations in the number, size, and migration of cells^[7-10]. Mice with deleted^[7,11] or mutated^[12,13] PTEN in the cerebellar granule neurons exhibit characteristics similar to Lhermitte-Duclos disease. This condition is characterized by multiple hamartomas in different tissues, which could lead to tumor formation. Furthermore, PTEN knockout mice demonstrate early embryonic lethality, highlighting the importance of PTEN during embryogenesis^[14-17].

PTEN mutations are associated with mental retardation and core behaviors in autism spectrum disorders^[18,19]. Accordingly, PTEN deletion in mouse cortical and hippocampal neurons induced abnormal social interaction and exaggerated responses to stimuli, which were related to the activation of the AKT/mTOR/S6k pathway^[19]. Moreover, PTEN knockdown in gamma-aminobutyric acid neurons resulted in impaired motor coordination, repetitive behaviors, and deficits in social and learning abilities^[20]. Interestingly, these mice exhibited anxiety or anxiolytic-like behaviors depending on which PTEN neuronal subtype was deleted. Furthermore, loss of PTEN in cerebellar Purkinje cells also resulted in repetitive behavior and deficits in motor learning and sociability^[21]. Although the exact mechanisms remain unclear, several reports suggest that these PTEN-behavioral deficits occur through the activation of the AKT pathway and its downstream targets, such as mTOR/S6k^[18-20].

At the synapse, PTEN plays an important role in plasticity. In healthy conditions, the major excitatory neurotransmitter in the CNS, glutamate, binds to N-methyl-D-aspartate (NMDA) receptors, which are composed of Ca²⁺-permeable channels, thus mediating synaptic plasticity, excitotoxicity, learning, and memory formation^[22]. Research on the connection between PTEN and NMDA receptors has suggested that activating NMDA receptors evoke an interaction between PTEN and postsynaptic density-95 dependent on the PDZ domain in the postsynaptic vesicles. This interaction is essential for memory consolidation, demonstrating that PTEN is required at the synapse for the modulation of NMDA receptor-dependent long-term depression and is central to excitatory synapses^[23].

Voluntary physical exercise is an intervention with well-known benefits on brain functions, leading to cognitive improvement, as it increases brain activity, synaptic plasticity, and neurogenesis and triggers better performance in learning and memory^[24-27]. Research has revealed that physical exercise triggers the activation of genes encoding neurotrophic factors, such as brain-derived neurotrophic factor, which plays key roles in neuroplasticity and neuronal resistance against brain damage and neurodegenerative diseases^[28,29]. In addition, physical exercise is related to synaptic transmission by positively modulating NMDA receptor subunits, resulting in an increased expression of these subunits and their phosphorylated forms^[30].

Van Praag *et al.*^[31] reported that a short protocol of voluntary running is sufficient to increase neurogenesis, a finding supported by other studies as well^[32,33]. More recently, it was reported that short-term voluntary running can induce long-term morphological changes in synapses, resulting in augmented synaptic plasticity^[34]. Therefore, the present study aimed to investigate the effects of short-term voluntary running in PTEN-conditioned knockout mice, focusing on behavioral (anxiety, fear memory, and social interaction), and biochemical aspects (glutamate receptors, synaptophysin, and PTEN/AKT/S6 pathway protein expressions).

In our study, we observed that regardless of genotype or treatment, all groups spent more time in the periphery of an open field arena and in the closed arms of an elevated plus maze apparatus. In addition, fear memory was present in all groups. Our findings also suggest that 10 days of voluntary running cannot counteract social recognition memory deficit in PTEN neuronal haploinsufficient mice.

2. Materials and methods

2.1. Animals and the voluntary physical exercise protocol

Pten^{loxP/loxP} (donated by Dr. Antonio Di Cristofano from Albert Einstein College of Medicine, Bronx, NY, USA) were crossed with neuron-specific enolase *Nse-Cre*⁺ mice (B6.Cg-Tg[Eno2-cre]39Jme/J), from Jackson Laboratory, Bay Harbor, ME, USA) to generate the *Pten*^{loxP/+}/*Nse-Cre*⁺ lineage. Up to five mice were housed in Micro-Isolator plastic cages at 22 ± 2°C with a 12-h light/dark cycle at the mouse facility of the Department of Pharmacology, Institute of Biomedical Sciences, University of São Paulo, São Paulo, Brazil. All experimental procedures were approved by the Ethical Committee for Animal Research of the Institute of Biomedical Sciences (CEUA/ICB/USP, protocol 114/2014). In this study, we used *Pten*^{loxP/+}/*Nse-Cre*⁺ animals, that is, heterozygous mice with PTEN deletion (HT, PTEN^{+/-}).

Pten^{+/+}/*Nse-Cre*⁺, *Pten*^{loxP/+}/*Nse-Cre*⁺, or *Pten*^{loxP/loxP}/*Nse-Cre*⁺ were considered wild-type (WT, PTEN^{+/+}) since they present a regular PTEN expression.

Females of the *Pten*^{loxP/+}/*Nse-Cre*⁺ lineage were divided into four groups: WT sedentary (WTS), HT sedentary (HTS), WT exercise (WTE), and HT exercise (HTE). The voluntary physical exercise protocol^[31] involved providing a rotating wheel inside the mouse home cage, allowing the mice to engage involuntary physical exercise for 10 days. Before starting the experimental procedure, the mice were evaluated for 96 h to verify their motivation to walk on the wheels. An apparatus that detects the number of wheel turns was used when the animals were in the cage. The body mass and food intake of each female were evaluated weekly throughout the experimental period. After 10 days of physical exercise, behavioral tests were performed, starting with the open field test, followed by the elevated plus maze, social behavior, and passive avoidance tests. The time interval between the behavior tests was 24 h. One day after the last behavior test, the mice were euthanized, and the cerebral cortex was dissected and kept frozen at -80°C until protein extraction for western blotting assay.

2.2. Behavioral tasks

All behavioral tasks were recorded using a video camera connected to a computerized digital system controlled through the software Anymaze[®] (Stoelting, IL, USA).

2.2.1. Open field

Following the methodology described by Kawamoto *et al.*^[35], mice were positioned in the center of a 40 cm \times 40 cm open field apparatus, and their time spent in the center or the periphery of the apparatus was recorded for 10 min. The main objective of this test was to evaluate the preservation of the animal's locomotor activity and anxiety-like behavior, using the amount of time the animal remained in the center or the periphery of the apparatus.

2.2.2. Elevated plus maze

To evaluate anxiety-like behavior, we used an elevated plus maze based on Texel *et al.*^[36], with modifications. The maze used was a cross-shaped wooden apparatus with arms measuring 25 cm \times 5 cm, elevated by a 60 cm holder. Two opposite arms were enclosed by a 20 cm wall, while the other two arms were left open. Mice were individually placed at the center of the maze, facing one of the closed arms. Their movements within the maze were observed for 5 min. The exploration profile regarding the areas of the apparatus (open and closed arms) was analyzed, with a particular focus on the profile of open-arm exploration to assess anxiety-like behavior.

2.2.3. Social behavior

The social interaction test measures the integration between individuals of the same species in the same environment for a certain period^[37]. Following the protocol by Nadler *et al.*^[38], a box measuring 20 cm \times 40.5 cm \times 22 cm was used, with two partitions placed to form three chambers: one central and two laterals. This division was made using two transparent plates with a 3.5 cm diameter opening, allowing the animals to move from one chamber to another. Sociability was measured in the first phase of the test. In the first phase, the test mouse was placed in the center of the box for 5 min for habituation. After that, the test mouse was removed, and two grid cages were added to the lateral chambers of the box: An empty cage and another containing a non-familiar mouse (the non-familiar animal was previously habituated to the apparatus), which had not interacted previously with the test animal. The test mouse was then placed back in the center of the apparatus, and the time spent exploring the "empty" side or the non-familiar mouse was measured. This observation period lasted for 10 min. After each mouse, the apparatus was cleaned using 5% alcohol, and the arrangement of the empty object with the one containing the non-familiar mouse was alternated. The social novelty or social recognition memory phase was conducted 10 min later. In this phase, the previously encountered non-familiar mouse was placed on one of the sides of the apparatus, while a novel animal, which had been previously habituated to the apparatus but had no prior contact with the test mouse, was placed on the other side. The time spent exploring the familiar or the novel mouse was then measured, with observations conducted for 10 min. After each mouse's observation, the apparatus was cleaned using 5% alcohol.

2.2.4. Passive avoidance

The passive avoidance apparatus (Insight, São Paulo, Brazil) is a device composed of two same-sized chambers, one clear and the other dark, separated by an automatic door. The floor of the compartments was made of stainless-steel rods, and only the dark chamber floor was electrified. On the 1st day (exposure session), each mouse was placed in the clear chamber, and the automatic door was opened. Once the mouse entered the dark compartment, the door was closed, and the mouse received an electric foot shock (0.5 mA, 2 s in duration) through the grid floor. Immediately after the shock, the mouse was removed from the dark compartment and returned to its home cage. After 24 h, the mouse was subjected to the test (probe session), and the measurement of fear-motivated memory was obtained from the latency to move to the dark compartment. Mice that failed to enter the dark compartment within 5 min were removed from the apparatus and assigned a ceiling score of 300 s^[39].

2.3. Protein extraction

As described by Vasconcelos *et al.*^[40], the cerebral cortex was homogenized in a Dounce homogenizer filled with ice-cold lysis buffer (10 mM HEPES, 1.5 mM MgCl₂, 10 mM KCl, 0.1 mM EDTA) containing protease inhibitors (0.5 mM phenylmethylsulfonyl fluoride, 2 µg/ml leupeptin, and 2 µg/ml antipain) and phosphatase inhibitors (30 mM sodium fluoride, 3 mM sodium orthovanadate, and 20 mM sodium pyrophosphate). The samples were then centrifuged at 12,000 ×g for 30 s at 4°C. The supernatant was removed, and the pellet was re-suspended with the same lysis buffer described above. After 10 min on ice, 10% v/v NP-40 was added to each sample, vigorously shaken for 30 s, and then centrifuged at 1,000 ×g for 30 s at 4°C. The supernatant was collected for the western blotting assay. Protein concentration was measured using the Bradford colorimetric method^[41].

2.4. Western blotting

Western blotting assay was used to evaluate the expression of AKT, phospho-AKT, NR1, phospho-NR1, NR2B, PTEN, synaptophysin, S6, and phospho-S6. The protocol used was based on that described by Laemmli^[42]. The amount of protein in the samples was adjusted to 2.0 µg/µL with the sample buffer (125 mM Tris-HCl, 4% SDS, 20% v/v Glycerol, 200 mM DTT, 0.02% bromophenol blue, and pH 6.8), incubated for 5 min at 95°C, and then immediately placed on ice. Subsequently, each sample containing 10 µg total protein was applied to a 10% SDS-polyacrylamide (acrylamide/bisacrylamide (37.5:1) gel; 1% SDS) for size-separation of the proteins present. The assay was run for 2 h at 90 V. Finally, the proteins were transferred to a nitrocellulose membrane (BioRad, Hercules, CA, USA) for approximately 90 min at 400 mA.

Next, the membranes were stained with Ponceau red solution (0.5% Ponceau-S, 5% trichloroacetic acid). The excess dye solution was removed by washing with distilled water. Subsequently, the membranes were incubated for 1 h in a solution containing bovine serum albumin in TBS-T (100 mM Tris-base, 0.9% NaCl, 0.05% Tween 20) to block non-specific antibody binding. Following this step, the membranes were incubated with the primary antibody overnight. The next day, after the washing steps, the membranes were incubated with the secondary antibody for 2 h. The chemiluminescence kit (Millipore, Billerica, MA, USA) was used for detection, and the resulting blots were photographed using the G-Box photo documentation system (Syngene/Synoptics, Cambridge, England).

2.5. Statistical analysis

The data obtained from the western blotting assay were quantitatively analyzed using optical density analysis

with the ImageJ program (National Institutes of Health, USA). For western blotting, food intake, body mass, and behavioral data (open field, elevated plus maze, and social behavior), statistical analysis was conducted using a two-way analysis of variance (ANOVA) test, followed by a Tukey post-test for multiple comparisons. For behavioral data related to the passive inhibitory avoidance task, non-parametric statistics were employed due to the use of a 300-s ceiling in probe sessions. The Kruskal–Wallis analysis of variance was performed, followed by Dunn's multiple comparison test. Social behavior data were analyzed using a two-way ANOVA test, and Fisher's lysergic acid diethylamide post-tests were conducted^[43]. Statistical significance was set at $P < 0.05$. All graphs were plotted as mean values ± scanning electron microscopy using GraphPad Prism 8.

3. Results

3.1. Voluntary running increased food intake and body mass in both genotypes

Females of *Pten*^{loxP/+}/*Nse-Cre*⁺ lineage were divided into four groups: WTS, HTS, WTE, and HTE. Food intake and body mass were measured after 10 days of physical exercise.

The results suggested that mice of both genotypes (WT and HT) presented a higher food intake after 10 days of voluntary running compared to sedentary mice ($F[1,24] = 41.87$, $P < 0.0001$ for the treatment factor, $P < 0.001$ for WTS vs. WTE and HTS vs. HTE). No significant difference in food intake was observed between genotypes (genotype factor, $F[1,24] = 0.3964$, $P = 0.5349$; interaction factor, $F[1,24] = 0.0009911$, $P = 0.9751$) (Figure 1A).

When analyzing body mass over the same period, the results indicated a difference in body mass between the sedentary and exercise groups (group factor, $F[1,48] = 10.14$, $P = 0.0025$; time factor, $F[1,48] = 0.2000$, $P = 0.6567$; and interaction factor, $F[1,48] = 0.07137$, $P = 0.7905$) (Figure 1B).

3.2. PTEN^{+/+} and PTEN^{+/-} animals traveled similar distances over 10 days of running

To verify whether there was a difference in exercise motivation between the WT (PTEN^{+/+}) and HT (PTEN^{+/-}) mice, the distance traveled over 10 days was measured. When comparing the daily performance of animals using the distance traveled on day 1, we observed that both WT and HT mice covered more distance in a genotype-independent manner from the 5th and 7th day, respectively (time factor, $F[9,200] = 13.6$, $P < 0.0001$; genotype factor, $F[1,20] = 3.74$, $P = 0.0544$; and interaction factor, $F[9,200] = 0.65$, $P = 0.7446$) (Figure 2A).

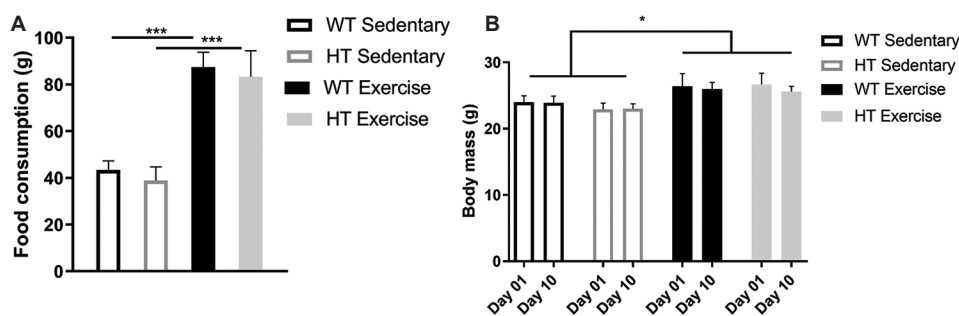


Figure 1. Determination of total body mass and food consumption. (A) Determination of the difference in food intake between the 1st and 10th days after voluntary exercise. (B) The total body mass of animals measured on the 1st and 10th days after voluntary physical exercise. Values are expressed as mean \pm standard error of the mean (sedentary WT [SWT], $n = 8$; sedentary HT (SHT), $n = 7$; exercise WT (EWT), $n = 7$; and exercise HT (EHT), $n = 6$). In (A), $***P < 0.001$ for EWT versus SWT and EHT versus SHT. In (B), $*P < 0.05$ for the exercise group versus the sedentary group. Food intake data were analyzed by repeated measures of two-way ANOVA followed by Turkey post-test. Repeated measures of three-way ANOVA were performed to evaluate body mass changes over the time course for each group.

Abbreviations: WT: Wild-type; HT: Heterozygous; ANOVA: Analysis of variance.

3.3. Voluntary running induced no changes in anxiety-like behavior and locomotor activity

Open field and elevated plus maze apparatus were used to assess anxiety-like behavior in all experimental groups. In addition, locomotor activity was also evaluated in the open field. Results for the time spent in the closed and open arms of the elevated plus maze, as well as at the center and periphery of the open field, were analyzed as a within-subjects factor, considering the time spent in different areas. The time spent in different areas of the apparatus is a repeated measure of the same subject^[44].

In the open field task, all groups exhibited similar exploratory activity in the open field apparatus (interaction factor, $F[1,33] = 0.2956$, $P = 0.5903$; genotype factor, $F[1,33] = 0.1084$, $P = 0.7440$; and treatment factor, $F[1,33] = 1.280$, $P = 0.2661$) (Figure 2B). Regarding the time spent in each zone of the open field, all groups explored the periphery more than the center of the apparatus (interaction factor, $F[3,65] = 6.473$, $P = 0.0007$; group factor, $F[3,65] = 0.1140$, $P = 0.9516$; and zone factor, $F[1,65] = 262.0$, $P < 0.0001$) (Figure 3A).

In relation to the elevated plus maze, we observed that all groups explored the closed arms more than the open ones (interaction factor, $F[3,59] = 4.574$, $P = 0.0060$; group factor, $F[3,59] = 0.7239$, $P = 0.5417$; and arm factor, $F[1,59] = 1.375$, $P < 0.0001$) (Figure 3B).

Taken together, the data from the open field and elevated plus maze data indicate that neither voluntary running nor genotype-induced changes in anxiety-like behavior.

3.4. Voluntary physical exercise did not rescue social recognition memory in PTEN^{+/-} mice

According to the literature, PTEN-deleted animals present some characteristics that resemble autism spectrum

disorder, such as abnormalities in social behavior. A social interaction task was performed to verify whether a 10-day voluntary running protocol could alter social behavior in PTEN mice.

This task was performed in a chamber divided into three compartments, and the test was divided into two phases: First, an unfamiliar mouse was placed in one part of the chamber, while the other part of the apparatus was empty. Ten minutes later, in the second part of this task, we introduced a novel mouse to one part of the chamber and a familiar mouse to the other part of the chamber.

During the first phase of the test, which is related to sociability, we did not observe any differences among the groups (chamber factor [$F \times N$], $F[1,70] = 0.4201$, $P = 0.5190$; group factor, $F[3,70] = 0.7762$, $P = 0.5112$; and interaction factor, $F[3,70] = 0.2378$, $P = 0.8697$) (Figure 4A).

During the second phase of the test, sedentary PTEN^{+/-} mice spent more time with the novel mouse compared to the familiar one ($P = 0.0120$), and a deficit in social recognition memory was observed in PTEN^{+/-} mice ($P = 0.0268$). Voluntary running did not counteract this effect in PTEN^{+/-} animals ($P = 0.7373$). Although not statistically significant, physical exercise showed a tendency to keep social recognition memory in PTEN^{+/-} mice ($P = 0.1318$) (group factor, $F[3,68] = 1.273$, $P = 0.2907$; chamber factor [$F \times N$], $F[1,68] = 6.472$, $P = 0.0132$; and interaction factor, $F[3,68] = 1.170$, $P = 0.3276$) (Figure 4B).

3.5. Voluntary physical exercise maintained a positive effect on fear memory

To investigate the effect of voluntary running on fear memory, an inhibitory avoidance task was performed. In this task, the animals were placed in an illuminated compartment of the apparatus, and the latency to enter

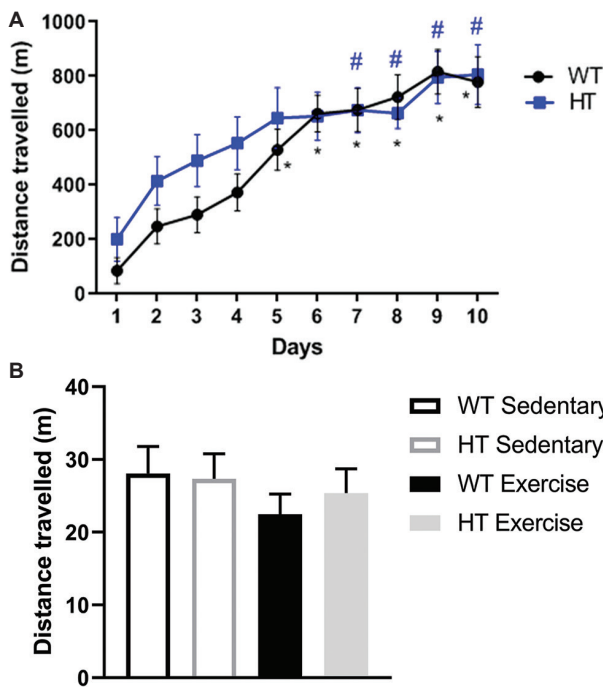


Figure 2. (A) Evaluation of the distance traveled by female mice submitted to a voluntary physical exercise in the running wheel present in the animal cage. (B) Distance traveled measured in the open field apparatus. Values are expressed as mean ± standard error of the mean (WT, *n* = 13; HT, *n* = 9). WT animals: **P* < 0.05 vs. day 01. HT animals: **P* < 0.05 vs. day 01. Repeated measures of two-way ANOVA were performed, followed by Tukey post-test. Abbreviations: WT: Wild-type; HT: Heterozygous; ANOVA: Analysis of variance.

the dark chamber was measured in seconds (exposure session). After entering the dark compartment, the mice received an electric foot shock (0.5 mA, 3 s in duration) through the grid floor. Once a mouse was shocked, it was immediately removed from the dark compartment and returned to its home cage. Twenty-four hours later, the mouse was subjected to the test (probe session), and the fear-motivated memory was measured by recording the latency to enter the dark compartment.

Data obtained from the inhibitory avoidance task were analyzed using the nonparametric Kruskal–Wallis test, followed by post-test Dunn’s multiple comparison tests. The results suggested an important variation between the exposure and probe tests (*P* < 0.0001 and Kruskal–Wallis test = 33.40). Post-test analysis indicated that all groups remembered the aversive stimulus after 24 h (*P* = 0.0242 for WTS [exposure] vs. WTS [probe], *P* = 0.0368 for HTS [exposure] vs. HTS [probe], *P* = 0.0034 for WTE [exposure] vs. WTE [probe], and *P* = 0.0366 for HTE [exposure] vs. HTE [probe]) (Figure 5).

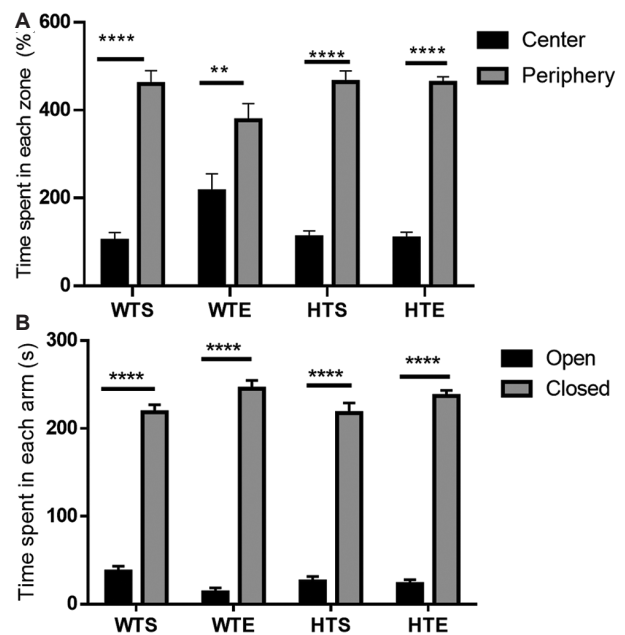


Figure 3. (A) Time spent in each zone (center or periphery). (B) Time spent in the open or closed arms of the elevated plus maze apparatus. The results are expressed as mean ± standard error of the mean and were analyzed by two-way ANOVA followed by the Turkey post-test. *****P* < 0.0001 and ***P* < 0.01 for time spent at the center versus the periphery and *****P* < 0.0001 for time spent in the open arm versus closed arm in wild-type sedentary (WTS, *n* = 10), heterozygous sedentary (HTS, *n* = 10), heterozygous exercise (HTE, *n* = 9), and wild-type exercise (WTE). Abbreviation: ANOVA: Analysis of variance.

3.6. Voluntary physical exercise reduced S6 phosphorylation and increased total NR1 expression in the frontal cortex of PTEN^{+/-} mice

To investigate the signaling pathways modulated by PTEN that might be altered in HT mice compared to WT mice in the presence or absence of voluntary running exercise, western blotting assay was performed on the frontal cortex (Figure 6). The data were analyzed using a two-way ANOVA followed by the Tukey multiple comparisons test. The results revealed that female HTE mice presented a reduction in the phospho-S6/S6 ratio compared to HTS mice (*F*[1,18] = 6.529, *P* = 0.0199 for treatment factor, *P* = 0.0208 for HTS vs. HTE) (Figure 6A). No significant differences were observed in the expressions of total S6 (genotype factor, *F*[1,19] = 1.063, *P* = 0.3154; treatment factor, *F*[1,19] = 0.3854, *P* = 0.5421; and interaction factor, *F*[1,19] = 1.185, *P* = 0.2900), synaptophysin (genotype factor, *F*[1,16] = 0.001934, *P* = 0.9655; treatment factor, *F*[1,16] = 0.06041, *P* = 0.8090; and interaction factor *F*[1,16] = 0.9265, *P* = 0.3501), or PTEN (genotype factor, *F*[1,19] = 0.2200, *P* = 0.6444; treatment

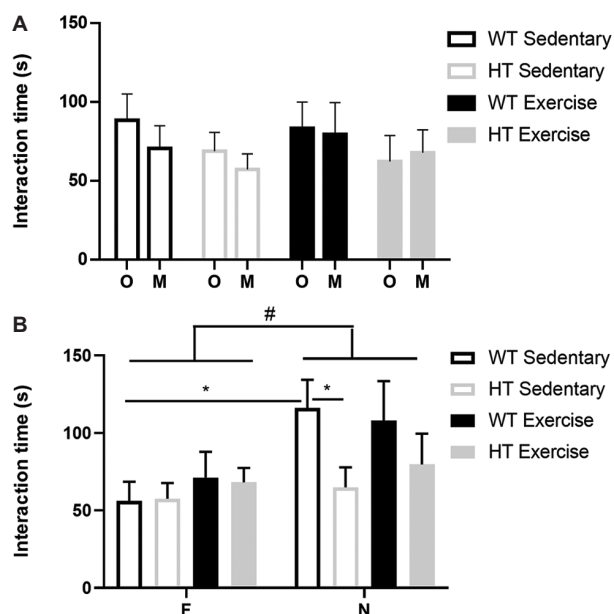


Figure 4. (A) Time of exploration (s) in the chambers with an animal (M) or the “empty” (O) part of the chamber and (B) time of exploration with a familiar (F) or a novel (N) animal within the social behavior test apparatus, by sedentary or exercised mice. Sedentary WT, $n = 10$; sedentary HT, $n = 10$; exercise WT, $n = 9$; and exercise HT, $n = 9$. The results are expressed as mean \pm standard error of the mean and were analyzed by a two-way ANOVA test ($*P = 0.0132$) followed by Fisher's LSD post-test. $*P < 0.05$ for WT sedentary (familiar vs. novel) and novel (WT sedentary vs. HT sedentary).

Abbreviations: WT: Wild-type; HT: Heterozygous; ANOVA: Analysis of variance; LSD: Lysergic acid diethylamide.

factor, $F[1,19] = 5.834$, $P = 0.0260$; and interaction factor, $F[1,19] = 1.192$, $P = 0.2886$) (Figure 6B-D).

The analysis of total NR1 expression suggested an increase caused by the genotype factor ($F[1,17] = 5.568$, $P = 0.0305$) (Figure 6E). No statistical difference was observed in the phospho-NR1 among the groups (genotype factor, $F[1,16] = 1.126$, $P = 0.3043$; treatment factor, $F[1,16] = 2.685$, $P = 0.1208$; and interaction factor, $F[1,16] = 0.1818$, $P = 0.6755$) (Figure 6F). No change was observed in the total NR2B (genotype factor, $F[1,18] = 0.4542$, $P = 0.5089$; treatment factor, $F[1,18] = 0.7405$, $P = 0.4008$; and interaction factor, $F[1,18] = 0.3413$, $P = 0.5663$) (Figure 6G), in phospho-S473 AKT (genotype factor, $F[1,14] = 0.007380$, $P = 0.9328$; treatment factor, $F[1,14] = 0.0005750$, $P = 0.9812$; and interaction factor, $F[1,14] = 0.2053$, $P = 0.6574$) (Figure 6H), and in the total AKT (genotype factor, $F[1,14] = 0.5788$, $P = 0.4594$; treatment factor, $F[1,14] = 0.8711$, $P = 0.3665$; and interaction factor, $F[1,14] = 2.059$, $P = 0.1733$) (Figure 6I).

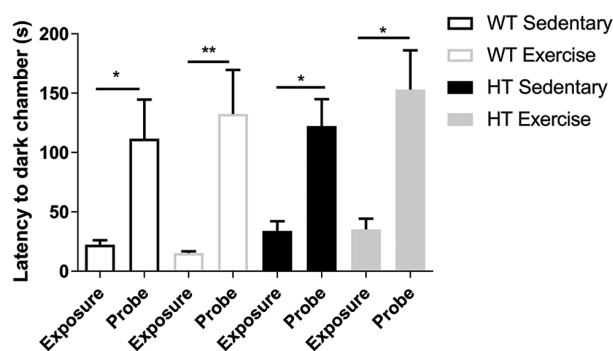


Figure 5. Latency to enter the dark chamber in both exposure and probe sessions in the passive avoidance test. Sedentary WT, $n = 10$; sedentary HT, $n = 10$; exercise WT, $n = 9$; and exercise HT, $n = 9$. Kruskal-Wallis test was conducted, followed by Dunn's *post hoc* test: $*P < 0.05$ for exposure versus probe in sedentary WT, sedentary HT, and exercise HT groups, $**P < 0.01$ for exposure versus probe in exercise WT group.

Abbreviations: WT: Wild-type; HT: Heterozygous.

4. Discussion and conclusion

This study aimed to evaluate the effects of 10-day voluntary running in PTEN neuronal haploinsufficient mice. We chose to conduct the experiments using female mice for two reasons. First, previous studies in the literature have primarily focused on male mice. In addition, female mice have been reported to exhibit higher running activity than their male counterparts^[45-47].

While we acknowledge that the presence of running wheels in the animal home cage may be considered a form of environmental enrichment, we tightly controlled the distance traveled using an apparatus that detected the number of wheel turns in each home cage, allowing us to account for the potential effects of running in the present study.

Physical exercise has emerged as one of the most effective on-pharmacological strategies for preventing neurodegenerative processes^[48] and managing cognitive decline in aging brains^[49]. Besides, physical exercise seems to be a strategy to treat and prevent Alzheimer's disease and other types of dementia^[50]. Physical exercise benefits have been observed for the management of autism spectrum disorder^[51].

An increase in food intake between the 1st and 10th day of voluntary physical exercise was observed in both WT and HT mice (Figure 1A), consistent with similar results reported in the literature^[52,53]. In addition, the total body mass of females that practiced voluntary running differed from that of sedentary females (Figure 1B). During the 10 days of voluntary physical exercise, the distance

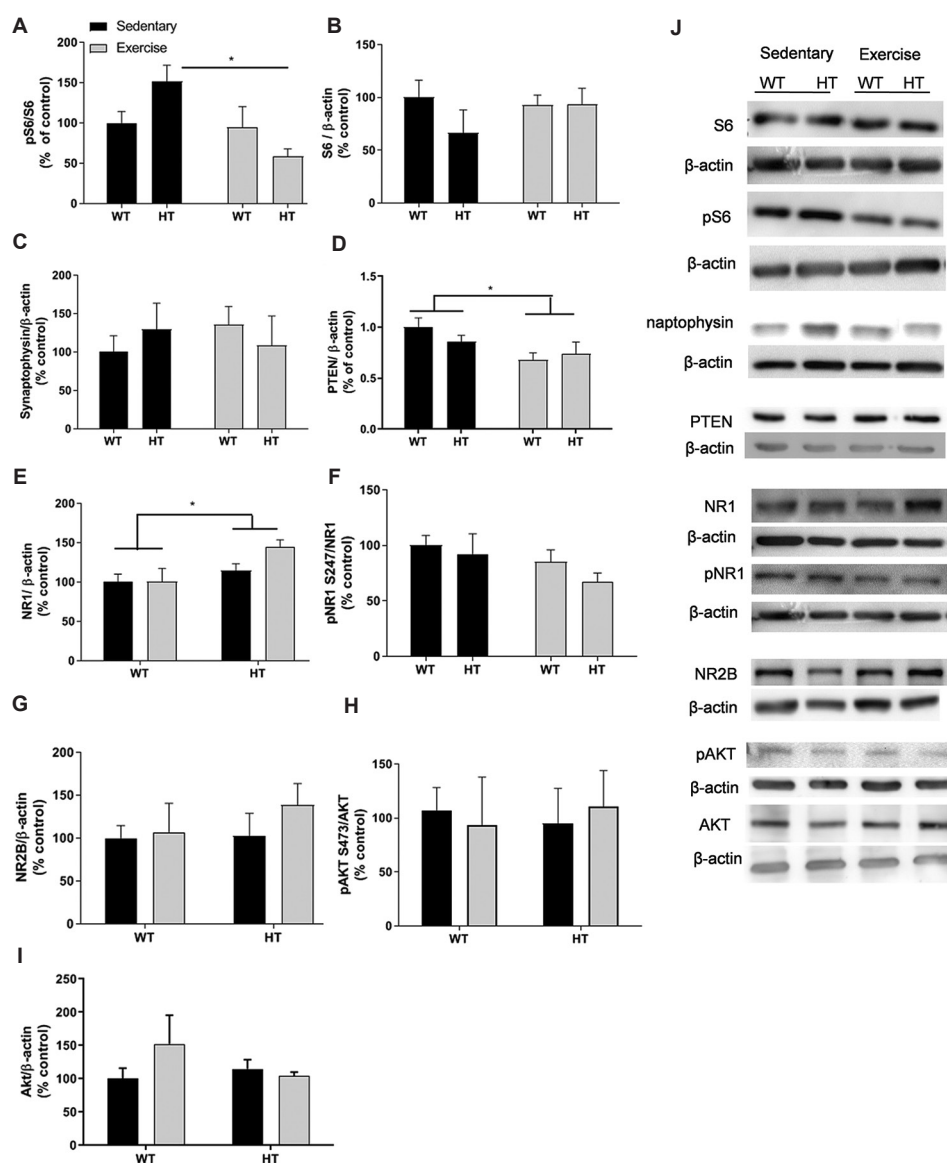


Figure 6. Analysis of the expression of the phosphorylated (A) and total (B) forms of S6; synaptophysin (C); PTEN (D); total (E) and phosphorylated (F) forms of NR1; total form of NR2B (G); phosphorylated (H); and total (I) forms of AKT from the cortical extract of mice that were and were not subjected to voluntary physical exercise (sedentary WT [$n = 6$], sedentary HT [$n = 5$], exercise WT [$n = 6$], exercise HT [$n = 6$], except for AKT (I) sedentary WT [$n = 5$], sedentary HT [$n = 5$], and exercise WT [$n = 4$], exercise HT [$n = 4$]). (J) Representative bands of each protein. The results are expressed as mean \pm standard error of the mean and were analyzed by two-way ANOVA followed by Turkey post-test. In (A): $*P < 0.05$ for sedentary HT versus Exercise HT; in (D): $*P < 0.05$ for exercise group versus sedentary group; in E: $*P < 0.05$ for WT versus HT.

Abbreviations: PTEN: Phosphatase and tensin homolog deleted on chromosome 10; WT: Wild-type; HT: Heterozygous; ANOVA: Analysis of variance.

traveled increased regardless of genotype. Interestingly, on the 1st day, HT mice traveled twice the distance compared to WT mice (WT: 85.5 ± 45.8 m; HT: 201.5 ± 76.3 m). However, after the 5th day, WT animals began to travel significantly higher distances daily, whereas HT animals began to travel significantly higher distances after the 7th day (Figure 2A). In contrast, Clipperton-Allen *et al.*^[54] reported that PTEN haploinsufficient female mice

(PTEN^{+/-}) made fewer running wheel rotations than WT mice, suggesting that PTEN deletion in specific brain areas can induce distinct behavioral outcomes. In our study, the PTEN deletion driven by the enolase promoter had no effect on the entire brain, unlike conventional knockout animals. The observed running wheel effect appears to be influenced by gender, as PTEN-conditioned Nse-Cre knockout male mice exhibited less activity than WT male

mice^[55]. Locomotion was also evaluated in the arena of the open field (Figure 2B).

In behavioral tasks, such as the arena of the open field (Figure 3A), anxiety-like behavior can also be evaluated, alongside locomotion. For PTEN knockout male mice, an increase in anxiety-like behavior and locomotor activity has been previously described^[56]. However, for females, no difference in the time spent in the center of the apparatus was observed between PTEN^{+/+} and PTEN^{+/-} mice^[54]. Our results showed that all the groups of mice spent more time in the periphery of the open field (Figure 3A) and in the closed arms of elevated plus maze apparatus (Figure 3B), indicating anxiogenic-like behavior, regardless of physical exercise and animal genotype.

In the sociability task, we observed no difference among groups (Figure 4A). However, we did not find that social recognition memory was preserved in sedentary WT animals, while HT mice exhibited impaired social recognition memory (Figure 4B). This pattern of abnormalities in social behavior resembles what is usually observed in autistic patients^[57-59], and similar deficits in social behavior have been reported by Lugo *et al.*^[56] and Kwon *et al.*^[19]. It is worth noting that voluntary running did not counteract this memory deficit (Figure 4B). These results suggest that 10 days of voluntary running may be insufficient to induce changes in social recognition memory damage, and a longer period of running might be needed to reverse this behavior effect, as reported by other studies^[52,60]. The contradictory data among studies could be attributed to various factors, such as gender, age, animal lineage, running wheel, diet, and environment^[53]. In relation to the environment, although some studies in the literature have used protocols similar to ours (i.e., the use of one animal and one running wheel per cage to ensure that all runners indeed ran in the wheel)^[61,62], the varying results could be due to differences in mouse lineage (background lineage of PTEN-conditioned knockout driven by enolase promoter) and the gender (female) as our results did not show an improvement in sociability induced by voluntary running in WT animals. Therefore, further studies are necessary to determine whether a longer period of voluntary physical exercise can counteract PTEN-induced social recognition memory deficit.

In the inhibitory avoidance test, all the groups demonstrated memory of the avoidance stimulus (Figure 5). In this study, female mice did not exhibit impaired aversive memory, which contrasts with the results observed in male mice from the same lineage in our previous study. In that study, a 30-day of intermittent fasting protocol was able to recover fear memory deficit in male HT mice^[39]. These findings align with the fact that the

incidence of autism spectrum disorder is about 3 – 4 times higher in boys than in girls^[63,64]. Similar to social behavior data, 10 days of physical exercise did not induce any changes in fear memory. Therefore, the mice remembered that the dark side of the chamber was associated with foot shock.

According to previous studies in the literature, physical exercise has been shown to be related to synaptic transmission by positively modulating the NMDA receptor subunits. This modulation includes an increased expression of these subunits but also their phosphorylated forms^[30]. As we did not observe any effects of physical exercise on animal behavior, we also did not observe any alterations in terms of NMDA receptor subunit modulation, except for the fact that HT mice showed an increase in NR1 expression (Figure 6E). Interestingly, this effect of increased NR1 expression in HT mice aligns with the findings from experiments where PTEN expression was deleted using siRNA^[65]. This increase in NR1 expression observed in HT mice could potentially contribute to explaining the increased excitability observed in autism spectrum disorder^[66,67].

Children prenatally exposed to valproic acid are more vulnerable to developing autism spectrum disorders^[68,69]. According to Rinaldi *et al.*^[70], valproic acid increases the expression of NMDA receptor subunits NR2A and NR2B while decreasing PTEN gene expression. In the present study, we did not observe any differences among the groups in the expression of the phosphorylated form of NR1 and the total NR2B. However, we observed an increase in total NR1 expression in HT mice (Figure 6E). Some studies with autism spectrum disorder models, as reviewed by Wang *et al.*^[71], have shown that both an increase and decrease in NMDAR1 phosphorylation can occur.

Another protein that can be modulated by the PI3K-AKT pathway is S6K1, which, in turn, phosphorylates S6. S6 is a ribosomal 40S constituent involved in regulating protein translation and, subsequently, cell growth and proliferation^[5]. Furthermore, S6K can also regulate protein translation^[72]. Studies have demonstrated that exercise can augment the phosphorylation of S6K in skeletal muscle, which seems to be related to an increase in muscle mass^[73,74]. In addition to this, S6K seems to be involved in modulating synaptic plasticity, as shown by Caccamo *et al.*^[75], who observed that suppression of S6K1 expression improved synaptic plasticity and spatial memory deficits in an Alzheimer's disease animal model. This improvement could be explained by the fact that sustained glutamatergic signaling activation, which has been shown to occur in neurodegenerative processes^[76], can inhibit S6K^[77]. Our study showed that HT mice have

an increased expression of NR1, which could be related to the fact that HT mice present neuronal hypertrophy and increased synapses in the cerebral cortex and hippocampus^[19]. This increase in NR1 expression may be associated with the activation of excitatory synapses^[78,79]. Ten days of running induced a reduction in S6 phosphorylation, specifically in HT mice, possibly due to a combined effect of glutamatergic signaling activation induced by running in other glutamate receptors such as AMPA or metabotropic receptors and the activation of glutamatergic signaling induced by PTEN knocking down itself (Figure 6E), leading to decreased S6 phosphorylation in HT mice.

Other studies have shown similar results, including the role of S6K1 in learning and memory^[80-82]. In our study, we observed that voluntary running decreased S6 phosphorylation (Figure 6A), suggesting a decreased activity/expression of S6K. This effect could be a protective effect of running, which reduces dysregulated cell growth, possibly related to a downregulation of tumor suppressor expression/activity, such as PTEN. The pathway responsible for the decrease in S6 phosphorylation induced by physical exercise appears to be independent of AKT and PTEN signaling, as we observed no differences among the groups regarding AKT expression and activity (Figures 6H and I). In addition, we observed that physical exercise caused a reduction in PTEN expression (Figure 6D), which could induce S6 phosphorylation through the PIP3-PDK-P70S6K-S6 signaling pathway^[83]. Further investigation of other proteins related to S6K signaling is necessary to understand the voluntary running induced decreased S6 phosphorylation in HT mice.

Studies in the literature have demonstrated that 10 weeks of running can increase PTEN expression in the mouse skin tissue. This suggests that exercise may play a role in preventing skin cancer development^[84]. On the other hand, studies have shown that PTEN levels are increased in the synapses of the brains of Alzheimer's disease patients as the disease progresses, associated with synaptic failure^[85]. These observations suggest that both increased and decreased PTEN levels could have varying effects on cell survival. In our study, we observed that exercise led to a reduction in PTEN levels in the cerebral cortex of both WT and HT mice. Further, analyses will be necessary to better understand the short-term running effects on PTEN expression in the brain.

Female PTEN-conditioned mice were used in the present study, as female animals are rarely used in research due to potential hormonal interference with data interpretation. Therefore, it is essential to consider gender when evaluating

the effects of strategies such as physical exercise in both females and males, given evidence of sex-dependent effects in rodents and humans under physical exercise, as reviewed by Rosenfeld^[86]. In addition, our previous observations indicated differences in basal levels of proteins, such as PTEN, mTOR, and FoxO3a, between male and female mice^[87]. These differences may contribute to varying susceptibilities to developing conditions such as autism spectrum disorder^[64,88], potentially leading to distinct responses to therapeutic treatments. Furthermore, while literature has reported that a short protocol of voluntary running causes morphological changes in synapses^[34] and boosts neurogenesis^[31], the present study's short-term running protocol did not fully counteract behavioral deficits. Further studies are warranted to validate these findings.

Acknowledgments

We thank Larissa de Sá Lima for her technical assistance. We also thank Editage for the English editing service.

Funding

This study was financially supported by *Fundação de Amparo à Pesquisa do Estado de São Paulo* to Elisa Mitiko Kawamoto (FAPESP, grant number 2016/22996-9) and to Cristoforo Scavone (FAPESP grant number 2016/07427-8). Ana Maria Orellanais supported by the postdoc fellowship from *Coordenação de Aperfeiçoamento de Pessoal de Nível Superior* (CAPES). Natália Prudente de Mello and Amanda Galvão Paixão were supported by the MSc fellowship from FAPESP. Elisa Mitiko Kawamoto and Cristoforo Scavone are research fellows of *Conselho Nacional de Desenvolvimento Científico e Tecnológico* (CNPq).

Conflict of interest

The authors declare no competing interests.

Author contributions

Conceptualization: Diana Zukas Andreotti, Cristoforo Scavone, Elisa Mitiko Kawamoto

Formal analysis: Diana Zukas Andreotti, Elisa Mitiko Kawamoto

Investigation: Diana Zukas Andreotti, Natália Prudente de Mello, Amanda Galvão Paixão, Ana Maria Orellana

Writing – original draft: Diana Zukas Andreotti, Cristoforo Scavone, Elisa Mitiko Kawamoto

Ethics approval and consent to participate

All experimental procedures were approved by the Ethical Committee for Animal Research of the Institute of

Biomedical Sciences (CEUA/ICB/USP, protocol 114/2014).

Consent for publication

Not applicable.

Availability of data

All data generated during this study are included in this article.

References

- Steck PA, Pershouse MA, Jasser S, *et al.*, 1997, Identification of a candidate tumor suppressor gene, MMAC1, at chromosome 10q23.3 that is mutated in multiple advanced cancers. *Nat Genet*, 15: 356–362.
<https://doi.org/10.1038/ng0497-356>
- Li J, Yen C, Liaw D, *et al.*, 1997, PTEN, a putative protein tyrosine phosphatase gene mutated in human brain, breast and prostate cancer. *Science*, 275: 1943–1947.
<https://doi.org/10.1126/science.275.5308.1943>
- Maehama T, Dixon JE, 1998, The tumor suppressor PTEN/MMAC1, dephosphorylates the lipid second messenger phosphatidylinositol 3,4,5-triphosphate. *J Biol Chem*, 273: 13375–13378.
<https://doi.org/10.1074/jbc.273.22.13375>
- Ruvinsky I, Sharon N, Lere T, *et al.*, 2005, Ribosomal protein S6 phosphorylation is a determinant of cell size and glucose homeostasis. *Genes Dev*, 19: 2199–2211.
<https://doi.org/10.1101/gad.351605>
- Ruvinsky I, Meyuhas O, 2006, Ribosomal protein S6 phosphorylation: From protein synthesis to cell size. *Trends Biochem Sci*, 31: 342–348.
<https://doi.org/10.1016/j.tibs.2006.04.003>
- Perandones C, Costanzo RV, Kowaljow V, *et al.*, 2004, Correlation between synaptogenesis and the PTEN phosphatase expression in dendrites during postnatal brain development. *Brain Res Mol Brain Res*, 128: 8–19.
<https://doi.org/10.1016/j.molbrainres.2004.05.021>
- Backman SA, Stambolic V, Suzuki A, *et al.*, 2001, Deletion of Pten in mouse brain causes seizures, ataxia and defects in soma size resembling Lhermitte-Duclos disease. *Nat Genet*, 29: 396–403.
<https://doi.org/10.1038/ng782>
- Groszer M, Erickson R, Scripture-Adams DD, *et al.*, 2001, Negative regulation of neural stem/progenitor cell proliferation by the Pten tumor suppressor gene *in vivo*. *Science*, 294: 2186–2189.
<https://doi.org/10.1126/science.1065518>
- Kwon CH, Zhu X, Zhang J, *et al.*, 2001, Pten regulates neuronal soma size: A mouse model of Lhermitte-Duclos disease. *Nat Genet*, 29: 404–411.
<https://doi.org/10.1038/ng781>
- Marin S, Krimpenfort P, Leung C, *et al.*, 2002, PTEN is essential for cell migration but not for fate determination and tumorigenesis in the cerebellum. *Development*, 129: 3513–3522.
<https://doi.org/10.1242/dev.129.14.3513>
- Kwon CH, Zhu X, Zhang J, *et al.*, 2003, mTor is required for hypertrophy of Pten-deficient neuronal soma *in vivo*. *Proc Natl Acad Sci U S A*, 100: 12923–12928.
<https://doi.org/10.1073/pnas.2132711100>
- Liaw D, Marsch DJ, Li J, *et al.*, 1997, Germline mutations of the PTEN gene in Cowden disease, an inherited breast and thyroid cancer syndrome. *Nat Genet*, 16: 64–67.
<https://doi.org/10.1038/ng0597-64>
- Marsh DJ, Coulon V, Luneeta KL, *et al.*, 1998, Mutation spectrum and genotype-phenotype analyses in Cowden disease and Bannayan-Zonana syndrome, two hamartoma syndromes with germline PTEN mutation. *Hum Mol Genet*, 7: 507–515.
<https://doi.org/10.1093/hmg/7.3.507>
- Di Cristofano A, Pesce B, Cordon-Cardo C, *et al.*, 1998, Pten is essential for embryonic development and tumor suppression. *Nat Genet*, 19: 348–355.
<https://doi.org/10.1038/1235>
- Podsypanina K, Ellenson LH, Nemes A, *et al.*, 1999, Mutation of Pten/Mmac1 in mice causes neoplasia in multiple organ system. *Proc Natl Acad Sci U S A*, 96: 1563–1568.
<https://doi.org/10.1073/pnas.96.4.1563>
- Stambolic V, Suzuki A, de la Pompa JL, *et al.*, 1998, Negative regulation of PKB/Akt-dependent cell survival by the tumor suppressor PTEN. *Cell*, 95: 29–39.
[https://doi.org/10.1016/s0092-8674\(00\)81780-8](https://doi.org/10.1016/s0092-8674(00)81780-8)
- Suzuki A, de La Pompa JL, Stambolic V, *et al.*, 1998, High cancer susceptibility and embryonic lethality associated with mutation of the PTEN tumor suppressor gene in mice. *Curr Biol*, 8: 1169–1178.
[https://doi.org/10.1016/s0960-9822\(07\)00488-5](https://doi.org/10.1016/s0960-9822(07)00488-5)
- Butler MG, Dasouki MJ, Zhou XP, *et al.*, 2005, Subset of individuals with autism spectrum disorders and extreme macrocephaly associated with germline PTEN tumour suppressor gene mutations. *J Med Genet*, 42: 318–321.
<https://doi.org/10.1136/jmg.2004.024646>
- Kwon CH, Luikart BW, Powell CM, *et al.*, 2006, Pten regulates neuronal arborization and social interaction in mice. *Neuron*, 50: 377–388.
<https://doi.org/10.1016/j.neuron.2006.03.023>

20. Shin S, Santi A, Huang S, 2021, Conditional Pten knockout in parvalbumin- or somatostatin-positive neurons sufficiently leads to autism-related behavioral phenotypes. *Mol Brain*, 14: 24.
<https://doi.org/10.1186/s13041-021-00731-8>
21. Cupolillo D, Hoxha E, Faralli A, *et al.*, 2016, Autistic-like traits and cerebellar dysfunction in Purkinje cell PTEN Knock-out mice. *Neuropsychopharmacology*, 41: 1457–1466.
<https://doi.org/10.1038/npp.2015.339>
22. Zhu S, Stein RA, Yoshioka C, *et al.*, 2016, Mechanism of NMDA receptor inhibition and activation. *Cell*, 165: 704–714.
<https://doi.org/10.1016/j.cell.2016.03.028>
23. Jurado S, Benoist M, Lario A, *et al.*, 2010, PTEN is recruited to the postsynaptic terminal for NMDA receptor-dependent long-term depression. *EMBO J*, 29: 2827–2840.
<https://doi.org/10.1038/emboj.2010.160>
24. Gligoroska JP, Manchevska S, 2012, The effect of physical activity on cognition – Physiological mechanisms. *Mater Sociomed*, 24: 198–202.
<https://doi.org/10.5455/msm.2012.24.198-202>
25. Creer DJ, Romberg C, Saksida LM, *et al.*, 2010, Running enhances spatial pattern separation in mice. *Proc Natl Acad Sci U S A*, 107: 2367–2372.
<https://doi.org/10.1073/pnas.0911725107>
26. Kempermann G, Fabel K, Ehninger D, *et al.*, 2010, Why and how physical activity promotes experience-induced brain plasticity. *Front Neurosci*, 4: 189.
<https://doi.org/10.3389/fnins.2010.00189>
27. van Praag H, 2008, Neurogenesis and exercise: Past and future directions. *Neuromolecular Med*, 10: 128–140.
<https://doi.org/10.1007/s12017-008-8028-z>
28. Seifert T, Brassard P, Wissenberg M, *et al.*, 2010, Endurance training enhances BDNF release from the human brain. *Am J Physiol Regul Integr Comp Physiol*, 298: R372–R377.
<https://doi.org/10.1152/ajpregu.00525.2009>
29. Mattson MP, 2012, Energy intake and exercise as determinants of brain health and vulnerability to injury and disease. *Cell Metab*, 16: 706–722.
<https://doi.org/10.1016/j.cmet.2012.08.012>
30. Dietrich MO, Mantese CE, Porciuncula LO, *et al.*, 2005, Exercise affects glutamate receptors in postsynaptic densities from cortical mice brain. *Brain Res*, 1065: 20–25.
<https://doi.org/10.1016/j.brainres.2005.09.038>
31. van Praag H, Kempermann G, Gage FH, 1999, Running increases cell proliferation and neurogenesis in the adult mouse dentate gyrus. *Nat Neurosci*, 2: 266–270.
<https://doi.org/10.1038/6368>
32. Allen DM, van Praag H, Ray J, *et al.*, 2001, Ataxia telangiectasia mutated is essential during adult neurogenesis. *Genes Dev*, 15: 554–566.
<https://doi.org/10.1101/gad.869001>
33. Persson AI, Naylor AS, Jonsdottir IH, *et al.*, 2004, Differential regulation of hippocampal progenitor proliferation by opioid receptor antagonists in running and non-running spontaneously hypertensive rats. *Eur J Neurosci*, 19: 1847–1855.
<https://doi.org/10.1111/j.1460-9568.2004.03268.x>
34. Lattanzi D, Savelli D, Pagliarini M, *et al.*, 2022, Short-term, voluntary exercise affects morpho-functional maturation of adult-generated neurons in rat hippocampus. *Int J Mol Sci*, 23: 6866.
<https://doi.org/10.3390/ijms23126866>
35. Kawamoto EM, Scavone C, Mattson MP, *et al.*, 2013, Curcumin requires tumor necrosis factor α signaling to alleviate cognitive impairment elicited by lipopolysaccharide. *Neurosignals*, 21: 75–88.
<https://doi.org/10.1159/000336074>
36. Texel SJ, Camandola S, Ladenheim B, *et al.*, 2012, Ceruloplasmin deficiency results in an anxiety phenotype involving deficits in hippocampal iron, serotonin, and BDNF. *J Neurochem*, 120: 125–134.
<https://doi.org/10.1111/j.1471-4159.2011.07554.x>
37. Moy SS, Nadler JJ, Perez A, *et al.*, 2004, Sociability and preference for social novelty in five inbred strains: An approach to assess autistic-like behavior in mice. *Genes Brain Behav*, 3: 287–302.
<https://doi.org/10.1111/j.1601-1848.2004.00076.x>
38. Nadler JJ, Moy SS, Dold G, *et al.*, 2004, Automated apparatus for quantification of social approach behaviors in mice. *Genes Brain Behav*, 3: 303–314.
<https://doi.org/10.1111/j.1601-183X.2004.00071.x>
39. Cabral-Costa JV, Andreotti DZ, Mell NP, *et al.*, 2018, Intermittent fasting uncovers and rescues cognitive phenotypes in PTEN neuronal haploinsufficient mice. *Sci Rep*, 8: 8595.
<https://doi.org/10.1038/s41598-018-26814-6>
40. Vasconcelos AR, Yshii LM, Viel TA, *et al.*, 2014, Intermittent fasting attenuates lipopolysaccharide - induced neuroinflammation and memory impairment. *J Neuroinflammation*, 11: 85.
<https://doi.org/10.1186/1742-2094-11-85>
41. Bradford MM, 1976, A rapid and sensitive methods for the quantification of microgram quantities of protein utilizing the principle of protein-dye binding. *Anal Biochem*, 72: 248–254.
<https://doi.org/10.1006/abio.1976.9999>
42. Laemmli UK, 1970, Cleavage of structural proteins during

- the assembly of the head of bacteriophage T4. *Nature*, 227: 680–685.
<https://doi.org/10.1038/227680a0>
43. Chiang MC, Huang AJY, Wintzer ME, *et al.*, 2018, A role for CA3 in social recognition memory. *Behav Brain Res*, 354: 22–30.
<https://doi.org/10.1016/j.bbr.2018.01.019>
44. Vasconcelos AR, da Paixão AG, Kinoshita PF, *et al.*, 2021, Toll-like receptor 4 signaling is critical for the adaptive cellular stress response effects induced by intermittent fasting in the mouse brain. *Neuroscience*, 465: 142–153.
<https://doi.org/10.1016/j.neuroscience.2021.04.022>
45. Rhodes JS, Garland T, Gammie SC, 2003, Patterns of brain activity associated with variation in voluntary wheel-running behavior. *Behav Neurosci*, 117: 1243–1256.
<https://doi.org/10.1037/0735-7044.117.6.1243>
46. Konhilas JP, Maass AH, Luckey SW, *et al.*, 2004, Sex modifies exercise and cardiac adaptation in mice. *Am J Physiol Heart Circ Physiol*, 287: H2768–H2776.
<https://doi.org/10.1152/ajpheart.00292.2004>
47. De Bono JP, Adlam D, Paterson DJ, *et al.*, 2006, Novel quantitative phenotypes of exercise training in mouse models. *Am J Physiol Regul Integr Comp Physiol*, 290: R926–R934.
<https://doi.org/10.1152/ajpregu.00694.2005>
48. Liu Y, Yan T, Chu JM, *et al.*, 2019, The beneficial effects of physical exercise in the brain and related pathophysiological mechanisms in neurodegenerative diseases. *Lab Invest*, 99: 943–957.
<https://doi.org/10.1038/s41374-019-0232-y>
49. Barnes JN, 2015, Exercise, cognitive function and aging. *Adv Physiol Educ*, 39: 55–62.
<https://doi.org/10.1152/advan.00101.2014>
50. Tabei KL, Satoh M, Ogawa JI, *et al.*, 2018, Cognitive function and brain atrophy predict non-pharmacological efficacy in dementia: The mihama-kiho scan project 2. *Front Aging Neurosci*, 10: 87.
<https://doi.org/10.3389/fnagi.2018.00087>
51. Sefen JAN, Al-Salmi S, Shaikh Z, *et al.*, 2020, Beneficial use and potential effectiveness of physical activity in managing autism spectrum disorder. *Front Behav Neurosci*, 14: 587560.
<https://doi.org/10.3389/fnbeh.2020.587560>
52. Otsuka A, Shiuchi T, Chikahisa S, *et al.*, 2015, Voluntary exercise and increased food intake after mild chronic stress improve social avoidance behavior in mice. *Physiol Behav*, 151: 264–271.
<https://doi.org/10.1016/j.physbeh.2015.07.024>
53. Manzanares G, Brito-da-Silva G, Gandra PG, 2018, Voluntary wheel running: Patterns and physiological effects in mice. *Braz J Med Biol Res*, 52: e7830.
<https://doi.org/10.1590/1414-431X20187830>
54. Clipperton-Allen AE, Page DT, 2014, Ptenhaploinsufficient mice show broad brain overgrowth but selective impairments in autism-relevant behavioral tests. *Hum Mol Genet*, 23: 3490–3505.
<https://doi.org/10.1093/hmg/ddu057>
55. Ogawa S, Kwon CH, Zhou J, *et al.*, 2007, A seizure-prone phenotype is associated with altered free-running rhythm in Pten mutant mice. *Brain Res*, 1168: 112–123.
<https://doi.org/10.1016/j.brainres.2007.06.074>
56. Lugo JN, Smith GD, Arbuckle EP, *et al.*, 2014, Deletion of PTEN produces autism like behavioral deficits and alterations in synaptic proteins. *Front Mol Neurosci*, 7: 27.
<https://doi.org/10.3389/fnmol.2014.00027>
57. Pierce K, Conant D, Hazin R, *et al.*, 2011, Preference for geometric patterns early in life as a risk factor for autism. *Arch Gen Psychiatry*, 68: 101–109.
<https://doi.org/10.1001/archgenpsychiatry.2010.113>
58. Zhou J, Parada LF, 2012, PTEN signaling in autism spectrum disorders. *Curr Opin Neurobiol*, 22: 873–879.
<https://doi.org/10.1016/j.conb.2012.05.004>
59. Hill EL, Frith U, 2003, Understanding autism: Insights from mind and brain. *Philos Trans R Soc Lond B Biol Sci*, 358: 281–289.
<https://doi.org/10.1098/rstb.2002.1209>
60. Zhang Y, Niu L, Zhang D, *et al.*, 2019, Social-emotional functioning explains the effects of physical activity on academic performance among Chinese primary school students: A mediation analysis. *J Pediatr*, 208: 74–80.
<https://doi.org/10.1016/j.jpeds.2018.11.045>
61. Van Praag H, 2005, Exercise enhances learning and hippocampal neurogenesis in aged mice. *J Neurosci*, 25: 8680–8685.
<https://doi.org/10.1523/JNEUROSCI.1731-05.2005>
62. Moon HY, Becke A, Berron D, *et al.*, 2016, Running-induced systemic cathepsin B secretion is associated with memory function. *Cell Metab*, 24: 332–340.
<https://doi.org/10.1016/j.cmet.2016.05.025>
63. Loomes R, Hull L, Mandy WPL, 2017, What is the male-to-female ratio in autism spectrum disorder? A systematic review and meta-analysis. *J Am Acad Child Adolesc Psychiatry*, 56: 466–474.
<https://doi.org/10.1016/j.jaac.2017.03.013>
64. Kim YS, Leventhal BL, Koh YJ, *et al.*, 2011, Prevalence of

- autism spectrum disorders in a total population sample. *Am J Psychiatry*, 168: 904–912.
<https://doi.org/10.1176/appi.ajp.2011.10101532>
65. Liu G, Feng D, Wang J, *et al.*, 2018, rTMS ameliorates PTSD symptoms in rats by enhancing glutamate transmission and synaptic plasticity in the ACC via the PTEN/AKT signaling pathway. *Mol Neurobiol*, 55: 3946–3958.
<https://doi.org/10.1007/s12035-017-0602-7>
66. Rubenstein JLR, 2010, Three hypotheses for developmental defects that may underlie some forms of autism spectrum disorder. *Curr Opin Neurol*, 23: 118–123.
<https://doi.org/10.1097/WCO.0b013e328336eb13>
67. Marchese M, Conti V, Valvo G, *et al.*, 2014, Autism-epilepsy phenotype with macrocephaly suggests PTEN, but not GLIALCAM genetic screening. *BMC Med Genet*, 15: 26.
68. Christensen J, Gronborg TK, Sorensen MJ, *et al.*, 2013, Prenatal valproate exposure and risk of autism spectrum disorders and childhood autism. *JAMA*, 309: 1696–1703.
<https://doi.org/10.1001/jama.2013.2270>
69. Bescoby-Chambers N, Forster P, Bates G, *et al.*, 2001, Foetal valproate syndrome and autism: Additional evidence of an association. *Dev Med Child Neurol*, 43: 847.
<https://doi.org/10.1017/s0012162201211542>
70. Rinaldi T, Kulangara K, Antonello K, *et al.*, 2007, Elevated NMDA receptor levels and enhanced postsynaptic long-term potentiation induced by prenatal exposure to valproic acid. *Proc Natl Acad Sci U S A*, 104: 13501–13506.
<https://doi.org/10.1073/pnas.0704391104>
71. Wang X, Kery R, Xiong Q, *et al.*, 2018, Synaptopathology in autism spectrum disorders: Complex effects of synaptic genes on neural circuits. *Prog Neuropsychopharmacol Biol Psychiatry*, 84: 398–415.
<https://doi.org/10.1016/j.pnpbp.2017.09.026>
72. Fenton TR, Gout IT, 2011, Functions and regulation of the 70kDa ribosomal S6 kinase. *Int J Biochem Cell Biol*, 43: 47–59.
<https://doi.org/10.1016/j.biocel.2010.09.018>
73. Baar K, Esser K, 1999, Phosphorylation of p70(S6k) correlates with increased skeletal muscle mass following resistance exercise. *Am J Physiol*, 276: C120–C127.
<https://doi.org/10.1152/ajpcell.1999.276.1.C120>
74. Terzis G, Spengos K, Mascher H, *et al.*, 2010, The degree of p70S6k and S6 phosphorylation in human skeletal muscle in response to resistance exercise depends on the training volume. *Eur J Appl Physiol*, 110: 835–843.
<https://doi.org/10.1007/s00421-010-1527-2>
75. Caccamo A, Branca C, Talboom JS, *et al.*, 2015, Reducing ribosomal protein S6 kinase 1 expression improves spatial memory and synaptic plasticity in a mouse model of Alzheimer's disease. *J Neurosci*, 35: 14042–14056.
<https://doi.org/10.1523/JNEUROSCI.2781-15.2015>
76. Rothman SM, Olney JW, 1986, Glutamate and the pathophysiology of hypoxic-ischemic brain damage. *Ann Neurol*, 19: 105–111.
<https://doi.org/10.1002/ana.410190202>
77. Lenz G, Avruch J, 2005, Glutamatergic regulation of the p70S6kinase in primary mouse neurons. *J Biol Chem*, 280: 38121–38124.
<https://doi.org/10.1074/jbc.C500363200>
78. Weston MC, Chen H, Swann JW, 2012, Multiple roles for mammalian target of rapamycin signaling in both glutamatergic and GABAergic synaptic transmission. *J Neurosci*, 32: 11441–11452.
<https://doi.org/10.1523/JNEUROSCI.1283-12.2012>
79. Williams MR, DeSpensa T Jr., Li M, *et al.*, 2015, Hyperactivity of newborn PTEN knock-out neurons results from increased excitatory synaptic drive. *J Neurosci*, 35: 943–959.
<https://doi.org/10.1523/JNEUROSCI.3144-14.2015>
80. Antion MD, Merhav M, Hoeffler CA, *et al.*, 2008, Removal of S6K1 and S6K2 leads to divergent alterations in learning, memory, and synaptic plasticity. *Learn Mem*, 15: 29–38.
<https://doi.org/10.1101/lm.661908>
81. Cammalleri M, Lutjens R, Berton F, *et al.*, 2003, Time-restricted role for dendritic activation of the mTOR-p70S6K pathway in the induction of late-phase long-term potentiation in the CA1. *Proc Natl Acad Sci U S A*, 100: 14368–14373.
<https://doi.org/10.1073/pnas.2336098100>
82. Raymond CR, Redman SJ, Crouch MF, 2002, The phosphoinositide 3-kinase and p70 S6 kinase regulate long-term potentiation in hippocampal neurons. *Neuroscience*, 109: 531–536.
[https://doi.org/10.1016/s0306-4522\(01\)00500-0](https://doi.org/10.1016/s0306-4522(01)00500-0)
83. Paez JG, Sellers WR, 2003, PI3K/PTEN/AKT pathway. A critical mediator of oncogenic signaling. *Cancer Treat Res*, 115: 145–167.
84. Yu M, King B, Ewert E, *et al.*, 2016, Exercise activates p53 and negatively regulates IGF-1 pathway in epidermis within a skin cancer model. *PLoS One*, 11: e0160939.
<https://doi.org/10.1371/journal.pone.0160939>
85. Gonzalez MD, Buberaman A, Morales M, *et al.*, 2021, Aberrant synaptic PTEN in symptomatic Alzheimer's patients may link synaptic depression to network failure. *Front Synaptic Neurosci*, 13: 683290.
<https://doi.org/10.3389/fnsyn.2021.683290>
86. Rosenfeld CS, 2017, Sex-dependent differences in voluntary

physical activity. *J Neurosci Res*, 95: 279–290.

<https://doi.org/10.1002/jnr.23896>

87. de Mello NP, Andreotti DZ, Orellana AM, *et al.*, 2020, Inverse sex-based expression profiles of PTEN and Klotho in mice. *Sci Rep*, 10: 20189.

<https://doi.org/10.1038/s41598-020-77217-5>

88. Auyeung B, Taylor K, Hackett G, *et al.*, 2010, Foetal testosterone and autistic traits in 18 to 24-month-old children. *Mole Autism*, 1: 11.

<https://doi.org/10.1186/2040-2392-1-11>

ORIGINAL RESEARCH ARTICLE

Relationship between sleep outcomes and lifestyle factors in young adults who sustained traumatic brain injury in childhood

Edith Botchway-Commey^{1,2,3*}, Celia Godfrey^{1,2,3}, Christian L. Nicholas^{1,4,5}, Vicki Anderson^{1,2,3,4}, and Cathy Catroppa^{1,2,3,4}¹Clinical Sciences, Murdoch Children's Research Institute, Victoria, Australia²Department of Psychology, Royal Children's Hospital, Victoria, Australia³Department of Paediatrics, University of Melbourne, Victoria, Australia⁴School of Psychological Sciences, University of Melbourne, Victoria, Australia⁵Institute for Breathing and Sleep, Austin Health, Victoria, Australia**Abstract**

This study investigated the relationships between subjective and objective sleep outcomes and lifestyle factors (i.e., nap duration, screentime, chronotype, use of tobacco, alcohol, caffeine, and medications) in young adults who sustained traumatic brain injury (TBI) in childhood. The study was conducted at the Murdoch Children's Research Institute and Royal Children's Hospital (Australia). It reports cross-sectional data collected at 20 years post-childhood TBI, as part of a prospective study. Participants included 54 young adults with TBI (mean age, 27.7; standard deviation [SD], 3.2 years) who were assessed at 20 years post-injury (mild [$n = 14$], moderate [$n = 27$], and severe [$n = 13$] TBI) and 13 healthy controls (mean age, 26.0; SD, 2.1 years). Sleep was assessed with the Pittsburgh Sleep Quality Index and actigraphy, and lifestyle factors were assessed with a study-designed questionnaire. Objective sleep efficiency was not significantly different between the TBI and control groups, but the control group presented with significantly better subjective sleep quality compared to the mild and moderate TBI severity groups. Poor subjective sleep quality was significantly associated with evening chronotype ($P < 0.001$) and tobacco use ($P < 0.001$), while being a parent ($P = 0.038$) and alcohol use ($P = 0.035$) were significantly associated with poorer objective sleep efficiency in the TBI group. These preliminary findings highlight interesting associations between poor sleep quality and lifestyle factors in young adults who sustained TBI in childhood. They highlight the need to further explore these relationships in this TBI population to inform on potential avenues for sleep interventions.

Keywords: Traumatic brain injury; Childhood; Young adulthood; Sleep; Lifestyle factors

***Corresponding author:**
Edith Botchway-Commey
(edith.botchway@mcri.edu.au)

Citation: Botchway-Commey E, Godfrey C, Nicholas CL, *et al.*, 2023, Relationship between sleep outcomes and lifestyle factors in young adults who sustained traumatic brain injury in childhood. *Adv Neuro*, 2(3): 0876. <https://doi.org/10.36922/an.0876>

Received: April 28, 2023

Accepted: July 10, 2023

Published Online: August 3, 2023

Copyright: © 2023 Author(s). This is an Open-Access article distributed under the terms of the Creative Commons Attribution License, permitting distribution, and reproduction in any medium, provided the original work is properly cited.

Publisher's Note: AccScience Publishing remains neutral with regard to jurisdictional claims in published maps and institutional affiliations.

1. Introduction

Traumatic brain injury (TBI) refers to an alteration to brain function, or other evidence of brain pathology, caused by an external force^[1,2]. Sustaining TBI in childhood has been associated with poor outcomes in several domains including cognition, behavior, mental

health, and sleep^[3,4]. Sleep disturbances such as insomnia (i.e., prolonged sleep onset and sleep maintenance problems) and daytime sleepiness (i.e., increased propensity to fall asleep during the day) are common in survivors of childhood TBI^[3]. The presence of these sleep disturbances in young TBI survivors is problematic considering the important role of sleep in memory consolidation and learning, behavior regulation, mental health, and well-being^[5-7], and its essence for body and brain recovery following potentially devastating incidents such as TBI^[8]. Proposed origins of these sleep disturbances include the impact of TBI on sleep-wake contingent brain areas and neural mechanisms^[9,10], and secondary sleep-related factors such as pain, fatigue, anxiety, and depression. In addition to these proposed causes, studies in typically developing individuals show that sleep can be affected by lifestyle factors such as screentime, having young children, smoking, and use of caffeine and certain medications^[11-13], but the relationships between sleep disturbances and lifestyle factors have not been explored in survivors of childhood TBI.

Studies have reported that sleep disturbances can persist several years following childhood TBI^[3,14,15] and are associated with injury severity, age at injury (older age for mild TBI^[16], younger age for moderate-severe TBI)^[17-19] sex, anxiety, depression, pain, and fatigue in children and adolescents with TBI^[3,17], although reports on some associations are inconsistent (e.g., male vs. female sex). We recently extended these findings in a cross-sectional study that showed a higher rate of subjective sleep disturbance in young adults who sustained TBI in childhood (39%)^[20], compared to controls (15%), and to rates reported in typically developing young adults (10 – 35%)^[21].

Young adulthood is a developmental period typically associated with increased professional, social, and family commitments, all of which can impact sleep and well-being. During this developmental stage, there may be an adaptation of lifestyles and related coping mechanisms (e.g., parenting, caffeine use, screen time, work and social patterns, and medications), which may contribute to alterations in sleep patterns and increase risk of sleep disturbance even in healthy young people^[21]. Some may engage in late night social activities, or work for long hours on computer screens, and therefore adopt an evening chronotype (i.e., delayed bedtime and extended wake-up time) to meet work and social expectations. In typically developing adults, high levels of screentime on mobile phones have been associated with increased risk of sleep problems and depression^[11], while cigarette smoking has a 2-fold risk for mental health disorders^[13]. To help manage the sleep and mental health problems associated with these

lifestyle factors, individuals may adopt late night behaviors, increase the use of alcohol, caffeine, and tobacco/cigarette, and use sleep and psychotropic medications (stimulants and antidepressants)^[22].

The relationship between sleep and lifestyle factors is yet to be investigated in survivors of childhood TBI; however, some studies involving adult survivors of TBI have reported significant associations between poor sleep and these lifestyle factors^[23,24], with studies in healthy adults reporting similar outcomes^[25-28]. Considering the vulnerability of the brain to stress and related consequences following brain injuries^[9,10], survivors of childhood brain injury may be at a greater risk of these lifestyle-related impacts on sleep. In previous publications involving the current sample, subjective sleep problems in the young adults with TBI were associated with increased symptoms of anxiety and pain^[20], fatigue, depression, and poorer general health^[29]; all of which may have been related to lifestyle choices. Identifying lifestyle factors that impact on sleep in the long-term following childhood TBI can further knowledge regarding factors impacting sleep after childhood brain injury and provide insights into modifiable risk factors that can be targeted to improve this critical biological phenomenon that facilitates our mental health and well-being.

The aim of the present study is to explore the relationships between sleep and lifestyle factors in young adults who sustained TBI in childhood. The following lifestyle factors were explored based on their known impact on sleep in studies involving individuals who sustained TBI in adulthood^[23,24] and studies of healthy adults^[25-28]: Parenting status; nap duration; screen time, chronotype; use of tobacco, alcohol, caffeine, and medication. Consistent with evidence from the broader sleep literature about the relationship of these lifestyle factors and sleep outcomes^[12,25-28,30], we predict that significant associations would be identified between sleep and these lifestyle factors.

2. Materials and methods

2.1. Study design and ethics

This study was approved by the Human Research Ethics Committee of The Royal Children's Hospital (RCH – HREC Ref No: 30064), Melbourne, Australia. It forms part of a longitudinal, prospective study of long-term outcomes of childhood TBI^[31] and reports cross-sectional outcomes at 20-year post-injury.

2.2. Participants

Participants for this 20-year follow-up included young adults with a history of childhood TBI recruited from

consecutive admissions to the neurosurgical ward of The RCH between 1993 and 1997. Inclusion criteria in the original study were^[32]: (i) Age at injury between 0 and 12 years; (ii) documented evidence of TBI, including a period of altered consciousness at the time of injury; and (3) English speaking. Exclusion criteria were: (i) Penetrating head injury; (ii) head injury resulting from abuse; (iii) history of previous head injury; and (iv) evidence of pre-existing physical, neurological, psychiatric or developmental disorder. No additional inclusion/exclusion criteria were applied in this 20-year follow-up due to the longitudinal nature of this study and attrition. The study originally included 172 children with TBI and 35 typically developing controls (TDC), identified through the families of the injured children and local schools, and matched to the TBI group on age, sex, and socioeconomic status (SES). Reasons for dropouts in previous follow-ups were unwillingness to continue the study (9); deceased (2). Of the 196 invited for the 20-year follow-up, 67 participated and the reasons provided for not participating were: time constraints (1), loss of interest (3), and death (2); declined participation (13); declined participation after consenting (6); could not be contacted even with updated state electoral registration information (102); and did not complete some of the questionnaires presented in this study (2). The questionnaire data presented here are based on 67 participants (mild = 14; moderate = 27; severe = 13; and TDC = 13), while the actigraphy data are based on 58 participants (mild = 12; moderate = 22; severe = 11; and TDC = 13) due to technical problems with this measure.

TBI severity classification was based on the following: (i) Mild TBI ($n = 44$): Glasgow coma scale (GCS) score on admission of 13 – 15, post-traumatic amnesia (PTA) <24 h, and no abnormality on computed tomography (CT) or magnetic resonance imaging (MRI) scan; (ii) moderate TBI ($n = 81$): GCS on admission = 9 – 12, PTA 1 – 7 days, and/or abnormalities on CT or MRI scan; and (iii) severe TBI ($n = 47$): GCS = 3 – 8 at the time of admission, PTA > 7 days, and abnormalities on CT or MRI scan.

2.3. Procedure

A detailed account of the recruitment procedure and questionnaire administration methods has been reported previously^[20,33]. Briefly, all participants provided written consent and completed all questionnaires either in hardcopies (sent through post) or online through REDCap, and all actigraphy watches were sent to participants through post.

2.4. Measures

2.4.1. Demographic and injury-related information

A demographic questionnaire and medical records of participants provided information on sex, age at injury,

current age, employment status, level of education, and injury severity.

2.4.2. Lifestyle factors

General lifestyle factors were evaluated through administration of a study-designed questionnaire. Mean responses from these questions were assessed over a 14-day period (during which the actigraphy data were collected) to assess the following lifestyle factors:

- (i). Parenting status (*Do you have children? Yes/No*)
- (ii). Substance use: Frequency of alcohol and cigarette intake (*During the past 2 months which of these substances have you used?*).
- (iii). Screen time: Duration (*Number of hours spent using electronic device today, scored on a scale of 1 – 12 h*), daytime naps (*total time I spent napping during the day today, in hours*).
- (iv). Caffeine use (*How many caffeinated drinks did you take today, e.g., coke, coffee, tea, energy drink*). Options: 0, 1, 2, 3, 4, more than 4).
- (v). Medication use: Current or previous use of antidepressants, stimulants, and pain medications was assessed with this question in the study-designed questionnaire (*Have you, or are you currently taking any of these medications (e.g., antidepressants, stimulants)? Yes/No*).

2.4.3. Chronotype

Chronotype was assessed with the Morningness and Eveningness Questionnaire (MEQ), which assesses chronotype using 19 questions^[34]. The MEQ total score, obtained as a sum of responses from all items ranges from 16 to 86. Scores of 16 – 41, 42 – 58, and 59 – 86 were used to differentiate between participants with eveningness, intermediate, and morningness chronotypes, respectively.

2.4.4. Sleep outcomes

Subjective sleep quality was assessed with the Pittsburgh Sleep Quality Index (PSQI), which examines sleep quality over the past month using five descriptive questions and 14 multiple-choice questions. The PSQI produces a total score of 0 – 21, and scores above 5 indicated poor subjective sleep quality in this study^[35].

Objective sleep efficiency, defined as the ratio of total time spent asleep over total time spent in bed, was assessed using Actiwatch 2 (Phillips-Respironics). The actigraphy method estimates sleep and wake activity based on movement and correlates with key parameters on the polysomnography^[36]. We recorded actigraphy data and *Night Sleep Diaries* (used to validate actigraphy data) over 14 consecutive days. Consistent with previous actigraphy

studies, an actigraphy sleep efficiency score below 85% indicated poorer objective sleep^[37].

2.4. Statistical analysis

All analyses were performed using IBM SPSS Statistics (Version 29). Data were checked to ensure compliance with statistical assumptions using frequencies, distribution plots, skewness and kurtosis values, and with Shapiro–Wilk statistics. Differences in demographic factors between the TBI and TDC groups, and paired contrasts were conducted between the TDC and TBI severity groups using χ^2 tests, Mann–Whitney U tests, analysis of variance (ANOVA), and independent sample t -tests.

Before exploring the relationships between lifestyle factors and sleep outcomes, χ^2 tests and Mann–Whitney U test were used to compare the TBI severity groups to the TDC group on the sleep outcomes and lifestyle factors. Although we have previously reported similar comparisons in this sample for the sleep outcomes^[20,33], the current analysis extends the previous reports by looking at group differences in lifestyle factors and teasing out the differences in outcome between each TBI severity group and the control group.

To address the study aim, the relationships between subjective and objective sleep and lifestyle factors in the TBI group were explored using generalized linear models, since outcomes were mostly not normally distributed. Separate models were run for the subjective and objective sleep outcomes, with each model including these lifestyle factors: Caffeine use (morning, afternoon, evening, and total), screentime, nap duration, chronotype, substance use (alcohol and tobacco), parenting status, and medication use (stimulants, antidepressants, and pain medications). Age at follow-up was included in each model to control for its effect on the relationships assessed since age emerged as a potential confounding variable in the demographic comparisons and has been associated with sleep outcomes^[38]. Follow-up generalized linear models were conducted in just the TBI participants with poor subjective (PSQI > 5) or objective (sleep efficiency <85%) sleep outcomes to verify if similar factors predicted outcomes in this subgroup. To verify if the identified relationships were specific to the TBI group, similar analyses were conducted in the control group using Spearman correlations (since the small sample size was not suitable for generalized linear models). A statistical significance threshold of $P < 0.05$ was used for all analyses.

3. Results

3.1. Demographic characteristics

Demographic differences between 20-year follow-up TBI participants and non-participants (i.e., those who did not participate in this 20-year follow-up) have been

reported previously^[20] with results showing significantly more males ($\chi^2 [1, n = 172] = 9.33, P = 0.002$) and higher SES (median = 4.30, $U = 2541.50, P = 0.032$) in the non-participants compared to those who participated in this 20-year follow-up.

Table 1 presents results from demographic comparisons for this 20-year follow-up sample. Results show statistically significant differences in age at injury among the TBI severity groups ($P = 0.035$), with significant differences found between the mild and moderate TBI groups ($P = 0.032$). Age at follow-up was also significantly higher in the TBI compared to the TDC group ($P = 0.047$). The four group contrasts showed these significant differences in age at follow-up: TDC < mild TBI ($P = 0.002$) and mild TBI > moderate TBI ($P = 0.039$). The proportion of people with higher levels of education was also higher in the TDC compared to severe TBI group ($P = 0.037$).

3.2. Differences in lifestyle factors and sleep outcomes: TBI severity and TDC groups

Table 2 presents analyses comparing the TBI and TDC groups and the four groups (i.e., TDC, mild, moderate, and severe TBI), on lifestyle factors and sleep outcomes. There were significantly more parents in the TBI compared to TDC group ($P = 0.049$). All participants who have children were in the TBI group, and the majority of them (92%) had children below 8 years old. Pain medication use was higher in the TDC compared to the TBI group ($P = 0.048$). Subjective and objective sleep quality were not statistically different between the TBI and TDC groups, and neither were the proportion of participants presenting with poor subjective sleep quality (39% and 15%, $P = 0.109$), and poor objective sleep efficiency (67% and 81.8%, $P = 0.327$) significant in these group, respectively.

In the four group comparisons, there was a greater proportion of parents in the mild ($P = 0.037$) and severe ($P = 0.013$) TBI groups, compared to the TDC group. The proportion of young adults using pain medication was higher in the TDC compared to severe TBI group ($P = 0.018$), and stimulant medication use was higher in the mild compared to severe TBI group ($P = 0.037$). Evening caffeine use was significantly higher in the severe compared to mild TBI group ($P = 0.037$). Finally, subjective sleep quality was significantly poorer in the mild TBI compared to TDC ($P = 0.042$), and in the moderate TBI compared to the TDC ($P = 0.012$) and severe TBI ($P = 0.025$) groups.

3.3. Relationships between sleep outcomes and lifestyle factors in the TBI group

Results from generalized linear models assessing the relationships between sleep outcomes and lifestyle factors,

Table 1. Group differences in demographic characteristics

Demographic characteristics	TBI n=54	TDC n=13	P	Mild TBI (1) n=14	Moderate TBI (2) n=27	Severe TBI (3) n=13	Contrasts
Sex (male), n (%)	27 (50)	8 (61.5)	0.455	9 (64.3)	13 (48.1)	5 (38.5)	NS
Age at injury (years), M (SD)	6.5 (3.2)	-	-	8.4 (3.0)	5.7 (3.0)	6.0 (3.3)	1>2 ^c
Age at follow-up (years), M (SD)	27.7 (3.3)	25.9 (2.2)	0.047^a	29.2 (2.9)	27.1 (3.1)	27.1 (3.5)	TDC<1; 1>2 ^a
Socioeconomic status, M (SD)	4.1 (1.1)	3.4 (1.2)	0.095 ^b	3.7 (1.0)	4.2 (1.1)	4.2 (1.3)	NS ^b
Highest level of education							TC>3
<Year 10, n (%)	1 (1.9)	0	0.227	0	1 (3.7)	0	
Year 10 – 12, n (%)	12 (22.2)	5 (38.5)		2 (14.3)	8 (29.6)	2 (15.4)	
Technical education, n (%)	12 (22.2)	0		3 (21.4)	4 (14.8)	5 (38.5)	
Bachelor's and higher, n (%)	29 (53.7)	8 (61.5)		9 (64.3)	14 (51.9)	6 (46.2)	
Employment status			0.845				NS
Employed, n (%)	44 (81.5)	11 (84.6)		14 (100)	22 (81.5)	8 (61.5)	
Unemployed, n (%)	7 (13.0)	1 (7.7)		0	3 (11.1)	4 (30.8)	
Studying, n (%)	3 (5.6)	1 (7.7)		0	2 (7.4)	1 (7.7)	

Note: Bold font indicates significant group differences. Results are based on χ^2 tests, unless otherwise specified. ^aMann–Whitney U test, ^bIndependent sample t-test, ^cANOVA.

Abbreviations: NS: Not significant; TDC: Typically developing controls; TBI: Traumatic brain injury use.

Table 2. Group differences in lifestyle factors and sleep outcomes

	TBI n=54	TDC n=13	P	Mild TBI (1) n=14	Moderate TBI (2) n=27	Severe TBI (3) n=13	Contrasts
(A) Lifestyle factors							
Parenting status, n (%)	13 (24.1)	0	0.049	4 (28.6)	4 (14.8)	5 (38.5)	1 and 3>TDC
Screen time, M (SD)	4.7 (2.71)	4.41 (2.0)	0.893 ^a	5.3 (3.0)	4.6 (2.3)	4.4 (3.3)	NS ^a
Substance use							
Alcohol use, n (%)	47 (87.0)	11 (84.6)	0.818	11 (84.6)	11 (78.6)	11 (84.6)	NS
Tobacco use, n (%)	15 (27.8)	4 (30.8)	0.830	6 (42.9)	7 (25.9)	2 (15.4)	NS
Nap duration, M (SD)	5.3 (6.7)	6.2 (9.2)	0.981 ^a	4.6 (6.7)	6.7 (7.6)	3.1 (3.6)	NS ^a
Caffeine use, M (SD)							
Morning	0.8 (0.7)	0.8 (0.6)	0.874 ^a	0.9 (0.7)	0.8 (0.8)	0.7 (0.5)	NS ^a
Afternoon	0.5 (0.5)	0.4 (0.2)	0.353 ^a	0.4 (0.4)	0.6 (0.5)	0.6 (0.4)	NS ^a
Evening	0.4 (0.6)	0.3 (0.5)	0.839 ^a	0.1 (0.2)	0.5 (0.7)	0.4 (0.4)	3>1 ^a
Total	1.7 (1.2)	1.5 (0.8)	0.806 ^a	1.5 (1.0)	1.9 (1.5)	1.7 (0.9)	NS ^a
Medication use							
Stimulants, n (%)	7 (13)	2 (15.4)	0.818	4 (28.6)	3 (11.1)	0	1>3
Antidepressants, n (%)	9 (16.7)	1 (7.7)	0.415	1 (7.7)	4 (14.8)	2 (15.4)	NS
Pain medications, n (%)	21 (38.9)	9 (69.2)	0.048	7 (50.0)	11 (40.7)	3 (23.1)	TDC>3
Chronotype, M (SD)	53.5 (9.6)	54.0 (6.4)	0.793 ^a	54.3 (7.3)	53.0 (11.4)	53.5 (8.6)	NS ^a
(B) Sleep outcomes							
Subjective sleep quality, M (SD)	5.5 (2.9)	3.9 (1.9)	0.050 ^a	6.0 (3.1)	6.1 (2.7)	3.9 (2.5)	1>TDC; 2>TDC & 3 ^a
Actigraphy sleep efficiency, M (SD)	77.4 (12.8)	81.0 (5.4)	0.599 ^a	76.3 (16.8)	76.6 (13.3)	80.2 (5.4)	NS

Note: Bold font indicates significant group differences. Results are based on χ^2 tests, unless otherwise specified. Shift work and parenting: Yes or No; screen time: Scored on a scale of 1 – 12 h assessed over 14 days; substance use: In the last 2 month; daytime naps: Total time spent napping during the day assessed over 14 days; caffeine use: Number of caffeinated drinks take in a day, assessed over 14 days; medication use: Current or previous use; ^aMann–Whitney U test.

Abbreviations: NS: Not significant; TDC: Typically developing controls; TBI: Traumatic brain injury.

while controlling for the effect of age at follow-up in the TBI group, are presented in Table 3. The overall model assessing the lifestyle factors associated with poor subjective sleep quality was significant ($P < 0.001$), and two significant correlates were identified: Evening chronotype ($P < 0.001$) and use of tobacco in the past 2 months ($P < 0.001$). The model for objective sleep efficiency did not show a good fit ($P = 0.814$); however, being a parent was associated with poor objective sleep efficacy ($P = 0.038$). When these analyses were repeated in just the TBI participants who reported poor subjective (39%) and objective (67%) outcomes, tobacco use in the past 2 months again emerged as the only significant predictor ($P = 0.002$) of poor subject sleep quality, while being a parent ($P < 0.001$) and alcohol use in the past 2 months ($P = 0.035$) were associated with poor objective sleep efficiency. Figure 1 illustrates these findings.

3.4. Relationships between sleep outcomes and lifestyle factors in the TDC group

Results presented in Table S1 show a significant relationship only between morning chronotype and subjective sleep

quality ($P = 0.037$). No significant relationships were identified between objective sleep efficiency and lifestyle factors.

4. Discussion

This study explored the relationships between sleep (subjective and objective) and lifestyle factors in a sample of young adults who sustained TBI in childhood. In partial support of our hypothesis, subjective and objective sleep outcomes were predicted by some lifestyle factors in young adults with childhood TBI. Poor subjective sleep quality was significantly associated with evening chronotype and use of tobacco in the past 2 months, while being a parent and alcohol use in the past 2 months were associated with poor objective sleep efficiency. These findings provide preliminary insights into the relationships between sleep and lifestyle factors in young adulthood following childhood TBI.

Poorer subjective sleep quality was significantly associated with evening chronotype (i.e., a preference for later timing of sleep and wake) in the whole TBI group, but not in the TBI subgroup presenting with poor subjective

Table 3. Relationships between sleep outcomes and lifestyle factors in the TBI group

	Subjective sleep quality N=54				Objective sleep efficiency N=45			
	Estimates	SE	95% CI	P	Estimates	SE	95% CI	P
Caffeine use [†]								
Morning	81.1	211.2	-332.9, 495.1	0.701	16.4	1483.7	-2891.5, 2924.4	0.991
Afternoon	77.9	211.1	-335.9, 491.7	0.712	14.3	1483.3	-2892.8, 2921.5	0.992
Evening	80.3	211.1	-333.4, 494.12	0.704	23.4	1482.7	-2882.6, 2929.4	0.987
Total	-80.1	211.2	-494.1, 333.9	0.705	-13.2	1483.6	-2920.8, 2894.5	0.993
Screen time	-0.1	0.11	-0.3, 0.1	0.403	0.7	0.9	-1.0, 2.4	0.423
Nap duration	0.0	0.0	-0.1, 0.1	0.600	-0.5	0.4	-1.2, 0.2	0.144
Chronotype	-0.1	0.0	-0.2, -0.1	<0.001	0.2	0.3	-0.4, 0.8	0.440
Substance use								
Alcohol use	0.4	0.9	-1.4, 2.1	0.685	3.4	6.6	-9.4, 16.4	0.597
Tobacco use	-3.0	0.7	-4.4, -1.5	<0.001	3.1	5.7	-8.1, 14.3	0.585
Parenting status	0.1	0.7	-1.5, 1.4	0.685	-10.7	5.2	-20.9, -0.6	0.038
Medication use								
Stimulants	1.4	0.9	-0.3, 3.1	0.114	-4.6	6.9	-18.4, 8.9	0.506
Antidepressants	-1.5	0.8	-3.1, 0.1	0.061	-6.3	6.0	-18.1, 5.4	0.294
Pain medications	-0.9	0.6	-2.1, 0.3	0.125	-3.5	4.4	-12.1, 5.0	0.416
Age at follow-up	0.0	0.1	-0.2, 0.2	0.699	1.0	0.8	-0.5, 2.6	0.196

Note: Based on generalized linear models (controlling for the effect of age at follow-up). Bold face represents significant relationship between variables ($P < 0.05$). Caffeine use (number of caffeinated drinks take in a day), screen time duration (h), and nap duration (h) were averaged over 14 days; frequency of alcohol and tobacco use was based on the past 2 months; medication use results were based on current or previous usage. Fifty-four participants for subjective sleep variable include: Mild, $n=14$; moderate, $n=27$; and severe, $n=13$. Forty-five participants for objective sleep variable include: Mild, $n=12$; moderate, $n=22$; and severe, $n=11$.

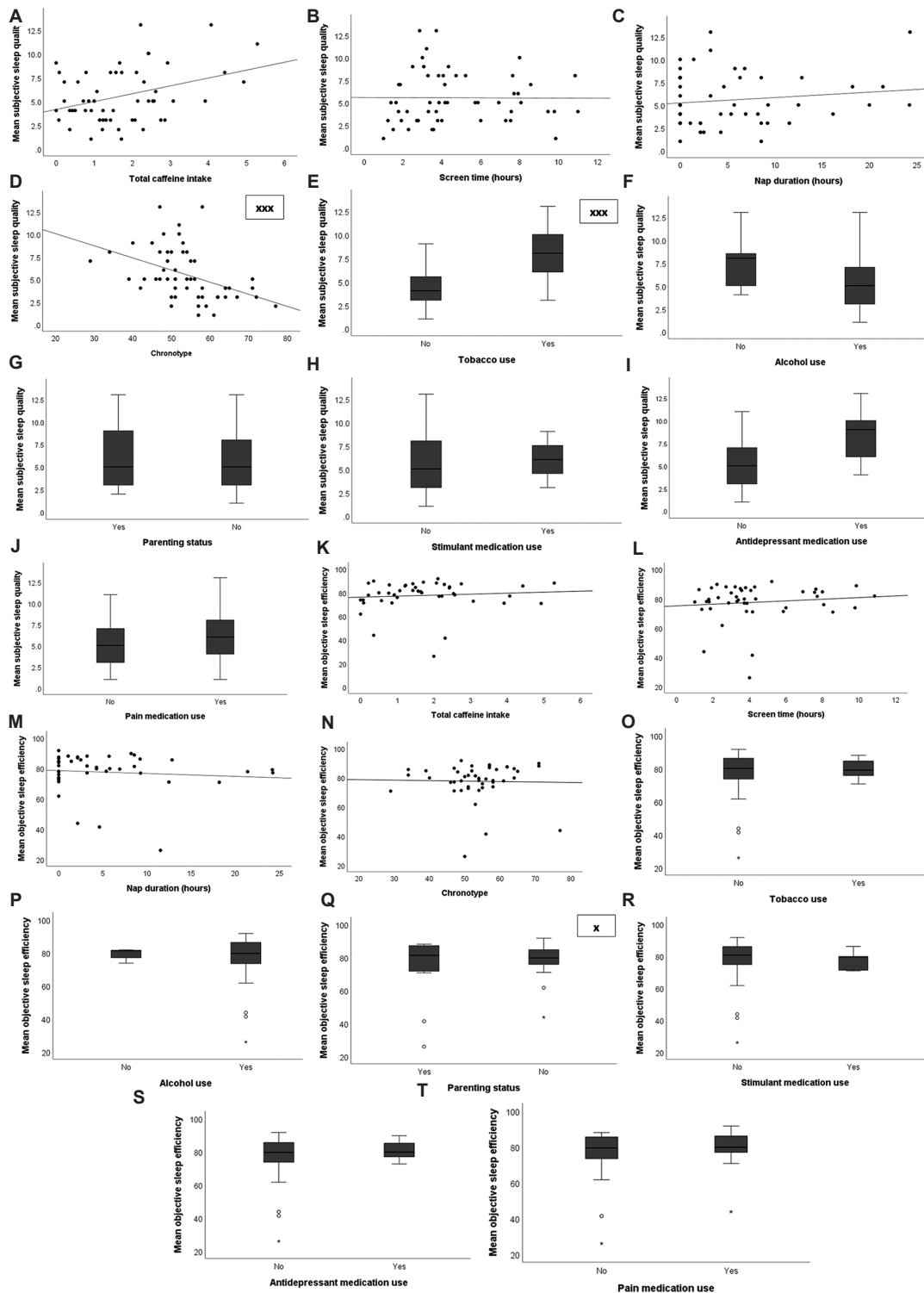


Figure 1. (A-T) Figure 1A-J illustrates the results on the relationships between subjective sleep and lifestyle factors. Figure 1K-T illustrate the results on the relationships between objective sleep and lifestyle factors. Results are based on generalized linear models (controlling for age at follow-up). Subjective sleep results were based on 54 participants including: Mild: $n = 14$; moderate: $n = 27$; severe $n = 13$. Objective sleep results are based on 45 participants including: Mild: $n = 12$; moderate: $n = 22$; and severe $n = 11$. Caffeine use (number of caffeinated drinks take in a day), screen time duration (h), and nap duration (h) were averaged over 14-days. Frequency of alcohol and tobacco use in the past 2 months; medication use results based on current or previous usage. *** $P < 0.001$; * $P < 0.05$.

sleep quality and chronotype did not differ between TBI and controls. This latter finding aligns with studies showing no differences in chronotype between adults who sustained TBI in adulthood and controls^[39]. Eveningness has been previously associated with increased insomnia symptoms^[28,40], poor sleep quality, and increased sleep debt (especially during week days) in healthy young adults^[41], but data on the relationship between chronotype and sleep quality in TBI are limited. Chronotype is a behavioral phenotype ensuing from the two processes that regulate sleep and wake: The internal circadian clock and sleep homeostasis^[42]. Evening chronotype is due to either a later circadian clock phase (later sleep and wake times), a slower homeostatic build-up of sleep pressure (causing a naturally low tendency of falling asleep early), or both, which are all possible explanations for the increased risk of poor sleep quality in our TBI participants with evening chronotype^[43]. A previous study in adults with TBI found no conclusive objective evidence of shift in circadian timing of sleep following TBI^[39], but the question of whether brain disruptions caused by childhood TBI contributes to shift in circadian timing or reduced homeostatic sleep regulation is a question for further research.

Tobacco use in the past 2 months was also significantly associated with poor subjective sleep quality in the whole TBI group, and in TBI participants who reported poor subjective sleep quality. This resonates with reports on the negative impact of smoking on sleep in population-based healthy smokers^[27]. Reviews on this relationship have indicated that cigarette smokers are more likely to experience difficulty initiating and maintaining sleep, breathing-related sleep problems, and daytime sleepiness^[44], and are about 47% more likely to experience sleep disturbance than non-smokers^[45]. Although the proportion of tobacco users were not significantly different between our TBI and TDC groups, this significant relationship was only found in the TBI group, suggesting greater vulnerability in this group to the negative effects of smoking on sleep quality. Clinically, smoking is associated with managing pain and depression, increased risk of snoring (e.g., due to upper airway inflammation), increased arousal, increased night waking (to sooth nicotine cravings especially in heavy smokers), and poor sleep hygiene (especially when people smoke close to bedtime)^[44,45]; all of which may have impacted subjective sleep quality in our TBI group. From a neurobiological perspective, the relationship identified in this TBI group may be because this group is more vulnerable to the known toxic effects of cigarette smoking on the brain (including increased oxidative stress, inflammation, and atherosclerosis)^[46]. This is likely because TBI may have interrupted the development of their sleep-related brain areas or hindered the effective regulation of

the sleep by the brain. We propose that the relationship between tobacco use and poor sleep quality in these young adults with childhood TBI may be related to a combination of these clinical and neurobiological factors, which can be examined in future studies.

Poor objective sleep efficiency was significantly associated with being a parent in the whole TBI group and in the subsample that reported poor objective sleep efficiency (<85% sleep efficiency). In this study, all participants with children were in the TBI group and 92% of them had children below 8 years old, suggesting that their poor sleep efficiency may be related to involvement with their children at night. Studies involving typically developing adults have reported that sleep quality can be affected in parent with younger children in instances where the child has sleep problems, family environment is stressful, parent is too involved in soothing the child at bedtime and during night awakenings, and parent has irregular routines^[47-50]. We hence propose that the significant relationship identified between being a parent and poor objective sleep efficiency in this sample is potentially due to some of these reasons.

Alcohol use in the last month was also significantly associated with poor sleep efficiency in the young adults with TBI who presented with poor sleep efficiency. This finding resonates with several studies that have associated alcohol consumption with poor sleep quality^[51,52]. Although many people use alcohol for its sleep-promoting effects, alcohol acts as a sedative and affects several neurotransmitter systems important for sleep regulation (e.g., GABAergic systems)^[53]. Alcohol reduces sleep quality through several mechanisms, including reducing sleep duration, increasing risk of breathing-related sleep problems, disrupting sleep architecture early in the night (when blood alcohol levels are high), and causing insomnia and abnormalities of circadian rhythms^[51,53]. Our finding regarding this relationship was present only in the young adults with TBI who had poor sleep efficiency (67% of TBI group), of which 83% endorsed using alcohol in the past 2 months. We propose that this finding indicates a greater effect of alcohol on this subgroup, potentially due to the negative impact of alcohol on their already vulnerable brain. The question of whether alcohol affects sleep efficiency in early TBI survivors through known mechanisms such as reduced melatonin secretion^[53], disrupted homeostatic regulation, or reduced neural sleep regulation^[51] remain open for future investigation.

4.1. Study limitations

Some limitations of the present study should be considered: (I) The small sample size used in this study limits the

robustness of the findings. (ii) Information about possible additional brain injuries in the TBI group in the years following their first injury is a potential confounding factor, which was not measured in this study. (iii) The findings regarding the significant relationships between sleep outcomes and substances such as alcohol and tobacco use should be interpreted with caution because critical questions around dose, type, timing, frequency, duration, and reason for using these substances were not assessed in the present study. (iv) We are unable to draw casual inferences between TBI and the identified factors due to the cross-sectional nature of this evaluation.

4.2. Clinical implications

Some clinical implications of our findings are as follows. The significant association between poor sleep quality and evening chronotype^[40] highlights greater vulnerability to sleep problems in young adults with childhood TBI who have an evening chronotype and suggests the need to pay attention to those with this risk factor. Although being a parent with a young child is a known risk factor for poor sleep^[47,49], young adults with TBI may be more vulnerable to such problems because of the potential impact of TBI on sleep-related brain mechanisms and should be supported with interventions to help improve their sleep outcomes. Clinicians and young people living with a childhood TBI should be informed about the identified relationship between tobacco, alcohol use, and sleep outcomes, with due consideration for the lack of information about dose, type of medication, duration of use, and frequency of use in this study.

5. Conclusion

This study investigated the relationships between sleep subjective and objective outcomes, and lifestyle factors in young adults who sustained TBI in childhood. Results highlight lifestyle factors associated with subjective (i.e., chronotype and tobacco use) and objective sleep (alcohol and being a parent) outcomes in this young adult TBI sample. These preliminary findings highlight some potential modifiable factors, raise interesting issues for clinical consideration, and indicate the need for further investigations of these relationships to identify more avenues for sleep interventions in young adult survivors of childhood TBI.

Acknowledgments

We thank the Victorian Electoral Commission (Australia) for their support with participant recruitment and appreciate all participating families for their dedication to this longitudinal study.

Funding

This project is supported by the Australian National Health and Medical Research Council project and fellowship funding, Victorian Operational Infrastructure fund. Edith Botchway-Commey was funded by the University of Melbourne International Fee Remission and the Melbourne International Research Scholarships.

Conflict of interest

The authors declare that they have no competing interests.

Author contributions

Conceptualization: Edith Botchway-Commey, Celia Godfrey, Vicki Anderson, Cathy Catroppa

Formal analysis: Edith Botchway-Commey, Christian L. Nicholas

Investigation: Edith Botchway-Commey, Celia Godfrey, Vicki Anderson, Cathy Catroppa

Methodology: All authors

Project administration: Edith Botchway-Commey, Celia Godfrey, Vicki Anderson, Cathy Catroppa

Supervision: Celia Godfrey, Vicki Anderson, Cathy Catroppa

Writing – original draft: Edith Botchway-Commey

Writing – review & editing: All authors

Ethics approval and consent to participate

This study was approved by the Human Research Ethics Committee of The Royal Children's Hospital (RCH – HREC Ref No: 30064), Melbourne, Australia.

Consent for publication

All participants provided written consent for this study, using the Study Information Statement and Consent Form, which included information about intentions to publish the results from this study in peer-reviewed journals.

Availability of data

Not applicable.

Further disclosure

Part of the findings (specifically mean group differences of subjective and objective sleep outcomes) has been previously published (DOI: 10.1089/neu.2018.5743; DOI: 10.1080/09638288.2019.1578422). However, the present analysis extends these previous reports by looking at group differences in lifestyle factors and teasing out the differences in outcome between each TBI severity group and the control group.

References

1. Roozenbeek B, Maas AIR, Menon DK, 2013, Changing patterns in the epidemiology of traumatic brain injury. *Nat Rev Neurol*, 9: 231–236.
<https://doi.org/10.1038/nrneurol.2013.22>
2. Menon DK, Schwab K, Wright DW, *et al.*, 2010, Position statement: Definition of traumatic brain injury. *Arch Phys Med Rehabil*, 91: 1637–1640.
<https://doi.org/10.1016/j.apmr.2010.05.017>
3. Gagner C, Landry-Roy C, Laine F, *et al.*, 2015, Sleep-wake disturbances and fatigue after pediatric traumatic brain injury: A systematic review of the literature. *J Neurotrauma*, 32: 1539–1552.
<https://doi.org/10.1089/neu.2014.3753>
4. Anderson V, Spencer-Smith M, Wood A, 2011, Do children really recover better? Neurobehavioural plasticity after early brain insult. *Brain*, 134: 2197–2221.
<https://doi.org/10.1093/brain/awr103>
5. Desseilles M, Dang-Vu T, Schabus M, *et al.*, 2008, Neuroimaging insights into the pathophysiology of sleep disorders. *Sleep*, 31: 777–794.
<https://doi.org/10.1093/sleep/31.6.777>
6. Van Der Werf YD, Altena E, Schoonheim MM, *et al.*, 2009, Sleep benefits subsequent hippocampal functioning. *Nat Neurosci*, 12: 122–123.
<https://doi.org/10.1038/nn.2253>
7. Tononi G, Cirelli C, 2014, Sleep and the price of plasticity: From synaptic and cellular homeostasis to memory consolidation and integration. *Neuron*, 81: 12–34.
<https://doi.org/10.1016/j.neuron.2013.12.025>
8. Zhou Y, Greenwald BD, 2018, Update on insomnia after mild traumatic brain injury. *Brain Sci*, 8: 223.
<https://doi.org/10.3390/brainsci8120223>
9. Baumann CR, Stocker R, Imhof HG, *et al.*, 2005, Hypocretin-1 (orexin A) deficiency in acute traumatic brain injury. *Neurology*, 65: 147–149.
<https://doi.org/10.1212/01.wnl.0000167605.02541.f2>
10. Imbach LL, Valko PO, Li T, *et al.*, 2015, Increased sleep need and daytime sleepiness 6 months after traumatic brain injury: A prospective controlled clinical trial. *Brain*, 138: 726–735.
<https://doi.org/10.1093/brain/awu391>
11. Thomée S, Härenstam A, Hagberg M, 2011, Mobile phone use and stress, sleep disturbances, and symptoms of depression among young adults - A prospective cohort study. *BMC Public Health*, 11: 66.
<https://doi.org/10.1093/sleep/31.4.473>
12. Leblanc M, Mérette C, Savard J, *et al.*, 2009, Incidence and risk factors of insomnia in a population-based sample. *Sleep*, 32: 1027–1038.
<https://doi.org/10.1093/sleep/32.8.1027>
13. Lawrence D, Mitrou F, Zubrick SR, 2009, Smoking and mental illness: Results from population surveys in Australia and the United States. *BMC Public Health*, 9: 285.
<https://doi.org/10.1186/1471-2458-9-285>
14. Botchway EN, Godfrey C, Anderson VA, *et al.*, 2019, A systematic review of sleep-wake disturbances in childhood traumatic brain injury: Relationship with fatigue, depression, and quality of life. *J Head Trauma Rehabil*, 34: 241–256.
<https://doi.org/10.1097/HTR.0000000000000446>
15. Luther M, Cordts KMP, Williams CN, 2019, Sleep wake disturbances in children surviving neurocritical care with traumatic brain injury: A systematic review. *Neurocrit Care*, 31: S304.
16. Djukic S, Phillips NL, Lah S, 2022, Sleep outcomes in pediatric mild traumatic brain injury: A systematic review and meta-analysis of prevalence and contributing factors. *Brain Inj*, 36: 1289–1322.
<https://doi.org/10.1080/02699052.2022.2140198>
17. Bogdanov S, Brookes N, Epps A, *et al.*, 2019, Sleep disturbance in children with moderate or severe traumatic brain injury compared with children with orthopedic injury. *J Head Trauma Rehabil*, 34: 122–131.
<https://doi.org/10.1097/HTR.0000000000000426>
18. Ekinci O, Okuyaz C, Günes S, *et al.*, 2017, Sleep and quality of life in children with traumatic brain injury and ADHD: A comparison with primary ADHD. *Int J Psychiatry Med*, 52: 72–87.
<https://doi.org/10.1177/0091217417703288>
19. Botchway-Commey E, Godfrey C, Ryan NP, *et al.*, 2022, The link between sleep and quality of life in childhood traumatic brain injury. In: Rajendram R, Preedy VR, Martin CR, editors. *Molecular, Physiological, and Behavioral Aspects of Traumatic Brain Injury*. Ch. 45. London: Academic Press, p563–573.
<https://doi.org/10.1016/B978-0-12-823036-7.00025-6>
20. Botchway EN, Godfrey C, Anderson V, *et al.*, 2019, Outcomes of subjective sleep-wake disturbances twenty years after traumatic brain injury in childhood. *J Neurotrauma*, 36: 669–678.
<https://doi.org/10.1089/neu.2018.5743>
21. Buysse DJ, Angst J, Gamma A, *et al.*, 2008, Prevalence, course, and comorbidity of insomnia and depression in young adults. *Sleep*, 31: 473–480.
<https://doi.org/10.1093/sleep/31.4.473>
22. Owens J, 2014, Adolescent Sleep Working Group, Committee

- on Adolescence, 2014, Insufficient sleep in adolescents and young adults: An update on causes and consequences. *Pediatrics*, 34: e921–e932.
<https://doi.org/10.1542/peds.2014-1696>
23. Ouellet MC, Beaulieu-Bonneau S, Morin CM, 2015, Sleep-wake disturbances after traumatic brain injury. *Lancet Neurol*, 14: 746–757.
[https://doi.org/10.1016/S1474-4422\(15\)00068-X](https://doi.org/10.1016/S1474-4422(15)00068-X)
24. Beaulieu-Bonneau S, Morin CM, 2012, Sleepiness and fatigue following traumatic brain injury. *Sleep Med*, 13: 598–605.
<https://doi.org/10.1016/j.sleep.2012.02.010>
25. Clark I, Landolt HP, 2017, Coffee, caffeine, and sleep: A systematic review of epidemiological studies and randomized controlled trials. *Sleep Med Rev*, 31: 70–78.
<https://doi.org/10.1016/j.smrv.2016.01.006>
26. Exelmans L, Van den Bulck J, 2016, Bedtime mobile phone use and sleep in adults. *Soc Sci Med*, 148: 93–101.
<https://doi.org/10.1016/j.socscimed.2015.11.037>
27. Cohrs S, Rodenbeck A, Riemann D, *et al.*, 2014, Impaired sleep quality and sleep duration in smokers - Results from the German Multicenter Study on Nicotine Dependence. *Addict Biol*, 19: 486–496.
<https://doi.org/10.1111/j.1369-1600.2012.00487.x>
28. Simor P, Zavecz Z, Pálosi V, *et al.*, 2015, The influence of sleep complaints on the association between chronotype and negative emotionality in young adults. *Chronobiol Int*, 32: 1–10.
<https://doi.org/10.3109/07420528.2014.935786>
29. Botchway EN, Godfrey C, Ryan NP, *et al.*, 2020, Sleep disturbances in young adults with childhood traumatic brain injury: Relationship with fatigue, depression, and quality of life. *Brain Inj*, 34: 1579–1589.
<https://doi.org/10.1080/02699052.2020.1832704>
30. Nicholas CL, Gourlay CG, Chan JKM, 2018, Social drinking: Current findings on acute and chronic effects upon sleep disturbance and brain activity in adolescents and young adults. In: Murphy PN, editor. *The Routledge International Handbook of Psychobiology*. UK: Routledge, p367–387.
31. Catroppa C, Anderson V, 2005, A prospective study of the recovery of attention from acute to 2 years following pediatric traumatic brain injury. *J Int Neuropsychol Soc*, 11: 84–98.
<https://doi.org/10.1017/S1355617705050101>
32. Anderson VA, Catroppa C, Rosenfeld J, *et al.*, 2000, Recovery of memory function following traumatic brain injury in pre-school children. *Brain Inj*, 14: 679–692.
<https://doi.org/10.1080/026990500413704>
33. Botchway EN, Godfrey C, Nicholas CL, *et al.*, 2020, Objective sleep outcomes 20 years after traumatic brain injury in childhood. *Disabil Rehabil*, 42: 2393–2401.
<https://doi.org/10.1080/09638288.2019.1578422>
34. Terman M, Terman JS, 2005, Light therapy for seasonal and nonseasonal depression: Efficacy, protocol, safety, and side effects. *CNS Spectr*, 10: 647–663.
<https://doi.org/10.1017/s1092852900019611>
35. Buysse DJ, Reynolds CF, Monk TH, *et al.*, 1989, The Pittsburgh Sleep Quality Index: A new instrument for psychiatric practice and research. *Psychiatry Res*, 28: 193–213.
[https://doi.org/10.1016/0165-1781\(89\)90047-4](https://doi.org/10.1016/0165-1781(89)90047-4)
36. Sadeh A, 2011, The role and validity of actigraphy in sleep medicine: An update. *Sleep Med Rev*, 15: 259–267.
<https://doi.org/10.1016/j.smrv.2010.10.001>
37. Blytt KM, Bjorvatn B, Husebo B, *et al.*, 2017, Clinically significant discrepancies between sleep problems assessed by standard clinical tools and actigraphy. *BMC Geriatr*, 17: 253.
<https://doi.org/10.1186/s12877-017-0653-7>
38. Kocavska D, Lysen TS, Dotinga A, *et al.*, 2021, Sleep characteristics across the lifespan in 1.1 million people from the Netherlands, United Kingdom and United States: A systematic review and meta-analysis. *Nat Hum Behav*, 5: 113–122.
<https://doi.org/10.1038/s41562-020-00965-x>
39. Steele DL, Rajaratnam SMW, Redman JR, *et al.*, 2005, The effect of traumatic brain injury on the timing of sleep. *Chronobiol Int*, 22: 89–105.
<https://doi.org/10.1081/cbi-200042428>
40. Raman S, Coogan AN, 2019, A cross-sectional study of the associations between chronotype, social jetlag and subjective sleep quality in healthy adults. *Clocks Sleep*, 2: 1–6.
<https://doi.org/10.3390/clockssleep2010001>
41. Carciofo R, 2020, Morningness-eveningness and affect: The mediating roles of sleep quality and metacognitive beliefs. *Sleep Biol Rhythms*, 18: 17–26.
<https://doi.org/10.1007/s41105-019-00238-9>
42. Borbély AA, Daan S, Wirz-Justice A, *et al.*, 2016, The two-process model of sleep regulation: A reappraisal. *J Sleep Res*, 25: 131–143.
<https://doi.org/10.1111/jsr.12371>
43. Dijk DJ, Lockley SW, 2002, Invited review: Integration of human sleep-wake regulation and circadian rhythmicity. *J Appl Physiol* (1985), 92: 852–862.
<https://doi.org/10.1152/jappphysiol.00924.2001>
44. Htoo A, Talwar A, Feinsilver SH, *et al.*, 2004, Smoking and sleep disorders. *Med Clin North Am*, 88: 1575–1591.

- <https://doi.org/10.1016/j.mcna.2004.07.003>
45. Amiri S, Behnezhad S, 2020, Smoking and risk of sleep-related issues: A systematic review and meta-analysis of prospective studies. *Can J Public Health*, 111: 775–786.
<https://doi.org/10.17269/s41997-020-00308-3>
46. Liu JT, Lee IH, Wang CH, *et al.*, 2013, Cigarette smoking might impair memory and sleep quality. *J Formos Med Assoc*, 112: 287–290.
<https://doi.org/10.1016/j.jfma.2011.12.006>
47. Sadeh A, Tikotzky L, Scher A, 2010, Parenting and infant sleep. *Sleep Med Rev*, 14: 89–96.
<https://doi.org/10.1016/j.smrv.2009.05.003>
48. Brand S, Gerber M, Hatzinger M, *et al.*, 2009, Evidence for similarities between adolescents and parents in sleep patterns. *Sleep Med*, 10: 1124–1131.
<https://doi.org/10.1016/j.sleep.2008.12.013>
49. Brand S, Hatzinger M, Beck J, *et al.*, 2009, Perceived parenting styles, personality traits and sleep patterns in adolescents. *J Adolesc*, 32: 1189–1207.
<https://doi.org/10.1016/j.adolescence.2009.01.010>
50. Merrill RM, Slavik KR, 2023, Relating parental stress with sleep disorders in parents and children. *PLoS One*, 18: e0279476.
<https://doi.org/10.1371/journal.pone.0279476>
51. Colrain IM, Nicholas CL, Baker FC, 2014, Alcohol and the sleeping brain. *Handb Clin Neurol*, 125: 415–431.
<https://doi.org/10.1016/B978-0-444-62619-6.00024-0>
52. de Zambotti M, Baker FC, Sugarbaker DS, *et al.*, 2014, Poor autonomic nervous system functioning during sleep in recently detoxified alcohol-dependent men and women. *Alcohol Clin Exp Res*, 38: 1373–1380. <https://doi.org/10.1111/acer.12384>
53. He S, Hasler BP, Chakravorty S, 2019, Alcohol and sleep-related problems. *Curr Opin Psychol*, 30: 117–122.
<https://doi.org/10.1016/j.copsyc.2019.03.007>

ORIGINAL RESEARCH ARTICLE

Cognition damage due to disruption of cyclic adenosine monophosphate-related signaling pathway in melatonin receptor 2 knockout mice

He-Zhou Huang^{1†}, Xiang Wang^{2†}, and Dan Liu^{3*}¹Department of Pathophysiology, Key Laboratory of Neurological Disorders of the Education Ministry, School of Basic Medicine, Tongji Medical College, Huazhong University of Science and Technology, Wuhan, China²Department of Histology and Embryology, Medical College, Jiangnan University, Wuhan, China³Department of Genetics, School of Basic Medicine, Tongji Medical College, Huazhong University of Science and Technology, Wuhan, China**Abstract**

Alzheimer's disease (AD) was characterized by the presence of neurofibrillary tangles and senile plaques. Although melatonin plays an important role in AD, its mechanism is still unknown. In this study, we found obvious cognition damage in melatonin receptor 2 knockout mice (MT2KO) and double knockout mice (DKO), but not in melatonin receptor 1 knockout mice (MT1KO). To explore the mechanism in-depth, we attempted to determine the levels of metabolites and amyloid- β peptide (A β). A high level of Cho/tCr (choline/total creatine) was detected in MT2KO and MT1KO by nuclear magnetic resonance (NMR), while a high level of myo-inositol/total creatine (ml/tCr) was only detected in MT1KO. A higher ratio of A β _{42/40} was found in MT2KO, but not in MT1KO and DKO. We also found an abnormal increase of plaque detected by the A3981 antibody in MT2KO and DKO. Furthermore, a huge decrease of postsynapses was confirmed in MT2KO and DKO, but not MT1KO, accompanied by a low level of phosphorylated cyclic adenosine monophosphate (cAMP) response element-binding protein (CREB) at the site of serine 133 and a low activity of protein kinase A. Finally, the cAMP, cyclic guanosine monophosphate, and cAMP-regulated guanine nucleotide exchange factor (EPAC) were detected. We observed a significant decrease of cAMP and EPAC2 in MT2KO, but not MT1KO. Thus, we identified that cAMP-related signaling pathway was disturbed in MT2KO and was critical for normal cognitive function.

Keywords: Melatonin receptor 2; Plaque; Cyclic adenosine monophosphate; cAMP response element-binding; Cognition

1. Introduction

Melatonin (N-acetyl-5-methoxy tryptamine, MT) was synthesized by the pineal gland, and its level was controlled by circadian rhythms. Melatonin plays a role in its signal transduction and acts as an antioxidant. Melatonin receptor is divided into two types: Melatonin receptor 1 (MT1) and melatonin receptor 2 (MT2). Both of them were G-protein-coupled receptors, which can activate protein kinase A (PKA), but their signal transduction is fundamentally different^[1].

[†]These authors contributed equally to this work.

***Corresponding author:**
Dan Liu
(liudan_echo@mail.hust.edu.cn)

Citation: Huang H, Wang X, Liu D, 2023, Cognition damage due to disruption of cyclic adenosine monophosphate-related signaling pathway in melatonin receptor 2 knockout mice. *Adv Neuro*, 2(3): 0974.
<https://doi.org/10.36922/an.0974>

Received: May 22, 2023

Accepted: July 13, 2023

Published Online: August 11, 2023

Copyright: © 2023 Author(s). This is an Open-Access article distributed under the terms of the Creative Commons Attribution License, permitting distribution, and reproduction in any medium, provided the original work is properly cited.

Publisher's Note: AccScience Publishing remains neutral with regard to jurisdictional claims in published maps and institutional affiliations.

MT1 receptor transduced several cellular responses through both pertussis toxin-sensitive and -insensitive pathways. Activation of the MT1 receptor through G_i protein inhibited forskolin-stimulated cyclic adenosine monophosphate (cAMP) formation, PKA activity, and phosphorylation of the cAMP-responsive element-binding protein (CREB)^[2] and through G_q increases intracellular calcium^[3]. Activation of recombinant MT2 receptors expressed in mammalian cells inhibited forskolin-stimulated cAMP formation^[4,5]. In COS-7 cells expressing the hMT2 receptor, melatonin induces c-Jun N-terminal kinase through pertussis toxin-sensitive (G_i) and -insensitive (G_{16}) proteins^[6].

It was already known that melatonin abnormality is involved in the pathogenesis of many diseases, such as autism, and Alzheimer's disease (AD)^[7,8]. In AD patients, the MT2 expression was decreased significantly, but the expression of MT1 was increased^[9]. During neurodegeneration, the cytoskeleton can be erroneously assembled in neuron and a deficit in signal transduction could happen in neuron^[10,11]. Melatonin has been demonstrated to accelerate cytoskeletal remodeling through a melatonin receptor-dependent pathway to promote nerve regeneration after telangiectasia^[12]. MT2 stimulated axonogenesis and enhances synaptic transmission by activating the Akt signaling pathway^[13]. Our experiment results also demonstrated that melatonin could effectively ameliorate tau hyperphosphorylation induced by wortmannin, calyculin A, and okadaic acid^[14-17].

Melatonin has also been shown to significantly decrease amyloid- β peptide ($A\beta$) production^[18,19]. It has been reported that melatonin could reduce soluble amyloid precursor protein (APP) by disturbing APP maturation and finally reducing $A\beta$ ^[20]. The APP mRNA was significantly decreased in PC12 cells following pretreatment with melatonin, but this effect was not present in human neuroblastoma^[21]. In addition, the binding of melatonin with $A\beta_{40}$ and $A\beta_{42}$ *in vitro* strongly inhibited the formation of senile plaque and β -folding^[18]. The binding occurred at the residue of 29–40, which shows hydrophobic properties^[22].

Our results showed that melatonin could effectively reduce $A\beta$ in wild-type N2a and N2a/APP^[23]. However, it has also been reported that melatonin does not affect the stability of $A\beta_{40}$ and $A\beta_{42}$ ^[24]. These results demonstrated that melatonin has a strong effect on the $A\beta$, but it was unknown how melatonin executes its effect on AD, considering its antioxidant properties. Here, we used the melatonin receptor knockout mice, including C3H, MT1 knockout (MT1KO), MT2 knockout (MT2KO), and double knockout mice (DKO). We found cognition damage

in MT2KO mice. Then, we used $A\beta$ ELISA to determine the amount of $A\beta_{40}$ and $A\beta_{42}$ and found a relatively high $A\beta_{42}$ level in MT2KO mice but a comparable $A\beta_{40}$ level in three types of knockout mice. A3981, a special antibody, was used to label the senile plaque; we found that there were lots of plaque in the hippocampus of MT2KO mice. Golgi staining and Western blot showed that postsynaptic proteins were obviously decreased in MT2KO mice due to the disruption of cAMP-related signaling pathway.

2. Materials and methods

2.1. Animals

The transgenic mice were obtained from Professor D. Weaver of the University of Massachusetts Medical School. All animals were kept in a room on a 12 h light-dark cycle and set at 25°C and were given sufficient food and water. All animal experiments were carried out according to the "Policies on the Use of Animals and Humans in Neuroscience Research" revised and approved by the Society for Neuroscience in 1995. A total of 40 mice were divided into four groups: C3H, MT2KO mice, MT1KO mice, and DKO mice.

2.2. Step-down inhibitory avoidance task

The step-down inhibitory avoidance task was carried out in adherence to the procedures described in detail elsewhere. The testing apparatus consisted of an acrylic box (30 × 30 × 30 cm) with a floor made of a parallel stainless steel grid (1.0 mm in diameter) spaced 1 cm apart. A safe platform (5 cm in height, 5 cm in diameter) was fixed at one corner of the box. Each mouse was placed initially on the safe platform and an electric shock (36 V, 1.5 mA, alternate current, 50 Hz) was delivered to the grid. Before testing commenced, each mouse was habituated to the apparatus for 3 min. When the mice stepped down onto the grid floor, they received a foot shock and jumped back onto the safe platform. For a while, the mice went up and down between the platform and the grid, and eventually, they remained on the platform. The time the mice spent on learning on the platform continuously for 5 min was recorded as the latency of the acquisition test (day 1). The mice were tested for retention 24 h later (day 2) and were tested for recall 5 days later (day 7), by placing the mice on the platform, and the step-down latency was recorded for a maximum of 3 min.

2.3. Functional magnetic resonance imaging and NMR

The volume of the hippocampus was measured from the *in vivo* anatomical images with a manual approach. The volume of the hippocampus of each animal was measured from the anatomical images in their native space by

drawing a region of interest (ROI) representing the bilateral hippocampus on the photograph. The total volume of the hippocampus can be determined by adding up the volume measured from each anatomical image.

All proton NMR ($^1\text{H NMR}$) experiments were performed on a Bruker-500 spectrometer at room temperature. A pulse-acquisition sequence was used with a 90° flip angle, a 13 s relaxation delay to ensure full relaxation, a spectral width of 10,000 Hz, 32 k data points, and 64 scans. The spectra were zero-filled to 64 k, corrected manually for phase and baseline, and referenced to the chemical shift of the trimethylsilyl-propionic-2,2,3,3-d₄ acid (TSP) methyl peaks at 0 ppm. Peak area integration was performed using standard routines provided by the Topspin software package (version 2.0, Bruker). Using TSP as the external reference, the absolute concentrations of metabolites were determined from the spectra and calculated in the unit of mmol/kg wet tissue weight.

2.4. Antibodies and kits

NR2B antibody against N-methyl-D-aspartic acid receptor (NMDA) receptor subunit 2B was obtained from Abcam (Cambridge, UK). NR2A subunit of NMDA receptors (NR2A) antibody against NMDA receptor subunit 2A glutamate receptor type 1 (Glur1) antibody against was obtained from Millipore. Glur1s845 antibody against phosphor-AMPA receptor 1 at serine 845, PKA α antibody against PKA catalytic subunit α isoform, and PKA β antibody against PKA type I β regulatory subunit were obtained from Santa Cruz. Postsynaptic protein-95 (PSD95) antibody against postsynaptic density protein 95 and postsynaptic protein-93 (PSD93) antibody against postsynaptic density protein 93 were obtained from Abcam. pS133-CREB antibody against CREB at serine 133, CREB antibody against CREB, and P-APP antibody against APP at threonine 668 were obtained from cell signaling. Vesicle-associated membrane protein 2 antibody against vesicle-associated membrane protein 2 and MunC18 antibody against MunC18 were obtained from Abcam. Synaptophysin antibody against synaptophysin was acquired from Sigma. 4G8 antibody against APP was obtained from Covance. 22C11 antibody against APP N-terminus was obtained from Millipore. A3981 antibody against senile plaque was acquired from Sigma. Anti-rabbit IRDye and anti-mouse IRDye were purchased from Li-Cor Biosciences (Lincoln, NE, USA). The BCA kit was purchased from Pierce (Rockford, IL, USA).

2.5. Western blot

Hippocampus was removed from the brain and homogenized in tissue homogenate buffer containing NaCl 50 mM, Tris 10 mM, EDTA- $\text{Na}_2 \cdot 2\text{H}_2\text{O}$ 1 mM,

$\text{Na}_3\text{VO}_4 \cdot 12\text{H}_2\text{O}$ 0.5 mM, NaF 50 mM, benzyl benzene 1 mM, and phenylmethylsulfonyl fluoride 1 mM. The tissue was added to one-third sample buffer containing 8% sodium dodecyl sulfate (SDS), tris 200 mM, and 40% glycerol and boiled for 10 min. Lysate was centrifuged at $12,000 \times g$ for 10 min at 4°C , and then, the supernatant was stored at -80°C . The supernatant's protein concentration was detected using the BCA method. The same amount of protein was separated by SDS-polyacrylamide gel electrophoresis (10%) and then transferred to the nitrocellulose filter membrane. The membranes containing the protein were blocked by the 3% bovine serum albumin (BSA) and incubated with the antibody at 4°C overnight.

Using goat anti-mouse secondary antibody, conjugate to IRDyeTM (1:10000, LI-COR Biosciences), combined with mouse-derived primary antibody, or goat anti-rabbit secondary antibody, conjugate to IRDyeTM (1:10000, LI-COR Biosciences), combined with rabbit-derived primary antibody, the nitrocellulose membrane was incubated with the corresponding secondary antibody at room temperature for 1 h and then scanned using Odyssey[®] Imager (LI-COR Biosciences).

2.6. Immunohistochemistry

Mice were anesthetized with 6% chloral hydrate and perfused with 300 mL saline rapidly and then perfused with 500 mL 4% paraformaldehyde for 2 h. The brain was removed from the skull and sliced into 30 μm with Vibratome (Leica, VT1000S, Germany) after being post-fixed in the same fixative in a 50 mL centrifuge tube. The brain slice was soaked in the PBS-0.5% Triton-0.3% H_2O_2 to remove the endogenous hydrogen peroxidase and then block with 3% BSA for 30 min. After that, the slice was incubated with an antibody (1:200) for 48 h at 4°C . Then, the slice was incubated with a biotin-labeled secondary antibody for 1 h in a 37°C oven and dyed with the diaminobenzidine tetrachloride system (Bei Jing, ZSGB, 9032). The images were taken with a light microscope (Olympus BX60, Tokyo, Japan).

2.7. Nissl staining

The slides were dewaxed in xylene I and xylene II for 15 min in each solution. Then, the slides were hydrated in a series of gradient alcohol (100% alcohol I, 100% alcohol II, 95% alcohol, 90% alcohol, 80% alcohol, 70% alcohol, and 50% alcohol) for 5 min in each alcohol. The slides were then soaked in distilled water 3 times, for 5 min each time. Then, the slides were put in a 60°C incubator and dyed with 1% toluidine blue for 40 min (or dyed with tar violet for 30 s). After the excess dye was washed away with distilled water, the slides were dehydrated in 70%, 80%, 95%, and 100% ethanol, respectively, and then

cleared with xylene. Finally, a neutral gum seal was used for coverslipping.

2.8. Golgi staining

The mice were anesthetized with 6% chloral hydrate, the perfusion tube was inserted into the aorta of the mice, and the normal saline containing 0.5% sodium nitrite at 37°C was used for perfusion for about 5 min until the blood of the mice was removed. The perfusion solution was replaced with 4% polymethyl methacrylate.

The first 100 mL of the perfusion solution was dripped quickly, and then, the rest was dripped slowly for about 2 h; next, the perfusion solution was replaced with mordant solution (1000 mL mordant solution containing 50 g chloral hydrate, 50 g potassium dichromate, and 100 mL 40% formaldehyde solution). The fixed brain tissues of mice were immersed in mordant solution at room temperature for 3 days, and then, the specimens were placed in silver nitrate solution in the dark for 3 days, and the solution was changed every day. Finally, the specimens were washed with ultrapure water, and the brain slices were cut into 30 μm thick brain slices with an oscillating microtome. The cut brain slices were pasted on a clean slide, dehydrated and cleared, and covered with a cover slip for observation under an optical microscope.

2.9. cAMP and Cyclic guanosine monophosphate (cGMP) ELISA

cAMP and cGMP ELISA kits were purchased from YaJi Biological (Shanghai, China). A protein sample was added to each well of the 96-well plate set at 37°C and was let to stand for 20 min. Antibody with biotin was added to each well and incubated at 37°C for 60 min. Finally, the horseradish peroxidase-labeled avidin working solution was added and incubated at 37°C for 60 min. The optical density (OD) value was read at the wavelength of 450 nm.

2.10. PKA activity assay

PKA activity assay kit was purchased from GenMed Scientifics Inc. (U.S.A) (GMS50059.2.3 v.A). Sixty-five microliters of reagent C, 10 μL of reagent D, 10 μL of reagent E, and reagent F were added to each well of a 96-well plate. The plate was then shaken gently and mixed well, and incubated at 30°C for 3 min. Five microliters of reagent G were added to the blank well, and 50 μg of protein was added to the sample well. The plate was then shaken gently to mix well, and immediately, the OD values were read at the wavelength of 340 nm with a microplate reader at 0 min, 5 min, and 10 min.

In our system, the activity of PKA can be calculated using this formula: $A = 10.7 \times \text{OD}$, where A is PKA activity, and OD is the absorbance value.

2.11. Statistical analysis

For statistical analysis, differences between the groups were tested by analysis of variance followed by the least significant difference *post-hoc* test using SPSS 17.0. For a single comparison, the significance of differences between means was determined by *t*-test. $P < 0.05$ was considered statistically significant.

3. Results

3.1. MT2KO and DKO mice, instead of MT1KO mice, exhibited a deficit in learning and memory

Due to the weak eyesight of the C3H mice, we chose the contextual fear conditioning test to examine hippocampus-dependent learning and memory. A step-down inhibitory avoidance task was administered to all groups, and statistical latency and error times were measured to determine the deficit in memory. We found an obvious increase in the errors (Figure 1A) and short latency in MT2KO and DKO mice 2 h later (Figure 1B). Then, we also detected the long-term memory after 24 h and obtained the same results (Figures 1C and 1D). This demonstrated that MT2KO and DKO mice have a significant deficit in memory.

3.2. High quantity of choline and myo-inositol without change of neuron number in the hippocampus of MT1KO, MT2KO, and DKO mice

NMR results suggested a high quantity of choline (Cho) in MT2KO and MT1KO mice (Figure 2A) and a high quantity of myo-inositol (mI) in MT1KO mice (Figure 2B), while no significant change of N-Acetyl-L-aspartic acid (NAA) in melatonin receptor knockout mice (Figure 2C). Functional magnetic resonance imaging (fMRI) results suggested no statistical difference in hippocampus volume (Figure 2D). Furthermore, Nissl staining proved that there was no change in the number of neurons in the hippocampus of melatonin receptor knockout mice (Figure 2E and 2F).

3.3. Aberrant A β accumulation in MT2KO and DKO mice, instead of MT1KO mice

The deposition of A β was another important pathologic change in the AD brain. We performed immunohistochemical staining using 4G8 antibody (Figure 3A) and found a high density of staining in MT1KO and DKO mice (Figure 3B). Our further results showed high levels of A β 42 in MT2KO mice and high levels of A β 40 and high total levels of A β 40 and A β 42 in MT1KO mice (Figure 3C). The ratio of A β 42 and A β 40 was very high in MT2KO mice (Figure 3D), indicating dysregulation of APP metabolism. Therefore, we used the senile plaque antibody A3981 to explore the deposit of A β

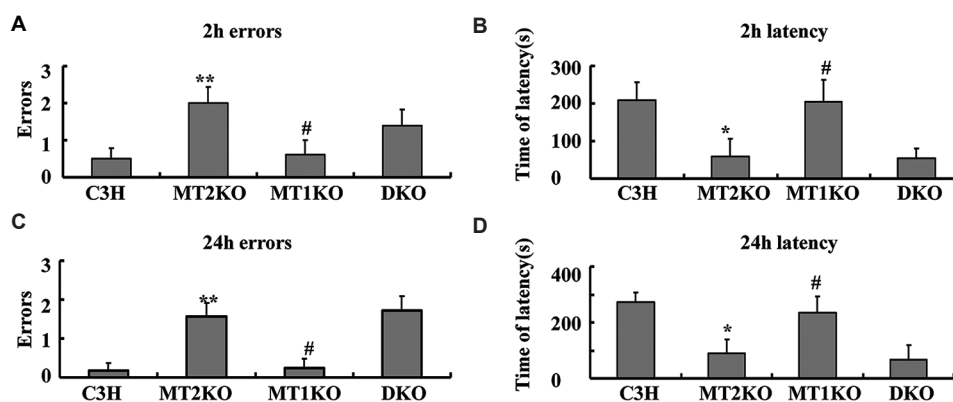


Figure 1. Decreasing learning and memory in MT2KO and DKO mice. (A) The errors of jump from the platform after 2 – 4 h. ** $P < 0.01$, compared with C3H mice; * $P < 0.05$ compared to MT2KO mice. (B) The latency time of jump from the platform after 24 h. ** $P < 0.01$, compared with C3H mice; * $P < 0.05$ compared to MT2KO mice. (C) The errors of jump from the platform after 2 h. * $P < 0.05$, compared with C3H mice; * $P < 0.05$ compared to MT2KO mice. (D) The latency time of jump from the platform after 24 h. * $P < 0.05$, compared with C3H mice; * $P < 0.05$ compared to MT2KO mice. Abbreviations: MT2KO: Melatonin receptor 2 knockout; DKO: Double knockout.

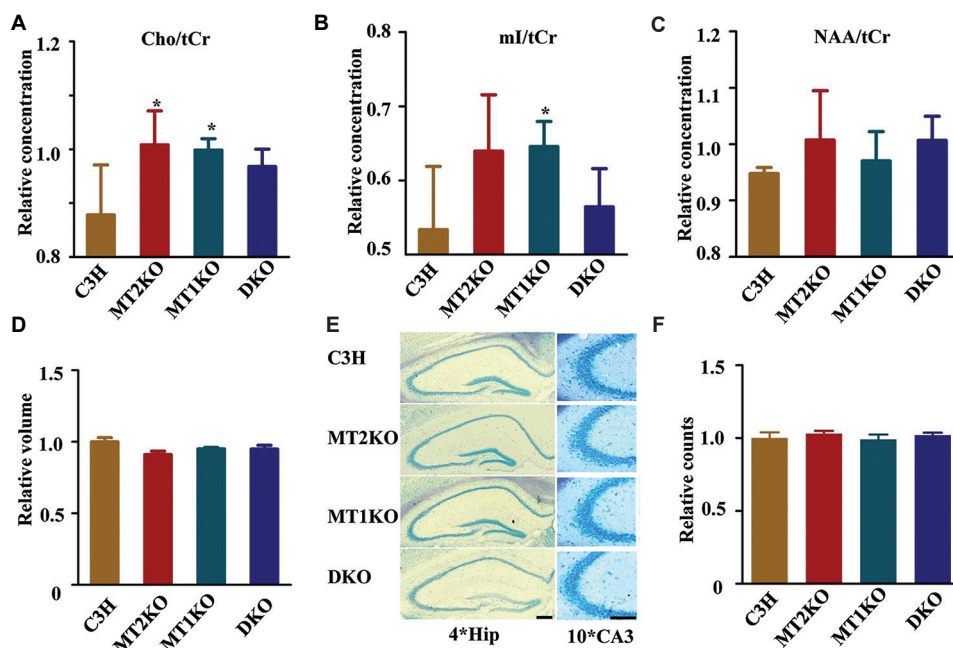


Figure 2. Detection of the change of metabolites and hippocampus area by fMRI. (A) Relative quantification of Cho. * $P < 0.05$, compared with C3H mice. (B) Relative quantification of mI. * $P < 0.05$, compared with C3H mice. (C) Relative quantification of NAA. (D) The relative volume of the hippocampus from four groups. (E) Representative photomicrographs of Nissl staining from four groups. (F) The relative counts of neuron. Abbreviations: fMRI: Functional magnetic resonance imaging; NAA: N-Acetyl-L-aspartic acid.

and found an increased plaque in MT2KO mice, instead of MT1KO mice (Figure 3E and F).

3.4. Abnormal dendritic spines and decreasing synaptic proteins in MT2KO and DKO mice, instead of MT1KO mice

Synapses were the basis of learning and memory. We examined the structure of the synapses with Golgi staining (Figure 4A). We found that the MT2KO and the DKO

mice exhibited a decreased density of dendritic spines (Figure 4B) and percentage of matured spines (Figure 4C). While the MT1KO mice exhibited normal dendritic spine morphology (Figure 4A–C). Meanwhile, in the purified crude synaptosomal fraction, we found that the levels of NR2B, NR2A, glutamate receptor 1 (GluR1), and GluR1-S845 in MT2KO and DKO mice were significantly reduced compared with control mice (Figure 4D and E). However, there were no alterations in the level of multiple

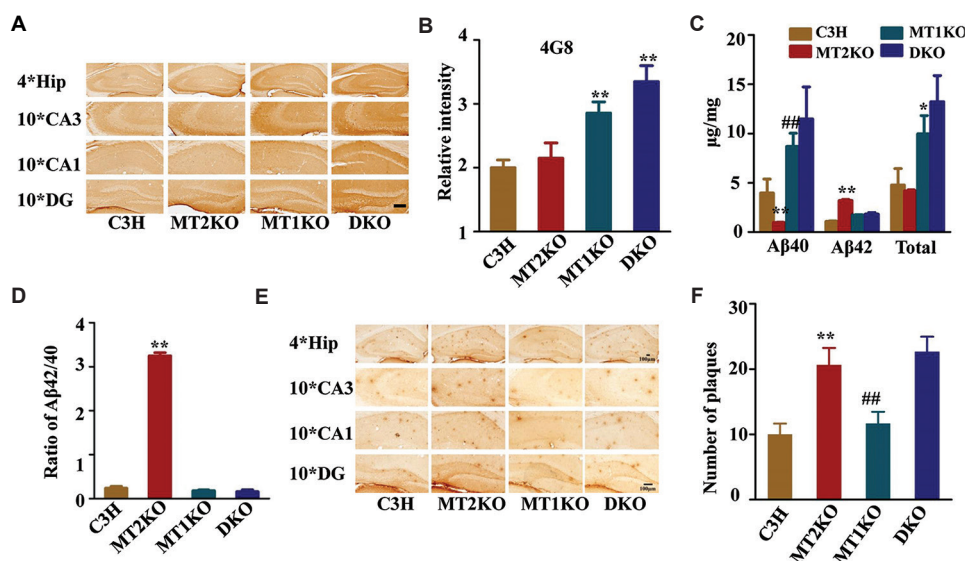


Figure 3. An obvious increase in the amount of A β 42 in MT2KO and DKO mice. (A) Immunohistochemistry for A β 42 in the hippocampus of DG, CA3, and CA1 in four groups. Scale bar = 100 μ m. (B) The relative intensity of 4G8 immunohistochemical staining in four groups. * P < 0.01, compared with C3H mice. (C) Relative quantification of A β 40, A β 42, and both of them in hippocampus. * P < 0.05 and ** P < 0.01, compared with C3H mice; ** P < 0.01, compared with MT2KO mice. (D) Ratio of A β 42/40. ** P < 0.01, compared with C3H mice. (E) Staining of plaques using A3981 antibody. Scale bar = 100 μ m. (F) The number of plaques in the hippocampus. ** P < 0.01, compared with C3H mice; ## P < 0.01, compared with MT2KO mice. Abbreviations: MT2KO: Melatonin receptor 2 knockout; DKO: Double knockout.

presynaptic proteins, such as VAMP-2, synaptophysin, MunC18, and postsynaptic markers, such as PSD93 and PSD95 (Figure 4F and G). These results suggested that MT2 knockout impaired the synaptic function through postsynaptic mechanisms.

3.5. Dysregulation of cAMP related signaling pathway in melatonin receptor knockout mice

As phosphorylated CREB at serine 133 (Ser133-CREB) is the main reason responsible for the new protein synthesis in the postsynaptic compartment, we examined the phosphorylation of CREB in the hippocampus. We found that both MT2KO and DKO mice display a dramatic increment in the phosphorylation of Ser133-CREB (Figure 5A and B). However, in the hippocampus of MT1KO mice, such abnormalities were not observed (Figure 5C and D).

We, then, queried how MTs knockout induces the differential regulation of memory and neuronal pathology. It has been reported that the cAMP and cGMP were the two major important downstream effectors of G-protein coupled receptors. Using specific ELISA kits, we measured the levels of cAMP and cGMP in the mice. We found that the concentration of cAMP was significantly reduced in MT2KO and MT1KO mice (Figure 5E), while the cGMP level was almost not altered in MT2KO, MT1KO, and DKO mice (Figure 5F). As the cAMP function is executed through PKA and EPAC2, we used Western blot and ELISA

kit to determine the activity of PKA and the quantity of EPAC2. The results suggested a significant decrease in PKA activity in MTs knockout mice (Figure 5G) and a special decrease of EPAC2 in MT2KO mice (Figure 5H and I).

4. Discussion

Melatonin has an important role in AD pathology largely due to its antioxidative stress. It has been reported that melatonin is used to treat AD^[25], day-night rhythm disturbances, and sundowning in AD. Malondialdehyde was elevated and superoxide dismutase enzyme activity was decreased in AD, indicating significant oxidative stress^[26]. Both of them were the main index of oxidative stress, and it has been demonstrated that oxidative stress was closely related to AD pathology. It has been demonstrated that decreasing the production of oxidants in the AD model could treat AD^[27]. Mitochondrial DNA damage is common in AD and aging due to oxidative stress^[28,29]. The level of basal peroxidation is increased in the cortex of AD patients^[30]. This line of evidence corroborates oxidative stress as a critical factor in AD pathology. Researchers have also reported a decreased MT2 expression^[31] and an increased MT1 expression in the hippocampus of AD patients^[32]. Although melatonin could pass through the blood-brain barrier and cell membrane, the role of the melatonin receptor remains unclear.

We also studied the hippocampus volume and neuron transmitters with fMRI and observed that there was no

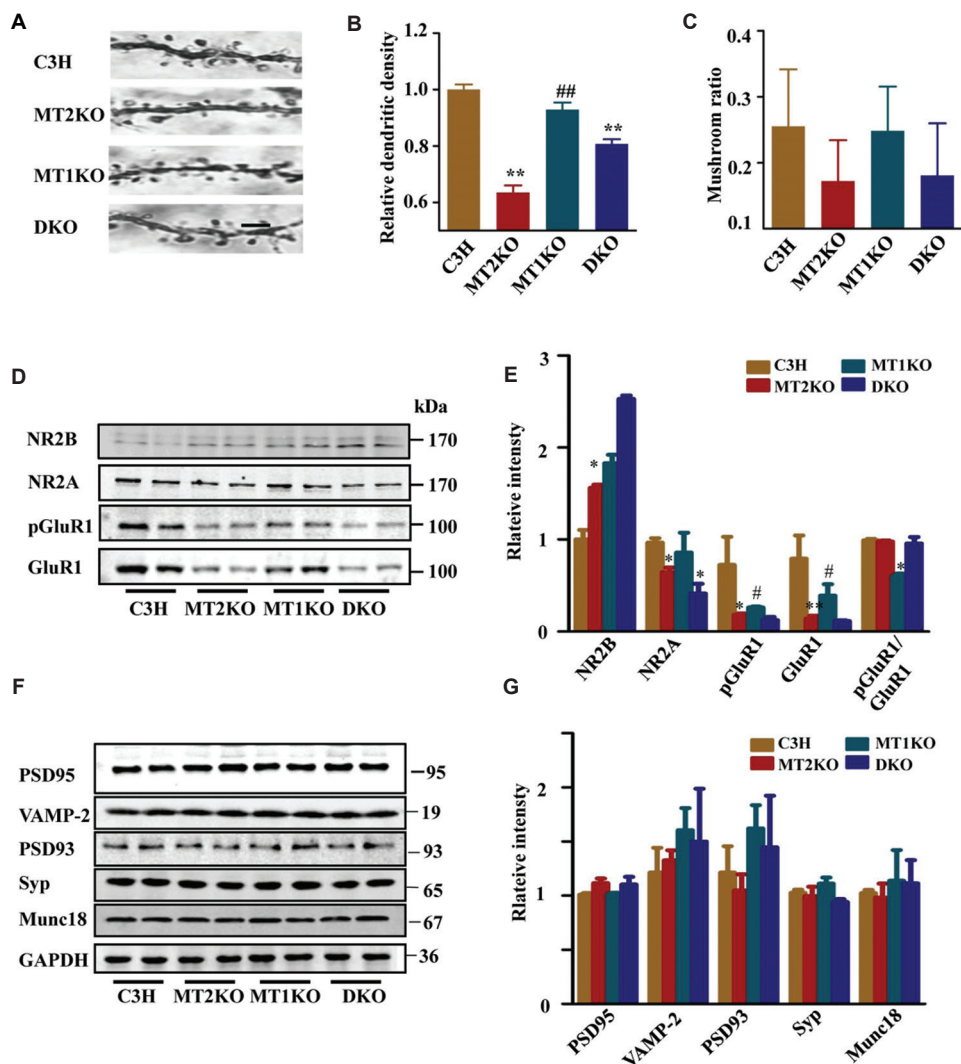


Figure 4. Deficit in expression of synaptic-related proteins in MT2KO and DKO mice. (A) Representative photomicrographs of Golgi staining from four groups. Scale bar = 20 μ m. (B) The relative dendritic density of four groups. ** $P < 0.01$, compared with C3H mice; ## $P < 0.01$, compared with MT2KO mice. (C) The relative ratio of mushroom spine computed by ImageJ software. (D) Western blot of NR2B, NR2A, GluR1, and pGluR1 (serine at the site of 845, s845). (E) Relative quantification of NR2B, NR2A, GluR1, and pGluR1 (GluR1s845). * $P < 0.05$, compared with C3H mice; ** $P < 0.01$, compared with C3H mice; # $P < 0.05$ compared to MT2KO mice. (F) Western blot of PSD95, VAMP-2, PSD93, Syp (synaptophysin), and munc18. (G) Relative quantification of PSD95, VAMP-2, PSD93, Syp (synaptophysin), and munc18. Abbreviations: MT2KO: Melatonin receptor 2 knockout; DKO: Double knockout; NR2B: NR2B subunit of NMDA receptors; NR2A: NR2A subunit of NMDA receptors; GluR1: Glutamate receptor 1; PSD95: Postsynaptic protein-95; PSD93: Postsynaptic protein-93.

change in the hippocampal volume but an increase in the Cho/tCr and mI/tCr. The Cho/tCr increase pointed to the damage in the neuron of the hippocampus. However, in the hippocampal region of the brain of AD patients, the Cho/tCr ratio did not change^[33], suggesting differences in intracerebral metabolism between MT2KO mice and AD patients. The mI/tCr increase demonstrated an influence on the activity of gliocyte^[34]. Therefore, an inflammatory response occurs in MT2KO and MT1KO mice due to melatonin receptor knockdown, but its physiological significance is still unclear.

Using ELISA, we also found an increase in A β 42 and a ratio of A β 42/A β 40 between MT2KO and MT1KO mice. Our results demonstrated that MT2 plays an important role in inhibiting the production of A β 42. It is already known that the expression of MT2 was decreased in the hippocampus. In view of this known fact and our results, the deficiency in MT2 signal transduction plays a critical role in the production of A β 42.

We found a small, but significant difference in cAMP concentration and PKA activity between MT2KO and

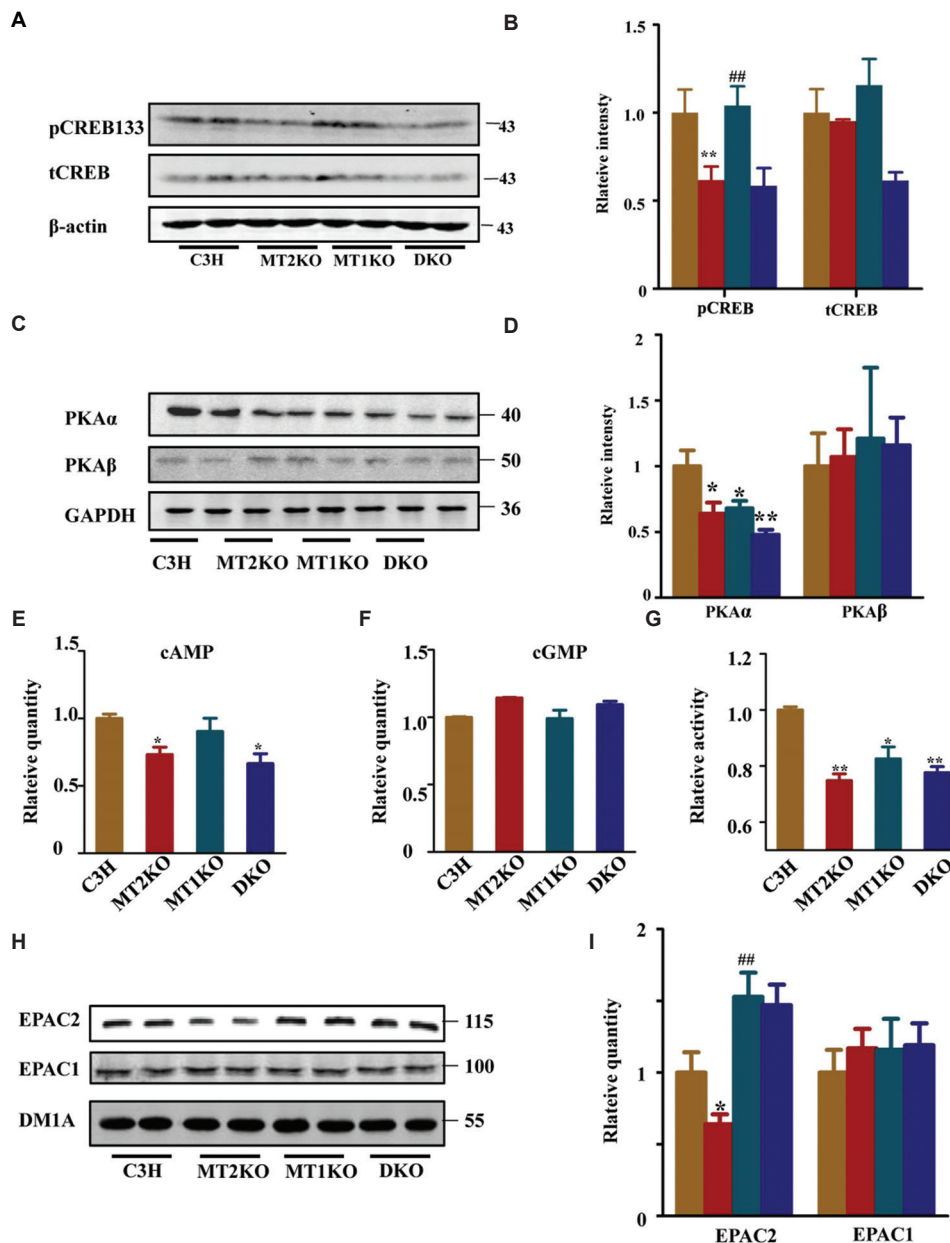


Figure 5. Perturbations of cAMP/PKA/CREB signaling pathway. (A) Western blot of CREB133 and total CREB. (B) Relative quantification of CREB133 and total CREB. ** $P < 0.01$, compared with C3H mice; ## $P < 0.01$, compared with MT2KO. (C) Western blot for PKA α and PKA β . (D) Relative quantification of PKA α and PKA β . * $P < 0.05$ and ** $P < 0.01$, compared with C3H mice. (E) Detection of PKA activity by ELISA. * $P < 0.05$ and ** $P < 0.01$, compared with C3H mice. (F) The quantification of cAMP by ELISA. * $P < 0.05$, compared with C3H mice. (G) The quantification of cGMP by ELISA. (H) Western blot of EPAC2 and EPAC1. (I) Relative quantification of EPAC2 and EPAC1. * $P < 0.05$, compared with C3H mice; ## $P < 0.01$, compared with MT2KO mice. Abbreviations: CREB: cAMP-responsive element binding protein; PKA α : Protein kinase A α ; PKA β : Protein kinase A β ; cGMP: Cyclic guanosine monophosphate; EPAC2: cAMP-regulated guanine nucleotide exchange factor II; ELISA: Enzyme-linked immunosorbent assay; MT2KO: Melatonin receptor 2 knockout.

MT1KO mice. It was known that PKA was the substrate of cAMP, and different concentration of cAMP has different effects on the substrate. This suggested that the different concentrations of cAMP may lead to different effects on the activity of PKA. The cAMP/PKA/CREB pathway plays

an important role in MT knockout mice, consistent with the behavior of the mice. Our results showed a slight but significant decrease in EPAC2 expression in MT2KO mice, and it has been shown that EPAC2 reduces GluR2/3 protein content in synapses, and this effect was not dependent on

PKA^[35]. It has been reported that the knockdown of EPAC2 inhibits dendritic spine morphology and suppresses synaptic density^[36]. Our results showed abnormal dendritic spine morphology, decreased synaptic density, and significantly more immature synapses in MT2KO mice, suggesting that decreased EPAC2 expression may also be involved in cognitive impairment in MT2KO mice.

5. Conclusion

Based on our findings, we believe that the decreased expression of the melatonin receptor and the impairment of its signal transduction may play a critical role in AD pathology. These molecular alterations could help us unravel the mechanism of AD and improve our therapeutic strategy.

Acknowledgments

We thank all the technicians and core facility in the Analytical and Testing Center, Huazhong University of Science and Technology for their support.

Funding

This study is supported by Major Project of “Brain Science and Brain-inspired Research” (2022ZD0206800), the National Natural Science Foundation of China (82030032, 82261138555, 32070960, 31721002), Top-Notch Young Talents Program of China of 2014, the Fundamental Research Funds for the Central Universities (2023BR027) to Dr. Ling-Qiang Zhu, and the Hubei Provincial Natural Science Foundation (2022CFA004) to Dr. Ling-Qiang Zhu.

Conflict of interest

The authors declare that they have no competing financial interests in this paper.

Author contributions

Conceptualization: Dan Liu

Formal analysis: He-Zhou Huang

Investigation: Xiang Wang, He-Zhou Huang

Writing – original draft: Xiang Wang

Writing – review & editing: Xiang Wang, Dan Liu

Ethics approval and consent to participate

The animal experiments have been reviewed and approved by the Medical Ethics Committee of Tongji Medical College of Huazhong University of Science and Technology (Approval ID: 2019S1873).

Consent for publication

Not applicable.

Availability of data

The original and supporting data can be obtained from corresponding author following formal request.

References

1. Dubocovich ML, 2007, Melatonin receptors: Role on sleep and circadian rhythm regulation. *Sleep Med*, 8: 34–42.
<https://doi.org/10.1016/j.sleep.2007.10.007>
2. Masana MI, Dubocovich ML, 2001, Melatonin receptor signaling: Finding the path through the dark. *Sci STKE*, 2001: pe39.
<https://doi.org/10.1126/stke.2001.107.pe39>
3. Brydon L, Roka F, Petit L, *et al.*, 1999, Dual signaling of human Mel1a melatonin receptors via G(i2), G(i3), and G(q/11) proteins. *Mol Endocrinol*, 13: 2025–2038.
<https://doi.org/10.1210/mend.13.12.0390>
4. Huete-Toral F, Crooke A, Martinez-Aguila A, *et al.*, 2015, Melatonin receptors trigger cAMP production and inhibit chloride movements in nonpigmented ciliary epithelial cells. *J Pharmacol Exp Ther*, 352: 119–128.
<https://doi.org/10.1124/jpet.114.218263>
5. Liu Y, Ni C, Li Z, *et al.*, 2017, Prophylactic melatonin attenuates isoflurane-induced cognitive impairment in aged rats through hippocampal melatonin receptor 2-cAMP response element binding signalling. *Basic Clin Pharmacol Toxicol*, 120: 219–226.
<https://doi.org/10.1111/bcpt.12652>
6. Palmer AM, Burns MA, 1994, Selective increase in lipid peroxidation in the inferior temporal cortex in Alzheimer's disease. *Brain Res*, 645: 338–342.
[https://doi.org/10.1016/0006-8993\(94\)91670-5](https://doi.org/10.1016/0006-8993(94)91670-5)
7. Roy J, Tsui KC, Ng J, *et al.*, 2021, Regulation of melatonin and neurotransmission in Alzheimer's disease. *Int J Mol Sci*, 22: 6841.
<https://doi.org/10.3390/ijms22136841>
8. Gagnon K, Godbout R, 2018, Melatonin and comorbidities in children with autism spectrum disorder. *Curr Dev Disord Rep*, 5: 197–206.
<https://doi.org/10.1007/s40474-018-0147-0>
9. Savaskan E, Jockers R, Ayoub M, *et al.*, 2007, The MT2 melatonin receptor subtype is present in human retina and decreases in Alzheimer's disease. *Curr Alzheimer Res*, 4: 47–51.
<https://doi.org/10.2174/156720507779939823>
10. Congdon EE, Sigurdsson EM, 2018, Tau-targeting therapies for Alzheimer disease. *Nat Rev Neurol*, 14: 399–415.
<https://doi.org/10.1038/s41582-018-0013-z>

11. Villemagne VL, Dore V, Burnham SC, *et al.*, 2018, Imaging tau and amyloid- β proteinopathies in Alzheimer disease and other conditions. *Nat Rev Neurol*, 14: 225–236.
<https://doi.org/10.1038/nrneurol.2018.9>
12. Liu CH, Chang HM, Yang YS, *et al.*, 2020, Melatonin promotes nerve regeneration following end-to-side neurorrhaphy by accelerating cytoskeletal remodeling via the melatonin receptor-dependent pathway. *Neuroscience*, 429: 282–292.
<https://doi.org/10.1016/j.neuroscience.2019.09.009>
13. Liu D, Wei N, Man HY, *et al.*, 2015, The MT2 receptor stimulates axonogenesis and enhances synaptic transmission by activating Akt signaling. *Cell Death Differ*, 22: 583–596.
<https://doi.org/10.1038/cdd.2014.195>
14. Deng YQ, Xu GG, Duan P, *et al.*, 2005, Effects of melatonin on wortmannin-induced tau hyperphosphorylation. *Acta Pharmacol Sin*, 26: 519–526.
<https://doi.org/10.1111/j.1745-7254.2005.00102.x>
15. Li XC, Wang ZF, Zhang JX, *et al.*, 2005, Effect of melatonin on calyculin A-induced tau hyperphosphorylation. *Eur J Pharmacol*, 510: 25–30.
<https://doi.org/10.1016/j.ejphar.2005.01.023>
16. Li SP, Deng YQ, Wang XC, *et al.*, 2004, Melatonin protects SH-SY5Y neuroblastoma cells from calyculin A-induced neurofilament impairment and neurotoxicity. *J Pineal Res*, 36: 186–191.
<https://doi.org/10.1111/j.1600-079x.2004.00116.x>
17. Wang YP, Li XT, Liu SJ, *et al.*, 2004, Melatonin ameliorated okadaic-acid induced Alzheimer-like lesions. *Acta Pharmacol Sin*, 25: 276–280.
18. Li Y, Zhang J, Wan J, *et al.*, 2020, Melatonin regulates A β production/clearance balance and A β neurotoxicity: A potential therapeutic molecule for Alzheimer's disease. *Biomed Pharmacother*, 132: 110887.
<https://doi.org/10.1016/j.biopha.2020.110887>
19. Panmanee J, Nopparat C, Chavanich N, *et al.*, 2015, Melatonin regulates the transcription of β APP-cleaving secretases mediated through melatonin receptors in human neuroblastoma SH-SY5Y cells. *J Pineal Res*, 59: 308–320.
<https://doi.org/10.1111/jpi.12260>
20. Lahiri DK, 1999, Melatonin affects the metabolism of the beta-amyloid precursor protein in different cell types. *J Pineal Res*, 26: 137–146.
<https://doi.org/10.1111/j.1600-079x.1999.tb00575.x>
21. Song W, Lahiri DK, 1997, Melatonin alters the metabolism of the beta-amyloid precursor protein in the neuroendocrine cell line PC12. *J Mol Neurosci*, 9: 75–92.
<https://doi.org/10.1007/BF02736852>
22. Skribanek Z, Balaspiri L, Mak M, 2001, Interaction between synthetic amyloid-beta-peptide (1–40) and its aggregation inhibitors studied by electrospray ionization mass spectrometry. *J Mass Spectrom*, 36: 1226–1229.
<https://doi.org/10.1002/jms.243>
23. Zhang YC, Wang ZF, Wang Q, *et al.*, 2004, Melatonin attenuates beta-amyloid-induced inhibition of neurofilament expression. *Acta Pharmacol Sin*, 25: 447–451.
24. Ono K, Hasegawa K, Yoshiike Y, *et al.*, 2002, Nordihydroguaiaretic acid potently breaks down pre-formed Alzheimer's beta-amyloid fibrils *in vitro*. *J Neurochem*, 81: 434–440.
<https://doi.org/10.1046/j.1471-4159.2002.00904.x>
25. Rudnitskaya EA, Maksimova KY, Muraleva NA, *et al.*, 2015, Beneficial effects of melatonin in a rat model of sporadic Alzheimer's disease. *Biogerontology*, 16: 303–316.
<https://doi.org/10.1007/s10522-014-9547-7>
26. Lopez N, Tormo C, De Blas I, *et al.*, 2013, Oxidative stress in Alzheimer's disease and mild cognitive impairment with high sensitivity and specificity. *J Alzheimers Dis*, 33: 823–829.
<https://doi.org/10.3233/jad-2012-121528>
27. Wang X, Wang LP, Tang H, *et al.*, 2014, Acetyl-L-carnitine rescues scopolamine-induced memory deficits by restoring insulin-like growth factor II via decreasing p53 oxidation. *Neuropharmacology*, 76: 80–87.
<https://doi.org/10.1016/j.neuropharm.2013.08.022>
28. Liu J, Ames BN, 2005, Reducing mitochondrial decay with mitochondrial nutrients to delay and treat cognitive dysfunction, Alzheimer's disease, and Parkinson's disease. *Nutr Neurosci*, 8: 67–89.
<https://doi.org/10.1080/10284150500047161>
29. Reddy PH, 2006, Mitochondrial oxidative damage in aging and Alzheimer's disease: Implications for mitochondrially targeted antioxidant therapeutics. *J Biomed Biotechnol*, 2006: 31372.
<https://doi.org/10.1155/JBB/2006/31372>
30. Pena-Bautista C, Baquero M, Vento M, *et al.*, 2019, Free radicals in Alzheimer's disease: Lipid peroxidation biomarkers. *Clin Chim Acta*, 491: 85–90.
<https://doi.org/10.1016/j.cca.2019.01.021>
31. Savaskan E, Ayoub MA, Ravid R, *et al.*, 2005, Reduced hippocampal MT2 melatonin receptor expression in Alzheimer's disease. *J Pineal Res*, 38: 10–16.
<https://doi.org/10.1111/j.1600-079X.2004.00169.x>
32. Savaskan E, Olivieri G, Meier F, *et al.*, 2002, Increased melatonin 1a-receptor immunoreactivity in the hippocampus of Alzheimer's disease patients. *J Pineal Res*, 32: 59–62.
<https://doi.org/10.1034/j.1600-079x.2002.00841.x>

33. Block W, Jessen F, Traber F, *et al.*, 2002, Regional N-acetylaspartate reduction in the hippocampus detected with fast proton magnetic resonance spectroscopic imaging in patients with Alzheimer disease. *Arch Neurol*, 59: 828–834.
<https://doi.org/10.1001/archneur.59.5.828>
34. Chang L, Munsaka SM, Kraft-Terry S, *et al.*, 2013, Magnetic resonance spectroscopy to assess neuroinflammation and neuropathic pain. *J Neuroimmune Pharmacol*, 8: 576–593.
<https://doi.org/10.1007/s11481-013-9460-x>
35. Woolfrey KM, Srivastava DP, Photowala H, *et al.*, 2009, Epac2 induces synapse remodeling and depression and its disease-associated forms alter spines. *Nat Neurosci*, 12: 1275–1284.
<https://doi.org/10.1038/nn.2386>
36. Jones KA, Sumiya M, Woolfrey KM, *et al.*, 2019, Loss of EPAC2 alters dendritic spine morphology and inhibitory synapse density. *Mol Cell Neurosci*, 98: 19–31.
<https://doi.org/10.1016/j.mcn.2019.05.001>

ORIGINAL RESEARCH ARTICLE

Estimated glomerular filtration rate and serum neurofilament light chain: Insight from National Health and Nutrition Examination Survey

Jiangwen Liu*

Department of Cardiology, 928 Hospital of Joint Logistics Support Force of PLA, Haikou, 571100, Hainan, China

Abstract

The neurofilament light chain is a protein biomarker associated with neurodegenerative diseases. Neurofilament light chain levels may increase as kidney function declines due to reduced clearance. However, the relationship between estimated glomerular filtration rate (eGFR) and serum neurofilament light chain (sNfL) has not been extensively studied. Therefore, the objective of this study was to examine the association between eGFR and sNfL levels. Health survey data from 2071 eligible participants in the National Health and Nutrition Examination Survey (NHANES) were used in three multivariate-adjusted weighted linear regression models to analyze the correlation between eGFR and sNfL. Subsequently, segmental linear regression analysis was employed to determine the inflection point of eGFR. Finally, through subgroup analysis, we aimed to assess the impact of all covariates on the association between eGFR and sNfL. According to our results, sNfL levels decreased as eGFR increased. The segmental linear regression model analysis identified an inflection point at 59.9. When eGFR reached 59.9 or exceeded it, each unit increase in eGFR was associated with a 1 pg/mL decrease in sNfL ($\beta = -0.1, P = 0.01$). Furthermore, subgroup analysis revealed that hypertension exhibited a significant interaction with the association between eGFR and sNfL ($P = 0.01$). These findings suggest that eGFR holds promise as a potential marker for neurodegenerative disorders, and hypertension could affect this association to some extent. Moreover, these results could have significant implications for the early detection and prevention of neurodegenerative diseases in patients with kidney disease. However, further research is needed to corroborate these results and elucidate the underlying mechanisms.

*Corresponding author:

Jiangwen Liu
(2020203020029@whu.edu.cn)

Citation: Liu J, 2023, Estimated glomerular filtration rate and serum neurofilament light chain: Insight from National Health and Nutrition Examination Survey. *Adv Neuro*, 2(3): 1394.
<https://doi.org/10.36922/an.1394>

Received: July 26, 2023**Accepted:** September 14, 2023**Published Online:** September 27, 2023**Copyright:** © 2023 Author(s).

This is an Open-Access article distributed under the terms of the Creative Commons Attribution License, permitting distribution, and reproduction in any medium, provided the original work is properly cited.

Publisher's Note: AccScience Publishing remains neutral with regard to jurisdictional claims in published maps and institutional affiliations.

Keywords: Estimated glomerular filtration rate; Serum neurofilament light chain; Kidney; National Health and Nutrition Examination Survey

1. Introduction

Kidney disease and neurological disorders are increasingly prevalent and debilitating health problems worldwide. The kidneys serve a critical role in filtering and eliminating waste products from the blood^[1], while the nervous system governs and coordinates all bodily functions^[2]. Despite their distinct functions, recent evidence suggests a correlation between kidney function and neurological health^[3]. One potential biomarker that has emerged as a promising indicator of both kidney and neurological health is the serum

neurofilament light chain (sNfL). This protein, known as sNfL, is released into the bloodstream when nerve cells sustain damage, rendering it a valuable tool for detecting and monitoring neurological disorders^[4].

In a recent study, sNfL was found to be linked with kidney function^[5], suggesting its potential utility as a marker for assessing kidney health. As widely acknowledged, one approach to evaluating kidney function is through the estimated glomerular filtration rate (eGFR)^[6], a measure of the kidneys' blood-filtering efficiency. eGFR is calculated by assessing the concentration of creatinine in the blood, with a decrease in eGFR indicating a decline in kidney function^[7]. A recent clinical study revealed that sNfL levels increased with age in elderly individuals over 65 years old, and a negative correlation was observed between sNfL and eGFR^[8]. The previous studies have regarded eGFR as a confounding factor in investigating the relationship between sNfL and neurodegenerative diseases, including multiple sclerosis^[9,10]. Nevertheless, there has been limited research examining the link between eGFR and sNfL in the general population. Given this gap, our study aimed to explore the relationship between eGFR and sNfL using data from the NHANES database.

2. Method

2.1. Data and population

NHANES, an acronym for the National Health and Nutrition Examination Survey, is a crucial survey led by the Centers for Disease Control and Prevention (CDC). Its primary objective is to assess the health and nutritional status of both adults and children throughout the United States. NHANES employs a comprehensive and nationally representative survey methodology, using a complex sampling design to ensure that the collected data accurately reflects the entire U.S. population. The program has maintained continuity since 1999, with new data released in 2-year cycles. For our study, we utilized physical examination and self-reported data from the 2013–2014 cycle, as sNfL information was exclusively recorded during this period. Participants with missing eGFR and sNfL information were excluded from the study, resulting in a final study cohort of 2071 participants (age ≥ 20). All NHANES protocols have received approval from the National Center for Health Statistics Research Ethics Review Board. All participants provided written informed consent, and the researcher had access to the database without the need for additional application^[11].

2.2. Calculation of eGFR

The estimated glomerular filtration rate, a measure of kidney function, is calculated using the CKD-EPI

equation^[12]. The CKD-EPI equation is a widely employed formula that incorporates the serum creatinine (Scr) level, age, sex, and race of the patient. The equation is represented as follows:

$$eGFR = 141 \times \min\left(\frac{Scr}{\kappa}, 1\right)^\alpha \times \max\left(\frac{Scr}{\kappa}, 1\right)^{-1.209} \times 0.993^{Age} \times 1.018[\text{if female}] \times 1.159[\text{if black}] \quad (1)$$

In Equation 1, κ is a constant set at 0.7 for females and 0.9 for males, while α , another constant, is defined as -0.329 for females and -0.411 for males. The equation uses “min” to represent the minimum of Scr/κ or 1, and “max” to indicate the maximum of Scr/κ or 1.

2.3. Measurement of sNfL

Serum samples from participants in the NHANES 2013–2014 cohort, aged 20–75 years, were used to perform sNfL immunoassays. The immunoassay was conducted using the Attelica platform from Siemens Healthineers, employing acridinium ester (AE) chemiluminescence and paramagnetic particles. The assay process involved incubating the serum sample with AE-labeled antibodies specifically designed to bind to the sNfL antigen. Subsequently, paramagnetic particles coated with capture antibodies were introduced, resulting in the formation of complexes comprising the sNfL antigen bound to AE-labeled antibodies and paramagnetic particles. Following the removal of unbound AE-labeled antibodies, chemiluminescence was initiated by adjusting the pH, and the resulting light emission was quantified.

2.4. Assessment of covariates

In this study, we adjusted for potential confounding factors by including age, sex, education, marital status, and self-reported information on smoking, drinking, heart failure (HF), myocardial infarction (MI), and stroke. Chronic kidney disease (CKD) is characterized by either kidney damage or reduced kidney function, as indicated by an eGFR < 60 ml/min/1.73 m² or a urine albumin-creatinine ratio of 30 or higher^[13]. Metabolic syndrome is diagnosed when a person has three or more of the following risk factors: High waist circumference, elevated triglycerides, reduced high-density lipoprotein (HDL) cholesterol, high blood pressure, and high fasting glucose levels^[14]. Hyperlipidemia is diagnosed if at least one of the following criteria is met^[15]: A total cholesterol level of 200 mg/dL or higher, a triglyceride level of 150 mg/dL or higher, an HDL cholesterol level of 40 mg/dL or lower in males and 50 mg/dL or lower in females, or a low-density lipoprotein (LDL) cholesterol level of 130 mg/dL or higher. Alternatively, individuals using cholesterol-

lowering medications are also considered to have hyperlipidemia. The criteria for hypertension include a blood pressure reading of 140/90 mmHg or higher or a documented history of taking medication to control high blood pressure^[16].

2.5. Statistical analysis

To obtain a representative estimate of the US adult population, sample weights provided by NHANES were used for analysis. In the baseline characteristics, participants' eGFR was divided into quartiles, and its association with all covariates was calculated. Mean \pm standard error represented continuous variables, while numbers and percentages were used for categorical variables. Weighted linear regression was used for univariate analysis to calculate the relationship between sNfL and eGFR, along with other covariates. To further explore the relationship between eGFR and sNfL, three linear regression models were used. Model 1 adjusted for demographic variables (age, sex, education, and marital status); Model 2 adjusted for alcohol consumption, smoking, CKD, HF, MI, metabolic syndrome (MetS), and diabetes mellitus (DM) based on Model 1; and Model 3 adjusted for hypertension, hyperlipidemia, and stroke based on Model 2. Sensitivity analysis involved dividing eGFR into quartiles to assess the robustness of the relationship with sNfL. A two-stage linear regression model was utilized to identify any potential inflection points in the curve and explore the potential correlation between eGFR and sNfL using a generalized additive model. Statistical analysis was conducted using Empower Stats and R, with significance set at $P < 0.05$.

3. Results

Our study involved a sample size of 2071 participants, and Table 1 provides the baseline characteristics. From the table, it is evident that age ($P < 0.01$), gender ($P = 0.03$), and marital status ($P < 0.01$) exhibited significant correlations with eGFR. In addition, several comorbidities such as CKD ($P < 0.01$), hyperlipidemia ($P < 0.01$), hypertension ($P < 0.01$), and diabetes ($P < 0.01$) were also associated with eGFR (Table 1). Subsequently, univariate analyses were performed to explore the association between sNfL levels, eGFR, and other covariates. The results indicated that age ($\beta = 0.38$, $P < 0.01$) and all comorbidities were positively correlated with sNfL levels (Table 2), while eGFR exhibited a significantly negative correlation with sNfL levels ($\beta = -0.31$, $P < 0.01$) (Table 2). After adjusting for demographic and clinical covariates in a multivariate model, our findings revealed that eGFR remained negatively associated with sNfL levels ($P < 0.01$). This association remained valid for eGFR when considered as both a continuous variable ($\beta = -0.2$, $P < 0.01$) and a categorical

variable (Q2/Q1: $\beta = -4.8$, $P = 0.03$; Q3/Q1: $\beta = -7.28$, $P = 0.01$; Q4/Q1: $\beta = -5.78$, $P = 0.01$) (Table 3). Notably, this relationship persisted even after adjusting for all covariates (Table 3). Using a generalized additive model followed by a threshold effect analysis, we identified an inflection point at an eGFR value of 59.9. Specifically, for each unit increase in eGFR < 59.9 , a corresponding decrease ($\beta = -1.0$, $P < 0.01$) of 1 pg/ml in sNfL levels was observed (Table 4 and Figure 1). Given that CKD is typically defined as an eGFR < 60 , we conducted interaction and subgroup analyses to explore the potential impact of CKD on the relationship between eGFR and sNfL levels. However, the results indicated no significant interaction between CKD and eGFR (Table 5). However, we did find a significant interaction between eGFR and hypertension ($P = 0.01$), which we included in our subgroup analysis (Table 5). Specifically, this study suggests that hypertension may modulate the effect of eGFR on sNfL levels.

4. Discussion

The present study aimed to investigate the correlation between eGFR and sNfL in the adult population using data from the NHANES database for the years 2013 – 2014. Our analysis revealed a negative correlation between eGFR and sNfL after adjusting for demographic and clinical covariates. These findings align with previous research that has reported an association between decreased kidney function and increased neuronal injury, manifested as elevated levels of sNfL^[17]. It is worth noting that the previous research focused on sNfL levels in elderly individuals with atrial fibrillation. In contrast, our study aimed to broaden the scope to encompass a wider population.

Interestingly, we identified an inflection point at an eGFR of 59.9. When eGFR reached 59.9 or higher, each unit increase in eGFR corresponded to a concomitant decrease of 1 pg/mL in sNfL ($P = 0.01$). Conversely, when eGFR was below 59.9, each unit increase in eGFR was associated with a decline of 0.1 pg/mL in sNfL ($\beta = -1.0$, $P < 0.01$). This inflection point is particularly noteworthy because CKD is defined as an eGFR < 60 . We considered the presence of CKD in our analysis, suggesting that the observed inflection point may reflect a different mechanism than the one underlying the pathophysiology of CKD. One potential explanation for this observation is that an eGFR < 60 may represent a threshold at which the decline in kidney function becomes significant enough to induce neurotoxicity and elevated sNfL levels.

Furthermore, our subgroup analysis revealed a significant interaction between hypertension and eGFR ($P = 0.01$). A previous meta-analysis reported that prehypertension or hypertension can serve as predictors of decreased eGFR^[18].

Table 1. Characteristics of population based on eGFR quartiles

Variables	Total	eGFR				P-value
		Q1	Q2	Q3	Q4	
Age (years)	45.05±0.45	56.77±1.04	49.89±0.77	42.16±0.98	30.65±0.29	<0.01
BMI (kg/m ²)	29.36±0.25	29.89±0.43	29.07±0.37	29.11±0.38	29.34±0.51	0.34
Sex (n [%])						0.03
Female	1081 (52.2)	263 (50.27)	240 (45.11)	271 (53.50)	307 (56.73)	
Male	990 (47.8)	255 (49.73)	277 (54.89)	248 (46.50)	210 (43.27)	
Marital (n [%])						<0.01
Never	396 (19.12)	49 (8.76)	65 (14.06)	95 (17.66)	187 (37.65)	
Alone*	386 (18.64)	159 (25.06)	92 (15.03)	81 (13.57)	54 (8.75)	
Partner [†]	1289 (62.24)	310 (66.19)	360 (70.91)	343 (68.77)	276 (53.59)	
Education (n [%])						0.01
<High school	451 (21.78)	92 (10.36)	113 (13.76)	131 (19.12)	115 (19.91)	
High school	431 (20.81)	106 (19.51)	88 (16.17)	112 (20.92)	125 (23.83)	
>High school	1186 (57.27)	319 (70.09)	316 (70.07)	276 (59.96)	275 (55.82)	
Missing	3 (0.14)	1 (0.04)	0 (0.00)	0 (0.00)	2 (0.44)	
CKD (n [%])						<0.01
No	1759 (84.93)	365 (75.59)	481 (94.97)	457 (88.46)	456 (88.45)	
Yes	299 (14.44)	150 (23.75)	33 (4.70)	59 (10.67)	57 (10.76)	
Missing	13 (0.63)	3 (0.65)	3 (0.33)	3 (0.87)	4 (0.78)	
HF (n [%])						0.05
No	2016 (97.34)	485 (95.11)	510 (99.01)	512 (98.17)	509 (98.74)	
Yes	54 (2.61)	33 (4.89)	6 (0.94)	7 (1.83)	8 (1.26)	
Missing	1 (0.05)	0 (0.00)	1 (0.05)	0 (0.00)	0 (0.00)	
MI (n [%])						0.04
No	2009 (97.01)	484 (94.41)	505 (97.88)	511 (97.86)	509 (98.95)	
Yes	61 (2.95)	34 (5.54)	12 (2.12)	8 (2.14)	7 (0.91)	
Missing	1 (0.05)	0 (0.00)	0 (0.00)	0 (0.00)	1 (0.13)	
Hyperlipidemia (n [%])						<0.01
No	655 (31.63)	103 (21.19)	141 (28.91)	190 (37.98)	221 (43.59)	
Yes	1416 (68.37)	415 (78.81)	376 (71.09)	329 (62.02)	296 (56.41)	
Hypertension (n [%])						<0.01
No	1240 (59.87)	205 (45.44)	289 (61.32)	336 (66.09)	410 (80.39)	
Yes	831 (40.13)	313 (54.56)	228 (38.68)	183 (33.91)	107 (19.61)	
MetS (n [%])						<0.01
No	1365 (65.91)	266 (55.66)	350 (69.72)	363 (70.76)	386 (74.77)	
Yes	688 (33.22)	251 (44.05)	167 (30.28)	154 (28.89)	116 (21.89)	
Missing	18 (0.87)	1 (0.29)	0 (0.00)	2 (0.35)	15 (3.34)	
Smoke (n [%])						0.01
Never	1155 (55.77)	276 (55.25)	280 (54.00)	270 (53.32)	329 (62.91)	
Former	460 (22.21)	146 (27.40)	131 (27.89)	113 (20.80)	70 (12.92)	
Now	455 (21.97)	96 (17.35)	105 (18.05)	136 (25.88)	118 (24.17)	
Missing	1 (0.05)	0 (0.00)	1 (0.06)	0 (0.00)	0 (0.00)	

(Cont'd...)

Table 1. (Continued)

Variables	Total	eGFR				P-value
		Q1	Q2	Q3	Q4	
Stroke (n [%])						0.04
No	2019 (97.49)	493 (95.79)	507 (98.12)	505 (96.84)	514 (99.65)	
Yes	52 (2.51)	25 (4.21)	10 (1.88)	14 (3.16)	3 (0.35)	
DM (n [%])						<0.01
No	1820 (87.88)	413 (83.88)	458 (90.92)	460 (91.08)	489 (95.20)	
Yes	251 (12.12)	105 (16.12)	59 (9.08)	59 (8.92)	28 (4.80)	
Drink (n [%])						0.02
Never	253 (12.22)	65 (10.13)	60 (11.02)	65 (9.71)	63 (11.46)	
Former	295 (14.24)	108 (16.70)	82 (12.92)	67 (11.21)	38 (6.60)	
Now	1360 (65.67)	315 (68.21)	348 (71.94)	337 (70.86)	360 (73.29)	
Missing	163 (7.87)	30 (4.96)	27 (4.12)	50 (8.22)	56 (8.66)	

Notes: Q1 (1.86–82.82), Q2 (82.82–98.39), Q3 (98.39–111.39), Q4 (111.39–159.93). *Including divorced, separated, widowed; †Including married, living with partner. BMI: Body mass index; CKD: Chronic kidney disease; DM: Diabetes mellitus; eGFR: Estimated glomerular filtration rate; HF: Heart failure; MetS: Metabolic syndrome; MI: Myocardial infarction.

Table 2. Univariate analysis for sNfL

Variables	β (95% CI [upper limit, lower limit])	P-value
Age (years)	0.38 (0.27, 0.49)	<0.01
BMI (kg/m ²)	0.09 (–0.05, 0.23)	0.19
Sex		
Female	1.00 (ref)	
Male	2.02 (–0.30, 4.34)	0.08
Marital		
Never	1.00 (ref)	
Alone*	6.26 (0.64, 11.88)	0.03
Partner†	2.57 (0.62, 4.52)	0.01
Education		
<High school	1.00 (ref)	
High school	0.61 (–3.54, 4.75)	0.76
>High school	0.9 (–2.91, 4.70)	0.62
CKD		
No	1.00 (ref)	
Yes	10.42 (5.50, 15.34)	<0.01
HF		
No	1.00 (ref)	
Yes	11.98 (2.96, 21.01)	0.01
MI		
No	1.00 (ref)	
Yes	9.56 (1.47, 17.64)	0.02
Hyperlipidemia		
No	1.00 (ref)	
Yes	5.19 (1.35, 9.03)	0.01

(Cont'd...)

Table 2. (Continued)

Variables	β (95% CI [upper limit, lower limit])	P-value
Hypertension		
No	1.00 (ref)	
Yes	9.4 (4.37, 14.43)	0.01
MetS		
No	1.00 (ref)	
Yes	6.82 (2.72, 10.93)	0.01
Smoke		
Never	1.00 (ref)	
Former	5.42 (–0.35, 11.20)	0.06
Now	2.37 (–0.01, 4.75)	0.05
Stroke		
No	1.00 (ref)	
Yes	24.97 (–16.08, 66.02)	0.21
DM		
No	1.00 (ref)	
Yes	12.82 (5.20, 20.43)	0.01
Drink		
Never	1.00 (ref)	
Former	6.12 (–4.89, 17.12)	0.25
Now	–2.78 (–8.16, 2.60)	0.28
eGFR (ml/min/1.73 m ²)	–0.31 (–0.42, –0.19)	<0.01

Notes: *Including divorced, separated, widowed; †Including married, living with partner. BMI: Body mass index; CI: Confidence interval; CKD: Chronic kidney disease; DM: Diabetes mellitus; eGFR: Estimated glomerular filtration rate; HF: Heart failure; MetS: Metabolic syndrome; MI: Myocardial infarction; sNfL: Serum neurofilament light chain.

Table 3. Multivariate analysis of the association between eGFR and sNfL

Variables	Model 1		Model 2		Model 3	
	β (95% CI [upper limit, lower limit])	P-value	β (95% CI [upper limit, lower limit])	P-value	β (95% CI [upper limit, lower limit])	P-value
eGFR	-0.22 (-0.34, -0.10)	0.01	-0.2 (-0.31, -0.10)	0.01	-0.2 (-0.30, -0.10)	<0.01
eGFR						
Q1	1.00 (ref)		1.00 (ref)		1.00 (ref)	
Q2	-6.06 (-11.20, -0.91)	0.03	-4.81 (-9.31, -0.30)	0.04	-4.8 (-9.21, -0.39)	0.03
Q3	-7.22 (-12.82, -1.61)	0.02	-7.05 (-12.33, -1.77)	0.01	-7.28 (-12.63, -1.92)	0.01
Q4	-5.8 (-10.60, -1.01)	0.03	-5.63 (-9.98, -1.29)	0.01	-5.78 (-10.24, -1.31)	0.01

Notes: Q1 (1.86–82.82), Q2 (82.82–98.39), Q3 (98.39–111.39), Q4 (111.39–159.93). Model 1: Adjust age + sex + education + marital; Model 2: Adjust model 1 + drink+smoke + CKD + HF + MI + MetS + DM; Model 3: Adjust model 2 + hyperlipidemia + hypertension + stroke. CI: Confidence interval; eGFR: Estimated glomerular filtration rate; sNfL: Serum neurofilament light chain.

Table 4. Threshold effect analysis of eGFR on sNfL by the two-piecewise linear regression

Variable	β (95% CI [upper limit, lower limit])	P-value
Fitting by standard linear model	-0.20 (-0.20, -0.10)	<0.01
Fitting by two-piecewise linear model		
Inflection point	59.9	
eGFR <59.9	-1.00 (-1.30, -0.80)	<0.01
eGFR >59.9	-0.10 (-0.10, 0.00)	0.01
Log-likelihood ratio	<0.001	

Abbreviations: CI: Confidence interval; eGFR: Estimated glomerular filtration rate.

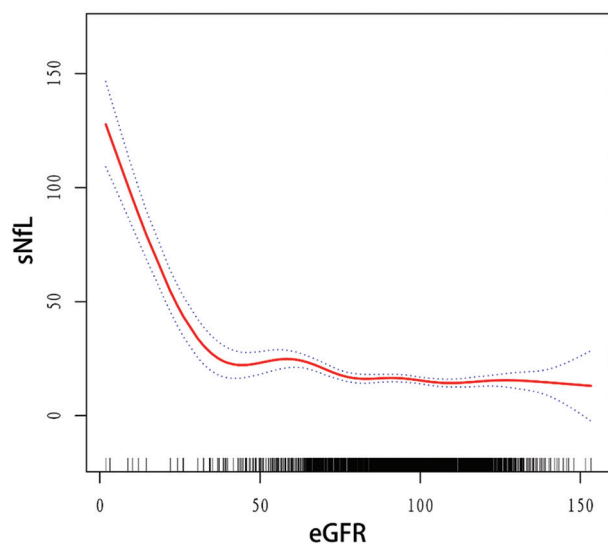


Figure 1. Association of estimated glomerular filtration rate with serum neurofilament light chain levels.

Abbreviations: eGFR: Estimated glomerular filtration rate; sNfL: Serum neurofilament light chain.

Subsequent research has also demonstrated that individuals with higher blood pressure experience a faster annual decline in eGFR^[19]. These findings suggest that hypertension may modify the effect of eGFR on sNfL levels. One plausible

mechanism is that hypertension could lead to vascular damage and inflammation, contributing to neuronal injury and increased sNfL levels in individuals with decreased eGFR. Neuronal damage can result in an elevation of sNfL levels^[20,21]. Hypertension can increase the expression of adhesion factors in brain endothelial cells, leading to platelet deposition. This, in turn, activates glial cells and NF- κ B signal transduction, ultimately resulting in neuronal damage^[22]. Furthermore, sustained intracranial hypertension can cause cerebral perfusion damage and neuronal injury, resulting in secondary brain injury^[23]. It has been found that hypertension is associated with sNfL levels, and previous studies have reported a correlation between sNfL levels in cerebrospinal fluid and idiopathic intracranial hypertension^[24,25].

In previous studies, age has been identified as an important factor affecting sNfL levels, with a more significant impact observed in participants aged 60 or older^[26]. Our research findings align with this observation. In our subgroup analysis, when adjusting for other covariates except for age, we observed a higher influence ratio of participants aged 60 years or older ($\beta = -0.36$, $P = 0.07$) on the relationship between eGFR and sNfL compared to participants younger than 60 years ($\beta = -0.17$, $P < 0.01$), although the P -value for the former was not statistically significant.

Table 5. Subgroup analysis

Variables	β (95% CI [upper limit, lower limit])	P-value	P for interaction
Age (years)			0.44
<60	-0.17 (-0.24, -0.10)	<0.01	
\geq 60	-0.36 (-0.75, 0.04)	0.07	
Sex			0.39
Female	-0.17 (-0.27, -0.06)	0.01	
Male	-0.23 (-0.41, -0.05)	0.02	
BMI (kg/m ²)			0.21
<5	-0.17 (-0.30, -0.03)	0.02	
25–30	-0.09 (-0.19, 0.01)	0.07	
\geq 30	-0.20 (-0.34, -0.06)	0.01	
Hypertension			0.01
No	-0.05 (-0.09, -0.01)	0.02	
Yes	-0.33 (-0.50, -0.15)	0.01	
DM			0.45
No	-0.14 (-0.26, -0.02)	0.02	
Yes	-0.40 (-0.61, -0.18)	0.01	
CKD			0.57
No	-0.15 (-0.33, 0.03)	0.10	
Yes	-0.30 (-0.54, -0.07)	0.01	

Abbreviations: BMI: Body mass index; CI: Confidence interval; CKD; Chronic kidney disease; DM; Diabetes mellitus.

Moreover, a recent cross-sectional study demonstrated that diabetes was associated with elevated sNfL levels, and this correlation remained significant even after accounting for related covariates^[27]. Coincidentally, Maalmi *et al.*^[28] have also identified sNfL as a potential novel biomarker for early diabetic sensorimotor polyneuropathy. In light of these findings, we included diabetes mellitus in our subgroup analysis and found no significant interaction with eGFR. The inclusion of diabetes mellitus in the subgroup analysis and the absence of a significant interaction offer valuable insights. This observation suggests that while diabetes may contribute to elevated sNfL levels, its interaction with eGFR may differ from that of hypertension. This nuanced distinction prompts us to explore the distinct molecular pathways through which diabetes impacts neuronal health. This distinction holds the potential to tailor interventions aimed at customizing neuroprotection strategies for individuals with varying comorbidities.

A recent study has demonstrated that urine sNfL could effectively differentiate between individuals with neuronal damage and those without^[29]. This non-invasive and fast detection method could be valuable for detecting neurological damage. Nevertheless, our study still has

some limitations. First, the cross-sectional design of our study limits our ability to establish causality between eGFR, sNfL levels, and hypertension. Longitudinal studies are needed to better understand the temporal relationship and potential causal pathways. Second, our study focused on a specific time frame and the American adult population. The results may not be fully generalized to other regions or age groups, and variations in health-care systems, genetics, and lifestyles should be considered. For further research, conducting longitudinal studies with multiple time points would allow for tracking changes in all variables, providing more insight into the causal relationship and potential predictive value. What's more, comparing the utility of sNfL with other established biomarkers in assessing kidney function and neurological damage could provide a broader context for the potential clinical applications of sNfL. In conclusion, our findings emphasize the significance of considering both kidney function and hypertension status when evaluating sNfL levels.

5. Conclusion

Our findings emphasize the significance of considering both kidney function and hypertension status when evaluating sNfL levels. Our research demonstrates a strong relationship between the eGFR and sNfL. To summarize, our study reveals a negative correlation between eGFR and sNfL levels in the adult population, with a turning point at an eGFR of 59.9. These findings contribute to the growing body of literature highlighting the potential utility of sNfL as a biomarker for kidney function and hypertension-induced neurological damage. Future research could explore whether monitoring sNfL levels facilitates the monitoring of kidney disease progression.

Acknowledgments

We thanked all the researchers and participants of the NHANES study for their critical review and profound contributions.

Funding

None.

Conflict of interest

The author declares that the research was conducted in the absence of any commercial or financial relationships that could be construed as a potential conflicts of interest.

Author contributions

This is a single-authored article.

Ethics approval and consent to participate

All NHANES protocols have received approval from the National Center for Health Statistics Research Ethics Review Board. All participants provided written informed consent, and the researcher had access to the database without the need for additional application.

Consent for publication

All participants provided written informed consent, and the researcher had access to the database without the need for additional application.

Data availability

All datasets can be found and downloaded from the official website: <https://www.cdc.gov/nchs/nhanes/>

References

- Lidberg KA, Muthusamy S, Adil M, *et al.*, 2022, Serum protein exposure activates a core regulatory program driving human proximal tubule injury. *J Am Soc Nephrol*, 33: 949–965.
<https://doi.org/10.1681/ASN.2021060751>
- Proulx ST, Engelhardt B, 2022, Central nervous system zoning: How brain barriers establish subdivisions for CNS immune privilege and immune surveillance. *J Intern Med*, 292: 47–67.
<https://doi.org/10.1111/joim.13469>
- Wang M, Ding D, Zhao Q, *et al.*, 2021, Kidney function and dementia risk in community-dwelling older adults: The Shanghai Aging Study. *Alzheimers Res Ther*, 13: 21.
<https://doi.org/10.1186/s13195-020-00729-9>
- Steinacker P, Anderl-Straub S, Diehl-Schmid J, *et al.*, 2018, Serum neurofilament light chain in behavioral variant frontotemporal dementia. *Neurology*, 91: e1390–e1401.
<https://doi.org/10.1212/WNL.0000000000006318>
- Tang R, Panizzon MS, Elman JA, *et al.*, 2022, Association of neurofilament light chain with renal function: Mechanisms and clinical implications. *Alzheimers Res Ther*, 14: 189.
<https://doi.org/10.1186/s13195-022-01134-0>
- Breeze CE, Batorsky A, Lee MK, *et al.*, 2021, Epigenome-wide association study of kidney function identifies trans-ethnic and ethnic-specific loci. *Genome Med*, 13: 74.
<https://doi.org/10.1186/s13073-021-00877-z>
- Lang J, Scherzer R, Tien PC, *et al.*, 2014, Serum albumin and kidney function decline in HIV-infected women. *Am J Kidney Dis*, 64: 584–591.
<https://doi.org/10.1053/j.ajkd.2014.05.015>
- Ladang A, Kovacs S, Lengelé L, *et al.*, 2022, Neurofilament light chain concentration in an aging population. *Aging Clin Exp Res*, 34: 331–339.
<https://doi.org/10.1007/s40520-021-02054-z>
- Revendova KZ, Zeman D, Bunganic R, *et al.*, 2022, Serum neurofilament levels in patients with multiple sclerosis: A comparison of SIMOA and high sensitivity ELISA assays and contributing factors to ELISA levels. *Mult Scler Relat Disord*, 67: 104177.
<https://doi.org/10.1016/j.msard.2022.104177>
- Rebelos E, Rissanen E, Bucci M, *et al.*, 2022, Circulating neurofilament is linked with morbid obesity, renal function, and brain density. *Sci Rep*, 12: 7841.
<https://doi.org/10.1038/s41598-022-11557-2>
- Zhao L, Sun Y, Cao R, *et al.*, 2022, Non-linear association between composite dietary antioxidant index and depression. *Front Public Health*, 10: 988727.
<https://doi.org/10.3389/fpubh.2022.988727>
- Levey AS, Stevens LA, Schmid CH, *et al.*, 2009, A new equation to estimate glomerular filtration rate. *Ann Intern Med*, 150: 604–612.
<https://doi.org/10.7326/0003-4819-150-9-200905050-00006>
- Kidney Disease: Improving Global Outcomes (KDIGO) Glomerular Diseases Work Group. 2021, KDIGO 2021 clinical practice guideline for the management of glomerular diseases. *Kidney Int*, 100: S1–S276.
<https://doi.org/10.1016/j.kint.2021.05.021>
- Grundy SM, Cleeman JI, Daniels SR, *et al.*, 2005, Diagnosis and management of the metabolic syndrome: An American Heart Association/National Heart, Lung, and Blood Institute Scientific Statement. *Circulation*, 112: 2735–2752.
<https://doi.org/10.1161/CIRCULATIONAHA.105.169404>
- Mahemuti N, Jing X, Zhang N, *et al.*, 2023, Association between systemic immunity-inflammation index and hyperlipidemia: A population-based study from the NHANES (2015–2020). *Nutrients*, 15: 1177.
<https://doi.org/10.3390/nu15051177>
- Fan H, Zhou J, Huang Y, *et al.*, 2022, A proinflammatory diet is associated with higher risk of peripheral artery disease. *Nutrients*, 14: 3490.
<https://doi.org/10.3390/nu14173490>
- Polymeris AA, Helfenstein F, Benkert P, *et al.*, 2022, Renal function and body mass index contribute to serum neurofilament light chain levels in elderly patients with atrial fibrillation. *Front Neurosci*, 16: 819010.
<https://doi.org/10.3389/fnins.2022.819010>
- Garofalo C, Borrelli S, Pacilio M, *et al.*, 2016, Hypertension and prehypertension and prediction of development of decreased estimated gfr in the general population: A meta-

- analysis of cohort studies. *Am J Kidney Dis*, 67: 89–97.
<https://doi.org/10.1053/j.ajkd.2015.08.027>
19. Yu Z, Rebholz CM, Wong E, *et al.*, 2019, Association between hypertension and kidney function decline: The atherosclerosis risk in communities (ARIC) study. *Am J Kidney Dis*, 74: 310–319.
<https://doi.org/10.1053/j.ajkd.2019.02.015>
 20. Siller N, Kuhle J, Muthuraman M, *et al.*, 2019, Serum neurofilament light chain is a biomarker of acute and chronic neuronal damage in early multiple sclerosis. *Mult Scler*, 25: 678–686.
<https://doi.org/10.1177/1352458518765666>
 21. Benkert P, Meier S, Schaedelin S, *et al.*, 2022, Serum neurofilament light chain for individual prognostication of disease activity in people with multiple sclerosis: A retrospective modelling and validation study. *Lancet Neurol*, 21: 246–257.
[https://doi.org/10.1016/S1474-4422\(22\)00009-6](https://doi.org/10.1016/S1474-4422(22)00009-6)
 22. Bhat SA, Goel R, Shukla R, *et al.*, 2017, Platelet CD40L induces activation of astrocytes and microglia in hypertension. *Brain Behav Immun*, 59: 173–189.
<https://doi.org/10.1016/j.bbi.2016.09.021>
 23. Rosenthal C, Wolf S, Weber-Carstens S, *et al.*, 2012, Intracranial hypertension-therapeutic options. *Anesthesiol Intensivmed Notfallmed Schmerzther*, 47: 30–38; quiz 39.
<https://doi.org/10.1055/s-0032-1301379>
 24. Beier D, Korsbæk JJ, Madsen JS, *et al.*, 2020, Neurofilament light chain as biomarker in idiopathic intracranial hypertension. *Cephalalgia*, 40: 1346–1354.
<https://doi.org/10.1177/0333102420944866>
 25. Engel S, Halcour J, Ellwardt E, *et al.*, 2023, Elevated neurofilament light chain CSF/serum ratio indicates impaired CSF outflow in idiopathic intracranial hypertension. *Fluids Barriers CNS*, 20: 3.
<https://doi.org/10.1186/s12987-022-00403-2>
 26. Koini M, Pirpamer L, Hofer E, *et al.*, 2021, Factors influencing serum neurofilament light chain levels in normal aging. *Aging (Albany NY)*, 13: 25729–25738.
<https://doi.org/10.18632/aging.203790>
 27. Ciardullo S, Muraca E, Bianconi E, *et al.*, 2023, Diabetes mellitus is associated with higher serum neurofilament light chain levels in the general US population. *J Clin Endocrinol Metab*, 108: 361–367.
<https://doi.org/10.1210/clinem/dgac580>
 28. Maalmi H, Strom A, Petrera A, *et al.*, 2023, Serum neurofilament light chain: A novel biomarker for early diabetic sensorimotor polyneuropathy. *Diabetologia*, 66: 579–589.
<https://doi.org/10.1007/s00125-022-05846-8>
 29. Kohlhase K, Frank F, Wilmes C, *et al.*, 2023, Brain-specific biomarkers in urine as a non-invasive approach to monitor neuronal and glial damage. *Eur J Neurol*, 30: 729–740.
<https://doi.org/10.1111/ene.15641>

OUR JOURNALS



Tumor Discovery is a peer-reviewed and open-access journal that aims to present new cancer research with strong emphasis on fundamental and translational studies. *Tumor Discovery* covers topics, including but not limited to the following:

- Etiology and pathogenesis of cancer
- Mechanisms and molecular pathways underlying cancer initiation and progression
- Tumor metastasis
- Tumor evolution and heterogeneity
- Tumor microenvironment and tumor-host interactions
- Cancer genetics and genomics
- Cancer characterization using omics approaches
- Discovery and validation of cancer biomarker
- Discovery of new therapeutic targets
- New approaches of diagnostic and treatment modalities
- Statistical methods in cancer research

Global Translational Medicine is a quarterly journal that focuses on medicine, biological sciences, and biomaterials engineering. The goal of *Global Translational Medicine* is to provide a platform to researchers for showcasing their latest research works in translational medicine so as to advance the field towards the betterment of human health. Despite the advancement of omics and new technologies, the process of transforming these technologies and scientific research results into effective therapies and putting them into clinical use still has a long way to go. *Global Translational Medicine* provides a platform to fill the gaps in preclinical and inter-disciplinary research, to promote clinical translation of scientific research results, and to contribute to the conception of new and improved preventive measures as well as diagnostic and therapeutic techniques of diseases.

Global Translational Medicine covers the following themes: cardiovascular disease, metabolism/diabetes/obesity, neuroscience/neurology, cancer, biomaterials and their applications in medicine, proteomics/metabolomics, pharmacogenomics, biomarkers, bioinformatics and data mining, animal and clinical research, and medical methods arising from interdisciplinary crossover.



Start a new journal

Write to us via email if you are interested to start a new journal with AccScience Publishing. Please attach your CV, professional profile page and a brief pitch proposal in your email. We shall inform you of our decision whether we are interested to collaborate in starting a new journal.

Contact: info@accscience.com

<https://accscience.com/journal/AN>



Contact

www.accscience.com

8 Burn Road, #15-03 Trivex, Singapore 369977

Email: editorial@accscience.com

Phone: +65 8182 1586